Departamento de Química Física

Centro Singular de Investigación en Química Biolóxica e Materiais Moleculares

UNIVERSIDADE DE SANTIAGO DE COMPOSTELA

THERMODYNAMIC AND STRUCTURAL STUDIES ON THE INTERACTION OF GUESTS WITH MACROCYCLES

Vítor Manuel dos Santos Francisco

Santiago de Compostela, Julio 2013

USC
UNIVERSIDADE
DE SANTIAGO
DE COMPOSTELA

D. Luis García Río,

Catedrático de Química Física de la Universidad de Santiago de Compostela

CERTIFICA

Que el trabajo descrito en esta memoria con el título "Thermodynamic and structural studies on the interaction of guests with macrocycles" presentado por D. Vítor Manuel dos Santos Francisco, Graduado en Química, para optar al Grado de Doctor en Química, ha sido realizado bajo su dirección en el Departamento de Química Física de la Universidad de Santiago de Compostela.

Para que así conste firma la presente en Santiago de Compostela a

31 de Julio de 2013

Luis García Río

USC
UNIVERSIDADE
DE SANTIAGO
DE COMPOSTELA

Agradecimientos

En primero lugar quiero agradecer a mi director de tesis, D. Luis García Río, por su constante apoyo y orientación en el desarrollo de este trabajo.

Também quero agradecerer a duas pessoas que me animaram a que eu desenvolve-se esta etapa da minha vida, professor José Moreira e Dr. Nuno Basílio.

Agradeço à Fundaçao para a Ciência e Tecnologia pelo apoio através da Bolsa de Doutoramento (SFRH/BD/43836/2008), financiada pelo POPH - QREN -Tipologia 4.1 - Formação Avançada, comparticipado pelo Fundo Social Europeu e por fundos nacionais do MCTES.

I would like to thank prof. José Moreira (Universidade do Algarve) and prof. Werner M. Nau (Jacobs University Bremen) for the opportunity to work in their labs.

A todos los compañeros del laboratorio que hicieran con que el tiempo que se pasa dentro de un laboratorio fuera más agradable: Borja, Fernando, Marcia, Mariluz , Maria, Miguel, Nuno, prof. Pedro, Pepita, Serxio, Silvia e Susana. Quiero agradecer también al Dr. Fernando Fernández por el apoyo en la Química Orgánica.

I would also like to thank my colleagues in Jacobs University, by the good hours spent inside and outside the lab: Alexandra, Indrajit, Frank, Khaleel, Garima, Amir and also Alex. Patras.

Quiero agradecer a todos los amigos que hice en esta bonita cuidad, en especial a Pedro, Santiago y Fátima. A Serxio por su amistad.

A todos os amigos da fronteira para baixo, mas em especial, Ana Teresa, Diana, Jorge e os meus sobrinhos Nuno e Sofia, que fizeram com que os fim-de-semana dessem para matar saudades.

E por ultimo, e mais importante, á minha familia mais proxima, os meus irmãos, mas em especial á minha Mãe.

A ti Rita, pelas pontes entre nós.

USC
UNIVERSIDADE
DE SANTIAGO
DE COMPOSTELA

"*A falta de coragem causa perda de momentos incriveis*"

USC
UNIVERSIDADE
DE SANTIAGO
DE COMPOSTELA

Table of Contents

USC
UNIVERSIDADE
DE SANTIAGO
DE COMPOSTELA

Abstract

This thesis describes the host-guest chemistry between different macrocycles with various guests in aqueous solution. The focus of this thesis is the influence of ionic molecules, which are typically neglected, in the binding affinities and thermodynamic parameters of the complexation of guests by macrocycles. In this sense, an extensively studied macrocycle and its counterion, often a inorganic cation, was selected as a host. The complexation of cations, others than the counterion, as well as a charged and a neutral guest by a water-soluble calixarene, *p*-sulfonatocalix[4]arene, was studied. This is the main topic of chapter 2, which is divided by the type of guest. In section 2.1, a microcalorimetric study of the inclusion of monovalent and divalent metal cations by *p*-sulfonatocalix[4]arene has been performed. The thermodynamic parameters for the complexation of alkali metal cations and also for Ag^+ were obtained for the first time at neutral pH. The cation Na^+ is routinely present as counterion of the calixarene in neutral aqueous solution, which needs to be taken into account in the determination of the thermodynamic parameters for the complexation of Na^+ as well as for the other cations by considering a sequential or a competitive binding scheme. The ΔH° and ΔS° values show that the inclusion process is entropically driven, although an influence of the temperature in the complexation reaction denotes that the enthalpic term is also an important contributor. The results also reveal that an enthalpy–entropy compensation balances the gain in one contribution against a corresponding loss in the other. The obtained thermodynamic data contrasts the results from previous microcalorimetric measurements, which point to orders of magnitude lower binding constants and in part enthalpically driven complexations, but which neglected the influence of the alkali metal counterions.

In section 2.2, calorimetric and NMR titration experiments have been done to measure the binding constant between *p*-sulfonatocalix[4]arene and a quaternary ammonium ion. The results show that the binding constants depend both on the calixarene concentration and on the presence of added Na^+. These results have been interpreted by considering the ion-exchange equilibrium between sulfonatocalixarene counterions and the added organic cation. In this way, it is necessary to extrapolate the

binding constants to zero calixarene concentration and zero added salts in order to get the true equilibrium constant.

In section 2.3, the complex stability constant for the complexation of a pyridine guest by the water-soluble calixarene have been determined in the presence of both alkali and transition-metal cations. Using isothermal titration calorimetry (ITC) and NMR experiments, we performed the structural investigation of the complex between 2-chloropyridine with *p*-sulfonatocalix[4]arene in different aqueous solutions containing Na^+ and Cu^{2+} ions at neutral pH. The experiments show the formation of a triple complex for both ions, with the presence of the alkali metal ion decreasing the host-guest binding constant, while the transition-metal cation leads to an increase in the binding constant indicating a positive cooperativity.

In order to confirm that the complexation of the counterion is not a specific case of sulfonatocalixarenes, in the next two chapters, chapter 3 and 4, is described the influence of the counterion/salt in other two macrocycles. In chapter 3, where the experiments were performed in collaboration with Borja Gómez, the complexation of an anionic guest by a cationic water-soluble pillararene is reported. ITC, ^{1}H NMR, ^{1}H and ^{19}F DOSY NMR experiments were employed to characterize the complex formation in aqueous neutral solution. The results from ITC and ^{1}H NMR show an inclusion of the guest in the cylindrical cavity of pillar[5]arene, where the binding constant is influenced by the counterion of the macrocycle. Diffusion experiments show that although a fraction of counterion is expelled from the host cavity upon complexation of the guest, a ternary complex is formed (pillarareno-counterion-guest). Furthermore, the diffusion experiments also showed that at higher concentration of guest, an external guest binding is observed in addition to the internal complexation of the guest.

In chapter 4, where the experiments were carried out in prof. Nau lab, host-guest complexation between a hemicyanine dye and cucurbit[6]uril was studied in neutral aqueous solution. The kinetics for the formation of the complex were determined by stopped-flow spectrofluorimetric experiments as a function of temperature, salt concentration and cation size. The results show a decrease in the binding affinity and also in the ingression rate constant as a consequence of the a competitive binding between the dye and the cations by the negative charged density portals of the cucurbituril.

The last chapter describes the interaction between surfactants and *p*-sulfonatocalix[4]arene. The chapter 5 is divided in two section due the different type of

surfactant studied. In section 5.1, where the synthesis and characterization of bolaforms were carried out in prof. José Moreira lab, the inclusion binding manners of bolaforms surfactants of type $C_nR_6^{2+}$ $2Br^-$ with different spacer length (n = 6 and 12) and terminal head group volume (R = methyl, ethyl and propyl) by the calixarene were studied by different NMR-methods and ITC experiments. The parameters obtained from ITC experiments (the binding constant, the enthalpy and the entropy of formation) allied with the chemical shifts and NOE cross peaks obtained upon complexes formation, allows the determination of the different binding modes between the bisquaternary ammonium guests and the water-soluble calixarene. The results point out that only the bolaforms with larger spacer length between the polar head groups enables the formation of 1:1 complexes as well as 2:1, while with the shorter spacer only form 1:1 complexes.

The results also show that the difference in the spacer length between the bolaforms studied is non-obstructive of 1:1 complex formation, with both polar head groups of the guest being accommodated in the cavity of the calixarene. Increasing the terminal head group volume of the bolaform, shows that the guest can form 1:1 complexes with only one polar head group inside the calixarene cavity, and where the alkyl spacer and the other terminal group of the bolaform is surrounding the calixarene cavity. The different binding modes obtained for the 1:1 stoichiometry can be related with the bolaform shape, but also with the flexibility and structure of the calixarene.

Finally in section 5.2, it is shown that the host-guest complex formed by *p*-sulfonatocalix[4]arene, and the single chain surfactant tetradecyltrimethylammonium bromide can yield vesicles after a sonication procedure. Such vesicles are stable for a period of four days. Moreover the vesicles can be dried by a lyophilization process and rehydrated without the need of further sonication, yielding vesicle aggregates of similar size. The complexation of a serine-based surfactant by *p*-sulfonatocalix[4]arene was also studied, where the preliminary results indicates a formation of region with supramolecular aggregates such as tubules, vesicles and supramolecular micelles.

USC
UNIVERSIDADE
DE SANTIAGO
DE COMPOSTELA

Chapter 1

1. Introduction

1.1. Definition of supramolecular chemistry

Supramolecular chemistry has become one of the most trendy areas of experimental chemistry.[1] Although is still a young field, has attracted a wide range of scientists from other fields, namely physicists, mathematicians, biologists, biochemists, among others. Nowadays, this research area can be defined by expressions as "the chemistry beyond molecules" or most commonly "the chemistry of molecular assemblies and of the intermolecular bond". Essentially, according to Jean-Marie Lehn, it is a result from the association of chemical species by intermolecular forces, where the properties of the resulting supermolecules are different and often better than the properties of the individual components.[2]

Supramolecular chemistry can be classified basically in two main categories: molecular recognition chemistry and molecular self-assembly (Scheme 1). Molecular recognition is generally associated with the inclusion of guest species by receptor molecules, forming supramolecular host-guest complexes (section 1.4), while the molecular assembly deals with the association of species to give well-organized supramolecular aggregates (section 1.5). Despite these two categories, some other categories can be found due the different size of the molecular system, such as the chemistry of molecules to build specific shapes.

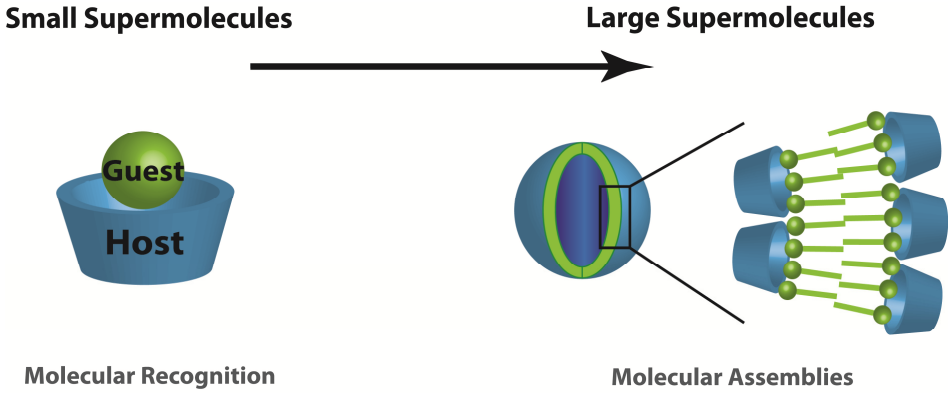

Scheme 1

Typical forces such as hydrogen bonds, hydrophobic, π–π stacking, cation–π, electrostatic and van der Waals dominates the interactions in supramolecular chemistry. The advantage of these type of interactions in comparison with the covalent bonds, can be related with the strength and reversibility of the intermolecular interactions.[2,3] Since most of the biological processes take place in water, and involve reversible and weak non-covalent interactions between molecular species, it is of great importance to understand intermolecular interactions to create new supramolecular systems.[4,5]

1.2. Non-covalent interactions

As stated above, in supramolecular chemistry, non-covalent interactions are the typical driving force between a host and a guest. Often a combination of the following intermolecular interactions describe below are responsible for the formation of host-guest complexes.

Electrostatic Interactions: These interactions are Coulombic interactions, that result from the attraction between two oppositely charged molecules. Commonly can be divided in ion-ion, ion-dipole, permanent dipole-permanent-dipole and permanent dipole-induced dipole interactions.[1,6] Within the electrostatic interactions, the ion-ion are the strongest non-covalent interactions available, with a bond energy up to 350 kJ/mol, which can be comparable in strength to covalent bonding.[1,6] These interactions are independent of direction, while ion-dipole interactions need to be arranged in a certain direction in order to achieve maximum strength.[1,6]

Permanent dipole-permanent dipole interactions involve interactions between molecules that have a permanent dipole, which is partially positive at one end and partially negative at the other end. Regarding with permanent dipole-induced dipole interactions, they take place generally when a molecule with a permanent dipole and a nonpolar molecule approach each other. The interaction energy of electrostatic interactions is related to the distance, *r*, between the two atoms or molecules. In the case of ion-dipole, the interaction energy decreases by r^2 as the distance increases, r^3 with increasing distance for permanent dipole-permanent dipole interactions and for ion-induced dipole interactions the decrease is r^4 with increasing distance.[7] The larger interaction energy decrease as distance increases is observed for the permanent dipole-induced dipole interactions, with a decrease by r^6.

Typical examples of electrostatic interactions can be found in the interactions between cationic guests and the electron rich carbonyl-lined rims of cucurbit[*n*]urils, as well as the binding between cations and crown ethers.

Hydrogen Bonding: This type of interaction involves donor-acceptor interactions between two atoms to form a special type of dipole-dipole attraction. While one atom, A-H, will act as a proton donor, the another atom, B, will act as a proton acceptor,[8,9] resulting in the hydrogen bond A-H···B. Atom A should be sufficiently electronegative to withdraw electron density from the proton so that atom B can donate electron density to the proton. Atom B should have a lone pair or polarizable π electrons in order to act as a hydrogen bond acceptor.[8] The strength of hydrogen bonds can vary significantly and can be divided into three broad categories: (i) while the stronger hydrogen bonds can be almost as strong as covalent bonds with bond energy in the order of 60–120 kJ mol^{-1}, (ii) the weaker hydrogen bonds have similar strength to van der Waals interactions,[1,8] with bond energies lower than ≈20 kJ mol^{-1},[1,9] (iii) and the moderate hydrogen bonds are somewhat similar to some electrostatic interactions, with a bond energy between 20-60 kJ mol^{-1}.[1]

The strength of a hydrogen bond interaction such as A-H···B can be basically influenced by three factors: (i) the distance between atoms A and H, (ii) the distance between atoms B and H, (iii) and the bond angle between A, H and B. It is well known that the shorter the distance between the proton and atoms A and B, the stronger the hydrogen bond will be. Hydrogen bonds are directional interactions, and will be stronger when the A-H···B angle is between 175–180°, making the bond more linear.[1,9] On the other hand, hydrogen bonds of moderate strength will be slightly bent with bond angles between approximately 130 and 180°, while weak hydrogen bonds can have angles between 90 and 150°.[1]

The hydrophobic Effect: This effect generally relates with the tendency of nonpolar substances to aggregate in aqueous solution where the water molecules are excluded, and it is important to explain a variety of phenomenon, such as the formation of micelles, the poor solubility of nonpolar solutes in aqueous solution and also protein folding.[10,11] As referred above, water interacts strongly with other water molecules due to hydrogen bonding, however these interactions are interrupted by the presence of a hydrophobic solute that occupies space and prevents the water to form hydrogen bond

with itself. Although water can also interact with the nonpolar solute, such as through van der Waals interactions and π– π stacking attractions, these interactions are generally weaker than the hydrogen bonding interactions occurring between water molecules.[6,3]

Regarding with supramolecular chemistry, the hydrophobic effects may be divided by the influence into the two thermodynamic parameters: the enthalpy and the entropy. The entropic hydrophobic effect arises from the release of water molecules due complexation of a nonpolar guest into the hydrophobic receptor site of a host molecule. This behavior is favorable since it results is an increase in the entropic term.[6] The enthalpic hydrophobic effect can be related to the fact that the release of water molecules from the host receptor, induces that these water molecules can be more readily to form hydrogen bonds with other water molecules in the solvent. Hosts such as cyclodextrins, cyclophanes and cucurbiturils bind guests largely due to the hydrophobic effect.[1,12]

Van der Waals Interactions: These interactions are well known by the intermolecular interactions between molecules that have an instantaneous dipole and an induced dipole, resulting in a weak electrostatic interaction. However, these interactions become important when they are observed between large numbers of molecules.[13,7] In supramolecular chemistry, this type of interactions are important in the complexation of small guests by hosts, since they are loosely included in the cavity of the macrocycle.[14] Depending on the distance between the atoms involved, generally these forces can be either attractive or repulsive. The dispersion (London) interactions are attractive from a distance and become more attractive as the molecules approach each other, but as the molecules become very close together, the interactions become repulsive due to repulsions between the electron clouds of the two molecules. The energy of interaction for van der Waals interactions is dependent on the distance, *r*, between the two atoms or molecules involved. In the case of dispersion interactions, the interaction energy decreases very rapidly with a dependence of r^{-6}.[7]

The π–π stacking interactions: These interactions occur between aromatic rings, , where one of the rings is relatively electron rich while the other is electron poor. These situation can be related with the planar rings that contain delocalized π electrons above and below the plane of the ring. The polarizable nature of the delocalized π-electrons present allows for dispersion interactions, which can be further enhanced by the

presence of softer, more polarizable nuclei in the rings. Moreover, the C-H bond is slightly polar ($C^{\delta-}$–$H^{\delta+}$), in the way that the π electrons near the carbon atoms have a slight negative charge while the outer edge of the aromatic group tends to be slightly electropositive. Generally the aromatic π–π stacking interactions can be considered as a combination of electrostatic and dispersion interactions.[15] The electrostatic component of π–π interactions involves a directional interaction, while the van der Waals component is considered to be a non-directional interaction. The most common arrangements between π-stacked aromatic rings are the face-to-face and edge-to-face arrangements, although a wide variety of intermediate geometries are known (Scheme 2).[16]

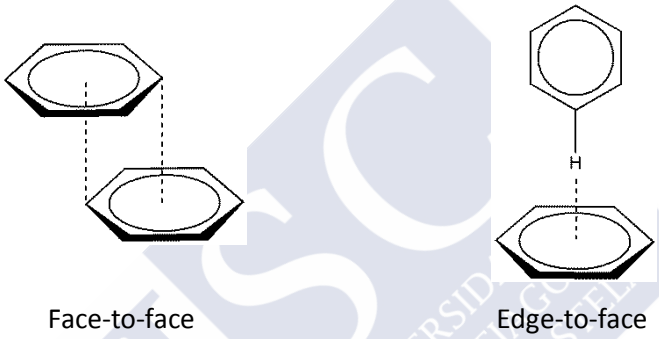

Scheme 2

In the face-to-face π-stacking interactions, the rings are parallel to each other but are offset from each other in order to allow oppositely charged regions of the molecules to align with each other. While in the edge-to-face arrangement, the slightly negatively charged π-electrons in one ring are attracted to the slightly positive hydrogen atoms on the edge (in the plane) of another ring, so that the two rings are arranged perpendicular to each other.

1.3. Complexes characterization

A large variety of techniques has been used to characterize the supramolecular systems. Depending on the system to study, techniques as nuclear magnetic resonance (NMR) spectroscopy, isothermal titration calorimetry (ITC), UV-visible spectroscopy, fluorescence spectroscopy and X-ray crystallography has been employed. These techniques can provide information about the binding constant, the stoichiometry of the host-guest system studied, and the location of the binding between the host and the guest within their relative structures. In the following section a brief description will be given with the main techniques used in this thesis (NMR and ITC).

Nuclear Magnetic Resonance (NMR) spectroscopy

This is perhaps the most versatile characterization tool available in studying supramolecular systems. The complexation of guests by hosts induced changes in the shielding of protons due the proximity between them, which generally results in changes of chemical shifts, $\Delta\delta$ values, of the protons of hosts and guests.[17,18] This can therefore provide information regarding the structural location of the guest inside of the host, since it may reveal which guest protons are encapsulated and which are not by the host. The appearances of the change of the host and guest proton resonances can vary depending if the exchange rate is fast or slow on the NMR timescale.[1,19,18] In the case of host-guest complexes, the interconversion between the "free" and the "bound" state for a particular nucleus is dependent on the frequency difference between the two states of the nucleus. If a nucleus' exchange between two states is faster than the frequency difference between the two states, the system is said to exhibit fast exchange behavior. On contrary, if a nucleus' exchange rate between the two states is slower than the difference in frequencies between the two states, the system is said to be a slow exchange system compared to the NMR timescale.[20,21] In the case of a fast exchange behavior, only a time averaged spectrum of the host-guest complex is observed, while for a slow exchange rate, both unbound and bound species can be seen in the spectrum. There is also a case where the host-guest exchange occurs on a time scale similar to the NMR timescale, which leads to a broadening of the species peaks.

The magnitude of the $\Delta\delta$ shifts observed change depending on the supramolecular system studied. As an example, guests encapsulated by cyclodextrin hosts reveal relatively modest shifts, while guests bound with calixarene hosts can have chemical

shifts in the order of 1-2 ppm. There are also macrocycles that can induced both positive and negative shifts in the guest. The complexation of guests by cucurbiturils displays upfield shifts up to 1 ppm when they are in the centre of the shielding cavity and downfield shifts when the protons are near the deshielding portals. Typically, since the protons are closer to the exterior of the molecules, ^{1}H is the nuclei more useful (then ^{13}C which is more deeply buried) for supramolecular systems.

Nowadays, NMR instruments are able to obtain good quality spectra with concentration of species as low as 10^{-4} M, enabling NMR to be suitable to determine binding constants up to 10^{6} M^{-1}.[18]

In addition to ^{1}H NMR experiments, Nuclear Overhauser Effect (NOE)-based experiments, such as the most common two-dimensional NOESY and ROESY, are frequently used. The NOE interactions are based on through-space interactions (via cross-relaxation) as opposed to through-bond interactions observed in NMR coupling. As a result, NOE experiments can be used to determine if protons from the host and guest come in close proximity, as would be the case in a host-guest interaction. The effect depends strongly on the internuclear distance *r*, in that the rate of transmission of the NOE is proportional to r^{-6}.[22]

Diffusion Ordered Spectroscopy (DOSY) experiments can also be used in supramolecular chemistry, since they provide a way to separate the different compounds in a mixture based on the differing translation diffusion coefficients.[23] Differences in the size and shape of the molecule, as well as physical properties of the surrounding environment such as viscosity, temperature, etc, influences the diffusion constant of each chemical species in the solution. In a simple way, it can be regarded as a special chromatographic method for physical component separation, but unlike those techniques, it maintains the innate chemical environment of the sample during analysis.

The measurement of diffusion is carried out by observing the attenuation of the NMR signals during a pulsed field gradient experiment. As can be seen in Figure 1, the peak on the left decays faster with increasing gradient strength and therefore will have a higher diffusion constant than the peak on the right.

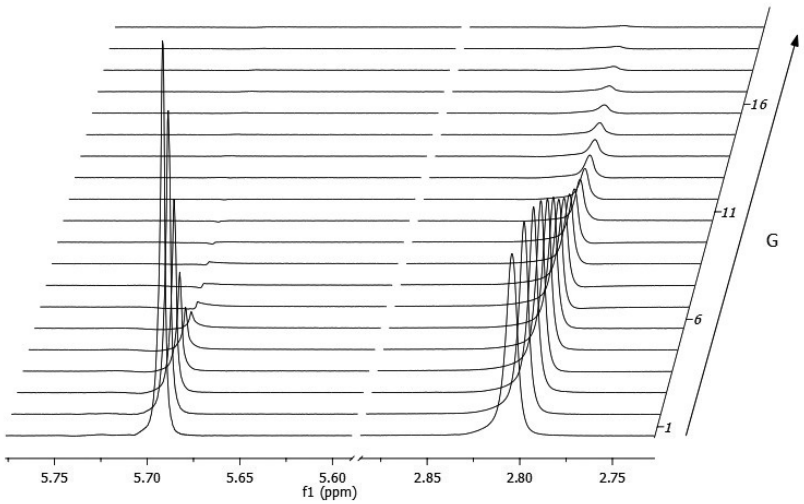

Figure 1. ^{1}H NMR diffusion experiment for a mixture of a host and a guest in D_2O.

Isothermal titration calorimetry

ITC which is a powerful technique in the study of biological systems, can also be used to study the interaction between macromolecule and guest molecules. With one experiment, we can obtain not only the binding constant for the complex formation, but also the full thermodynamic parameters using the relationships shown in eq 1.

$$\Delta G = -RT\ln K = \Delta H - T\Delta S \qquad (1)$$

In an ITC experiment, the host is usually placed in the sample cell, where it is titrated with a guest molecule placed in a syringe, and the binding affinity is determined by direct measurement of heat exchange with the environment. The successful extraction of thermodynamic parameters from the calorimetric data relies upon the use of nonlinear least squares curve fitting while employing an appropriate model that describes the interaction under study. The shape of the calorimetric curve can be related with the concentration of the macromolecule, [M], and the equilibrium constant, K, by the so-called Wiseman "c" parameter ($c = nK$[M], where n is the number of binding sites per receptor M) (Figure 2).[24]

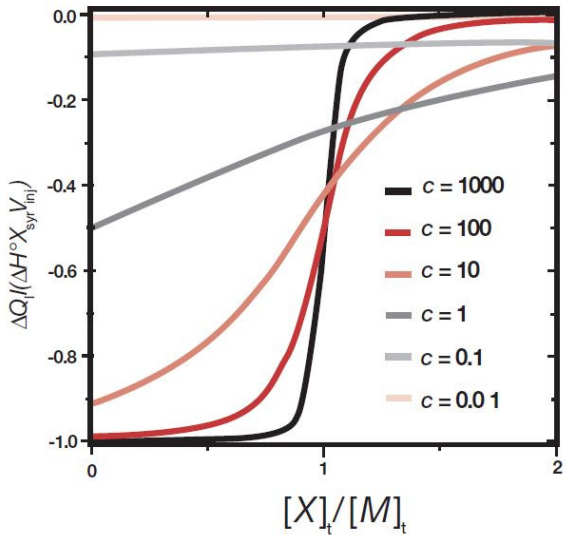

Figure 2. Traditional depiction of the Wiseman isotherm.[25]

At higher *c*-values, the curve is clearly sigmoidal, and allows the determination of the enthalpy, binding constant, but also the stoichiometry of the reaction, *n*. However, at lower c-values, the inflection point becomes poorly defined and the binding stoichiometry has to be fixed. This limitation arises from the strong correlation between ΔH° and *n* in the analysis of low-*c* data, which makes it difficult to determine both of these simultaneously.[26] Although there was some discussion in the past regarding the use of ITC to determine complex formation with low c-values, nowadays it is shown that the technique can be employed to determine high affinity but also low affinity systems.

1.4. Host-guest chemistry

Host-guest chemistry is a central topic in supramolecular chemistry and refers to the interaction of a receptor (host), with another molecule (guest). The interactions are usually based on the molecular recognition through non covalent interaction between the host and the guest molecules. Commonly the host is a large molecule possessing a cavity, while the guest can be a cation, anion, neutral species or more sophisticated molecules such as hormones or neurotransmitters. Regarding to the hosts, intensive research has been focused on the design and synthesis of macrocyclic receptors with specific properties and functions revealing their affinity and selectivity towards relevant molecules. After the first artificial host molecules discovered, the crown ethers,[27] other macrocycles were synthesized. Besides the artificial hosts there are also some natural

cyclic hosts, such as cyclodextrins. Scheme 3 shows the most common host molecules documented in the literature.

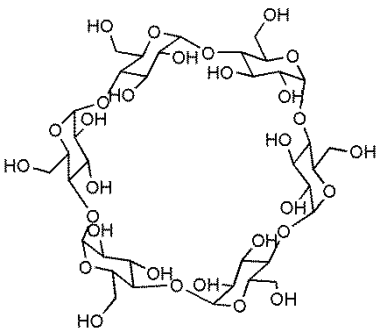
Cyclodextrin

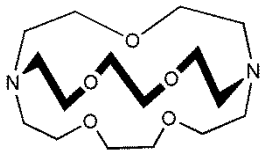
Cryptand

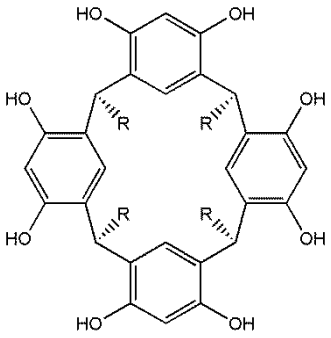
Resorcinarene

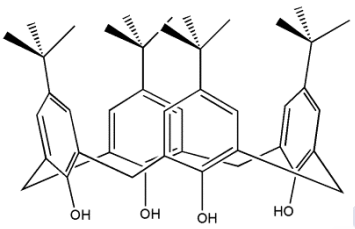
Calixarene

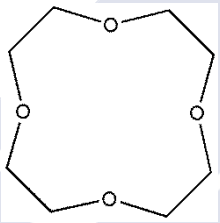
Crown ether

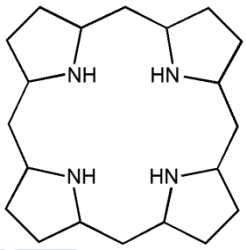
Porphyrin

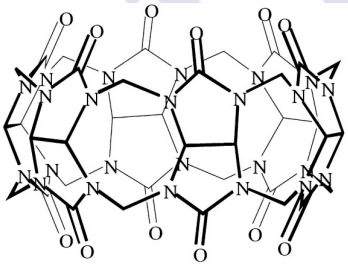
Cucurbituril

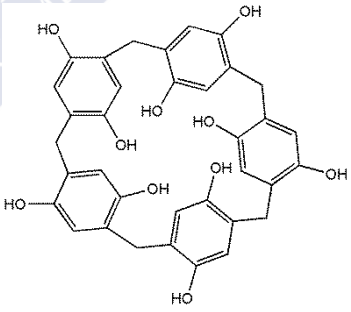
Pillararene

Scheme 3

As can be seen, there exists a large variety of macrocycles with different sizes, charge density, flexibility and functional groups, that possess molecular recognition capabilities. When a host (H) and a guest (G) form a complex, typically an equilibrium between the free and bounded state is observed, where the binding constant, $K = [HG]/[H][G]$, is a measure of the affinity of the guest by the host. In the case where more than one guest is involved, the selectivity between the two guests can be given by eq 2.[28]

$$\text{Selectivity} = \frac{K(\text{Guest1})}{K(\text{Guest2})} \qquad (2)$$

The selectivity and molecular recognition process can also be given by the enthalpic and entropic contributions to the overall free energy of binding, ΔG.

In host-guest chemistry, there are two main factors to determine the affinity between the host and the guest molecules: the preorganisation and the complementarity. Many host-guest complexes are more stable than expected due the traditionally termed *macrocyclic effect*.[29] This effect is related with the organisation of the host binding sites prior the guest complexation. Although this makes the elaboration of macrocycles more difficult, the energy gain obtained from the preorganisation makes them stronger complexing agents. As an example, the complexation of Cu(II) with the macrocyclic from scheme 4a is about 10^4 times more stable than the less organized analogue (Scheme 4b).[29]

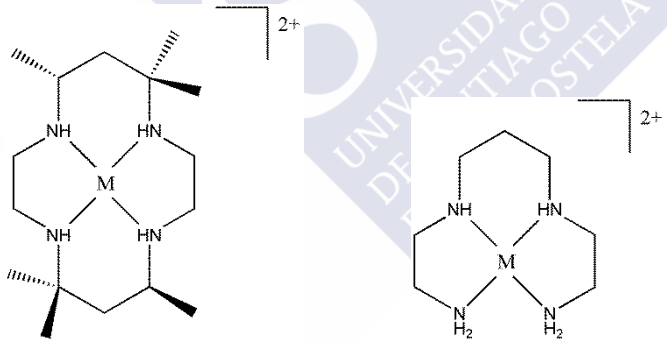

M = Cu^{2+}, Zn^{2+}

a **b**

Scheme 4

In thermodynamics terms, the well-organized macrocycle usually has less solvent-accessible surface area and therefore fewer solvent-ligand bonds to break, which contributes for the enthalpic term. For the entropic gain, it arises from the elaboration of more rigid macrocycles, which upon complexation with the guest lose less conformational freedom.

Although, the preorganisation is an important factor when synthesizing the macrocycle, the optimal stability of the host-guest complex is reached if the binding

sites between the host and the guest match each other. Crown ethers, a cyclic compound containing ethyleneoxy unit, are well known for their high affinity with certain cations. An influence of the repeating units of the macrocycle, and therefore the inner diameter, was studied in the complexation with K^+ cation.[3] As shown in Scheme 5, the crown ether with larger inner cores can accommodate better the cation then the smaller rings.

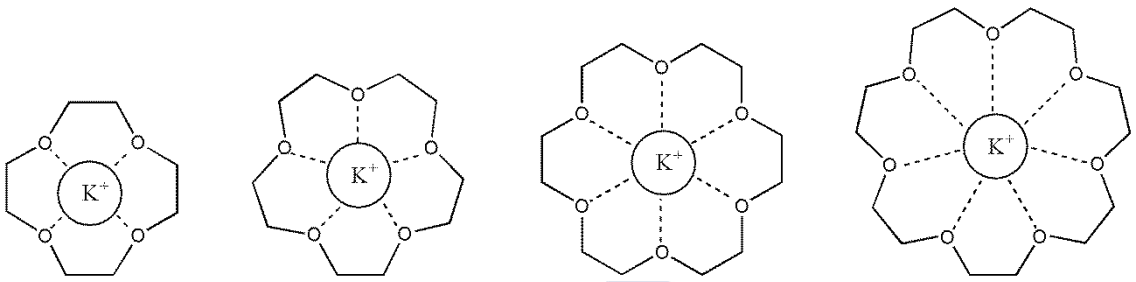

$K = 3.98 \times 10^1\ M^{-1}$ $K = 3.16 \times 10^3\ M^{-1}$ $K = 4.67 \times 10^5\ M^{-1}$ $K = 2.00 \times 10^4\ M^{-1}$

Scheme 5

Therefore, the complementarity between the guest size and the size of the macrocycle is critical to an efficient binding behavior. Moreover, the macrocyles can be functionalized with selected functional groups to increase their ability to complex specific guests. As mentioned above, there are several noncovalent forces that dominate the complexation of guests by hosts in supramolecular chemistry. This type of interactions are relatively weak when compared with the covalent bonds, which have typical bond energies higher than 200 kJ mol^{-1}. Although any single noncovalent bond is quite weak, several such bonds between the host and the guest can stabilize the host–guest complex. On the other hand, it is the magnitude of the noncovalent bonds energy, in the range from about 4 to 20 kJ mol^{-1} that is the key feature for the more reversible factor in the supramolecular chemistry.

This thesis is mainly concerned with the host-guest chemistry of calixarenes, although, studies with cucurbiturils and pillararenes were also performed. Therefore a general introduction of each macrocycle and host-guest complexation will be given in the following section.

1.4.1. Calixarenes

Calix[*n*]arenes are macrocyclic oligomers made of *n* phenol units linked by methylene bridges at the *ortho* position.[30,31] These compounds result from the condensation of *para*-substituted (usually *tert*-butyl groups) phenols with formaldehyde. Depending on the reaction conditions, calixarenes with four and/or up to 20 phenol units can be obtained,[32] though those with four, six and eight units are the most common (Scheme 6). The popularity of calixarenes in supramolecular chemistry can be attributed, at least partially, to their facile chemical functionalization. After removal of the *tert*-butyl groups from the calixarene framework using $AlCl_3$ in dry toluene, they can be readily and selectively functionalized at the hydroxyl groups (lower rim) and at the *para* positions (upper rim), owing to the different chemical reactivity of these groups.[31] Selective functionalization of the calixarene rims can be used to enhance their receptor ability and selectivity towards target guests or to develop sophisticated functional applications, such as rotaxanes and catenanes,[33–35] nanoparticles and monolayers,[36,37] sensors for enzyme assays,[38] drug delivery systems,[39] supramolecular polymers[40] and surfactants.[41]

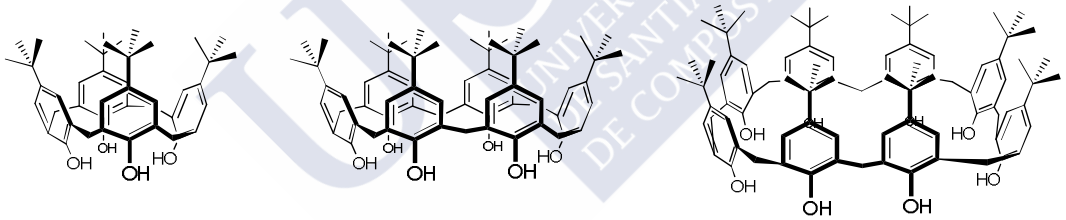

$n = 4$ $n = 6$ $n = 8$

Scheme 6. Structures of *tert*-butylcalix[*n*]arenes.

In addition to the diverse calixarene structures that can be devised by varying the size of the macrocycle and the nature of the substituents, their characteristic conformational isomerism can also contribute to further increase the diversity of functional molecules that can be constructed from the calixarene framework. While in Scheme 6 all three calixarenes are depicted in the so-called cone conformation, the phenol units can undergo rotation through the annulus, yielding other conformational isomers. In the case of calix[4]arene derivatives, four main conformations are possible: cone, partial cone, 1,2-alternate and 1,3-alternate (Scheme 7); while calix[6] and calix[8]arenes can display eight and sixteen main conformations, respectively.[30] It

should be noted that besides these "up-down" conformations, several others in which the aryl rings adopt planar orientations may be possible.

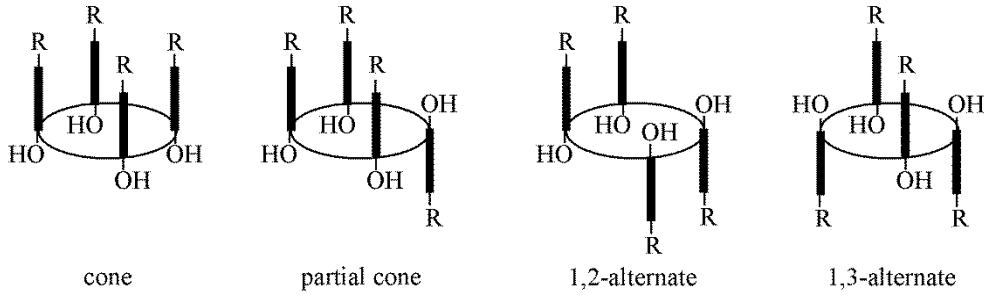

Scheme 7. Schematic representation of the four main conformations of calix[4]arenes.

Due the extremely versatile host framework and on their high degree of functionalization, a wide range of cations, anions and neutral molecules can be complexed by these macrocycles. Among the various types of calixarenes described in the literature, the water-soluble calixarenes functionalized with sulfonato groups in the upper rim are the most extensively studied. Moreover, the major part of this thesis has been performed on the sulfonatocalixarenes as hosts for host–guest complexation. Therefore, the following pages will briefly describe these host´s properties in host-guest chemistry.

p-sulfonatocalix[*n*]arene with four, six and eight monomer units are the most common derivatives studied in the literature (abbreviated as SC4, SC6 and SC8, respectively). These macrocycles were first synthesized by Shinkai[42,43] and can be obtained by three routes (Scheme 8), although the easiest is by direct *ipso*-sulfonation of the *p-tert*-butylcalix[*n*]arene.[44]

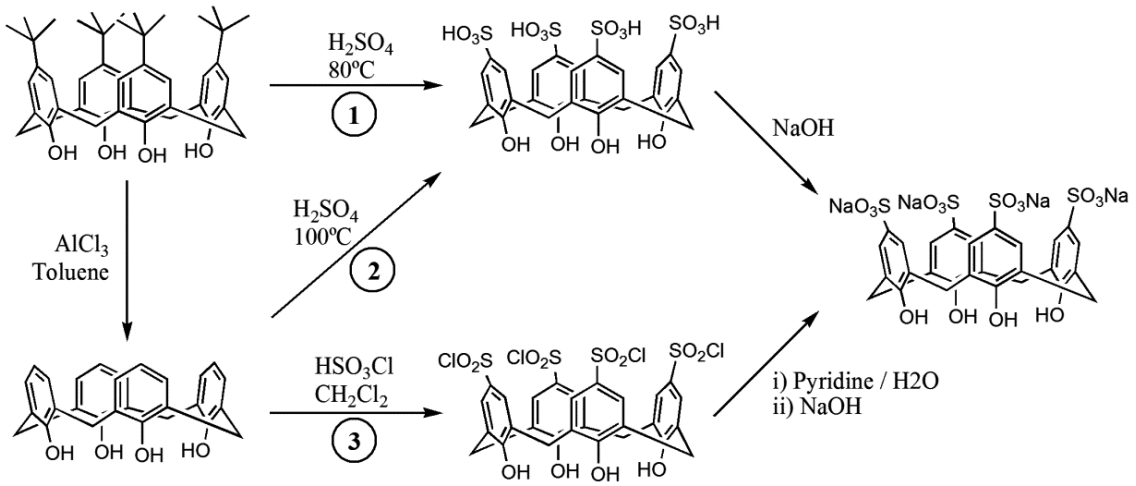

Scheme 8. Synthetic routes to obtain *p*-sulfonatocalix[4]arene. (1) Direct *ipso*-sulfonation, (2) *Ipso*-sulfonation, (3) *Chloro*-sulfonation.

In aqueous solution, the sulfonatocalixarenes are fully deprotonated at upper rim due the strongly acid groups, while at the lower rim the phenol groups are deprotonated according to the pH of the solution.[45] In comparison with the mononer *p*-hydrobenzenesulfonate (p$K_a \approx 9$), all three macrocycle have at least one phenolic group deprotonated, which can be related with the phenolate stabilization through intramolecular hydrogen bonds. The pK_a values obtained for the deprotonation of the common calixarenes are given in table 1.

Table 1. pK_a values for *p*-sulfonatocalix[*n*]arene (*n* = 4, 6, 8).[45]

p-sulfonatocalix[*n*]arene	pK_{a1}	pK_{a2}	pK_{a3}	pK_{a4}
4	3.28	11.5		
6	3.29	4.91	12.5	
8	3.44	4.26	7.78	10.3

In the literature, most of the experiments with these macrocycles are performed in acidic conditions (pH ≈ 2) or in neutral conditions (pH ≈7). This indicates that at lower pH only the sulfonato groups of the macrocycle will be deprotonated, while in neutral aqueous conditions, SC4, SC6 and SC8, have five, eight and ten negative charges, respectively. As mentioned above, the calixarenes can have different conformations and the sulfonatocalixarenes are not an exception. However, inside the homologues group, the SC4 has less possible conformations than the eight or sixteen conformations that the

SC6 and SC8 can have. In solid state, SC4 adopts a cone conformation,[46] while SC6 is found in a 1,2,3-alternated conformation,[47] but can adopt other conformations in the presence of guests.[48] The more flexible SC8 can be found in a *pleated loop*,[49] although resembling the SC6, can adopt various conformations in the presence of guests.[50] In solution, the same *cone* conformation can be found in SC4, which is stabilized by the intramolecular H-bonding among the hydroxyl groups.[47,51] However, due the higher flexibility in aqueous solution, a ring inversion between the two mirror-images of the *cone* conformation is observed, where the rate of conversion is influenced by the pH, and the presence of guest molecules(Scheme 9). Like SC4, SC6 also adopts the same conformation in solution as in the solid state, while SC8 can change between different possible conformations, although recently Kaliappan *et al.*[52] could arrest the macrocycle in a single conformation in solution by complexation with a guest.

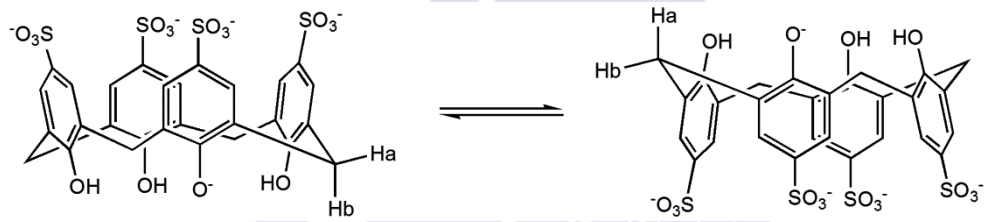

Scheme 9

Due the three dimensional π-rich cavity, flexibility and additional anchoring points offered by the charged sulfonate groups, the host-guest chemistry of the *p*-sulfonatocalixarenes has been extensively studied. The complexation of inorganic cations, a wide range of organic ammonium cations, neutral molecules, dye molecules, among other guests were studied by different groups at different conditions.[53] The binding affinities and the thermodynamics parameters were reported for the various guests with the three homologues, however, in most cases the counterion of the macrocycles has been neglected. As it will be addressed in chapter 2 of this thesis, the counterion has an important role in the host–guest complexation since it influences binding affinity and the thermodynamic parameters. Therefore a comparison between different guests from the same group can be misleading, however, the binding manners of inclusion of some guests will be described below.

From the three homologues, the sulfonatocalixarenes with four units are the most extensively investigated due to their preferred cone shape, and in particular with the

class of organic ammonium cations. Shinkai *et al.* studied the complexation of trimethylanilinium cation (TMA) by the three homologues.[54] The authors found that SC4 and SC6 formed 1:1 complexes with the guest, while SC8 can complex two molecules of the guest. They also found that TMA is complexed by SC4 and SC8 without regioselectivity (Scheme 10a), but selectivity included in the calixarene cavity by the ammonium group with SC6 (Scheme 10b). Due to the more efficient electrostatic interactions between the guest and SC4 or hydrophobic interactions when the host is SC8, the binding constant for the complexation of the guest by the two macrocycles is higher than the intermediary SC6.

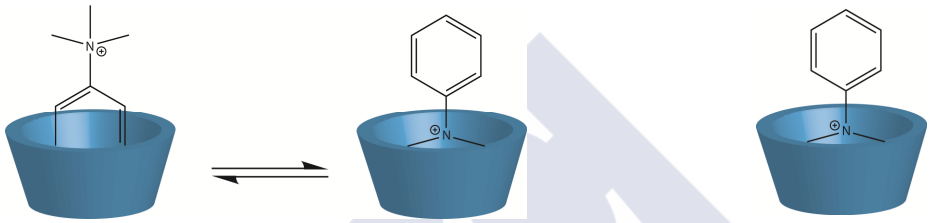

a **b**

Scheme 10

Although the cavity size of the calixarene influences the affinity towards the guests, the flexibility of the host also affects the binding abilities. Arena *et al.*studied the complexation of TMA with some other hosts blocked in the cone conformation.[55] From the results the authors concluded that the induced fit recognition is often more efficient than the complexation of guests by more pre-organized hosts.

As mentioned above, the complexation of neutral guests by the sulfonatocalixarenes was also investigated. Most of the guests studied form 1:1 inclusion complexes with the smaller SC4, although with low binding affinities (K < 100 M^{-1}).[56] An exception is, for example, the complexation of bicyclic azoalkane guests, with a binding constant for the complex formation one order of magnitude higher.[57] This behavior can be related with a better accommodation/complementarity of the guest by the host cavity. Moreover, the binding affinity of the bicyclic azoalkanes guests by SC4 is pH-dependent, since the protonated guest in acidic conditions (pD = 2.4) has a higher binding constant than the neutral species (pD = 7.4). This is in contrast with the increase of the binding constant with increasing the pH as observed for other guests.[58] However, while the latter is related with the first deprotonation of the phenolic hydroxyl of SC4 (pK_a = 3.28), which by producing the phenolate ion became better

electron-donating and promotes the cation–π interactions; the first is a result of the pK_a shifts observed when the guest molecules are complexed by the host. The enhancement of the binding constant are specially observed when the guests are very weak bases with pK_a values near 1.5. Since the observed increase of pK_a is in the order of 2 units, this allows the guest to be protonated when complexed with the host. The pK_a perturbation is not only observed with calixarenes, but also with other hosts, such as cyclodextrins and cucurbiturils. However, while calixarenes and cucurbiturils induced an increment in pK_a, the opposite is observed with cyclodextrins.[59]

The proposed mechanism to determine the p$K_a^{\prime}$ value of a complexed guest molecule is showed in Scheme 11.

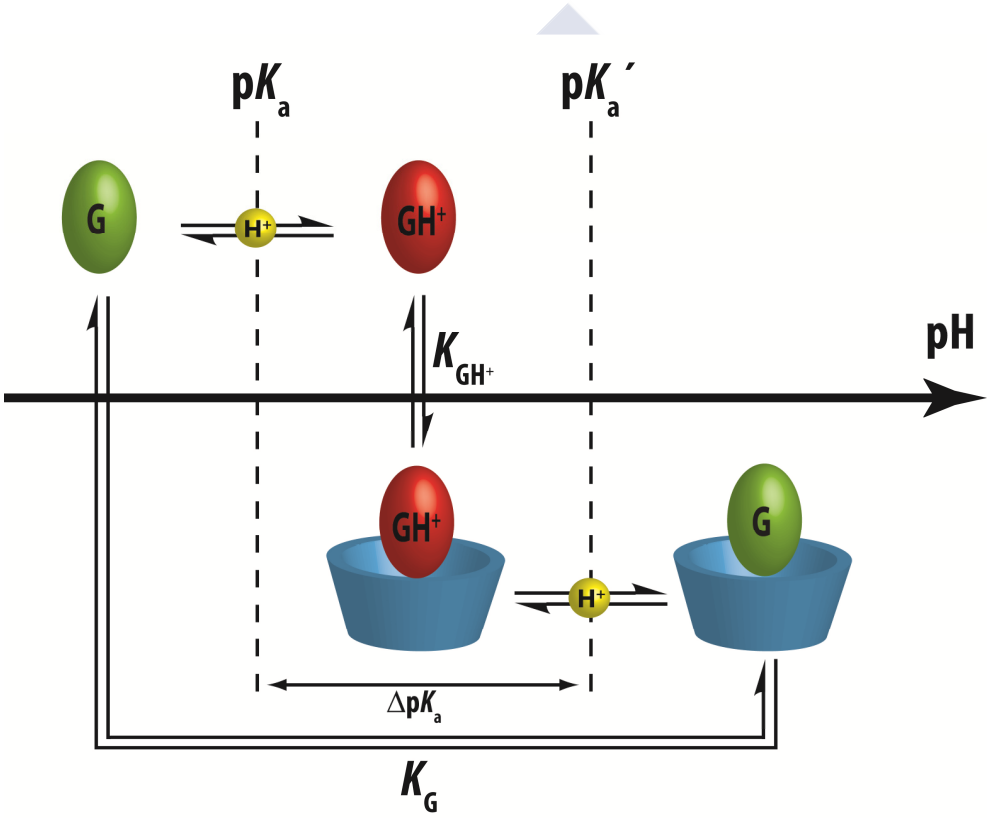

Scheme 11

This model involves a four-state species: the uncomplexed unprotonated and protonated guest, and the guest inside the cavity of the macrocycle in the unprotonated and protonated form state. The relation between the four equilibrium can be given by eq 3.

$$\frac{K_{\mathrm{GH}^+}}{K_G} = \frac{K_a}{K_a^{\prime}} \qquad (3)$$

Since the observation that enzymes modulate the pK_a values of residues of substrates, with shifts up to 5 units, the complexation-induced pK_a shifts of guest molecules approach has been used by Nau and coworkers to increase the solubility and stability of drug molecules.[39]

1.4.2. Cucurbiturils

Cucurbiturils are another family of macrocyclic compounds, which owes its name due the resemblance of the molecular shape with a pumpkin. They are self-assembled from an acid-catalyzed condensation reaction of glycoluril and formaldeyde. The most common derivative and the first one synthesized was the cucurbit[6]uril (CB[6]), which is based on six units of glycoluril enlaced by methylene groups. Although its synthesis was first reported in 1905 by Behrend and coworkers, its chemical nature and structure were unknown before the full characterization was reported by Mock.[60]In comparison with other macrocycles where the size of the macrocycle can be tuned by the number of repeating units, other homologues were isolated and characterized. The synthetic protocol of CB[*n*] homologues is similar to the conventional CB[6] synthesis, being the reaction temperature the key to obtain the homologues. As shown in Scheme 12, while CB[6] is obtained at temperatures higher than 110 °C, to obtain from cucurbit[5]uril to cucurbit[11]uril the temperature range is between 75 and 90 °C and using a milder acid concentration.[61]

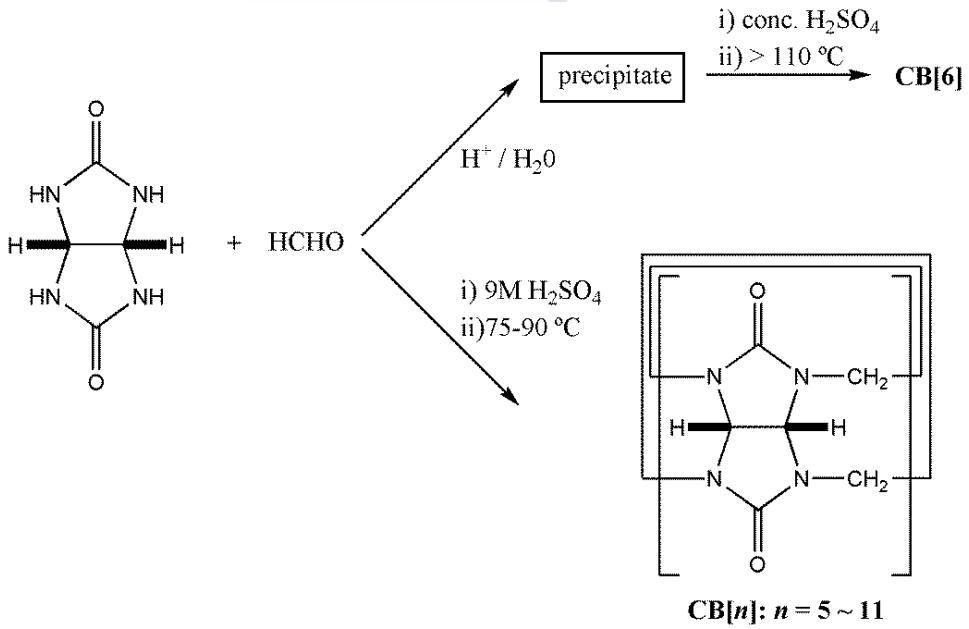

Scheme 12

The cavity size of the CB[*n*] varies with the value of *n*, where *n* refers to the number of glycoluril monomers per cucurbituril. However, it is not only the size cavity of the macrocycle that changes with *n*, but also their water solubility, guest affinity and binding stoichiometry. The cucurbiturils containing an odd number, such as CB[5] and CB[7], have better solubility in water than those composed of even numbers of units. Regarding with the change in the guest affinity and binding stoichiometry by changing the number of monomers (*n*), that is in accordance with the behavior observed with other macrocycles.

Frequently, the cucurbiturils are compared with other very well studied macrocycle, the cyclodextrins. In fact, these two receptor share some characteristics, such as size, shape and hydrophobic cavity. Table 2 shows a comparative of the cavity dimensions of cyclodextrins and cucurbiturils macrocycles.[62,63]

Table 2. Comparative of the cavity dimensions of cyclodextrins and cucurbiturils macrocycles.[62,63]

Dimensions (Å)	Monomer Units [*n*]	Cyclodextrin	Cucurbituril
Portal Diameter	6	4.7	3.9
	7	6.0	5.4
	8	7.5	6.9
Interior Cavity Diameter	6	5.3	5.8
	7	6.5	7.3
	8	8.3	8.8
Height	6–8	9.1	7.9
Cavity Volume	6	174	164
	7	262	279
	8	427	479

However, while cucurbiturils possess a symmetrical structure with two portals rims composed by ureido carbonyl groups, the cyclodextrins have a less symmetric geometry which allows to distinguishes the two macrocycles.

As observed in the case of other macrocycles, there are several different types of intermolecular interactions that promote the complexation of guests by cucurbiturils.

For example, while the hydrophobic interior provides a potential inclusion site for nonpolar molecules, the portals allow the complexation of molecules through charge-dipole and hydrogen bonding interactions. The hydrophobic effect can be related with the fact that frequently the complexation of guests by cucurbiturils are performed in aqueous solution.

Cucurbiturils are efficient host molecules and have a particularly high affinity for positively charged or cationic compounds. It was after the isolation of the different homologues that has increased the popularity of cucurbiturils as hosts. One of the guest groups well studied with the first member of the cucurbiturils to be synthesized, CB[6], were the diaminoalkanes and their ammonium mono– and di–cations. Diaminoalkanes thread themselves through the cavity of CB[6], until the aminogroups lie level with the oxygen ringed portals, resulting in a pseudorotaxane complex.[64] A few years later, Kim and coworkers were able to forming a rotaxane with CB[6], when a spermine was threaded though the cucurbituril and both ends of the guest were subsequently capped with 2,4–dinitrophenyl groups.

The complexation of CB[6] with fluorescent dyes has also been reported. For example, Li *et al*. studied the interaction of two alkaloid dyes with the cucurbituril by spectrofluometry.[65,66] They found a 1:1 host–guest stable complex with binding constants up to 10^4 M^{-1}, which is the same order of magnitude found for the other cucurbituril homologues. By the significant enhancement of the fluorescence intensity upon complexation with the host, they proposed a method for the determination of the alkaloids in urine and serum samples.

As mentioned above, the solubility of cucurbiturils with even number of glycoluril units are poor, which is the case of CB[6], although in the presence of alkali metals tend to improve significantly. This behavior was observed after the complexation of various alkali and alkaline earth metals.[67] Moreover with alkali cations such as sodium, it is possible to bind CB[6] with an organic guest, where the cations can cap one or both portals of the cucurbituril (Scheme 13).[68] However, this process can be reversible, since when a influence of the pH was studied, it is observed a change in the signals of the organic guest. Nau and coworkers, also reported that the presence of alkali ions in the host–guest complexation can have important effects on the binding constants, as well as their complexation ratio.[69]

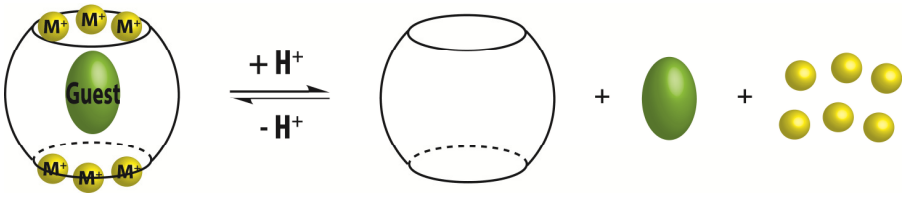

Scheme 13

Since the synthesis of other homologues of CB[*n*], one that become very popular is the CB[7]. This attractiveness became not only from the wider cavity that can accommodate other guests, but also due the increase in solubility when compared with CB[6]. Despite the difference in size, CB[7] is capable of binding neutral guests due to its hydrophobic cavity as well as cationic guest through electrostatic interactions with its portals. A wide range of cationic guests, from small ions such as alkali metal to larger polyciclic aromatic dyes, have been studied with CB[7] by different methods. As an example, the methylviologen guest has been well studied. With this guest, Kaifer and coworker were able to study the influence of salt in the binding affinity of CB[7].[70] When the concentration of salt in aqueous solution is increased, this leads to a decrease in the binding constant for the complexation of the methylviologen guest by the macrocycle, due a competitive binding. Years later, with this approach, Nau and coworkers proposed a useful method to induce the release of a guest, such as a drug, from the CB[7] cavity.[71] Again with methylviologen, Kaifer[72] but also Kim and coworkers,[73] evidence the importance of electrostatic interactions in the strengthening the binding of the guest with the electron rich portals. By changing the charge of the guest from double to singly charged, the binding constant decrease about two times. However, a higher decrease was observed for further reduction of the methylviologen to its neutral form. By comparison with a similar macrocycle with almost the size, β-CD, the inverse trend was observed.[73]

CB[7] has also been used for the complexation of a wide range of biological molecules. Host–guest complexes with anti-cancer drugs, such as albendazole[74] or camptothecin,[75] or other relevant guests, such as histamine H_2-receptor antagonist ranitidine,[76] have been reported. Remarkably high binding constants can be observed for the complexation of some guests. Affinities higher than 10^{10} M^{-1} can be found in the complexation of ferrocene and adamantane by CB[7].[77]

Fluorescent dyes are a class of guests that have been extensively studied with cucurbiturils. Since these type of guests are sensitive with the surrounding environment,

they are used to monitor the polarity of the media, such as the cases of supramolecular aggregates, but also studies in host-guest chemistry. Upon the complexation of the dye by the macrocycle, the microenvironmental parameters experiments a large change, which have been used to determine binding and rate constants, but also to perform displacement experiments. A lot of effort has been devoted by Nau and coworkers using CB[7] and fluorescent dyes as a novel approach towards enzyme assays.[78] The so called "supramolecular tandem assay" is based on the reversible and competitive binding of a dye and the substrate as well as the product of an enzymatic reaction to a macrocyclic host (Scheme 14).[38] In this way, the fluorescent dye, Dapoxyl, was used to monitor the conversion of a weak competitor, the amino acid, into a strong competitor, the product of the enzymatic decarboxylation of the amino acid. Therefore, the strong competitor formed will leads to a successive displacement of the dye, which have different fluorescence signal between its free and complexed form.[79] In this way the dye has to be carefully chosen, since it must have a binding constant higher than the weak competitor, but lower than the product of the enzymatic reaction.

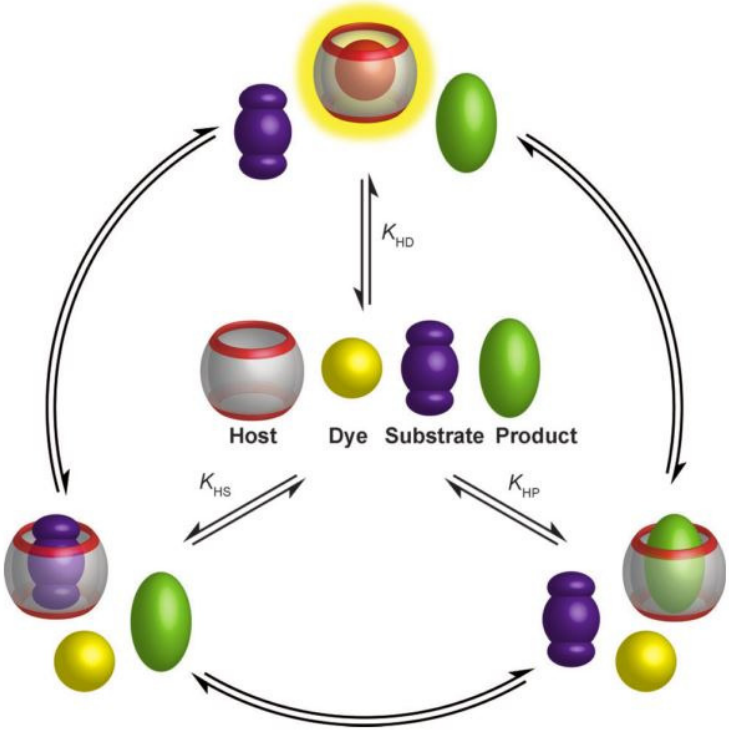

Scheme 14. Binding scheme for the equilibria involved in a supramolecular tandem assay.[38]

Another cucurbituril homologue that has been widely employed in host–guest chemistry is the CB[8]. An important feature of this homologue which differentiates from the other smaller cucurbiturils, is the ability to accommodate two guests simultaneously (although CB[7] can also complex some guests simultaneously, CB[8] is able with a wider variety of guests).[80–82] This feature is important in the way that CB[8] can act as a reaction vessel, with the reaction that occur inside the cavity depending if the two guest are identical (homo-guest pair) or different (hetero-guest pair). Homo-guest pairs such as viologen[80] or napthalene derivatives,[61] or hetero-guest pairs such as one viologen and one napthalene derivatives can be included in the CB[8] cavity. Biedermann *et al.* reported for the first time the existence of charge-transfer interactions between a variety of donor-acceptor pairs in the presence of CB[8] (Scheme 15).[83] However, the authors claim that the driven force for the formation of the ternary complex are electrostatic and solvation effects rather than charge-transfer phenomena.

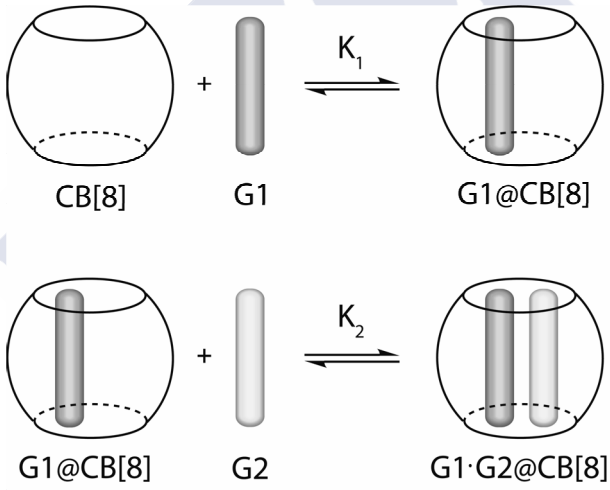

Scheme 15

In comparison with CB[7], where the charge of the methylviologen guest influences the binding constant, with CB[8] the charge of the guest influences the stoichiometry of the complex.[80] While the dicationic form of the guest favours the formation of a 1:1 complex, a ternary complex with two methylviologen incorporated in the CB[8] cavity is formed when the guest is in the monocationic form.

As conclusion of the host–guest chemistry of cucurbiturils, it is the electrostatic interaction (ion–dipole) between the host and the guest molecules, due the two carbonyl portals, and hydrophobic effect derived from the cavity nature of CB[*n*], that drives the inclusion of guests by the macrocycle. Recently, it was also demonstrated that the

formation of the host-guest complex involves the displacement of high-energy water molecules from the host cavity, which constitutes also an essential driving force in the complexation of guests by cucurbiturils.[84]

1.4.3. Pillararenes

Pillararenes were the last macrocycles to be incorporated in the host panorama. In contrast to the wide range of cyclooligomers *meta*-bridged, such as the already discussed calixarenes, very little is known about the *para*-bridge analogues. It was in 2008, when Ogoshi and coworkers describe the first route to synthesize these symmetrical pillar-shape macrocycles.[85] These analogues were initially obtained by condensation of 1,4-dimethoxybenzene with paraformaldehyde and an appropriate Lewis acid as a catalyst, $BF_3 \cdot O(C_2H_5)_2$. However, the yield for the formation of cyclic pentamer 1,4-dimethoxypillar[5]arene (DMpillar[5]arene) was 22 %, in which was also found a large amount of polymer. This is not an ideal synthesis, especially if the macrocycle want to be used in large scale. Therefore further experiments were performed to increase the reaction yield. This was obtained by increasing the amount of paraformaldehyde in relation to 1,4-dimethoxybenzene (3:1 equiv). As a results, DMpillar[5]arene was sucessfully obtained in a short time and with a high yield (71%), and then pillar[5]arene (R = H) almost in quantitative yield (route 1).[86] Nowadays, two more routes to obtain the macrocycle and homologues with different hydroquinone units can be employed (Scheme 16).

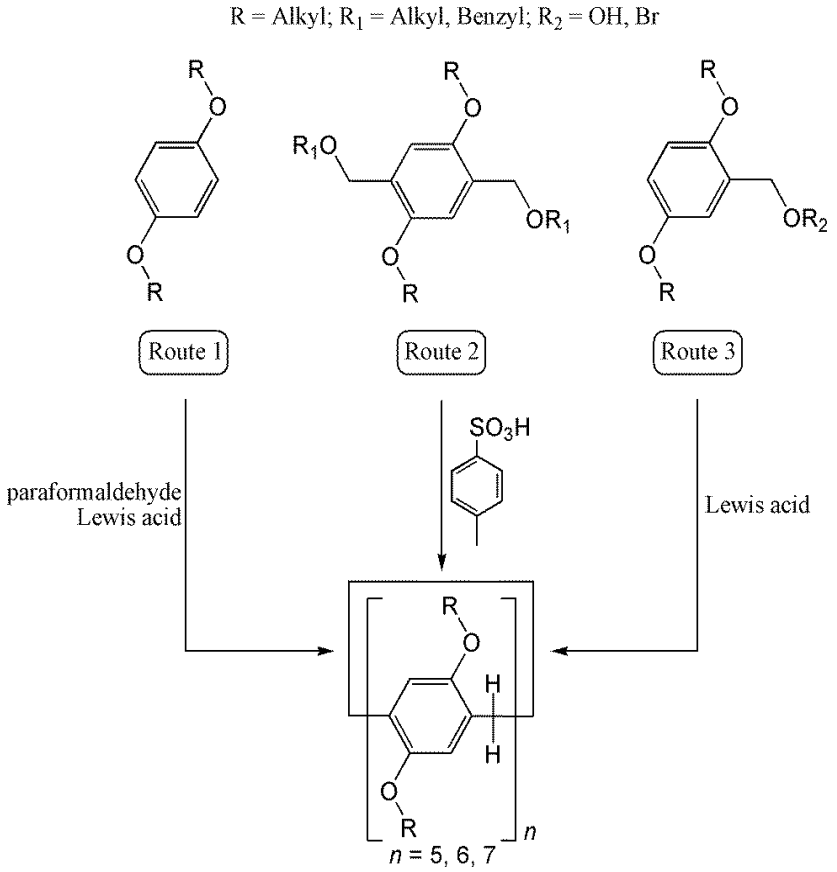

Scheme 16

Route 2, proposed by Cao and coworkers, consists in the condensation of 1,4-dialkoxy-2,5-bis(alkoxymethyl)benzene catalysed by *p*-toluenesulfonic acid. By this way, the authors were able to synthesize perfunctionalized pillar[5]arenes with R = Me, Et or *n*Bu with yields higher than 86 %, but pillar[6]arenes with R = Et or *n*Bu with a lower yield (<11 %).[87] However, two years later the same group were able to increase the yield to 35–45% and also with quantitative yields, the perhydroxylated pillar[*n*]arenes (*n* = 5, 6), ideal to obtain a wide range of perfunctionalize macrocycle derivatives.[88] The third strategy consists in the reaction of 2,5-dialkoxybenzyl alcohols or bromides with an appropriate Lewis acid as catalyst.[89]

As demonstrated above with the other two macrocycles discussed, the size of the macrocycle is an important characteristic in host-guest chemistry. In Table 3 are reported the calculated structural parameters for the perpropylated pillar[*n*]arenes (*n* = 5, 6, 7, R = C_3H_7) based on van der Waals radii of the atoms.[90]

Table 3. Cavity dimensions of perpropylated pillar[5]arene.[90]

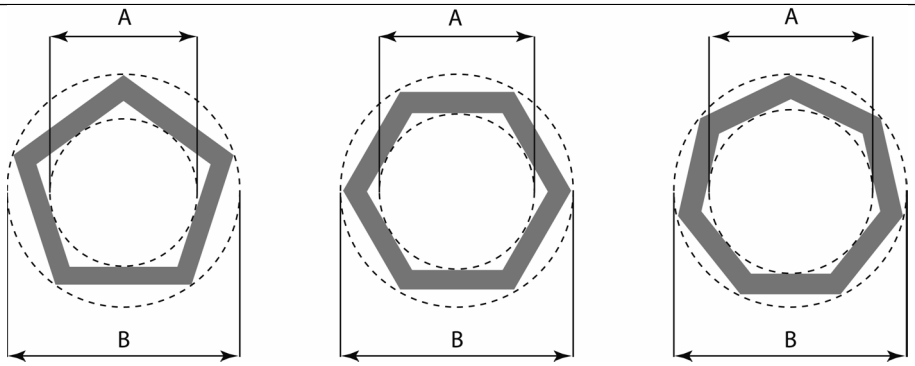

Pillar[*n*]arene	(A) Interior Cavity Diameter (Å)	(B) Portal Diameter (Å)	Cavity Volume (Å)
5	4.7	13.5	152
6	6.7	15.2	302
7	8.7	16.9	493

As can be seen in Table 3, by comparing with Table 2, cyclopentameric pillar[5]arenes are similar in terms of size with CB[6] and α-CD, while pillar[6]arenes and pillar[7]arenes can be compared with cucurbiturils and cyclodextrins with seven and eight monomer units, respectively. However, in terms of functionalization, the pillararenes can be compared with calixaranes, since both macrocycles are easily functionalized. Also, in the case of pillar[5]arene (R = H), by analogy with calix[4]arenes, can have various conformation, such as pillar-shape (*cone*) with all rings in the same orientation, partial pillar-shape (*partial cone*) where one ring is inverted, *1,2-alternative* and *1,3-alternative*, with two adjacent or non-adjacent rings inverted, respectively.[91]

Rapidly, pillar[5]arenes (R = mehtyl, ethyl, propyl, n-alkyl) and other perfunctionalized pillararenes showed molecular recognition of guests in organic solvents, such as neutral alkanediamines,[92,93] dinitriles,[94] dihaloalkane derivatives[95] as well as charged secondary ammonium salts,[96] alkyl ammonium salts,[97] among other guests. Also mono-guest-functionalized pillararenes were synthesized, which can form self-inclusion complex by changing the apolar solvent from acetone to chloroform (Scheme 17).[98]

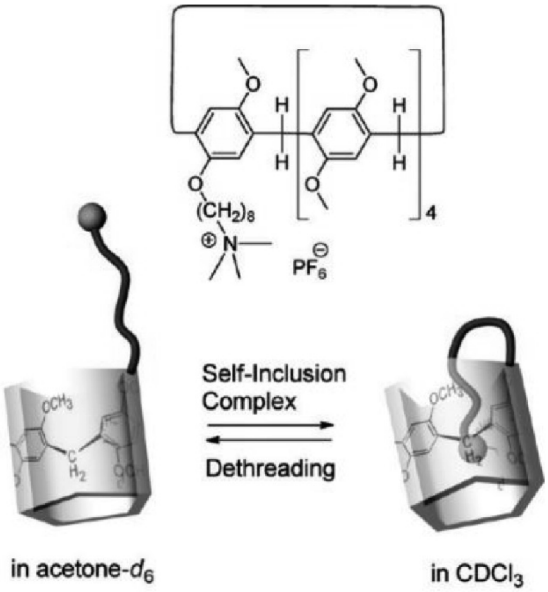

Scheme 17. Structural change of a mono-guest-functionalized pillar[5]arene observed in different organic medium.[98]

Although to a lesser extent, pillar[6]arenes were also studied in non aqueous solutions. As an example, a azobenzane-containing guest could be accommodated by the perpropylated pillar[6]arene to form a [2]pseudorotaxane, while the homologue pillar[5]arene cannot complex the guest. Moreover, the threading/dethreading switch of the guest from the host cavity induced by photoirradiation can lead to the formation of vesicle-like aggregates.[99]

In addition to pillararenes that were studied in organic media due the poor solubility in water, water-soluble pillararenes were also synthesized. In this case, also the pentamer host was investigated more extensively than the hexamer. Several guest, such as neutral[100] or charged molecules[101,102] could be complexed by the π-rich cavity or/and the charged portals of the host. Huang and coworkers reported the complexation of methylviologen by a percarboxylated pillar[6]arene.[103] By the formation of a very stable 1:1 [2]pseudorotaxane ($K = 1.02 \times 10^8$ M^{-1}), the authors were able to reduce the guest toxicity, due to the difficulty to generate its radical cation. The dicationic methylviologen was also studied by other homologues. In the case of percaboxylatedpillar[5]arene, it was observed that the binding constant decrease about 10^3 times,[104] while with perhydroxylated pillar[5]arene it was observed the formation of 2:1 external complexes.[105] Due the versatile and facile modifications of these recently

synthesized macrocycles, a bright future can be expected, with a large variety of potential applications.

In this brief introduction of host–guest chemistry, three types of macrocycles were showed. The calixarenes, which are characterized by their flexibility and facile modification, the more rigid cucurbiturils that are better known for their electro rich portals and the pillararenes which joint the facile modification of the analogues calixarenes with the rigid architecture of the cucurbiturils. With only these three macrocycles a wide variety of guest can be complex. Due the homologues with different number of monomer units, small guests as well as large guests, charged or non-charged, can be complexed with the proper macrocycle in order to maximize the binding affinity.

1.5. Supramolecular aggregates

As described above, *p*-sulfonatocalix[*n*]arenes (SCn) had attracted considerable attention due to their high water solubility, selective binding ability, catalytic properties and apparent biological compatibility.[53,106] In fact, several biological and medical potential applications that take advantage of the SCn properties have been described.[107] In addition to these interesting properties, *p*-sulfonatocalix[*n*]arenes can also be used as amphiphiles (or surfactants) that are able to self-assemble into well-defined nanostructures, such as micelles, when placed in aqueous solution. *p*-sulfonatocalixarene-based amphiphiles can be simply obtained by attaching hydrophobic alkyl chains to the phenolic oxygen atoms. These compounds can be, in principle, included in the same category of oligomeric surfactants (such as gemini dimeric, trimeric and tetrameric surfactants).[108,109] Besides sharing some of the appellative properties of open chain oligomeric surfactant, such as lower critical micelle concentration (CMC), calixarene-based surfactants are equipped with a host-guest recognition site, able to bind guest molecules and ions, which can be explored along with their self-association properties in order to develop new soft materials.

In addition to the synthesis of SCn-based surfactants by using irreversible covalent bonds, the recognition properties of SCn enable them to be also used as building blocks to construct supramolecular amphiphiles (or supra-amphiphiles). In these cases, the functional segments required to provide or improve the amphiphilic properties of the molecular species are linked by means of non-covalent interactions.[110] These

amphiphiles can be classified by the type of complex formed between the independent molecular species that are involved in their composition. In that sense, supra-amphiphiles comprising calixarenes or other macrocyclic receptors, such as cucurbiturils and cyclodextrins, can be placed in the host-guest category. In addition to host-guest complexes, charge-transfer, hydrogen bonded, ionic or coordination complexes, among others, with amphiphilic properties have been described and recently reviewed.[110]

The supramolecular approach is not only effective, but also capable of making the synthetic process simpler and highly reversible when compared with covalently bonded systems. The reversibility is in fact a key feature of these systems, since it allows the assembly process to be controlled by external stimuli and, thus, enables supra-amphiphiles to be applied as smart materials. In this section, it is provided an overview of the work published on the aggregation of SCn-based amphiphiles and supra-amphiphiles.

1.5.1. Amphiphilic sulfonatocalixarenes: structure-aggregation relationships

The first example of calixarenes with surface active properties was reported by Shinkai *et al.* back in 1986.[42,43] In this pioneering work, the authors described the synthesis of *p*-sulfonatocalix[6]arenes bearing alkyl chains at the lower rim. These compounds were obtained by sulfonation of the parent calix[6]arene with H_2SO_4, followed by neutralization and alkylation with alkyl halides in basic media (Scheme 18). It was found that compound **1b** forms small spherical micelles at a concentration above the CMC = 0.6 mM, with an aggregation number (*N*) of six or 19 unimers per micelle if determined by light scattering or estimated from the solubilization test of orange OT (1-(*o*-Tolylazo)-2-naphthol), respectively. On the other hand, for the **1c** derivative, some unexpected properties, such as the absence of a clear CMC, surface inactivity, *N* values of about two and formation of 1:1 host guest complexes with small dye molecules were reported. Based on these results, it was proposed that **1c** rather acts as a "unimolecular" micelle. A small angle x-ray scattering study of these compounds afforded values of *N* for **1b** compatible with that previously reported by Shinkai *et al.*, but the results obtained for **1c** are substantially different.[111] Specifically, the authors reported very high *N* values ranging from 84 to 217, depending on the concentration and on the assumptions

made for the estimation of this parameter. Nevertheless, these results are obviously inconsistent with the proposed unimolecular micelle.

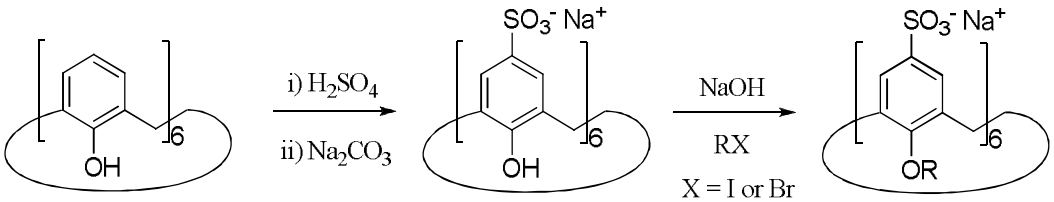

1a R = CH_3
1b R = C_6H_{13}
1c R = $C_{12}H_{25}$

Scheme 18. Synthesis of alkylated *p*-sulfonatocalix[6]arenes.

To complement their work on the self-assembly of amphiphilic sulfonatocalixarenes, the Shinkai group synthesized a new collection of derivatives (Scheme 19) and discussed possible structure-aggregation relationships.[112,113] Based on the ^{1}H NMR pattern of signals, it was possible to verify that the calix[4]arenes derivatives (**2a**, **2g** and **2j**) adopt a fixed cone conformation, while all amphiphilic calix[6]arenes and calix[8]arenes studied exchange between several possible conformations, due to the unhindered rotation of the phenolic units through the annulus.

2a	n = 4; R = C_4H_9	2d	n = 6; R = C_4H_9	2g	n = 4; R = H	2j	n = 4; R = *tert*-butyl
2b	n = 6; R = C_4H_9	2e	n = 6; R = C_6H_{13}	2h	n = 6; R = H	2k	n = 6; R = *tert*-butyl
2c	n = 8; R = C_4H_9	2f	n = 6; R = $C_{12}H_{25}$	2i	n = 8; R = H	2l	n = 8; R = *tert*-butyl

(**a**) (**b**)

Scheme 19. Amphiphilic sulfonatocalix[*n*]arenes bearing the hydrophilic SO_3^- group at the (a) upper rim and (b) lower rim.

The CMC's of these series of compounds were determined by conductance and surface tension measurements. The results obtained allowed the authors to propose a classification based on the aggregation properties of these types of calixarene derivatives. Accordingly, calixarenes that do not bear long alkyl chains (e.g., **1a**, **2g–i**)

do not form micelles and, thus, are classified as (i) nonmicellar calixarenes. On the other hand, calixarenes with moderate alkyl chain lengths (e.g., **1b**, **2a**–**e** and **2j**–**l**) self-assemble into micelles and are classified as (ii) micelle-forming calixarenes, while those with long alkyl chains (e.g., **1c** and **2f**) were placed in the category of (iii) unimolecular micelle calixarenes.

It was also observed that the ^{1}H NMR chemicals shifts for some protons of **2a** are displaced to a higher magnetic field when the concentration is increased above the CMC.[113] It was reported that the signals corresponding to the *endo* protons of the methylene bridge and to the OCH_2 protons of the alkyl chains were particularly affected, while, on the other hand, those corresponding to the aromatic protons hardly changed. By considering these observations, a model was proposed for the micellar aggregates in which the alkyl chains form the micellar core and the aromatic rings form stacks at the surface of the micelle. Results obtained from fluorescence polarization experiments suggested that the microviscosity of the calixarene-based micelles is generally higher than that of conventional surfactant micelles.

1.5.2. Conformational reorganization upon micellization

After the seminal work conducted by the Shinkai research group on the synthesis and aggregation of amphiphilic *p*-sulfonatocalix[*n*]arenes, these molecules have been sporadically revisited by several researchers, however, none of these works were focused on the aggregation properties of this special class of surfactants. Recently, our group has decided to undertake a systematic study on the self-assembly of such amphiphiles.[114–116] The work motivation was related to some physical characteristics of the micellar systems formed from calixarene-based surfactants, such as slow unimer-micelle exchange rates and low CMC's, which are not fully understood.[114]

In the first instance, it was decided to investigate the micellization of three calix[4]arene derivatives with alkyl chains of different lengths at the lower rim together with a calix[6]arene and a calix[8]arene, both bearing alkyl chains of the same length (hexyl) at the lower rim (Scheme 20).

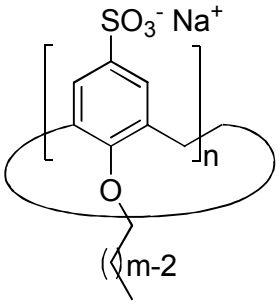

3a n = 4, m = 4
3b n = 4, m = 6
3c n = 4, m = 8
3d n = 6, m = 6
3e n = 8, m = 6

Scheme 20

With these five compounds, it is possible to establish correlations between the micellization properties with both the alkyl chain length and the number of phenolic units present in the macrocyclic ring (*i.e.*, the ring size). While all three calix[4]arene-based surfactants (**3a**–**c**) were found to be, as expected, blocked into the cone conformation, the hexamer **3d** adopts a pseudo-1,2,3-alternate conformation at concentrations below the CMC (Scheme 21). It must be noted that **3d** is not physically blocked into this conformation, but stabilized, presumably, by hydrophobic intramolecular interactions.[115] On the other hand, the octamer **3e** seems to present a loose structure, and its ^{1}H NMR spectra indicates that, below the CMC, the molecule undergoes fast exchange between several possible conformers.

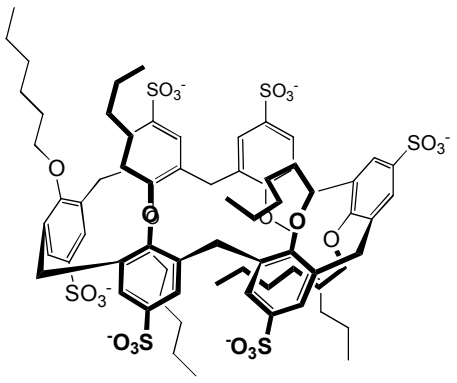

Scheme 21

By increasing the concentration of amphiphilic *p*-sulfonatocalix[*n*]arenes to values above the CMC, it was observed that these surfactants can undergo a structural reorganization upon aggregation to adopt the cone conformation in the micelles

(Scheme 22). This conformational change, induced by the aggregation process, demonstrates that the cone conformation is stabilized in the micelles. This result was expected, since in the micelles, the alkyl chains should point to the hydrophobic interior, while the sulfonate groups remain in contact with the solvent.[115] In the same article, it was also reported that the micelle diffusion coefficients obtained from diffusion ordered NMR spectroscopy (DOSY) experiments. From these results, it was suggested that the micellar assemblies formed from amphiphilic *p*-sulfonatocalix[*n*]arenes well above the CMC adopt ellipsoidal, rather than spherical, geometries.

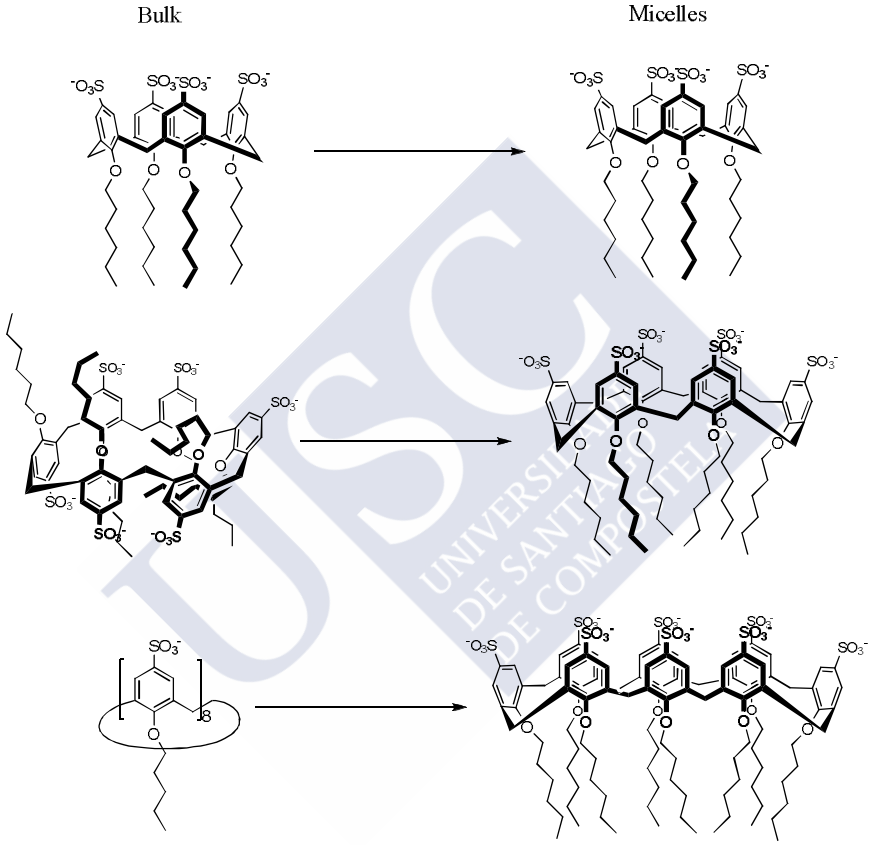

Scheme 22

1.5.3. *p*-Sulfonatocalixarene-based supramolecular amphiphiles

Among the various water soluble calixarenes, sulfonatocalixarenes have been more frequently employed in the last few years in building self-assembled nanostructures based on noncovalent interactions (Scheme 23). Our group reported for the first time the formation of micelles from the complexation of a single chain surfactant with calixarene derivatives in aqueous solution.[117] In that work, besides the formation of an expected host-guest complex between the alkyltrimethylammonium cation (**G1**) and the hexamethylated *p*-sulfonatocalix[6]arene (**4a**), the onset for the formation of micellar aggregates was observed to occur at concentration 70-fold below

the CMC of the pure surfactant, suggesting that the calixarene promotes the formation of micelles. The system was characterized by a wide variety of techniques, including NMR, surface tension and dynamic light scattering. The results indicate that for concentrations below the critical aggregation concentration (CAC), the calixarene **4a** forms a discrete 1:1 host-guest complex with **G1** that further aggregates into mixed micelles upon increasing the concentration of surfactant **G1** (Scheme 24). Saturation transfer difference NMR experiments point out that the ion-dipole interactions established between the OMe pendant groups of the host and the NMe_3^+ group of the surfactant play a significant role in stabilization of supramolecular amphiphile.[118]

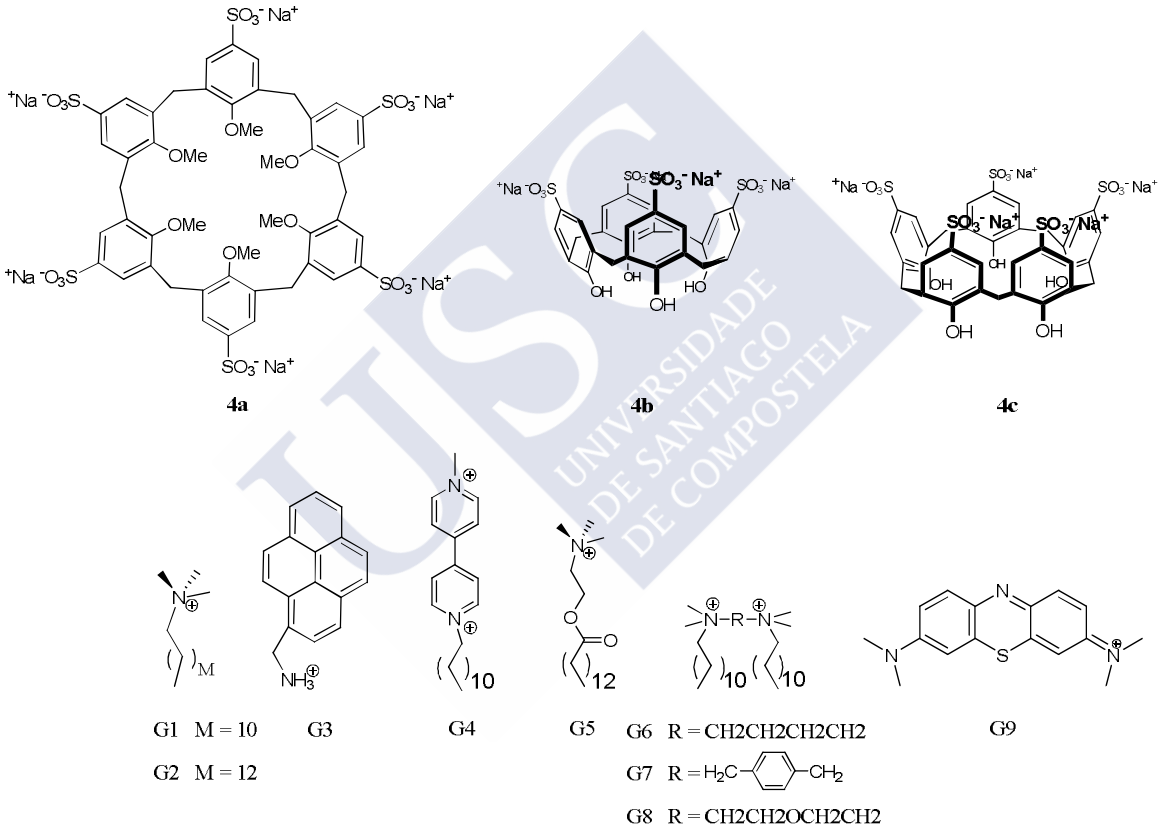

Scheme 23. Structures of *p*-sulfonatocalixarene hosts and cationic guests used for the assembly of supramolecular amphiphiles.

On the other hand, when the single chain surfactant is in the presence of a smaller and preorganized calixarene, such as *p*-sulfonatocalix[4]arene (**4b**), the formation of vesicles in aqueous solution was observed.[119] The unilamellar vesicles built from the complex formed between **G2** and host **4b** have, after sonication, a diameter of around 120 nm with the potential of being stored by lyophilization and then rehydrated without significant change in size or shape. While there are several host-guest complexes made

from **4b** and cationic species that display a bilayer-type arrangement in the solid state, the structure and composition of the vesicle bilayer remains unknown.[107] The critical packing parameter (CPP) is frequently invoked to predict the shape and type of aggregates formed from amphiphilic species.[120,121] The CPP can be defined as $V_H/l_c a_0$, where V_H is the volume occupied by the hydrophobic groups in the micellar core, l_c is its length and a_0 is the cross-sectional area occupied by the hydrophilic group at the micelle-solution interface. This parameter is a measure of the curvature at the aggregate-solution interface, and it can be used to predict the shape of the micelles based in the structure of the surfactant. For example, spherical micelles have CPP values below 1/3, rod-like micelles between 1/3 and 1/2 and lamellar structures are usually formed when CPP values are between 1/2 and 1.[122] On the basis of these considerations, it is important to remark that the formation of vesicles cannot be explained by a 1:1 complex, since, in this case, the a_0 parameter is expected to substantially increase, while V_H and l_c are subject to smaller variations. This will lead to a decrease in the CPP of the supramolecular amphiphile in comparison with the free surfactant guest, and thus, micelles should be formed. In order to explain the formation of vesicles, a high order 1:*n* calixarene:surfactant complex must be taken into account. In this case, V_H is multiplied by *n*, and thus, the CPP can conveniently increase to values higher than 1/2. Moreover, the charge neutralization of high-order complexes can also contribute to reduce the curvature of the interface between the hydrophilic and hydrophobic domains and, consequently, favor the formation of vesicles. In addition to the fact that the CPP model can fail in the prediction of vesicular structures for conventional surfactants, its application to SCn-based supra-amphiphiles presents serious limitations, due to the fact that the structure and composition of the complex or complexes are not currently known.[121]

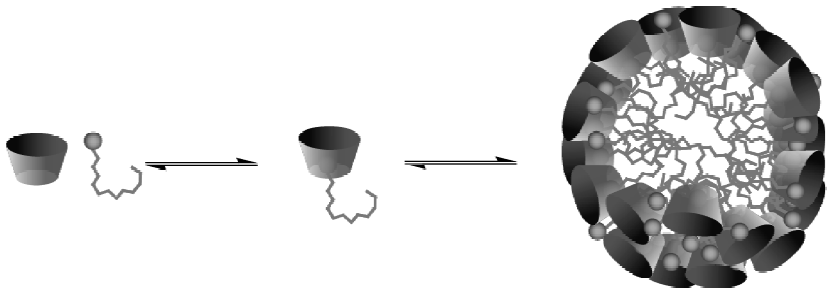

Scheme 24. Promoted aggregation of alkyltrimethylammonium surfactants through the formation of host-guest complexes with calix[6]arene **4a**.[118]

In the last two years, Liu and coworkers had made important contributions to the study of supramolecular binary vesicles assembled from host-guest complexes. In their published works, *p*-sulfonatocalixarene **4b** and **4c** were used as hosts, while molecules **G3**–**G8** were employed as guest.[123–126] In the first report, *p*-sulfonatocalix[5]arene (**4c**) and 1-pyrenemethylaminium (**G3**) were used to construct the vesicular assembly. The aggregation process can be followed by monitoring the polarity-dependent fluorescence spectra of the pyrene moiety. By performing this task in absence and presence of the calixarene, the authors determined the best molar fraction of the complex with the tendency toward self-aggregation.[125] The best mixing ratio for amphiphilic aggregation is when the calixarene **4c** is in the presence of four **G3** molecules, otherwise increasing the amount of calixarene leads to the formation of 1:1 inclusion complexes, accompanied by the disassembly of the amphiphilic aggregation (Scheme 25). The authors proposed a model for the unilamellar membrane, where the pyrene segments are stacked together and the inner- and outer-layer surfaces consist of hydrophilic phenolic hydroxyl groups of **4c** exposed to water.[125] This model is also depicted in Scheme 25.

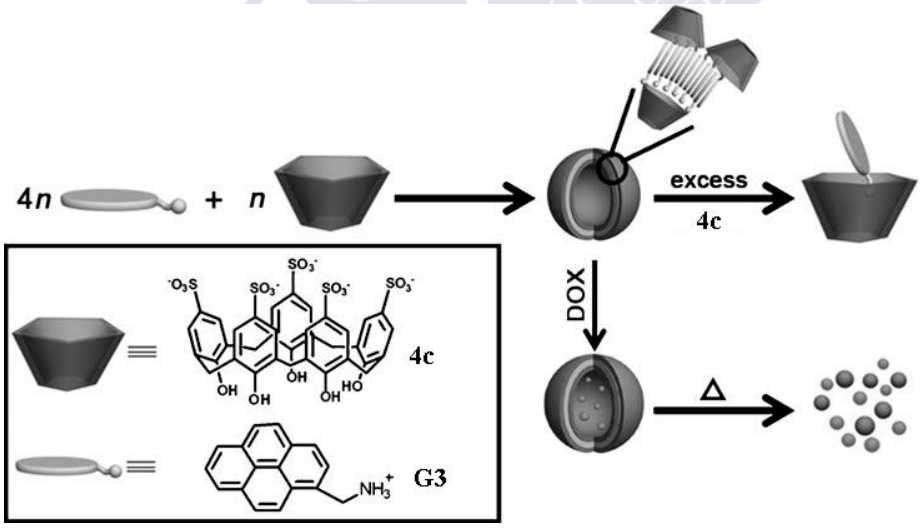

Scheme 25. Formation of supramolecular binary vesicles made from pyrene derivative **G3** and calixarene **4c**.[125]

Further development of this system was described in posterior reports. In the case of **4b** and 1-meth-yl-1'-dodecyl-4,4'-bipyridinium (**G4**), a value for **4b/G4** molar ratio of 0.5 was found to be the ideal for amphiphilic aggregation, while in the case of **4b** and gemini surfactants (**G6**–**G8**), a value of 0.4 was determined.[124–126] On the other hand, for the binary system composed by **4b** and myristoylcholine (**G5**), the results indicate

that a molar ratio of 0.1 should be used.[123] Similarly to the first report, increasing the concentration of calixarene affords a simple 1:1 inclusion complex between **4b** and the guests. The CAC's were also measured for the three guests in the presence and absence of calixarene **4b**. The most interesting feature was observed for the guests **G4** and **G6**–**G8** with a decrease of almost *ca.* 1000 in the CAC value after complexation by the host. For **G5** and **G3**, a decrease of 100- and 3-times were observed, respectively. It should be noted that **4b**, as well as **4c**, do not have any tendency to self-aggregation.[127] To obtain further evidences on the self-assembled morphology of this type of aggregate, the same common techniques in the study of other classes of vesicles are employed. Dynamic laser scattering (DLS), cryo-Transmission Electron Microscopy (Cryo-TEM), Scanning Electron Microscopy (SEM) and Atomic Force Microscopy (AFM) represent the first evidence of vesicle formation in the systems, undoubtedly proving the presence of an inner hollow sphere surrounded by a bilayer or a multilayer.[128]

The self-assembly process is defined in the literature as the spontaneous organization of individual components into an ordered structure.[129] The possible control over the characteristics of the components of these aggregates, as well as the interactions among them, makes fundamental investigations in this kind of structures especially tractable. Frequently, stimuli, such as pH, temperature, voltage, redox and light, are employed as a way to have control over the structure and enhance the possibility of using this kind of aggregate as a potential delivery model for special substrates.[130–135] The group of Liu and coworkers also study responsiveness of the binary supramolecular vesicles upon external stimuli. The aggregates formed by **4c** and **G3** can be assembled and disassembled with the variation of temperature.[125] The reason for these behaviors can be explained based on taking into account the type of complexation of the guest by the host and also by the π-π stacking of the guest, which are both enthalpy-driven and, therefore, can be weakened upon heating.[53,136,137] The process of disassembly of the aggregate was also confirmed by loading the vesicles with the doxorubicin hydrochloride (DOX) fluorescence dye, which is released upon increase of the temperature (Scheme 25).

Regarding the binary vesicles of **4b** and **G4**, the structure can respond to multiple external stimuli, such as temperature, host-guest competitive binding and redox.[124] Like in the previous report, by increasing the temperature, the aggregates can be disassembled into free **4b**, free **G4** and complex **4b:G4**. Control of the architecture can also be achieved by adding another macrocycle to the aqueous solution where vesicles

are present. Through the addition of α-, β- and γ-cyclodextrins, the disassembly of the vesicles was confirmed by the absence of Tyndall effect of the solution and also by DLS experiments. This behavior can be explained, since the alkyl chain moiety of the **G4** can form complexes with cyclodextrin and then disrupt the host-guest complex that forms vesicles. Additional experiments to have control of the aggregates were obtained by adding hydrazine and, therefore, changing the state of the guest. The size of the vesicles is smaller when **G4** is reduced from the dication state to the cation, and finally, the aggregate is disrupted in the neutral form of the guest. The self-assembly vesicles constructed with **4b** and **G5** can be controlled by cholinesterase, which induces the disassembly of the vesicles, since it is a specific enzyme to cleave the guest molecules.[123] With this approach, the authors were able to release the entrapped drugs inside the vesicles.

Colloidal aggregates were also obtained from the binary complex formed between methylene blue (**G9**) and SCn. The presence of such aggregates was demonstrated by resonance Rayleigh scattering measurements, where the presence of a band around 560 nm appears in the spectra of **G9** in the presence of three different hosts.[138] The most fascinating aspect of these supramolecular amphiphiles is that two components can self-assemble into higher-order structures, which exhibit particular properties and functions that the individual components cannot achieve.

1.6. References

1. J. W. Steed and J. L. Atwood, *Supramolecular Chemistry*, John Wiley & Sons, Ltd, Chichester, 2nd Editio., 2009.

2. J.-M. Lehn, *Supramolecular Chemistry: Concepts and Perspectives*, VCH, Weinheim, 1995.

3. K. Ariga and T. Kunitake, *Supramolecular Chemistry – Fundamentals and Applications*, Springer, Berlin, 2006.

4. G. V. Oshovsky, D. N. Reinhoudt, and W. Verboom, *Angew. Chem. Int. Ed.*, 2007, **46**, 2366–2393.

5. P. J. Cragg, *Supramolecular Chemistry: From Biological Inspiration to Biomedical Applications*, Springer, New York, 2010.

6. P. D. Beer, P. A. Gale, and D. K. Smith, *Supramolecular Chemistry*, Oxford University Press, Oxford, 2003.

7. P. S. Murthy, *J. Chem. Ed.em. Ed.*, 2006, **83**, 1010–1013.

8. G. A. Jeffrey, *An introduction to Hydrogen Bonding*, Oxford University Press, New York, 1997.

9. G. R. Desiraju, in *Encyclopedia of Supramolecular Chemistry*, Marcel Dekker, New York, 2004, pp. 658–665.

10. D. Chandler, *Nature*, 2005, **437**, 640–647.

11. E. E. Meyer, K. J. Rosenberg, and J. Israelachvili, *Proc. Nat. Acad. Sci. U.S.A.*, 2006, **103**, 15739–15746.

12. H.-J. Schneider, in *Encyclopedia of Supramolecular Chemistry*, 2004, pp. 673–678.

13. G. R. Desiraju, *Nature*, 2001, **412**, 397–400.

14. G. D. Andreetti, *J. Chem. Soc., Chem. Commun.*, 1979, 1005–1007.

15. C. A. Hunter, *Chem. Soc. Rev.*, 1994, **23**, 101–109.

16. C. A. Hunter, K. R. Lawson, J. Perkins, and C. J. Urch, *J. Chem. Soc., Perkin Trans. 2*, 2001, 651–669.

17. H.-J. Schneider and A. K. Yatsimirsky, *Principles and Methods in Supramolecular Chemistry*, John Wiley & Sons, Ltd, Chichester, 2000.

18. P. Thordarson, *Chem. Soc. Rev.*, 2011, **40**, 1305–1323.

19. L. Fielding, *Tetrahedron*, 2000, **56**, 6151–6170.

20. J. K. M. Sanders and B. K. Hunter, *Modern NMR Spectroscopy. A Guide for Chemists*, Oxford University Press, Oxford, 1988.

21. K. A. Connors, *Binding Constants. The Measurement of Complex Stability*, John Wiley & Sons, Ltd, New York, 1987.

22. M. P. Williamson, *Mod. Magn. Reson.*, 2006, 409–412.

23. P. S. Pregosin, P. G. A. Kumar, and I. Fernández, *Chem. Rev.*, 2005, **105**, 2977–2998.

24. T. Wiseman, S. Williston, J. F. Brandts, and L.-N. Lin, *Anal. Biochem*, 1989, **179**, 131–137.

25. W. B. Turnbull and A. H. Daranas, *J. Am. Chem. Soc.*, 2003, **125**, 14859–14866.

26. J. Tellinghuisen, *J. Phys. Chem. B*, 2005, **109**, 20027–20035.

27. C. J. Pedersen, *J. Am. Chem. Soc.*, 1967, **89**, 7017–7036.

28. H.-J. Schneider and A. K. Yatsimirsky, *Chem. Soc. Rev.*, 2008, **37**, 263–277.

29. D. K. Cabbiness and D. W. Margerum, *J. Am. Chem. Soc.*, 1969, **91**, 6540–6541.

30. A. Ikeda and S. Shinkai, *Chem. Rev.*, 1997, **97**, 1713–1734.

31. V. Bohmer, *Angew. Chem. Int. Ed.*, 1995, **34**, 713–745.

32. D. R. Stewart and C. D. Gutsche, *J. Am. Chem. Soc.*, 1999, **121**, 4136–4146.

33. C. Talotta, C. Gaeta, T. Pierro, and P. Neri, *Org. Lett.*, 2011, **13**, 2098–2101.

34. A. V. Leontiev, C. A. Jemmett, and P. D. Beer, *Chem. Eur. J.*, 2011, **17**, 816–825.

35. T. Pierro, C. Gaeta, C. Talotta, A. Casapullo, and P. Neri, *Org. Lett.*, 2011, **13**, 2650–2653.

36. H. J. Kim, M. H. Lee, L. Mutihac, J. Vicens, and J. S. Kim, *Chem. Soc. Rev.*, 2012, **41**, 1173–1190.

37. A. Wei, *Chem. Commun.*, 2006, 1581–1591.

38. R. N. Dsouza, A. Hennig, and W. M. Nau, *Chem. Eur. J.*, 2012, **18**, 3444–3459.

39. I. Ghosh and W. M. Nau, *Adv. Drug Deliv. Rev.*, 2012, **64**, 764–783.

40. D.-S. Guo and Y. Liu, *Chem. Soc. Rev.*, 2012, **41**, 5907–5921.

41. K. Helttunen and P. Shahgaldian, *New J. Chem.*, 2010, **34**, 2704–2714.

42. S. Shinkai, S. Mori, T. Tsubaki, T. Sone, and O. Manabe, *Tetrahedron Lett.*, 1984, **25**, 5315–5318.

43. S. Shinkai, S. Mori, H. Koreishi, T. Tsubaki, and O. Manabe, *J. Am. Chem. Soc.*, 1986, **108**, 2409–2416.

44. R. Lamartine, J.-B. Regnouf-de-Vains, P. Choquar, and A. Marcillac, 1997.

45. K. Suga, T. Ohzono, M. Negishi, and K. Deuchi, *Supramol. Sci.*, 1998, **5**, 9–14.

46. S. Shinkai, K. Araki, T. Matsuda, N. Nishiyama, H. Ikeda, I. Takasu, and M. Iwamoto, *J. Am. Chem. Soc.*, 1990, **112**, 9053–9058.

47. S. Shinkai, K. Araki, M. Kubota, T. Arimura, and T. Matsuda, *J. Org. Chem.*, 1991, **56**, 295–300.

48. S. J. Dalgarno, M. J. Hardie, M. Makha, and C. L. Raston, *Chem. Eur. J.*, 2003, **9**, 2834–2839.

49. S. J. Dalgarno, M. J. Hardie, J. L. Atwood, J. E. Warren, and C. L. Raston, *New J. Chem.*, 2005, **29**, 649–652.

50. F. Perret, V. Bonnard, O. Danylyuk, K. Suwinska, and A. W. Coleman, *New J. Chem.*, 2006, **30**, 987–990.

51. Y. Israëli and C. Detellier, *Phys. Chem. Chem. Phys.*, 2004, **6**, 1253–1257.

52. R. Kaliappan, Y. Ling, A. E. Kaifer, and V. Ramamurthy, *Langmuir*, 2009, **25**, 8982–8992.

53. D.-S. Guo, K. Wang, and Y. Liu, *J. Incl. Phenom. Macrocycl. Chem.*, 2008, **62**, 1–21.

54. O. M. Seiji Shinkai, Koji Araki, *J. Am. Chem. Soc.*, 1988, 7214–7215.

55. G. Arena, A. Casnati, A. Contino, F. G. Gulino, D. Sciotto, and R. Ungaro, *J. Chem. Soc., Perkin Trans. 2*, 2000, 419–423.

56. N. Kon, N. Iki, and S. Miyano, *Org. Biomol. Chem.*, 2003, **1**, 751–755.

57. H. Bakirci, A. L. Koner, and W. M. Nau, *J. Org. Chem.*, 2005, **70**, 9960–9966.

58. H. Bakirci and W. M. Nau, *Adv. Funct. Mater.*, 2006, **16**, 237–242.

59. X. Zhang, G. Gramlich, X. Wang, and W. M. Nau, *J. Am. Chem. Soc.*, 2002, **124**, 254–263.

60. W. A. Freeman, W. L. Mock, and N.-Y. Shih, *J. Am. Chem. Soc.*, 1981, **103**, 7367–7368.

61. J. Kim, I. Jung, S. Kim, E. Lee, J. Kang, S. Sakamoto, K. Yamaguchi, and K. Kim, *J. Am. Chem. Soc.*, 2000, **122**, 540–541.

62. J. W. Lee, S. Samal, N. Selvapalam, H.-J. Kim, and K. Kim, *Acc. Chem. Res.*, 2003, **36**, 621–30.

63. F. Hapiot, S. Tilloy, and E. Monflier, *Chem. Rev.*, 2006, **106**, 767–781.

64. W. L. Mock and N. Shih, *J. Org. Chem.*, 1986, **51**, 4440–4446.

65. C.-F. Li, L.-M. Du, W.-Y. Wu, and A.-Z. Sheng, *Talanta*, 2010, **80**, 1939–44.

66. C.-F. Li, L.-M. Du, and H.-M. Zhang, *Spectrochim. Acta Mol. Biomol. Spectros.*, 2010, **75**, 912–917.

67. H.-J. Buschmann, E. Cleve, K. Jansen, A. Wego, and E. Schollmeyer, *J. Incl. Phenom. Macrocycl. Chem.*, 2001, **40**, 117–120.

68. Y.-M. Jeon, J. Kim, D. Whang, and K. Kim, *J. Am. Chem. Soc.*, 1996, **118**, 9790–9791.

69. C. Márquez, R. R. Hudgins, and W. M. Nau, *J. Am. Chem. Soc.*, 2004, **126**, 5806–5816.

70. W. Ong and A. E. Kaifer, *J. Org. Chem.*, 2004, **69**, 1383–1385.

71. M. Shaikh, J. Mohanty, A. C. Bhasikuttan, V. D. Uzunova, W. M. Nau, and H. Pal, *Chem. Commun.*, 2008, 3681–3683.

72. W. Ong, M. Gómez-Kaifer, and A. E. Kaifer, *Org. lett.*, 2002, **4**, 1791–1794.

73. H.-J. Kim, W. S. Jeon, Y. H. Ko, and K. Kim, *Proc. Nat. Acad. Sci. U.S.A.*, 2002, **99**, 5007–5011.

74. Y. Zhao, D. P. Buck, D. L. Morris, M. H. Pourgholami, A. I. Day, and J. G. Collins, *Org. Biomol. Chem.*, 2008, **6**, 4509–4515.

75. N. Dong, S.-F. Xue, Q.-J. Zhu, Z. Tao, Y. Zhao, and L.-X. Yang, *Supramol. Chem.*, 2008, **20**, 663–671.

76. R. Wang and D. H. Macartney, *Org. Biomol. Chem.*, 2008, **6**, 1955–1960.

77. S. Liu, C. Ruspic, P. Mukhopadhyay, S. Chakrabarti, P. Y. Zavalij, and L. Isaacs, *J. Am. Chem. Soc.*, 2005, **127**, 15959–15967.

78. A. Hennig and W. M. Nau, *Nat. Methods*, 2007, **4**, 629–632.

79. D. M. Bailey, A. Hennig, V. D. Uzunova, and W. M. Nau, *Chem. Eur. J.*, 2008, **14**, 6069–6077.

80. W. S. Jeon, H.-J. Kim, C. Lee, and K. Kim, *Chem. Commun.*, 2002, 1828–1829.

81. A. Y. Ziganshina, Y. H. Ko, W. S. Jeon, and K. Kim, *Chem. Commun.*, 2004, 806–807.

82. M. Pattabiraman, A. Natarajan, R. Kaliappan, J. T. Mague, and V. Ramamurthy, *Chem. Commun.*, 2005, 4542–4544.

83. F. Biedermann and O. A. Scherman, *J. Phys. Chem. B*, 2012, **116**, 2842–2849.

84. F. Biedermann, V. D. Uzunova, O. A. Scherman, W. M. Nau, and A. De Simone, *J. Am. Chem. Soc.*, 2012, **134**, 15318–15323.

85. T. Ogoshi, S. Kanai, S. Fujinami, and T. Yamagishi, *J. Am. Chem. Soc.*, 2008, **130**, 5022–5023.

86. T. Ogoshi, T. Aoki, K. Kitajima, S. Fujinami, T. Yamagishi, and Y. Nakamoto, *J. Org. Chem.*, 2011, **76**, 328–331.

87. D. Cao, Y. Kou, J. Liang, Z. Chen, L. Wang, and H. Meier, *Angew. Chem. Int. Ed.*, 2009, **48**, 9721–9723.

88. H. Tao, D. Cao, L. Liu, Y. Kou, L. Wang, and H. Meier, *Sci. China Chem.*, 2012, **55**, 223–228.

89. Y. Ma, Z. Zhang, X. Ji, C. Han, J. He, Z. Abliz, W. Chen, and F. Huang, *Eur. J. Org. Chem.*, 2011, **2011**, 5331–5335.

90. M. I. N. Xue, Y. Yang, X. Chi, Z. Zhang, and F. Huang, *Acc. Chem. Res.*, 2012, **45**, 1294–1308.

91. T. Ogoshi, K. Kitajima, T. Aoki, T. Yamagishi, and Y. Nakamoto, *J. Phys. Chem. Lett.*, 2010, **1**, 817–821.

92. H. Deng, X. Shu, X. Hu, J. Li, X. Jia, and C. Li, *Tetrahedron Lett.*, 2012, **53**, 4609–4612.

93. N. L. Strutt, R. S. Forgan, J. M. Spruell, Y. Y. Botros, and J. F. Stoddart, *J. Am. Chem. Soc.*, 2011, **133**, 5668–5671.

94. X. Shu, S. Chen, J. Li, Z. Chen, L. Weng, X. Jia, and C. Li, *Chem. Commun.*, 2012, **48**, 2967–2969.

95. X. Shu, J. Fan, J. Li, X. Wang, W. Chen, X. Jia, and C. Li, *Org. Biomol. Chem.*, 2012, **10**, 3393–3397.

96. C. Han, G. Yu, B. Zheng, and F. Huang, *Org. Lett.*, 2012, **14**, 1712–1715.

97. M. Ni, Y. Guan, L. Wu, C. Deng, X. Hu, J. Jiang, C. Lin, and L. Wang, *Tetrahedron Lett.*, 2012, **53**, 6409–6413.

98. T. Ogoshi, K. Demachi, K. Kitajima, and T.-A. Yamagishi, *Chem. Commun.*, 2011, **47**, 7164–7166.

99. G. Yu, C. Han, Z. Zhang, J. Chen, X. Yan, B. Zheng, S. Liu, and F. Huang, *J. Am. Chem. Soc.*, 2012, **134**, 8711–817.

100. Y. Ma, M. Xue, Z. Zhang, X. Chi, and F. Huang, *Tetrahedron*, 2013, **69**, 4532–4535.

101. C. Li, X. Shu, J. Li, S. Chen, K. Han, M. Xu, B. Hu, Y. Yu, and X. Jia, *J. Org. Chem.*, 2011, **76**, 8458–65.

102. C. Li, J. Ma, L. Zhao, Y. Zhang, Y. Yu, X. Shu, J. Li, and X. Jia, *Chem. Commun.*, 2013, **49**, 1924–1926.

103. G. Yu, X. Zhou, Z. Zhang, C. Han, Z. Mao, C. Gao, and F. Huang, *J. Am. Chem. Soc.*, 2012, **134**, 19489–19497.

104. T. Ogoshi, M. Hashizume, T. Yamagishi, and Y. Nakamoto, *Chem. Commun.*, 2010, **46**, 3708–3710.

105. C. Li, Q. Xu, J. Li, and X. Jia, *Org. Biomol. Chem.*, 2010, **8**, 1568–1576.

106. F. Perret and A. W. Coleman, *Chem. Commun.*, 2011, **47**, 7303–7319.

107. O. Danylyuk and K. Suwinska, *Chem. Commun.*, 2009, 5799–5813.

108. R. Zana, *Adv. Colloid Interface Sci.*, 2002, **97**, 205–253.

109. F. M. Menger and J. S. Keiper, *Angew. Chem. Int. Ed.*, 2000, **39**, 1906–1920.

110. X. Zhang and C. Wang, *Chem. Soc. Rev.*, 2011, **40**, 94–101.

111. H. Matsuoka, M. Tsurumi, and N. Ise, *Phys. Rev. B*, 1988, **38**, 6279–6286.

112. S. Shinkai, K. Araki, and O. Manabe, *J. Chem. Soc., Chem. Commun.*, 1988, 187–189.

113. S. Shinkai, T. Arimura, K. Araki, H. Kawabata, H. Satoh, T. Tsubaki, O. Manabea, and J. Sunamoto, *J. Chem. Soc., Perkin Trans. 1*, 1989, 2039–2045.

114. N. Basilio, L. García-Río, and M. Martín-Pastor, *J. Phys. Chem. B*, 2010, **114**, 4816–4820.

115. N. Basílio, L. Garcia-Rio, and M. Martín-Pastor, *Langmuir*, 2012, **28**, 2404–2014.

116. N. Basílio and L. Garcia-Rio, *Chemphyschem*, 2012, **13**, 2368–2376.

117. N. Basilio and L. García-Río, *Chem. Eur. J.*, 2009, **15**, 9315–9319.

118. N. Basilio, M. Martín-Pastor, and L. García-Río, *Langmuir*, 2012, **28**, 6561–6568.

119. V. Francisco, N. Basilio, L. Garcia-Rio, J. R. Leis, E. F. Marques, and C. Vázquez-Vázquez, *Chem. Commun.*, 2010, **46**, 6551–6553.

120. D. J. Mitchell, B. W. Ninham, and J. N. Israelachvili, *J. Chem. Soc., Dalt. Trans. 2*, 1976, **72**, 1525–1568.

121. R. Nagarajan, *Langmuir*, 2002, **18**, 31–38.

122. K. Holmberg, B. Jönsson, B. Kronberg, and B. Lindman, *Surfactants and Polymers in Aqueous Solution*, John Wiley & Sons, Ltd, Chichester, UK, 3rd ed., 2002.

123. D.-S. Guo, K. Wang, Y.-X. Wang, and Y. Liu, *J. Am. Chem. Soc.*, 2012, **134**, 10244–10250.

124. K. Wang, D.-S. Guo, X. Wang, and Y. Liu, *ACS Nano*, 2011, **5**, 2880–2894.

125. K. Wang, D.-S. Guo, and Y. Liu, *Chem. Eur. J.*, 2010, **16**, 8006–8011.

126. Z. Li, C. Hu, Y. Cheng, H. Xu, X. Cao, X. Song, H. Zhang, and Y. Liu, *Sci. China Chem.*, 2012, **55**, 2063–2068.

127. M. Rehm, M. Frank, and J. Schatz, *Tetrahedron Lett.*, 2009, **50**, 93–96.

128. S. Segota and D. Tezak, *Adv. Colloid Interface Sci.*, 2006, **121**, 51–75.

129. G. M. Whitesides and M. Boncheva, *Proc. Nat. Acad. Sci. U.S.A.*, 2002, **99**, 4769–4774.

130. M. Lee, S.-J. Lee, and L.-H. Jiang, *J. Am. Chem. Soc.*, 2004, **126**, 12724–12725.

131. F. Chécot, S. Lecommandoux, Y. Gnanou, and H.-A. Klok, *Angew. Chem. Int. Ed.*, 2002, **41**, 1339–1343.

132. Y. Sumida, A. Masuyama, M. Takasu, T. Kida, Y. Nakatsuji, I. Ikeda, and M. Nojima, *Langmuir*, 2001, **17**, 609–612.

133. M. Johnsson, A. Wagenaar, and J. B. F. N. Engberts, *J. Am. Chem. Soc.*, 2003, **125**, 757–760.

134. K. N. Power-Billard, R. J. Spontak, and I. Manners, *Angew. Chem. Int. Ed.*, 2004, **43**, 1260–1264.

135. J. L. Mynar, A. P. Goodwin, J. a. Cohen, Y. Ma, G. R. Fleming, and J. M. J. Fr?chet, *Chem. Commun.*, 2007, 2081–2082.

136. Z. Chen, V. Stepanenko, V. Dehm, P. Prins, L. D. a Siebbeles, J. Seibt, P. Marquetand, V. Engel, and F. Würthner, *Chem. Eur. J.*, 2007, **13**, 436–449.

137. Z. Chen, A. Lohr, C. R. Saha-Möller, and F. Würthner, *Chem.Soc.Rev.*, 2009, **38**, 564–584.

138. O. Varga, M. Kubinyi, T. Vidóczy, P. Baranyai, I. Bitter, and M. Kállay, *J. Photochem. Photobiol., A*, 2009, **207**, 167–172.

USC
UNIVERSIDADE
DE SANTIAGO
DE COMPOSTELA

Chapter 2

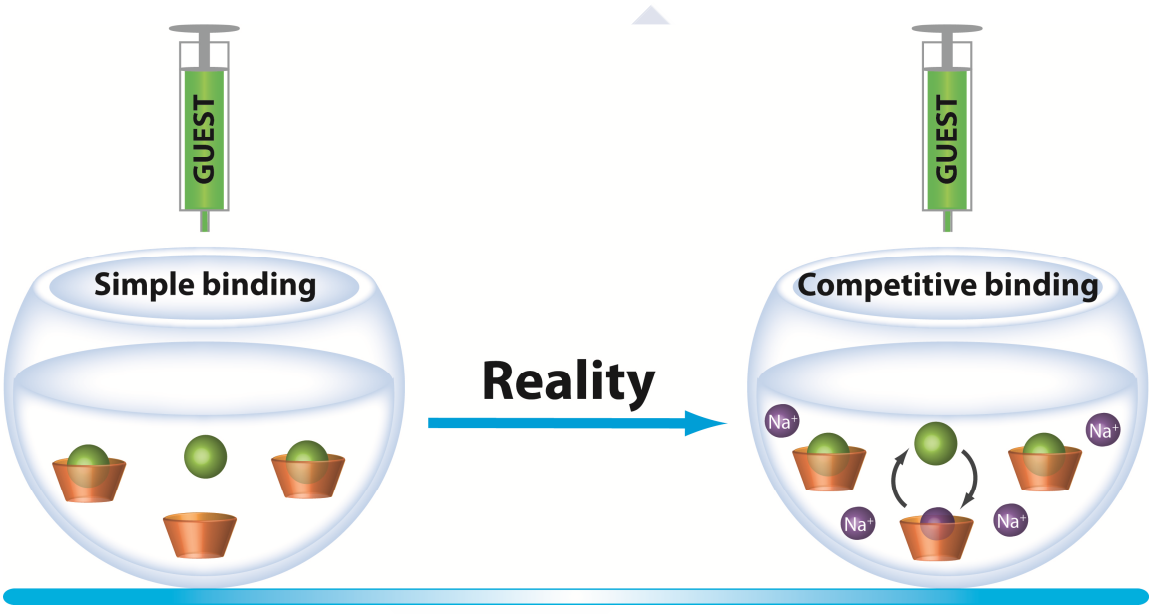
GUEST
Simple binding
Reality
GUEST
Competitive binding
Na+
Na+
Na+
Na+

USC
UNIVERSIDADE
DE SANTIAGO
DE COMPOSTELA

2. Complexation of guests by *p*-sulfonatocalix[4]arene

2.1. Complexation of inorganic metal cations by *p*-sulfonatocalix[4]arene: a thermodymanic study at neutral pH

2.1.1. Introduction

Calixarenes are a synthetically versatile class of macrocycles with high conformational flexibility that can accommodate a wide range of guest molecules.[1] *p*-sulfonatocalix[4]arene (SC4) is the prototype of a water-soluble calixarene that has been widely investigated, also due to its commercial availability, with many neutral or ionic guest, of different size and shape.[2–4] Knowledge of the absolute binding constants and its thermodynamics with salts, in particular alkali metal cations, is of exceptional practical importance for two reasons. On one hand, alkali metal cation binding would interfere with any biological or environmental application, of which many have been proposed for calixarenes in general. On the other hand, since SC4 possesses 4 highly acidic sulfonato groups and additionally one acidic phenolic hydroxyl group (pK_a ca. 3.3),[5,6] it exists as a pentaanion at neutral pH (Scheme 1), such that any application as well as measurements requires the presence of counterions, routinely sodium.

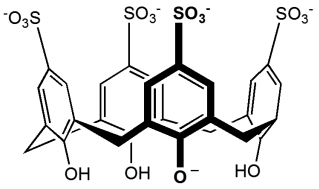

Scheme 1

Due to its importance, the putative interaction of SC4 with alkali metal cations has a rich and controversial scientific history. Despite early NMR-spectroscopic indications that alkali metal ions bind with SC4 because they affected the coalescence temperature at high concentrations at pH 8.9 (2.2 M NaCl),[7] it had soon become common practice – a habit persisting in part until to date – to assess binding constants of guests with SC4 in 0.1 M sodium phosphate buffer solutions.[8–15] Although it was noted that "buffering cannot be used here since CX (SC4) are all capable to interact strongly

with many buffers",[16] it was also concluded that "In fact, the (sodium) phosphate buffer (10 mM) has no influence on complexation."[17] Not surprisingly, in view of this uncertainty, efforts were subsequently made to study the binding of cations by sensitive methods, particularly isothermal titration calorimetry (ITC). An initial study suggested that "NH_4^+ has also been studied (by ITC) at pH 2 but no heat effect has been observed"[18] and a follow-up study also revealed no heat effects for NH_4^+ and K^+ at pH 7.5 by ITC.[19]

However, within the years 1998-2003 measurements by different groups at varying buffer concentrations provided many sets of binding constants, with extraordinary large variations, e.g., binding constants in the range from 100-6700 M^{-1} and from 200-3900 M^{-1} were reported for binding of lysine and arginine by SC4 in water at pH 1-2.[16,17,20,21] In parallel, it became firmly established that di- and trivalent metal ions bind to SC4 with significant binding constants.[18] Bakirci *et al*. showed in 2005 by fluorescence displacement titrations that alkali metal cations and ammonium – and therefore also the innocuous sodium ions ubiquitously used in buffers – bind indeed significantly to SC4, with binding constants from 80-280 M^{-1} between pH 2-8.[22] The same authors also emphasized that the presence of alkali metal cations prevents the measurement of the actual binding constants with other guests, which was suggested as a likely explanation for the observed large spread in binding constants, e.g., for amino acids.[16,17,20,21,23,24] Only one year later, another conflicting study appeared in which the same authors, which had previously not detected any heat effect in ITC measurement,[16,18] now were able to detect heat effects by using much higher (22 mM) SC4 concentrations;[25] alkali metal cations and ammonium were now reported to show detectable heat effects and affinities except for the crucial Na^+ ion and for Ag^+. But the binding constants ranged only between 2-15 M^{-1} – this would be sufficiently low to eventually again justify the use of buffers in binding constant determinations, especially since no heat effect was detected for the common Na^+ buffer ion; in this follow-up study,[25] no reference to the preceding study[22] was made in which sizable binding of Na^+ had been demonstrated. In 2010, Basilio *et al*. measured the binding constants by direct and competitive ^{23}Na diffusion NMR experiments and the authors obtained evidently sizable binding constants (on the order of 10^2 M^{-1}),[26] very similar to those determined by Bakirci *et al*.[22] In 2007 and 2009, Morel-Desrosiers and coworkers corrected their interim reported[25] binding constant for Cs^+, from 15 M^{-1} first to 22 M^{-1} and then to 45 M^{-1}, without providing a details.[27,28] Evidently, inorganic cation binding to SC4 has a

rich history, and the full "evolution" of binding constants for monovalent and divalent cations that has happened during the past 10 years is summarized in Table 1.

Unfortunately, although there is now independent experimental evidence by a variety of techniques from different research groups that alkali metal ion binding to SC4 is sizable and needs to be taken into account, the notion, based on the early conjectures and ITC studies, that binding of the common buffer ions Na^+, K^+, and NH_4^+ is very small or negligible and that the binding of K^+, Rb^+ and Cs^+ is enthalpically driven, pervades the literature and, unfortunately, is being amplified by recent reviews.[2,3,29] Herein, we have revisited the topic once more, in an effort to determine the "true" binding constants of inorganic cations with SC4 at neutral pH. The aim of this work was to determine the thermodynamic parameters for the complexation of Na^+, and also for other mono and also divalent inorganic cations by considering a comprehensive model for counterion exchange. As we will demonstrate, to obtain the "true" equilibrium thermodynamic data and binding constants, ITC measurements must be extrapolated to zero calixarene and zero added salt since the complexation of cationic guests occurs by an ion-exchange equilibrium.[30] Moreover, we find that the binding of simple alkali metal cations with SC4 is – as intuitively expected from desolvation effects – entropically driven, in contrast to the previous results.

Table 1. Reported binding constants (in M^{-1}) for 1:1 complexation of monovalent and divalent inorganic cations with SC4 at ambient temperature (recommended values shown in boldface).

	Method	ITC	ITC	Competitive titration	Competitive titration	ITC	NMR	NMR	ITC
Cation	pH [pD][a]	2	7.5	[2.4]	[7.4]	2	[Not given]	[6-7]	7
	Ref.	[18]	[19]	[22]	[22]	[25]	[28]	[26]	This work[f]
	Year	2001	2003	2005	2005	2006	2009	2010	This year
Li^+				70	80			80	**139**
Na^+			no heat[c]	75	85	no heat[c]		100	**183**
K^+			no heat[c]	100	115	2.9		110	**217**
Rb^+				110	135	5.9			**253**
Cs^+				150	280	14.6	45 [22][d]	280	**760**
H_3O^+				40[b]					
NH_4^+		no binding	no heat[c]	95	165	6.9			
Ag^+						no heat[c]			**271**
Tl^+						460	245		
Mg^{2+}		2000		1020	2190				**3800**
Ca^{2+}		2090		1590	3820				**7900**
Sr^{2+}				1810	4630				
Ba^{2+}				n.a.	6760				
Zn^{2+}					2000[e]				**5580**
Ni^{2+}									**5560**
Cu^{2+}									**5650**

[a] pD for measurements carried out in D_2O solution. [b] From ref. 31. [c] No data due to lack of significant heat effect. [d] Value from ref. 27. [e] From ref. 32. [f] See Tables 3 and 4 for errors.

2.1.2. Experimental Section

Materials: *p*-Sulfonatocalix[4]arene (SC4) was prepared by *ipso*-sulfonation of *p-tert* butylcalixarene in H_2SO_4 at 80 °C.[33–35] The pentasodium (SC4Na) or pentacesium salt (SC4Cs) of SC4 was obtained by neutralization of the acid form of SC4 with Na_2CO_3 or Cs_2CO_3 in H_2O.[34] The product was then decolorized with activated charcoal and filtered through Celite. The final solution was placed in an open flask and allowed to crystallize by slow evaporation of water. The crystals were recollected by filtration, dissolved in a minimum quantity of water, and precipitated with methanol. The operation was repeated at least three times. Finally, the product was dried at 80 °C under high vacuum for 3 days. The SC4 samples were characterized by nuclear magnetic resonance spectroscopy (NMR) and, to establish the identity of the counterion in the SC4Na and SC4Cs samples, by electrospray ionization-ion trap mass spectrometry (ESI-MS) in the negative ion mode (Figure, Figure). The SC4 samples were also analyzed by thermal gravimetric analysis (TGA) to assess volatile content.

NaCl from Fluka (assay ≥ 99.5%) and LiCl (assay ≥99%), KCl (assay ≥99%), RbCl (assay ≥99%), $AgNO_3$ (assay ≥99%), CsCl (assay ≥99.9%), $MgCl_2$ (assay ≥98%), $ZnCl_2$ (assay ≥99.9%), $CuCl_2$ (assay ≥99.9%), $Ni(NO_3)_2$ (assay ≥97%), $CaCl_2$ (assay ≥97%) from Sigma-Aldrich were used without further purification. All solutions were prepared with Milli-Q water. pH readings were taken with a Crison GLP 21 pH meter.

Microcalorimetry. The microcalorimetric titrations were performed on an isothermal titration microcalorimeter (VP-ITC) from Microcal Co. (Northampton, MA) at atmospheric pressure and 25 °C. In each run, a solution of guest in a 0.270 mL syringe was sequentially injected with stirring at 459 rpm into a solution of host in the sample cell (1.459 mL volume). Each solution was degassed and thermostatted by using a ThermoVac accessory before titration. In each titration the reference cell was filled with the same sample as in the sample cell. The concentration ranges to perform the experiments were determined by taking into account the results from this work for the complexation of the counterion Na^+ by SC4. From the presumed binding constant and the salt content at neutral pH (5 Na^+ per SC4 to neutralize all sulfonato groups and the hydroxyl group)[5,36] it is possible to calculate the degrees of complexation, see Figure 1.

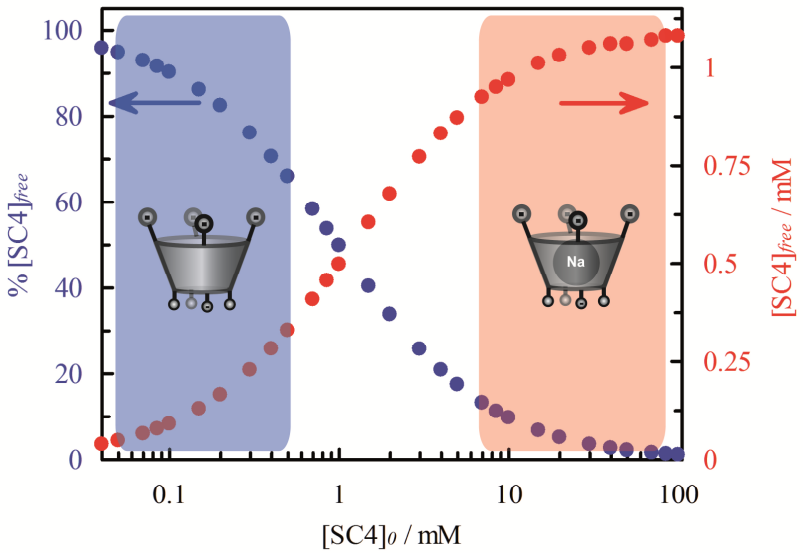

Figure 1. Percentage and concentration of free SC4 vs the total concentration of calixarene ($[SC4]_{\circ}$) by considering the presence of 5 Na^+ per SC4 and by taking the binding constant of 183 M^{-1} from this work for the counterion binding.

Since the binding constants of all monovalent cations are significant but the related heat effect for the complexation are very small, the experimental conditions must be carefully selected such that the total concentration of total SC4 is sufficiently low to allow for a relatively high percentage of free SC4, but sufficiently large to afford detectable absolute heats of complexation. As can be seen from Figure 1, total SC4 concentrations below 1 mM appear ideal for this purpose.

2.1.3. Results and Discussion

As the technique of choice, we employed isothermal titration calorimetry (ITC),[37] which provides the complex stability constant as well as the Gibbs free energy, and also enthalpy and entropy changes, in principle in a single experiment. In particular, it is suitable for determining the association of high-affinity ligands,[38] as well as low binding constants,[39] such as those expected for the complexation of metal cations.

Because the nearest pK_a values of SC4 lie at ca. 3.3 and ca. 12,[5,6] respectively, it should be noted at the outset that SC4 exists quantitatively (< 99%) in its pentaanion form at neutral pH (7.0). All analyses refer therefore to the pentaanion form in Scheme 1. Although the presence of different cations, varying ionic strengths, or the selection of different temperatures may lead to measurable shifts of these pK_a values (e.g., by up to 1

pK_a unit at 4 M $NaClO_4$),[5,40] they are too small to significantly affect the abundance of the pentaanion form of SC4 at neutral pH.

2.1.3.1. Thermodynamic model for Na^+ cation complexation

A representative result of the microcalorimetric titration curve of SC4 with Na^+ at 298.15 K is shown in Figure 2. The stepwise addition of NaCl solution resulted in exothermic changes (Figure 2, left), however, after correction for the (larger) exothermic heat of dilution, the titration of NaCl resulted in a net endothermic enthalpy change, see Figure 2, right.

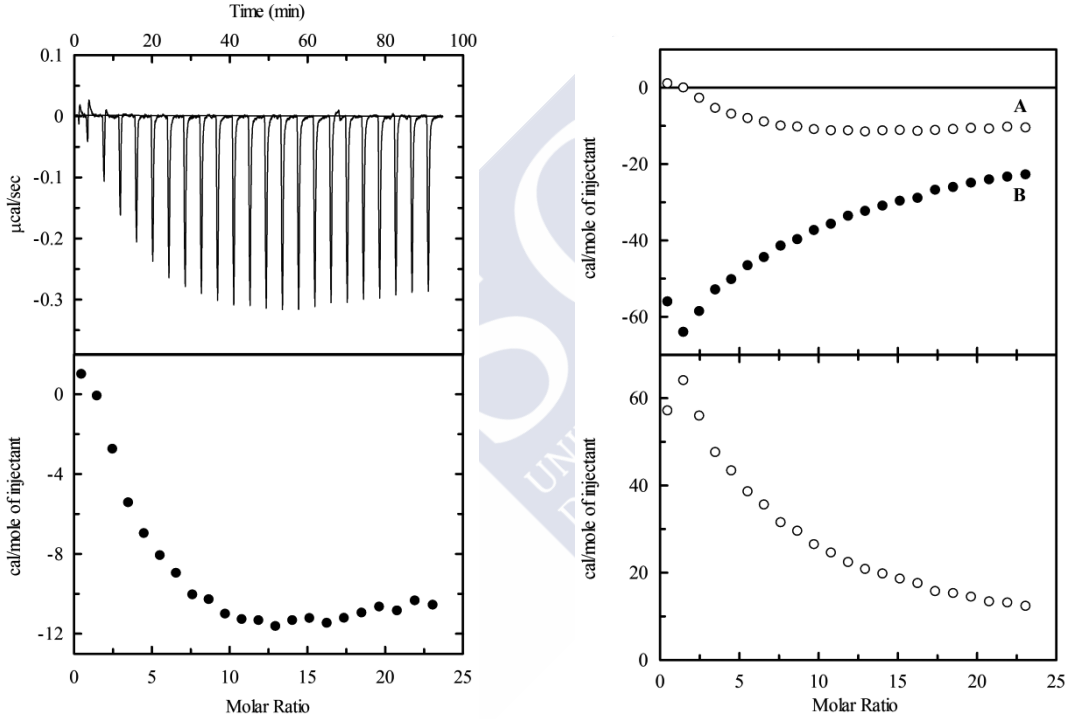

Figure 2. (Left) Microcalorimetric titration of SC4 with NaCl at 298.15 K in aqueous solution at neutral pH: (top) raw data for sequential 12 µL injections of NaCl (60 mM) into SC4 (0.5 mM); (bottom) heats of reaction as obtained from the integration of the calorimetric traces. (Right) (top) Complexation reaction of SC4 with NaCl (A) and heat effect of the dilution of the NaCl (B) and (bottom) "Net" heat effect obtained by subtracting the heat of dilution from the heat of reaction.

Although the heat effects for the complexation of the cations by SC4 are very small, ITC can be employed successfully for binding constants on the order of 10^{-4} or lower.[39,41] Higher binding constants are generally preferable since host saturation can be

achieved by adding usually 2 equiv. of the guest such that the stoichiometry can be determined more accurately. However, at low binding constant values, the stoichiometry and ΔH° are correlated and thereby difficult to determine simultaneously. Fortunately, for low-molecular weight macrocycles and analytes, the stoichiometry of the complex can be independently determined by other techniques. In particular, for the complexes of SC4 and monovalent cations, diffusion NMR experiments,[26] and fluorescence displacement titrations[22] have previously established a 1:1 binding stoichiometry, which was adapted in the ITC titrations.

In the range where the experiments were performed, *ca.* 26% of the host SC4 is occupied, which influences both the binding constant and also the thermodynamics parameters[30]. As a result, a sequential binding model where the Na^+ already present in solution in the sample cell was taken into account in the fitting of the microcalorimetric titrations. Concretely, the following chemical equilibrium was employed to provide the thermodynamical characterization of the system:

$$\mathrm{SC4 + Na} \overset{K_{Na}}{\rightleftharpoons} \mathrm{SC4Na} \qquad (1)$$

The experimental stepwise molar heat change, including the corrections due to the constant volume cell of the employed VP-ITC microcalorimeter, can be compared to:

$$q_i = \left[Q_j^{cum} + \frac{\Delta V_i}{2V} \left(Q_j^{cum} + Q_{j-1}^{cum} \right) - Q_{j-1}^{cum} \right] / \Delta n_i \qquad (2)$$

with ΔV_i being the volume of the solution in the syringe injected into the sample cell upon each titration, Δn_i the number of moles of Na^+ in ΔV_i, and V the volume of the cell. Q_j^{cum} is the cumulative heat involved in the mixing of SC4 with Na^+ in the sample cell of the calorimeter, after subtraction of the heat of dilution, when the concentration of the complex is [SC4Na]

$$Q_j^{cum} = V\{\Delta H_1 [SC4Na]\} \qquad (3)$$

Taking this into account and considering that the reaction of SC4 with the Na^+ counterion is present in all the performed experiments, a simultaneous fitting of the data

was performed. To keep a balanced weight of the systems, despite the magnitude of the absorbed or delivered heat in each experiment, the simulated annealing algorithm[42] was employed to minimize the following objective function χ^2 (eq 4) as a function of the adjustable parameters:[43]

$$\chi^2=\frac{1}{p-v}\sum_j\sum_i\frac{\left[Q_{ij}(\text{exp})-Q_{ij}(\text{mod})\right]^2}{\left[Q_{ij}(\text{exp})\right]^2} \tag{4}$$

where p stands for the number of experimental points, v stand for the number of adjustable parameters, "exp" and "mod" mean "experimental" and "model", and i, j run over all the concentrations and over the experimental curves, respectively. Note that without this normalization of χ^2 the fitting would be dominated by the solutions and concentrations with largest $|Q_i|$ and the simultaneous fitting would be meaningless. The numerical solution of eq 4, providing K_i and ΔH_i (i = 1,2), requires the determination of the concentration of every chemical species in the mixture. At this point, it needs to be taken into account that a fraction of SC4 is already complexed by Na^+ even before addition of NaCl solution. This is due to the unavoidable presence of counterions when working at neutral pH. At the employed 0.5 mM SC4 concentration, the concentration of Na^+ is 2.5 mM, resulting in 30% of host being complexed (this assumes a binding constant of 183 M^{-1}). Obviously, SC4 molecules already complexed with a sodium ion will not afford any heat effect upon addition of sodium, such that the heat effect needs to be normalized for the fraction of uncomplexed SC4 (and uncomplexed Na^+), which can be obtained from the following mass balance equations:

$$[SC4]_{Total}=[SC4]_{Free}+[SC4Na]=[SC4]_{Free}\left(1+K_{Na}[Na]_{Free}\right) \tag{5}$$

$$[Na]_{Total}=[Na]_{Free}+[SC4Na]=[Na]_{Free}\left(1+K_1[SC4]_{Free}\right) \tag{6}$$

The latter nonlinear system of coupled equations was solved for every concentration and iteration of the main numerical routine by using the Newton-Raphson algorithm.[43] The model gives a good approximation of the experimental data in every titration and the thermodynamic parameters characterizing the reactions and also the

distribution of all the chemical species as a function of the concentration in the sample cell.

Figure 3 shows the fitting of the experimental data and the distribution of the species for the complexation of Na^+ by SC4 at 298.15 K. Direct fitting of the ITC data according to a 1:1 complexation model provided a binding constant of 107 M^{-1}, similar to previous estimates,[22,26] while the consideration of sodium ions already present in solution afforded a significantly higher value of 183 M^{-1} (Figure S3). The latter value is extrapolated to zero salt concentration and can therefore be considered as the "true" binding constant of SC4 with Na^+ at neutral pH. The thermodynamic parameters obtained by the refined model afford positive ΔH° = 7.1 kJ mol^{-1} and $T\Delta S^\circ$ = 20.0 kJ mol^{-1} values, indicating that the complex formation is entropically driven. In a first approximation, for an entropically controlled reaction, the binding constant could increase with temperature, and towards this end, experiments at different temperatures were performed for the complexation of Na^+ with SC4.

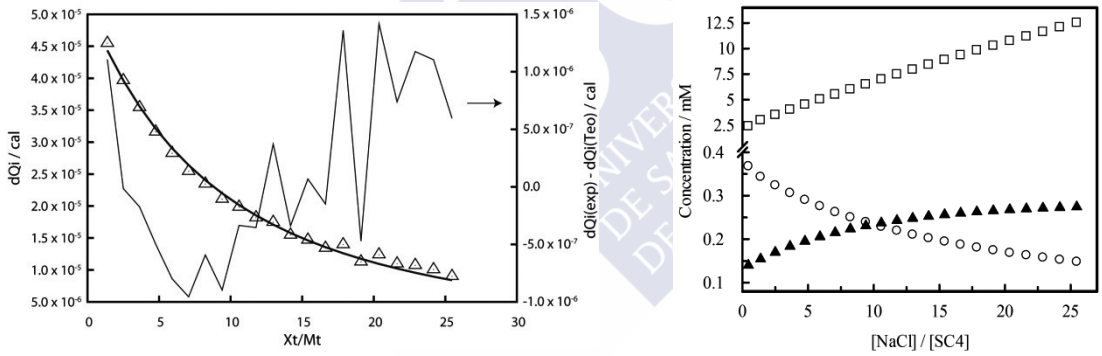

Figure 3. (Left) Experimental ITC data (Δ) and fitted curve (thick line) for the titration of NaCl to SC4 (0.5 mM) with Na^+ as a counterion at 298.15 K. The difference between the fitted and the experimental data is represented by the thin line (right scale). (Right) Concentration of free SC4 (○), free Na^+ (□), and complex Na@SC4 (▲) as a function of the [NaCl]/[SC4] ratio, calculated from the isotherm at 298.15 K, considering K = 183 M^{-1}.

The heat changes for the complexation of Na^+ by SC4 at different temperatures yielded always a positive heat deflection after correction for the dilution effect of the cation. In Figure 4 are shown the reaction heats obtained for the titrations of NaCl to a solution of 0.5 mM SC4 at five temperatures. The corresponding thermodynamic

parameters obtained by fitting to a 1:1 complexation model and correcting for the presence of Na^+ counterions are reported in Table 2.

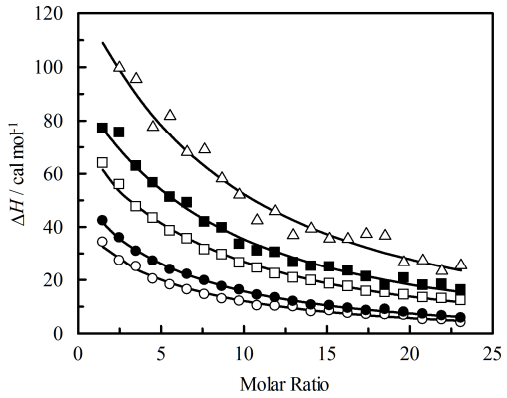

Figure 4. Heat effects, corrected for dilution, observed upon titration with Na^+ to 0.5 mM SC4 in water at neutral pH (7.0) for different temperatures. (○) 278.15 K, (●) 283.15 K, (□) 298.15 K, (■) 313.15 K and (Δ) 338.15 K.

Table 2. Thermodynamic parameters obtained from the counterion-considerate fitting of the ITC titrations of Na^+ to SC4@Na solution at neutral pH at different temperatures.

Cation	T / K	K/M^{-1} [a]	$\Delta G°$/ (kJ mol^{-1})[b]	$\Delta H°$/ (kJ mol^{-1})[b]	$T\Delta S°$/ (kJ mol^{-1})[b]
Na^+	278.15	275	–13.0	3.4	16.4
	283.15	250	–13.0	4.4	17.4
	298.15	183	–12.9	7.1	20.0
	313.15	167	–13.3	9.4	22.7
	338.15	143	–13.9	14.2	28.1

[a] 5% error. [b] Error ± 0.1 kJ mol^{-1}.

As can be seen, the binding constant decreases on increasing the temperature in the range studied. The values of K vary from 275 M^{-1} at T = 278.15 K to 143 M^{-1} at T = 338.15 K with positive enthalpy as well as entropy contributions. The change in the enthalpy and entropy is presumably related to the ordered water structure surrounding the cation and the sulfonato groups of the calixarene, which with increasing temperature leads to the structure of the hydration shell partially broken down. However, despite the fact that complexation is entropy-driven, the expected increase in the binding constant with increase in temperature is not observed. At 278.15 K, the entropy contribution is about five times higher than the enthalpic term, while at 338.15 K the entropy

contribution is only twice as large as the enthalpy contribution, which evidences the importance of the temperature dependence of the enthalpic term in the complexation, pointing to a heat capacity effect. A more detailed analysis of this behavior will be given after the results for the other monovalent cations have been presented.

2.1.3.2. Ion exchange model for the complexation of other cations

In contrast to the complexation of Na^+ by SC4 with Na^+ as counterion, the complexation of other cations by SC4 must take into account that the ions of the titrating solution compete with the Na^+ counterions in the binding to the SC4 cavity, such that formally one ion is exchanged or displaced by the other in the course of the titrations.[44] This displacement, and also the stoichiometric cation binding, is best rationalized through the involvement of an inclusion complex between the inorganic cations and SC4, as depicted in Scheme 2. In contrast to solid-state structures,[36,45] the precise position of the bound cation in solution (near the sulfonato rim, near the phenoxyl rim, or inside the cavity) cannot be deduced from the ITC experiments carried out herein. Nevertheless, in view of recent experimental investigations by NMR for Cs^+ and Tl^+ [27,28] and in view of the fact that the investigated alkali and earth alkaline metal cations displace also neutral guest molecules (which can be demonstrated by NMR to be positioned inside the SC4 cavity),[22] a binding inside the cavity is likely to be the dominant binding mode for the investigated inorganic cations in solution.

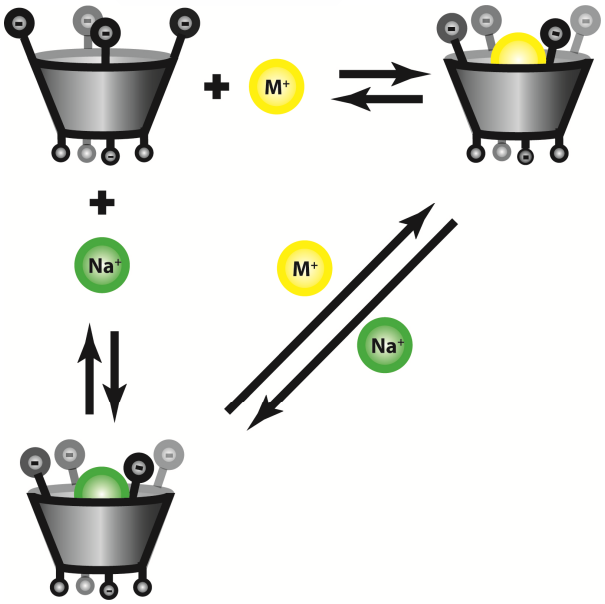

Scheme 2. Displacement reaction between metal cations and SC4 with Na^+ as counterion.

As a result, a competitive binding model was employed to fit the microcalorimetric titrations. More specifically, the next two independent chemical equilibria were employed to provide a complete thermodynamic characterization of the system:

$$SC4 + Na \overset{K_{Na}}{\rightleftharpoons} SC4Na \quad (1)$$

$$SC4 + M \overset{K_{M}}{\rightleftharpoons} SC4M \quad (7)$$

where Na is the SC4 counterion and M is the titrating ion. The net exchange reaction is given by:

$$SC4Na + M \overset{K_{1}}{\rightleftharpoons} SC4M + Na \quad (8)$$

and the corresponding equilibrium constant and enthalpy can be obtained by subtracting eq. (1) from eq. (7): $\Delta H_1 = \Delta H_M - \Delta H_{Na}$; and $K_1 = K_M/K_{Na}$. The experimental stepwise molar heat change was compared to eq. (2), however Q_j^{cum} has now one more parameter, the complex [SC4M].

$$Q_j^{cum}=V\{\Delta H_{Na}[SC4Na]+\Delta H_M[SC4M]\} \quad (9)$$

As was the case for Na^+ complexation by SC4Na, the objective function (eq. 4) was employed for all titration curves. The mass balance equations are given by:

$$[SC4]_{Total}=[SC4]_{Free}+[SC4Na]+[SC4M]=[SC4]_{Free}\left(1+K_{Na}[Na]_{Free}+K_M[M]_{Free}\right) \quad (10)$$

$$[Na]_{Total}=[Na]_{Free}+[SC4Na]=[Na]_{Free}\left(1+K_{Na}[SC4]_{Free}\right) \quad (11)$$

$$[M]_{Total}=[M]_{Free}+[SC4M]=[B]_{Free}\left(1+K_M[SC4]_{Free}\right) \quad (12)$$

The latter nonlinear system of coupled equations was solved for every concentration and iteration of the main numerical routine by using the Newton-Raphson algorithm.

The thermodynamic parameters obtained for the complexation of Li^+, K^+, Rb^+, Ag^+ and Cs^+ by SC4 and also the distribution of all chemical species as a function of the concentration in the sample cell are listed in Table 3 and in the appendix (Figures S4-S7).

As an example, in Figure 5 is shown the fitting for the Rb^+ cation as well as the species distribution. Contrary to the distribution of complex for the complexation of Na^+ cations by SC4, herein the concentration for the complex between the titrating ion and SC4 begins from zero concentration. It should also be noted that although the Na@SC4 complex decreases with increasing the concentration of the titrating RbCl, the complex coexists with the Rb@SC4 complex in solution.

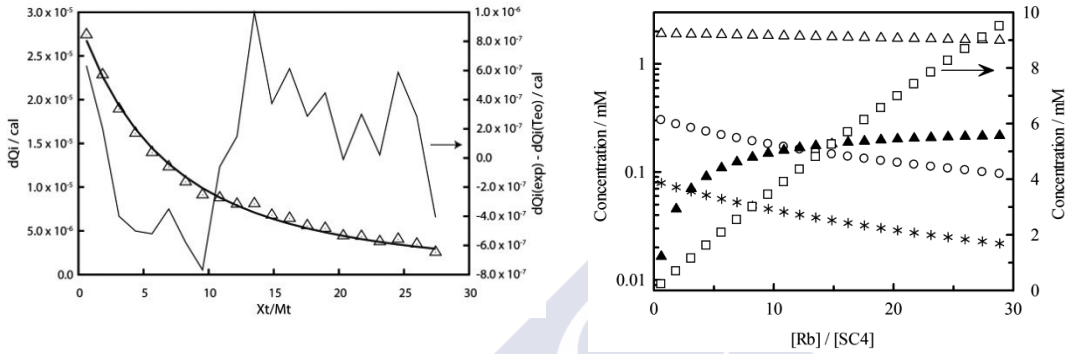

Figure 5. (Left) Experimental ITC data (Δ) and fitted curve (thick line) for the titration of Rb^+ on SC4 (0.4 mM) with Na^+ as a counterion at 298.15 K. The difference between the fitted and the experimental data is represented by the thin line (right scale). (Right) Concentration of free SC4 (○), free Na^+ (Δ), free Rb^+ (□), and complexes Na@SC4 (*), and Rb@SC4 (▲) as a function of the [RbCl] / [SC4] ratio, calculated from the isotherm at 298.15 K, considering K = 183 M^{-1} and K = 253 M^{-1} for the complexation of Na^+ and Rb^+, respectively.

Table 3. Thermodynamic parameters obtained from the counterion-considerate fitting of the ITC titrations for monovalent cations by SC4 in water at neutral pH (7.0) and 298.15 K.

Cation	K/M^{-1} [a]	$\Delta G°$/(kJ mol^{-1})[b]	$\Delta H°$/(kJ mol^{-1})[b]	$T\Delta S°$/(kJ mol^{-1})[b]
Li^+	139	–12.2	9.3	21.5
Na^+	183	–12.9	7.1	20.0
K^+	217	–13.3	5.3	18.6
Rb^+	253	–13.7	4.2	17.9
Ag^+	271	–13.9	7.9	21.8
Cs^+	760	–16.4	–0.2	16.2

[a] 5% error. [b] Error ± 0.1 kJ mol^{-1}.

As can be seen from Table, the results show that at pH ≈ 7 the binding constant increases from 139 M^{-1} for Li^+ to 760 M^{-1} for Cs^+. The obtained values, which we

contend provide the hitherto best measures of the "true" binding constants of monovalent cations with SC4, are on average a factor of 2 higher than previously reported binding constants for monovalent metal cations by competitive displacement of a fluorescent azoalkane guest[22] and also than those obtained by diffusion NMR experiments.[26] It has been concluded previously that measurements in the presence of metal ions result in the determination not of the true, but of apparent binding constants, and that the apparent ones are related to the true binding constant according to eq. 13 (which holds for excess metal ion concentrations):

$$K_{app} = \frac{K}{1 + K_M[M]} \tag{13}$$

Since the previous fluorescence displacement experiments at neutral pH were carried out with Na^+ as counterion at 1.6 mM concentration of SC4, the critical term in the denominator $K_M[M] = K_{Na}[Na] = 183\ M^{-1} \times 5 \times 1.6\ mM = 1.46$ becomes indeed nonnegligible, and it follows that $K \approx 2\ K_{app}$ for the previous set of experiments. The data from the 3 studies carried out at neutral pH (ref. 22,26 and this work), conducted with 3 independent experimental techniques (competitive titrations, NMR, and ITC), are therefore mutually consistent, but differ in the meaning of extracted binding constants.

However, our binding constants in Table 3 differ largely from the binding constants previously determined by ITC at pH = 2,[25] in which previous claims on the absence of heat effects had been revised.[18,19] Subsequent corrections for the binding constant of Cs^+ (from 15 M^{-1} to 45 M^{-1})[27,28] also leave a large variation to the value determined here (760 M^{-1}). These alternative ITC measurements have been determined with 22 mM concentrations of SC4 and, therefore, in the presence of ca. 88 mM concentration of a monovalent counterion (either H_3O^+ or Na^+, or a mixture of them). Moreover, these experiments were performed at pH 2.0, but since even a ca. 2 mM solution of SC4 (a very strong tetra- or pentaacid) affords a pH of 2.0, ca. 20 mM of SC4 must have been neutralized by counterions, presumably ca. 80 mM sodium (otherwise a much higher pH would result on the basis of simple strong-acid dissociation arguments). The denominator in eq. 13 adapts then indeed a very large value of ca. 16, which accounts largely for the more than one order of magnitude deviation. Additionally, variations in binding constants with pH (the binding of the tetraanion at pH 2 is naturally weaker than that of the pentaanion at pH 7)[17,19,20,22,46,47] and the possibility of higher-order complexes at the employed high concentrations can lead to additional deviations,

such that the previous set of low binding constants[25] provides a manifestation of the interference of cation binding rather than their quantification; the same conclusion holds for the previously reported thermodynamic parameters, which are obviously in similarly unsatisfactory agreement with the data in Table 3.

The stronger binding of Cs^+ than Li^+ suggests that the solvation and ionic radii of the cations have an influence on the binding constant, since the smaller, better solvated cations have a lower affinity than the bigger, less solvated ones. The thermodynamic parameters indicate that at neutral pH the complexation of the monovalent cations by SC4 is entropy-driven ($\Delta S^\circ > 0$ and $T\Delta S^\circ > |\Delta H^\circ|$). In Table 3, we also report for the first time the values for the complexation of the strongly hydrated Ag^+ cation by SC4, a cation whose complexation has eluded previous measurements.[25]

We also measured divalent cations by ITC at neutral pH in order to allow a more comprehensive comparison with previous measurements.[44] Table 4 shows the thermodynamic parameters for the complexation of Mg^{2+}, Ni^{2+}, Zn^{2+}, Cu^{2+} and Ca^{2+} fitted with the competitive binding model, i.e., again by explicitly considering the presence of sodium counterions even before addition of titrant. Again, there is a factor of ca. 2 difference to the previously reported values near neutral pH, which can be rationalized in the same manner as for the monovalent cations (see above, eq. 13).

Table 4. Thermodynamic parameters obtained from the simultaneous fitting of ITC titrations of divalent cations by SC4 in water at neutral pH (7.0) and 298.15 K.

Cation	K/M^{-1} [a]	$\Delta G°$/(kJ mol^{-1})[b]	$\Delta H°$/(kJ mol^{-1})[b]	$T\Delta S°$/(kJ mol^{-1})[b]
Mg^{2+}	3800	–20.4	11.9	32.3
Ni^{2+}	5560	–21.4	11.2	32.6
Zn^{2+}	5580	–21.4	11.3	32.7
Cu^{2+}	5650	–21.4	11.2	32.6
Ca^{2+}	7900	–22.2	11.6	33.9

[a] 5% error. [b] Error ± 0.1 kJ mol^{-1}.

From the comparison of the thermodynamic parameters of the monovalent cations (Table 3) with those of the more hydrated divalent cations (Table 4), it can be concluded that the association of the monovalent metal cations is dominated by electrostatic (charge-charge) interactions. The positive enthalpy and entropy changes for the association of the monovalent metal cations originate from the partial desolvation of M^+ and SO_3^- upon interaction and from the concomitant release of water molecules; for the

divalent cations, both solvation effects are larger due to their tighter and more extended solvation shell, resulting in more pronounced enthalpic and entropic effects, but in the same direction (both positive) as for the monovalent cations.

The thermodynamic parameters determined herein at pH 7 largely deviate from those reported in the previous ITC study at pH 2 (Table 5).[25] For the divalent cations, the enthalpic and entropic contributions are up to 10 kJ mol^{-1} more positive for our data set, and for the monovalent cations the enthalpic and entropic contributions are even opposite in most cases, which would suggest a switch-over from enthalpic to entropic control. Although the binding constants of cationic guests tend to be distinctly higher at neutral pH (compare data from competitive titrations entered in Table 1), the observed contrast in thermodynamic parameters is not expected, since ITC data for the complexation of several other guest molecules do not show such drastic pH changes.[17,19,20,46,47] Presumably, the deviation is due to the presence of large amounts of counterions (ca. 80 mM, see above) and large amounts of host used in the previous study. With a little hindsight, it is also not surprising that the previous ITC study has led to the assignment of enthalpically driven reactions: What is being measured at such high concentrations is actually solely the displacement of sodium from the cavity. The complexation enthalpies of Na^+ and Ag^+ are very similar (Table 3), such that no heat effects can then be detected by ITC for these two ions, as reported.[25] The complexation enthalpy of Na^+ is, on the other hand, more endothermic than those for K^+, Rb^+, and Cs^+ (Table 3) such that the displacement leads to an overall exothermic displacement reaction according to eq. 8. This rationalizes nicely the experimental observations, which, evidently, have been incorrectly interpreted: The heat release observed in the previous study[25] for K^+, Rb^+ and Cs^+ was presumably not due to the binding of these cations, but due to the exothermic release of Na^+ in the displacement process. We therefore do not draw further conclusions from the contrasting thermodynamic parameters reported in this study.[25]

Table 5. Reported thermodynamic parameters for the binding of monovalent and divalent inorganic cations by SC4 at ambient temperature by ITC (recommended values shown in boldface)

		ΔH°/(kJ mol^{-1})				$T\Delta S^\circ$/(kJ mol^{-1})		
	pH	2	7.5	2	7	2	2	7
Cation	Ref.	[18]	[19]	[25]	This work[d]	[18]	[25]	This work[d]
	Year	2001	2003	2006	This year	2001	2006	This year
Li^+					**9.3**			**21.5**
Na^+			≈ 0 [a,b]	≈ 0 [a]	**7.1**			**20.0**
K^+			≈ 0 [a,c]	–12.3	**5.3**		–9.7	**18.6**
Rb^+				–10.3	**4.2**		–5.9	**17.9**
Cs^+				–10.9	**–0.2**		–4.3	**16.2**
NH_4^+		≈ 0	≈ 0 [a,c]	–3.7			1.1	
Ag^+				≈ 0 [a]	**7.9**			**21.8**
Tl^+				–14.0			1.2	
Mg^{2+}		4.7			**11.9**	23.5		**32.3**
Ca^{2+}		3.0			**11.6**	22		**33.9**
Ni^{2+}					**11.2**			**32.6**
Zn^{2+}					**11.3**			**32.7**
Cu^{2+}					**11.2**			**32.6**

[a] No significant heat effect detected. [b] A very weak endothermic effect was assigned in retrospect (ref. 25). [c] A very weak exothermic effect was assigned in retrospect (ref. 25). [d] See Tables 3 and 4 for errors.

2.1.3.3. Temperature dependence for Cs^+ and K^+ cations

To confirm the temperature dependence observed for the complexation of Na^+ cation by SC4, experiments at different temperatures were also performed for two other monovalent cations and the thermodynamic parameters are entered in Table 6. As an example, Figure 6 shows the heat effects for the complexation of Cs^+ by SC4Na at four different temperatures. Interestingly, the formation of the complex is an exothermic process at lower temperatures but becomes endothermic at higher temperatures.

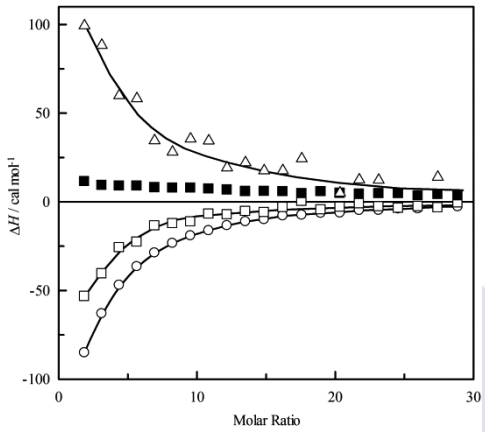

Figure 6. Heat effects, corrected for the dilution, observed upon titration of Cs^+ by 0.4 mM SC4Na in water at neutral pH (7.0) for different temperatures. (○) 283.15 K, (□) 298.15 K, (■) 313.15 K and (Δ) 338.15 K.

Although the complexation of Cs^+ by SC4 appears to be enthalpically favored at lower temperatures, after fitting the data with the competitive model, the enthalpy becomes at best slightly negative or almost negligible, suggesting that the complexation is almost purely entropy-driven. Therefore, the exothermic peaks observed in the microcalorimetric titration are due to the displacement of the sodium counterion from the cavity of the calixarene. Consequently, the binding of Cs^+ with SC4 cannot be detected by a direct titration, and it is only the heat effects related to the displacement of the sodium ions (and which is not thermoneutral) which allows one to follow the binding of Cs^+ "indirectly". We recommend here to always apply competitive titrations (whether by ITC or by other methods)[22] in cases where one cannot differentiate between negligible heat effects and negligible binding of "calorimetrically silent" guests. To independently confirm the purely entropically driven process at 298.15 K, an experiment using SC4 with a different counterion was also performed. After the

synthesis of the SC4, instead the neutralization with Na^+ cations to produce the pentaanion form of the host, the calixarene was neutralized with Cs^+ cations. When the ITC experiments were performed with a solution of CsCl in the syringe and SC4 with Cs^+ as a counterion in the sample cell, no heat effect was detected, confirming that at 298.15 K and in neutral aqueous solution, microcalorimetry is not a suitable technique to directly determine the interaction of the Cs^+ cation by SC4Cs (Figure S8). It should be noted that the binding constant of Cs^+ is higher than that of the other monovalent cations and therefore more SC4 is occupied with the counterion before addition of titrant. In the range of the titration, the host occupied goes from 57% to 84% (for K = 760 M^{-1}), which means an increment of 27%. For comparison, in the titration of Na^+ the increment is about 38%, therefore we can ruled out that the absence of heat involved in the complexation of Cs^+ by SC4Cs is only due to higher fraction of complexed host at the begin of the titration.

Table 6. Thermodynamic parameters obtained from the counterion-considerate fitting of the experiments corresponding to the titration of K^+ and Cs^+ in SC4@Na solutions as a function of the temperature at neutral pH (7.0).[a,b]

Cation	T (K)	K/M^{-1} [a]	$\Delta G°$/ (kJ mol^{-1})[b]	$\Delta H°$/ (kJ mol^{-1})[b]	$T\Delta S°$/ (kJ mol^{-1})[b]
K^+	283.15	374	–13.9	2.7	16.6
	298.15	217	–13.3	5.3	18.6
	313.15	227	–14.1	7.5	21.6
Cs^+	283.15	763	–15.6	–1.6	14.1
	298.15	760	–16.4	–0.2	16.2
	313.15	---	---	---	---
	338.15	393	–16.8	8.0	24.8

[a] 5% error. [b] Error ± 0.1 kJ mol^{-1}.

As can be seen from Tables 2 and 6, the binding constants for all 3 investigated alkali metal ions (Na^+, K^+ and Cs^+) decrease on increasing the temperature. Intuitively, for an endothermic process, an increase in the temperature would lead to an increase in the value of the binding constant in accordance with the LeChatelier principle. The fact that the expected increase in the binding constant with temperature is not observed points to a sizable temperature dependence of the (endothermic) enthalpy term, which apparently overwhelms the anticipated temperature effect on the entropic contribution.

The physical property of a system which characterizes the temperature dependence of the enthalpy is the heat capacity, in this case at constant pressure (ΔC_p°). Indeed, plotting ΔH° *versus* temperature (Figure 7) yielded a good linear correlation for each cation, from which ΔC_p° was calculated as the slope of the linear regression line according to the definition:

$$\Delta C_p^\circ = \left.\frac{\partial \Delta H^\circ}{\partial T}\right|_P \tag{14}$$

affording positive and very similar values of ΔC_p° = 178 ± 4 J mol^{-1} K^{-1} for Na^+, ΔC_p° = 160 ± 77 J mol^{-1} K^{-1} for K^+, and ΔC_p° = 179 ± 18 J mol^{-1} K^{-1} for Cs^+.

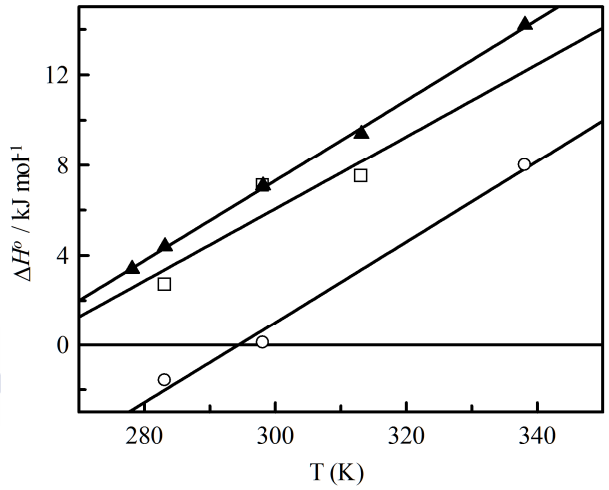

Figure 7. Temperature dependence of the binding enthalpy (ΔH°, determined by ITC) for the complexation of Na^+ (▲), K^+ (□) and Cs^+ (○) by SC4 at neutral pH.

The sign of the differential heat capacity indicates formally that the transfer of the monovalent cation from the aqueous solution to the macrocycle is an order-forming or order-destroying process.[48] Both positive and negative values have been reported for guest binding by macrocycles.[49] It is generally assumed that the hydration of a polar or charged solute is associated with a negative heat capacity, while for the dehydration of polar or ionic groups a positive heat capacity is expected.[50] Therefore, we attribute the positive heat capacity in the complexation of the alkali metal cations with SC4 tentatively to the dehydration of the sulfonato group of the calixarene and the cation itself. This means, in turn, that the affinity of the alkali metal cations to SC4 – although

the complexation is entropically driven – decreases with temperature, because of a positive heat capacity associated with the supramolecular process, particularly involving desolvation.

2.1.3.4. Enthalpy-entropy compensation

Enthalpy-entropy compensation has been widely studied in the formation of supramolecular host-guest assemblies[18,51,52]. By using the presently reported data for the complexation of SC4 with the alkali metal cations (Table 3 and Table 5), the entropy changes ($T\Delta S^{\circ}$) were plotted against the enthalpy changes (ΔH°) according to the equation:

$$T\Delta S^{\circ} = T\Delta S^{\circ}_{\circ} + \alpha\Delta H^{\circ} \qquad (15)$$

to give a good regression line (Figure 8, correlation coefficient $r = 0.94$) with a slope $\alpha = 0.66$ and an intercept $T\Delta S^{\circ}_{\circ} = 15.7$ kJ mol^{-1}. The first term of the equation ($T\Delta S^{\circ}_{\circ}$) is independent of the enthalpy change and describes the extent of complex stabilization in the absence of enthalpic contribution to the driving force; the second term is proportional to it ($\alpha\Delta H^{\circ}$) by a factor, α, that is considered as a quantitative measure of the magnitude of enthalpy-entropy compensation. The α value of 0.66 indicates that 34% of the increase in ΔH° contributes to the increase in complex stability. The positive value of $T\Delta S^{\circ}$ emphasizes that the complexation process is favored even in the absence of any enthalpic gain (*i.e.* $\Delta H^{\circ} = 0$). Enthalpy-entropy compensation effects occur when ΔG^{o} is approximately constant within a reaction series while ΔH° and ΔS° vary significantly.[53,54] Although there exists some criticism regarding the relevance of enthalpy-entropy compensation effects, the method employed in this study (ITC) by-passes some inherent limitations that will always lead to a statistical correlation of the two variables and that is always observed, for example, when thermodynamic parameters are derived from a van't Hoff analysis.[55]

Due to the limited available data for the complexation of monovalent cations by calixarenes and also keeping in mind that the results obtained for different host-guest systems may not be directly comparable as the species that form in supramolecular systems may result from different interactions and may display structural differences, only a qualitative analysis can be attempted. It is noteworthy that the value of the $T\Delta S^{\circ}_{\circ}$ term obtained is smaller than those obtained for the complexation of others

sulfonatocalixarenes with trivalent cations ($T\Delta S_{\circ}$ = 22.5 kJ mol^{-1}),[56] indicating that the entropic gain that arises from the desolvation upon guest inclusion is expectedly smaller for the monovalent cations.

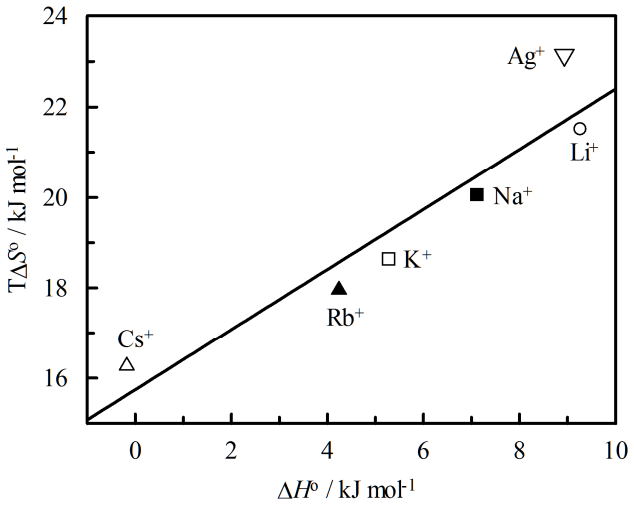

Figure 8. Enthalpy-entropy compensation plot for the complexation of monovalent cations by SC4.

Consequences of Alkali Metal Ion Binding for the Interpretation of Binding Constants and Thermodynamic Parameters of Guest Binding. At first glance, the fact that sodium, the most abundantly used buffer cation, binds significantly (K = 183 M^{-1} at neutral pH) to SC4 may appear like a mechanistic peculiarity and quantitative detail rather than an important experimental desideratum. However, since the notion of a negligible binding of sodium ions, which is additionally an omnipresent counterion of SC4, has been broadly accepted in the literature, numerous binding constants have been measured in buffers, frequently with up to 200 mM sodium ion concentrations. All these binding constants for many different guests, which have been compiled and reviewed for SC4 and its homologues,[3] are only apparent ones[22,24,26,30,31,47,57–60] and can only be compared in relative terms, and only when measured under identical concentrations of buffer, and, strictly speaking, at identical concentrations of SC4 (which supplies itself additional counterions). That the sodium concentration increases in the course of direct host-guest titrations due to the addition of SC4 presents another complication. Small changes in salt concentrations have very large effects on the binding constants and the

comparison of binding constants of different guest may even be misleading if the same buffer, but in different concentrations (e.g., 10 mM versus 100 mM) have been used.

Also important, essentially all thermodynamic parameters *hitherto* measured for SC4 and large sets of guest molecules, are incorrect in absolute terms. The extracted ΔH and ΔS values are actually not the enthalpies and entropies for complexation of the guest molecules, but rather the *difference* between the complexation enthalpies and entropies of the guest and the non-negligible enthalpies and entropies of the sodium ion. It can be readily seen that, with 100 mM sodium buffer, essentially all SC4 is complexed with a sodium ion (Figure 1), such that the addition of a guest and associated calorimetric effects refer to a displacement of sodium rather than to a direct binding event. Here, again, direct interpretations of the guest binding, e.g., in terms of intermolecular interactions or desolvation, are not possible, but only relative trends are meaningful, if the buffer concentration and also the SC4 concentration are both the same. The omnipresent binding of counterions reveals a pitfall of ITC measurements with SC4 as host: Instead of direct host-guest titrations, competitive ones are actually being performed but analyzed according to a direct binding model. The observation of negligible heat effects for a particular guest may actually indicate that the binding is endothermic, and the thermoneutral binding of a guest actually results in a net heat release.

2.1.4. Conclusions

The thermodynamic behavior for the complexation of monovalent and divalent cations by SC4 at neutral pH has been determined by ITC. Two distinct models were employed to fit the microcalorimetric titrations. For the complexation of Na^+ cations by SC4 a sequential model was employed, while for the other cations the competitive binding model was to be employed in order to take into account the counterion of the calixarene. The microcalorimetric study illustrates that, for all cations, the association process is enthalpically unfavorable ($\Delta H^o > 0$) but entropically favorable ($\Delta S^o > 0$), consistent with an electrostatic interaction involving desolvation of charged residues/guests. Experiments at different temperatures corroborate that the enthalpic contribution to guest binding is non-negligible, since the binding constant decreased with temperature (indicative of a positive heat capacity for the process), but did not increase as expected for a purely entropically driven process.

2.1.5. Appendix

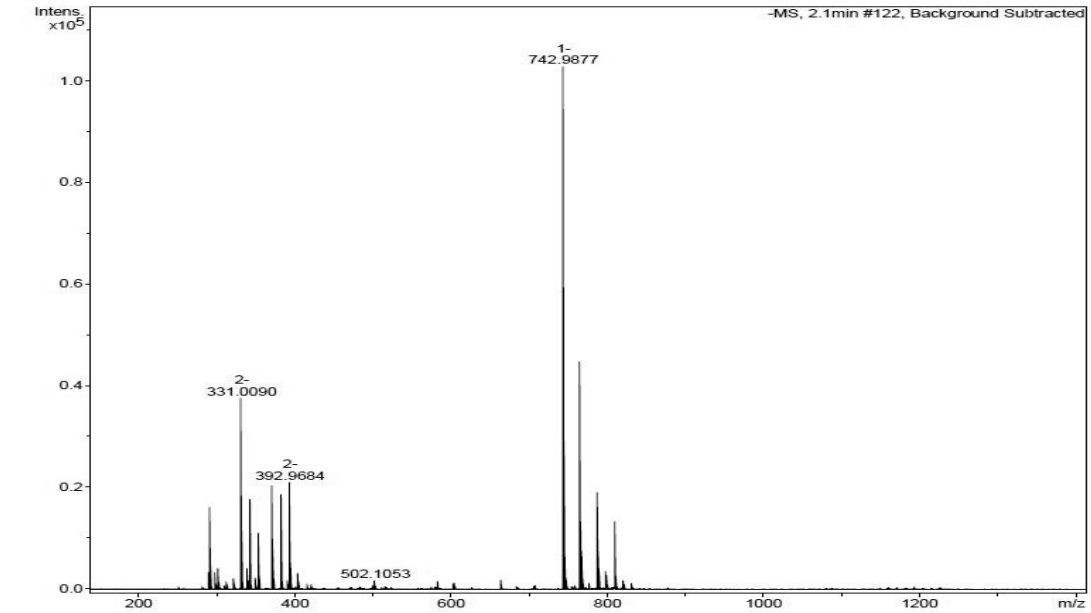

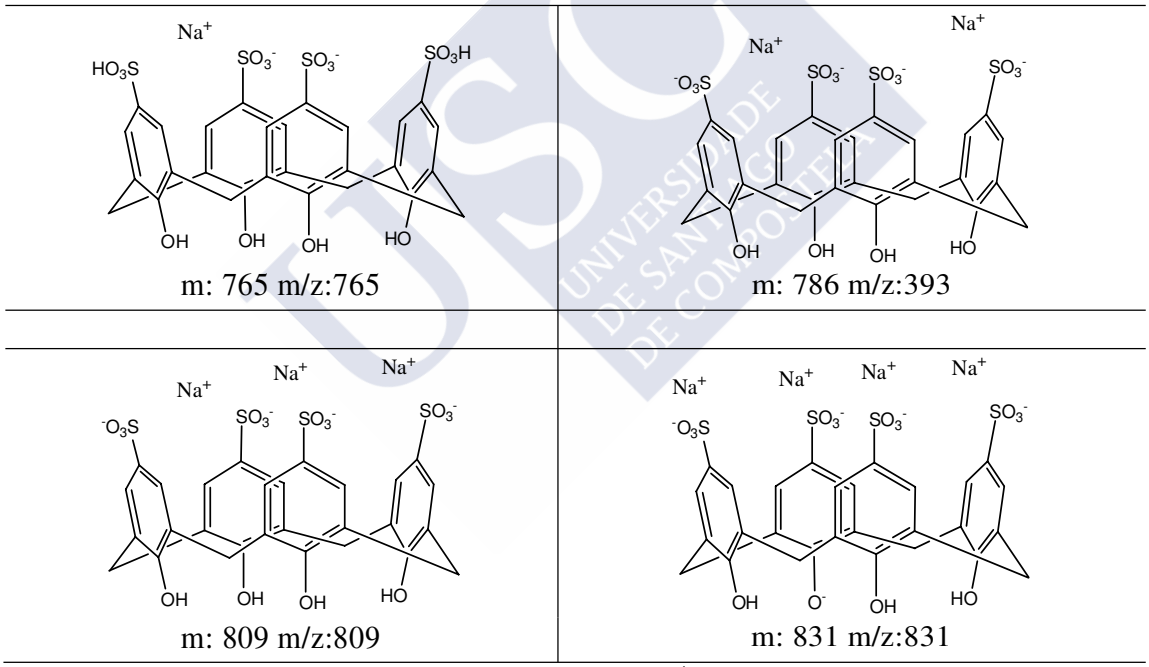

Figure S1. ESI-TOF mass spectrum of SC4 with Na^+ as a counterion.

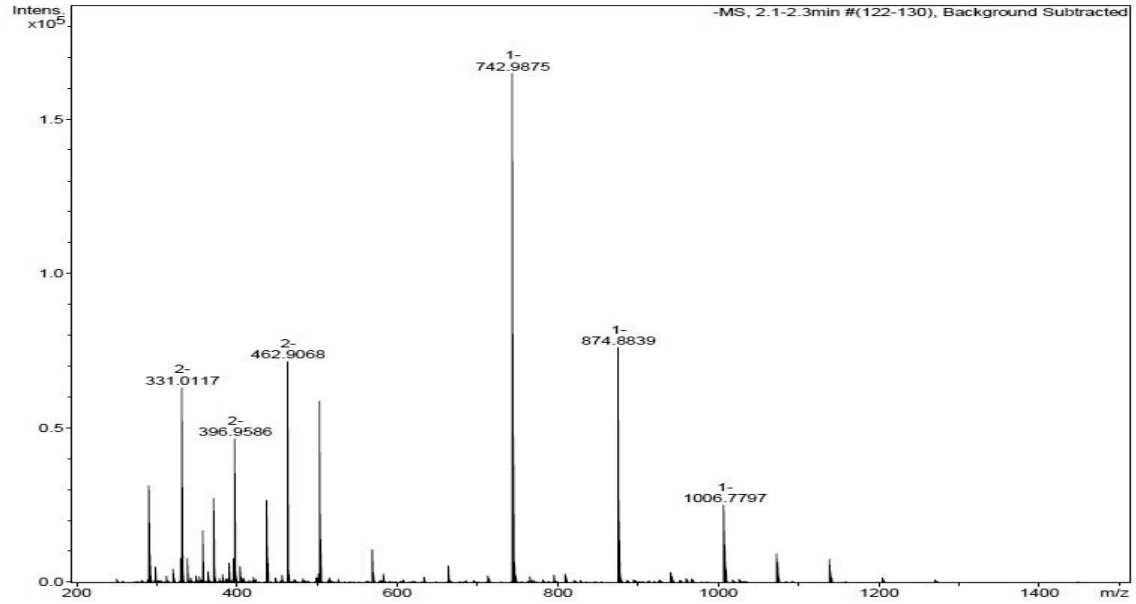

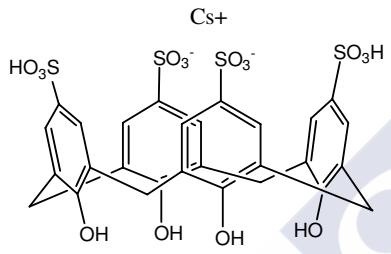

m:875 m/z:875

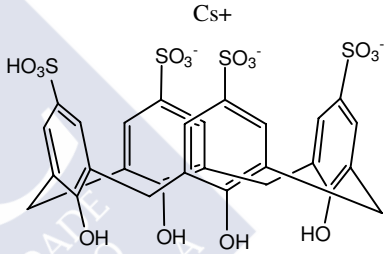

m:874 m/z:437

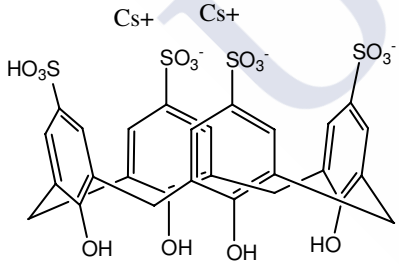

m:1007 m/z:1007

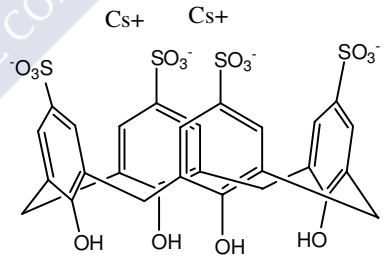

m:1006 m/z:503

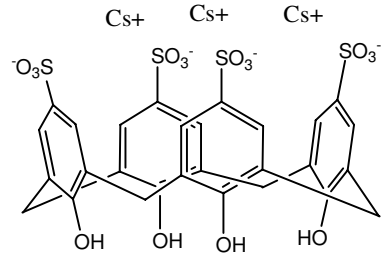

m:1139 m/z:1139

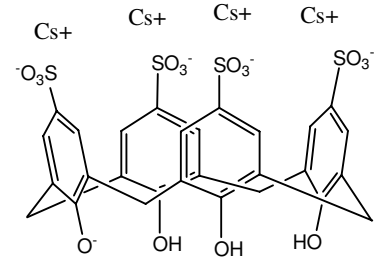

m:1271 m/z:1271

Figure S2. ESI-TOF mass spectrum of SC4 with Cs^+ as a counterion.

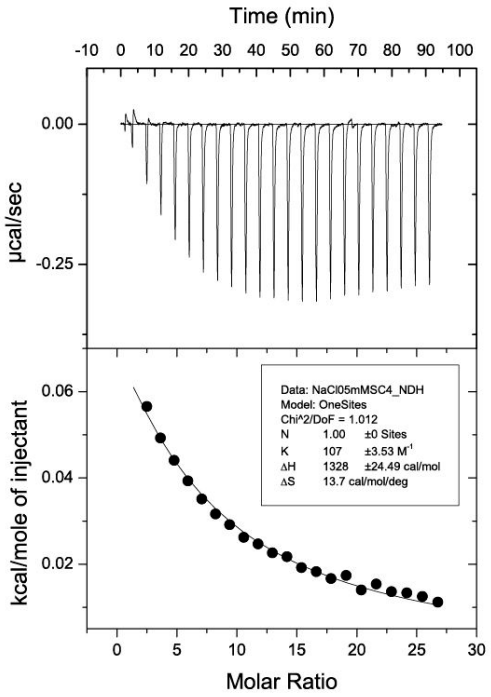

Figure S3. Microcalorimetric titration of SC4 with Na^+ at 298.15 K in aqueous solution: (upper) raw data for sequential 12 µL injections of Na^+ (60 mM) into SC4 (0.5 mM); (down) heat of reaction obtained from the integration of the calorimetric trace after subtracting the dilution heat from the reaction heat and fitted with "one set of binding sites" model.

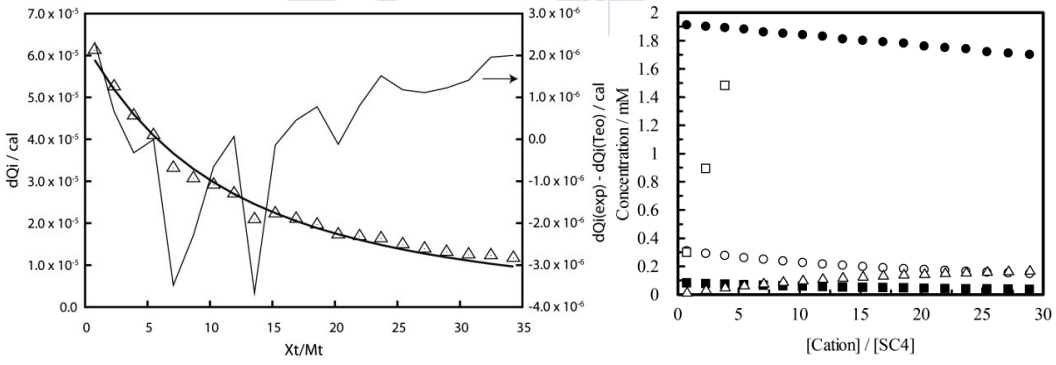

Figure S4. Experimental ITC data (Δ) and fitted curve (thick line) for the titration of Li^+ on SC4 (0.4 mM) with Na^+ as a counterion at 298.15 K. The difference between the fitted and the experimental data is represented by the thin line (right scale). (Right) Concentration of free SC4 (○), free Na^+ (●), free Li^+ (□), and complexes Na@SC4 (■), and Li@SC4 (Δ) as a function of the [LiCl]/[SC4] ratio, calculated from the isotherm at 298.15 K, considering K = 183 M^{-1} and K = 139 M^{-1} for the complexation of Na^+ and Li^+, respectively.

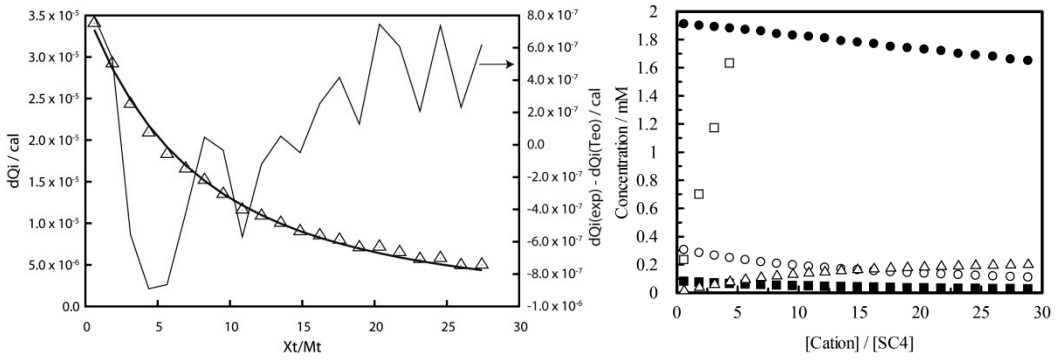

Figure S5. (Left) Experimental ITC data (Δ) and fitted curve (thick line) for the titration of K^+ on SC4 (0.4 mM) with Na^+ as a counterion at 298.15 K. The difference between the fitted and the experimental data is represented by the thin line (right scale). (Right) Concentration of free SC4 (○), free Na^+ (●), free K^+ (□), and complexes Na@SC4 (■), and K@SC4 (Δ) as a function of the [KCl]/[SC4] ratio, calculated from the isotherm at 298.15 K, considering K = 183 M^{-1} and K = 217 M^{-1} for the complexation of Na^+ and K^+, respectively.

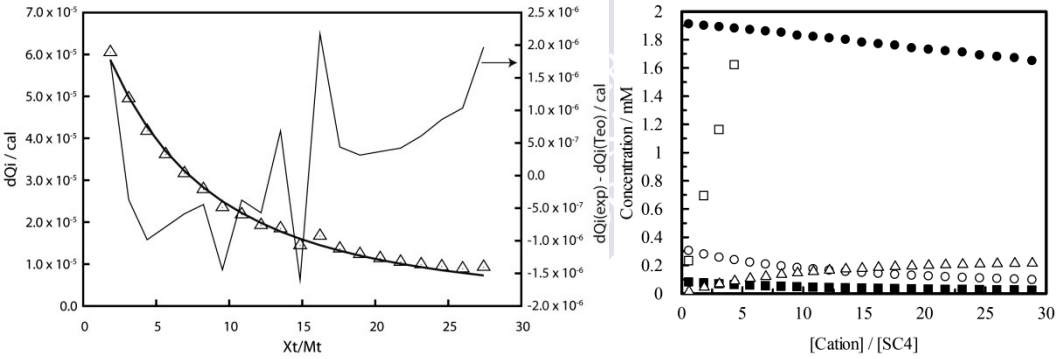

Figure S6. (Left) Experimental ITC data (Δ) and fitted curve (thick line) for the titration of Ag^+ on SC4 (0.4 mM) with Na^+ as a counterion at 298.15 K. The difference between the fitted and the experimental data is represented by the thin line (right scale). (Right) Concentration of free SC4 (○), free counterion Na^+ (●), free Ag^+ (□), and complexes Na@SC4 (■), and Ag@SC4 (Δ) as a function of the [AgCl]/[SC4] ratio, calculated from the isotherm at 298.15 K, considering K = 183 M^{-1} and K = 271 M^{-1} for the complexation of Na^+ and Ag^+, respectively.

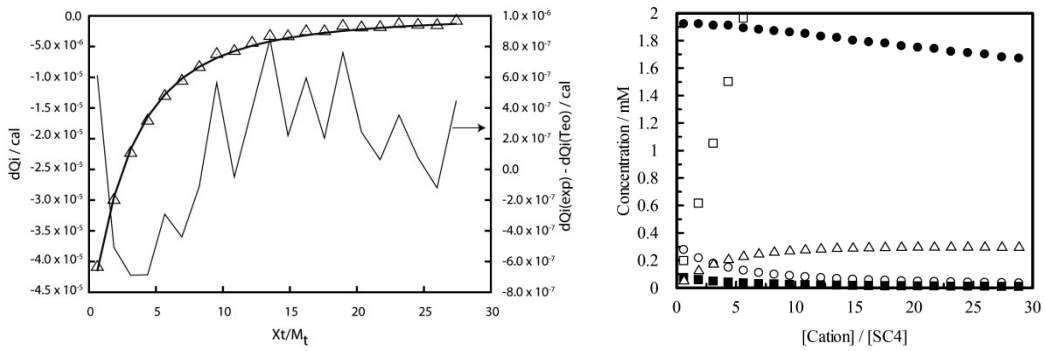

Figure S7. (Left) Experimental ITC data (Δ) and fitted curve (thick line) for the titration of Cs^+ on SC4 (0.4 mM) with Na^+ as a counterion at 298.15 K. The difference between the fitted and the experimental data is represented by the thin line (right scale). (Right) Concentration of free SC4 (○), free counterion Na^+ (●), free Cs^+ (□), and complexes Na@SC4 (■), and Cs@SC4 (Δ) as a function of the [CsCl]/[SC4] ratio, calculated from the isotherm at 298.15 K, considering K = 183 M^{-1} and K = 760 M^{-1} for the complexation of Na^+ and Cs^+, respectively.

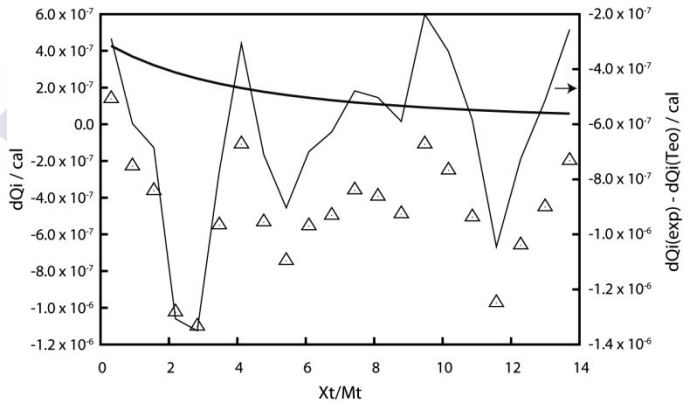

Figure S8. Experimental ITC data (Δ) and fitted curve (thick line) for the titration of Cs^+ on SC4 (0.4 mM) with Cs^+ as counterion at 298.15 K. The difference between the fitted and the experimental data is represented by the thin line (right scale).

2.1.6. References

1. Z. Asfari, V. Bohmer, J. Harrowfield, J. Vicens, *Calixarenes 2001*, Kluwer Academic Publishers, Dordrecht, The Netherlands, **2001**.

2. G. V. Oshovsky, D. N. Reinhoudt, W. Verboom, *Angew. Chem. Int. Ed.* **2007**, *46*, 2366–2393.

3. D.-S. Guo, K. Wang, Y. Liu, *J. Incl. Phenom. Macrocycl. Chem.* **2008**, *62*, 1–21.

4. W. Sliwa, T. Girek, *J. Incl. Phenom. Macrocycl. Chem.* **2010**, *66*, 15–41.

5. K. Suga, T. Ohzono, M. Negishi, K. Deuchi, *Supramol. Sci.* **1998**, *5*, 9–14.

6. I. Yoshida, N. Yamamoto, F. Sagara, D. Ishii, K. Ueno, S. Shinkai, *Bull. Chem. Soc. Jpn.* **1992**, *65*, 1012–1015.

7. S. Shinkai, K. Araki, T. Matsuda, N. Nishiyama, H. Ikeda, I. Takasu, M. Iwamoto, *J. Am. Chem. Soc.* **1990**, *112*, 9053–9058.

8. J.-M. Lehn, R. Meric, J.-P. Vigneron, M. Cesario, J. Guilhem, C. Pascard, Z. Asfari, J. Vicens, *Supramol. Chem.* **1995**, *5*, 97–103.

9. G. Arena, A. Casnati, A. Contino, G. G. Lombardo, D. Sciotto, R. Ungaro, *Chem. Eur. J.* **1999**, *5*, 738–744.

10. G. Arena, A. Contino, F. G. Gulino, A. Magrì, D. Sciotto, R. Ungaro, *Tetrahedron Lett.* **1999**, *40*, 1597–1600.

11. G. Arena, A. Casnati, A. Contino, F. G. Gulino, D. Sciotto, R. Ungaro, *J. Chem. Soc., Perkin Trans. 2* **2000**, 419–423.

12. G. Arena, A. Contino, F. G. Gulino, A. Magrì, D. Sciotto, R. Ungaro, *Tetrahedron Lett.* **2000**, *41*, 9327–9330.

13. N. Kon, N. Iki, S. Miyano, *Org. Biomol. Chem.* **2003**, *1*, 751–755.

14. M. Baur, *Tetrahedron* **2001**, *57*, 6985–6991.

15. Q. Li, D.-S. Guo, H. Qian, Y. Liu, *Eur. J. Org. Chem.* **2012**, *2012*, 3962–3971.

16. N. Douteau-Guével, A. W. Coleman, J. Morel, N. Morel-desrosiers, *J. Phys. Org. Chem.* **1998**, *11*, 693–696.

17. N. Douteau-Guével, A. W. Coleman, J.-P. Morel, N. Morel-Desrosiers, *J. Chem. Soc., Perkin Trans. 2* **1999**, 629–633.

18. C. Bonal, Y. Israëli, J.-P. Morel, N. Morel-Desrosiers, *J. Chem. Soc., Perkin Trans. 2* **2001**, 1075–1078.

19. F. Perret, J.-P. Morel, N. Morel-Desrosiers, *Supramol. Chem.* **2003**, *15*, 199–206.

20. N. Douteau-Guével, F. Perret, A. W. Coleman, J.-P. Morel, N. Morel-Desrosiers, *J. Chem. Soc., Perkin Trans. 2* **2002**, 524–532.

21. H.-J. Buschmann, L. Mutihac, E. Schollmeyer, *J. Incl. Phenom. Macrocycl. Chem.* **2003**, *46*, 133–137.

22. H. Bakirci, A. L. Koner, W. M. Nau, *Chem. Commun.* **2005**, 5411–5413.

23. A. Hennig, W. M. Nau, *Nature Methods* **2007**, *4*, 629–632.

24. W. M. Nau, G. Ghale, A. Hennig, H. Bakirci, D. M. Bailey, *J. Am. Chem. Soc.* **2009**, *131*, 11558–11570.

25. J.-P. Morel, N. Morel-Desrosiers, *Org. Biomol. Chem.* **2006**, *4*, 462–465.

26. N. Basilio, L. García-Río, M. Martín-Pastor, *J. Phys. Chem. B* **2010**, *114*, 7201–7206.

27. D. Cuc, D. Canet, J.-P. Morel, N. Morel-Desrosiers, P. Mutzenhardt, *Chemphyschem* **2007**, *8*, 643–645.

28. D. Cuc, S. Bouguet-bonnet, N. Morel-desrosiers, J. Morel, P. Mutzenhardt, D. Canet, *J. Phys. Chem. B* **2009**, *113*, 10800–10807.

29. L. M. Salonen, M. Ellermann, F. Diederich, *Angew. Chem. Int. Ed.* **2011**, *50*, 4808–4842.

30. V. Francisco, N. Basilio, L. García-Río, *J. Phys. Chem. B* **2012**, *116*, 5308–5315.

31. H. Bakirci, A. L. Koner, T. Schwarzlose, W. M. Nau, *Chem. Eur. J.* **2006**, *12*, 4799–4807.

32. H. Bakirci, A. L. Koner, M. H. Dickman, U. Kortz, W. M. Nau, *Angew. Chem. Int. Ed.* **2006**, *45*, 7400–7404.

33. R. Lamartine, J.-B. Regnouf-de-Vains, P. Choquar and A. Marcillac, *World Patent*, **1997**, WO 97/49677.

34. J. L. Atwood, A. W. Coleman, H. Zhang, S. G. Bott, *J. Incl. Phenom. Macrocycl. Chem.* **1989**, *7*, 203–211.

35. S. Shinkai, S. Mori, T. Tsubaki, T. Sone, O. Manabe, *Tetrahedron Lett.* **1984**, *25*, 5315–5318.

36. K. Fucke, K. M. Anderson, M. H. Filby, M. Henry, J. Wright, S. a Mason, M. J. Gutmann, L. J. Barbour, C. Oliver, A. W. Coleman, et al., *Chem. Eur. J.* **2011**, *17*, 10259–10271.

37. C. A. Schalley, in *Analytical Methods in Supramolecular Chemistry*, Wiley-VCH Verlag GmbH&Co. KGaA, Weinheim, Germany, **2012**, pp. 67–103.

38] A. Velazquez-Campoy, E. Freire, *Nature protocols* **2006**, *1*, 186–91.

39. J. Tellinghuisen, *Anal. Biochem.* **2008**, *373*, 395–397.

40. M. Faraji, A. Farajtabar, F. Gharib, *J. Serb. Chem. Soc.* **2013**, *78*, 681–688.

41. W. B. Turnbull, A. H. Daranas, *J. Am. Chem. Soc.* **2003**, *125*, 14859–14866.

42. W. H. Press, S. A. Teukolsky, W. T. Vetterling, B. P. Flannery, *Numerical Recipes in C++. The Art of Scientific Computing*, Cambridge University Press, Cambridge, UK, **2002**.

43. A private version of our software AFFINImeter was employed to perform all the calculations. For more details in the minimization of the objective function by the simulated annealing algorithm, as well as the determination of the complexed and uncomplexed species using the Newton-Raphson algorithm, see: P. Brocos, X. Banquy, N. Díaz-vergara, P. Silvia, M. Costas, and A. Piñeiro, *J. Phys. Chem. B*, 2011, **115**, 14381–14396.

44. The anion (chloride) was kept the same for the different types of cations, except for Ag^{+} and Ni^{2+} (nitrate), although anions were shown not to affect the complexation process (cf., C. Bonal, Y. Israëli, J.-P. Morel, and N. Morel-Desrosiers, *J. Chem. Soc., Perkin Trans. 2*, 2001, 1075–1078; Y. Israëli, C. Bonal, C. Detellier, J.-P. Morel, and N. Morel-Desrosiers, *Can. J. Chem.*, 2002, **80**, 163–168).

45. A. W. Coleman, S. G. Bott, S. D. Morley, C. M. Means, K. D. Robinson, H. Zhang, J. L. Atwood, *Angew. Chem. Int. Ed.* **1988**, *1*, 1361–1362.

46. K. Wang, D.-S. Guo, H.-Q. Zhang, D. Li, X.-L. Zheng, Y. Liu, *J. Med. Chem.* **2009**, *52*, 6402–6412.

47. D.-S. Guo, H.-Q. Zhang, F. Ding, Y. Liu, *Org. Biomol. Chem.* **2012**, *10*, 1527–1536.

48. A. Olvera, S. Pérez-Casas, M. Costas, *J. Phys. Chem. B* **2007**, *111*, 11497–11505.

49. M. Stödeman, N. Dhar, *J. Chem. Soc., Faraday Trans.* **1998**, *94*, 899–903.

50. A. I. Dragon, J. Klass, C. Read, M. E. A. Churchill, C. Crane-Robinson, P. L. Privalov, *J. Mol. Biol.* **2003**, *331*, 795–813.

51. Y. Inoue, Y. Liu, L.-H. Tong, B.-J. Shen, D. Jing, *J. Am. Chem. Soc.* **1993**, *115*, 10637–10644.

52. Y. Liu, H. Wang, L.-H. Wang, H.-Y. Zhang, *Thermochim. Acta* **2004**, *414*, 65–70.

53. O. Exner, *J. Phys. Org. Chem.* **1997**, *10*, 797–813.

54. O. Exner, *Chem. Commun.* **2000**, 1655–1656.

55. A. Cornish-Bowden, *J. Biosci.* **2002**, *27*, 121–126.

56. Y. Liu, H. Wang, L.-H. Wang, H.-Y. Zhang, *Thermochim. Acta* **2004**, *414*, 65–70.

57. H. Bakirci, A. L. Koner, W. M. Nau, *J. Org. Chem.* **2005**, *70*, 9960–9966.

58. D.-S. Guo, V. D. Uzunova, X. Su, Y. Liu, W. M. Nau, *Chem. Sci.* **2011**, *2*, 1722–1734.

59. V. Wintgens, L. Biczók, Z. Miskolczy, *Thermochim. Acta* **2011**, *523*, 227–231.

60. Y. Sueishi, H. Mori, N. Inazumi, *J. Incl. Phenom. Macrocycl. Chem.* **2013**, *75*, 235–238.

USC
UNIVERSIDADE
DE SANTIAGO
DE COMPOSTELA

2.2. Counterion Exchange as a Decisive Factor in the Formation of Host:Guest Complexes by *p*-Sulfonatocalix[4]arene

2.2.1. Introduction

Calixarenes are host frameworks that belong to the most versatile building blocks in supramolecular chemistry. When they are functionalized at upper rim with sulfonate groups, these calixarenes become water-soluble, which combined with a preorganized framework and biological compatibility,[1,2] allow that these calixarenes have a variety of applications in fields such as molecular recognition/sensing,[3] crystal engineering,[4,5] catalysis,[6] enzyme mimics/enzyme assays[7,8] and medicinal chemistry.[9,10] Consequently, *p*-sulfonatocalixarenes are one of the most studied derivatives in complexation of inorganic cations, organic ammonium cations, pyridiniums and viologens, neutral organic molecules and others.[11]

Depending on the guest, different types of interactions can be involved (ionic, hydrophobic, van der Waals, π–π, cation–π, hydrogen bonding,...), as demonstrated by the thermodynamic characterization of the binding process.[12] The binding affinities and the thermodynamics of *p*-sulfonatocalixarene upon metal ions were investigated by Bonal[13] and Morel-Desrosiers,[12] but according to the authors, significant heat effects were not detected for Na^+ and Ag^+, suggesting that these cations are not complexed. However, in the previous section (2.1), we quantified that SC4 fully binds an Na^+ counterion. Because of the anionic nature of SC4, Na^+ (or other counterions) are always present in solution and can introduce a competitive binding equilibria in the presence of other guests.

In addition to the complexation of inorganic cations by SC4, organic ammonium cations are other class of typical guest which has been extensively studied.[11] Most of these studies have been done by varying the concentration of the host or in the presence of a buffer solution.

Since Na^+ binds to the SC4, then a competition between the guest and the counterions should be considered. As a result, the binding constants should be affected by the SC4 concentration. Since most of the binding studies involving SC4 and guest species have been done by varying the host concentration, it is important to evaluate the effect of this parameter on the binding constants. In the present work, we show that contrary to the traditional point of view the binding constant of

benzyltrimethylammonium ion (BTA) decrease almost 10 times when the SC4 concentration is increased from 0.075mM to 7mM of SC4. NMR and isothermal titration calorimetry (ITC) experiments have been employed to measure the binding constant of the organic ammonium cation with SC4 at various concentrations.

2.2.2. Experimental Section

Materials. Benzyltrimethylammonium chloride (BTA) Aldrich (97%) and NaCl from Fluka (assay ≥ 99.5%) were used as received. *p*-Sulfonatocalix[4]arene (SC4) was prepared by *ipso*-sulfonation of *p-tert* butylcalixarene in H_2SO_4 at 80 °C.

The pK_a values of SC4 (3mM) was determined by pH-metric titration method and the pK_{a1} = 3.6 and pK_{a2} = 11.9 were obtained (the data were analyzed using the program HyperQuad,[14] see Appendix, Figure S1). These results are qualitatively in agreement with the results reported in the literature.[15]

Measurements of acid-dissociation constant. Fully automated titrations were performed using a Crison microBU 2031 autoburette and a Crison 2002 pH meter. The program controlling the experiments incorporated certain restrictions to ensure reproducibility and to avoid stabilization problems and electrode drift (Radiometer GK2401C, Ag/AgCl reference). After addition of the titrant and sample homogenization, the potential value was read every 3 s until obtaining a set of six values that complied with the condition that the difference between any two consecutive measurements was less than 0.2 mV. The actual value of the potential was then calculated as the average of the set of six measurements whenever the standard error of the average did not exceed 0.2 mV. If the restrictions were not fulfilled, a new process for potential measurement was started. Aqueous solutions of SC4 (3mM) and SC4 (3 mM) in the presence of BTA (3 mM) containing the definite concentration of HCl were placed in a thermostated cell at 298.0 ± 0.1 K and titrated by adding small aliquots KOH CO_2-free solution. Water-saturated N_2 was bubbled through the solution to maintain a CO_2-free atmosphere. Before each titration, the electrode was calibrated for H^+ ion concentration by titrating a strong acid (HCl) with a strong base (KOH).

Diffusion NMR. NMR spectra were recorded at 25°C on a Varian Inova 500 spectrometer by using DSS as an external reference and equipped with a 5 mm 1H/X indirect probe with Z-shielded gradients. The NMR experiments were processed with MestreC v.3.9 software (Mestrelab Inc.).^{1}H and ^{23}Na diffusion spectra were acquired with the Hahn spin-echo based PGSE pulse sequences.[16] In both cases, rectangular-shaped pulsed gradients (G) were applied with a power level linearly incremented from 4 to 65 G cm^{-1} in 32 steps. The duration of the pulse field gradients (δ) applied to encode and decode the diffusion was set to 1ms for ^{1}H and 3 ms for ^{23}Na. The diffusion delay period Δ of the experiment was optimized to 100 ms for ^{1}H and 40 ms for ^{23}Na. Such an optimized Δ value provided a convenient sampling of the exponential decay of the signal intensity during the diffusion experiment and this was essential to achieve accurate results for the determined diffusion coefficients.[17] Calibration of the absolute gradient strength was provided by the spectrometer and the particular probe was calibrated with the actual diffusion pulse sequence by using a compound of known diffusion as a reference.[18] The reference sample for the ^{1}H diffusion experiments was 99% D_2O at 25 °C (D) 1.87×10^{-5} cm^2 s^{-1}) and for the ^{23}Na diffusion experiments was 2 M NaCl solution in 10% D_2O in H_2O at 25 °C (D = 1.14×10^{-5} cm^2 s^{-1}). As expected, both reference samples provided the same gradient strength with an error of less than 1%.

Microcalorimetry. The microcalorimetric titrations were performed on an isothermal titration microcalorimeter (VP-ITC) from Microcal Co. (Northampton, MA) at atmospheric pressure and 25 °C. The ORIGIN software (Microcal Inc.), which was used to compute the binding constant (K) from a single titration curve, gave a standard deviation based on the scatter of the data points in the titration curve. The net reaction heat in each run was calculated by the ‘‘one set of binding sites’’ model. Additionally, the first point was removed from the titration curve before doing the curve-fit, because of the probably leakage resulting from having the syringe stirring all the time in the cell a long time before the first injection, giving a smaller heat effect than it should have. To check the accuracy of binding constant, two independent titration experiments were carried out and their average values were listed in the table.

2.2.3. Results and Discussion

A set of ^{1}H NMR spectra were recorded keeping constant the BTA concentration, at 1 and 7 mM (Figure 1), at different SC4 concentrations.

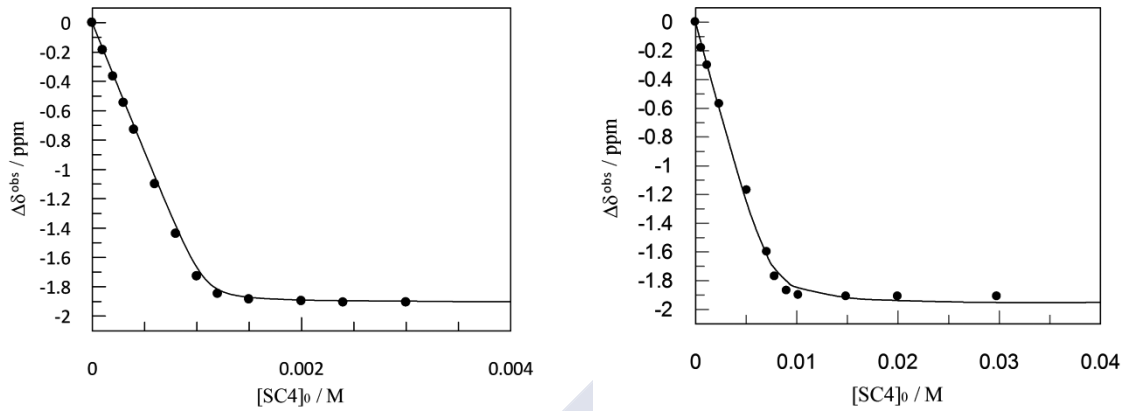

Figure 1. Plots of $\Delta\delta^{obs}$ (ppm) for trimethylammonium group signal of BTA *vs* SC4 concentration in D_2O at 25 °C. (Left) [BTA] = 1mM; (Right) [BTA]= 7mM. Solid lines were obtained by fitting the experimental data to eqs 4 and 2.

In all cases, the guest protons were observed as a single resonance due to the fast exchange between a free guest and a complexed one on the NMR time scales;[18] therefore, the chemical shifts observed (δ_{obs}) for the BTA signals in the spectra are given by

$$\delta^{obs} = \chi^f \delta^f + \chi^c \delta^c = (1 - \chi^c)\, \delta^f + \chi^c \delta^c \quad (1)$$

where χ^f and χ^c are the mole fraction of free and complexed BTA, respectively, and δ^f and δ^c are the chemical shifts for a specific signal of free and complexed BTA.

Defining chemical shift differences as $\Delta\delta^{obs} = \delta^{obs} - \delta^f$ and $\Delta\delta^{max} = \delta^c - \delta^f$ allows eq 1 to be expressed as

$$\Delta\delta^{obs} = \Delta\delta^{max}\, \chi^c \quad (2)$$

Since BTA forms a complex with 1:1 stoichiometry with SC4,[19] K_{obs} is defined as

$$K_{obs} = \frac{[BTA@SC4]}{[SC4][BTA]} \quad (3)$$

Solving the quadratic equation resulting from the insertion of the mass balance in eq 3, we can obtain the expression that depict the complex concentration variation as a function of the total concentration of host and guest (eq 4)

$$[BTA@SC4] = \frac{K_{\text{obs}}([SC4]_0 + [BTA]_0) + 1}{2K_{\text{obs}}} - \frac{\sqrt[2]{\{(K_{\text{obs}}[SC4]_0 - K_{\text{obs}}[BTA]_0)^2 + 2K_{\text{obs}}([SC4]_0 + [BTA]_0) + 1\}}}{2K_{\text{obs}}} \quad (4)$$

The K_{obs} values have been determined through an iterative method (eq 4 and eq 2), and the results have been fitted to the experimental values of δ^{obs}. The observed binding constants, K_{obs}, obtained for 1 mM and 7 mM were 3.25×10^5 M^{-1} and 1.7×10^4 M^{-1}, respectively. In order to corroborate these NMR data, we demonstrate by microcalorimetry that the observed binding constant of BTA by SC4 (K_{obs}) depends on the SC4 concentration. A representative titration curve is shown for 0.1 mM and 0.25 mM (Figure 2), and as can be seen, each titration of BTA into the sample cell gave an apparent reaction heat, caused by the formation of an inclusion complex between BTA and SC4.

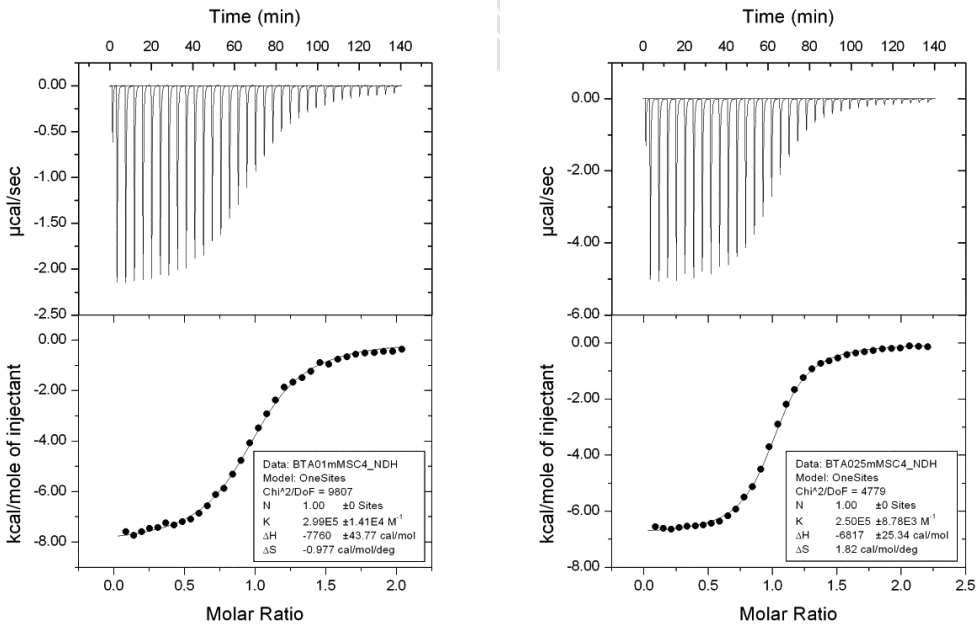

Figure 2. Microcalorimetric titration of BTA with SC4 at 25 °C: raw data for sequential 34 injections (8 μL per injection) of BTA solution (1 or 2.5 mM) injecting into SC4 solution (0.1 mM, left) and (0.25 mM, right): apparent reaction heat obtained from the integration of calorimetric traces.

The reaction heat decreases after each injection of BTA because less and less host molecules are available to form inclusion complexes. A control experiment was carried out in each run to determine the dilution heat by injecting BTA into Milli-Q water. The dilution heat determined to each run was subtracted from the apparent reaction heat measured in the titration experiments to give the net reaction heat. As can be seen in Figure 3, the K_{obs} values range from 3.05×10^5 M^{-1} to 3.40×10^4 M^{-1} by changing the SC4 concentration from 0.075 mM until 7 mM, and therefore corroborate the difference of K_{obs} obtained by NMR for the two selected concentration of host.

pH-metric titration curve of SC4 was measured in the presence of equimolar concentration of BTA (3 mM), and the values of pK_{a1} = 3.1 and pK_{a2} = 12.5 were obtained (see Appendix, Figure S1). If we compare with the values obtained for the SC4 without adding BTA, the pK_{a1} and pK_{a2} have a change of –0.5 and 0.6, respectively. Since the experiments were performed at neutral pH, this confirms that in the complexation the calixarenes do not release another proton that could yield a heat effect that interferes with the binding process.

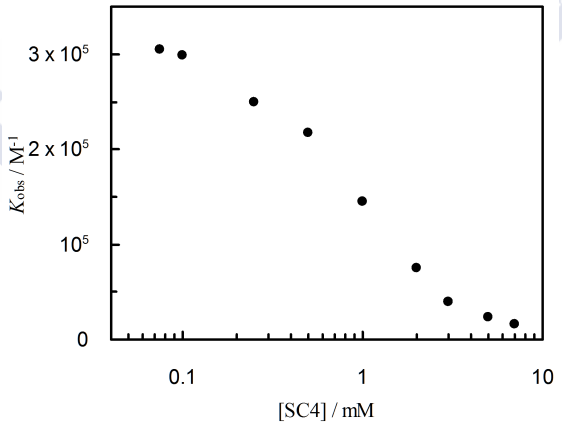

Figure 3. Influence of SC4 concentration on K_{obs} for the complex formation between BTA and SC4 at 25 °C. The K_{obs} values were obtained by microcalorimetric titrations and fitted to the "one set of binding sites" model.

In the previous section, we confirm by ITC that SC4 fully binds a Na^+ counterion with a binding constant of K_{Na} = 183 M^{-1}. Knowing the equilibrium constant of Na^+, we can calculate the fraction (%) of SC4 free of Na^+ cations that exists in solution as a function of the total calixarene concentration (Figure 4). In the figure, we show how the percentage and the concentration of sodium free SC4 varies compared to the total

concentration of the calixarene. As can be observed, the percentage of sodium free macrocycle decreases on increasing the total concentration of SC4. The absolute concentration of uncomplexed calixarene increases with increasing total concentration but not in a linear way.

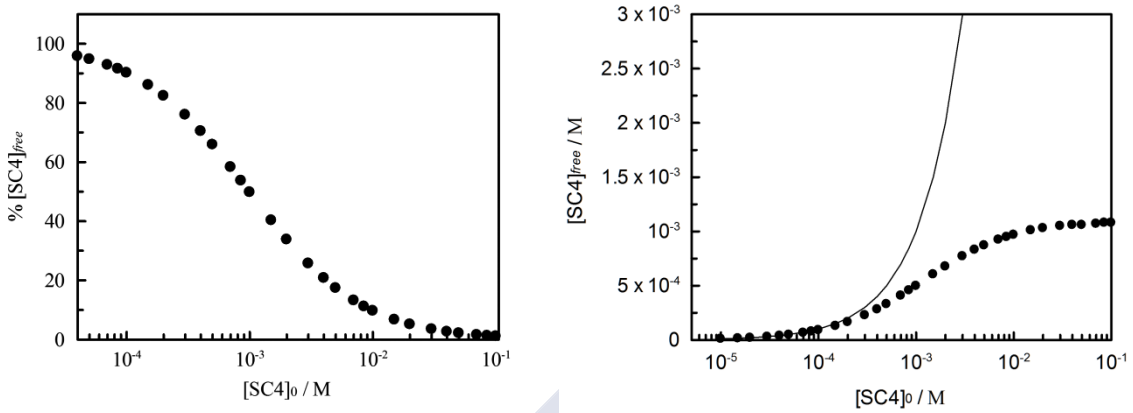

Figure 4. Percentage (left) and concentration of free SC4 (right) *vs* the total concentration of calixarene, $[SC4]_0$. The line represents the variation of the SC4 free *vs* the total concentration in the case where the complexation of Na^+ ions is neglected.

However, much of the studies between a guest and SC4 have been done by varying the concentration of host which implies a change in the state of complexation of SC4, or in the presence of a buffer solution. For example at 0.1 mM of SC4 ca. 92% is free of Na^+ cations but for 2 mM of calixarene only 38% of SC4 is uncomplexed (Figure 4). Our results show that the binding constant decrease on increasing the calixarene concentration, which is in agreement that at lower SC4 concentration, the fraction of Na^+ associated with SC4 is smaller than at higher SC4 concentration, and therefore, changing the SC4 concentration change the fraction of cation associated to SC4. Thus to determine the value of the binding constant of BTA to SC4 the values should be extrapolated at infinite dilution of calixarene.

In the literature, the stoichiometry for the BTA@SC4 complex show that SC4 can only accommodate one BTA molecule in its hydrophobic cavity. However, since inorganic cations can be complexed by SC4, it is important to demonstrate if the complexation of BTA by SC4 is an exchange process or if might exist another stoichiometry such as ternary complexes. To corroborate this hypothesis we performed ^1H and ^{23}Na DOSY experiments on 10 mM SC4 solution to which BTA is added successively. In a previous work[15] we demonstrate that in 10mM SC4 solution ca. 8mM

exists in the form of Na@SC4 complex, thereby if only a 1:1 complex between BTA and SC4 is present in solution, the diffusion coefficient of Na^+ should increase to a level close to that observed for free Na^+ when BTA is successively added.

Quantitative analysis of the intensity of a relevant echo peak in the diffusion spectrum provided the respective translational diffusion coefficient of the corresponding molecule or ion. This is achieved by nonlinear fitting of the signal intensity to the Stejskal-Tanner (eq 5) (ref 18 and references therein):

$$I = I_0 \exp[-D\gamma^2 G^2 \delta^2 (\Delta - \delta/3)] \qquad (5)$$

where I is the measured signal intensity, I_0 is the signal intensity at the lowest gradient pulse power, γ is the magnetogyric ratio of the observed nucleus, and the rest of the parameters are defined above in the experimental section. In all experiments, the intensity decay of the signals gave good fits to the monoexponential eq 5, which shows that they represent a single self-diffusion coefficient. As an example, the experimental intensities and the respective nonlinear fit to eq 5 of a ^1H and ^{23}Na signal are shown in Figure 5.

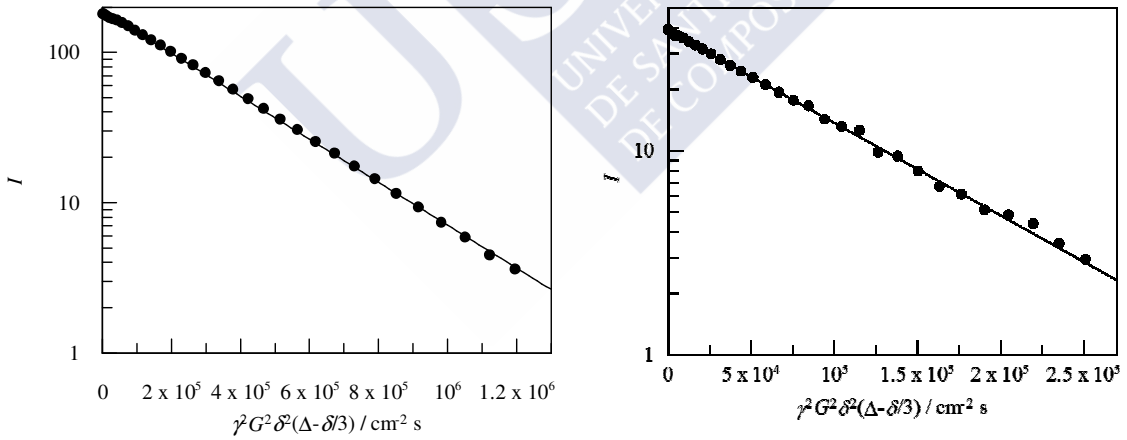

Figure 5. ^1H (left) and ^{23}Na (right) signal decay for a 10 mM SC4Na sample in D_2O at 25 °C. The solid line shows the nonlinear fit to the Stejskal–Tanner eq 5.

The diffusion coefficient obtained for SC4 does not vary significantly when adding BTA; however, as shown in Figure 6, the observed diffusion coefficient, D_{obs}, for the Na^+ cation increases to a value close to that of free Na^+ in bulk solution, suggesting that Na^+ is replaced by BTA molecules inside the calixarene. This excludes

the possibility of formation of ternary complexes and confirms both the formation of 1:1 complexes between BTA and SC4 and the presence of an exchange process (Scheme 1).

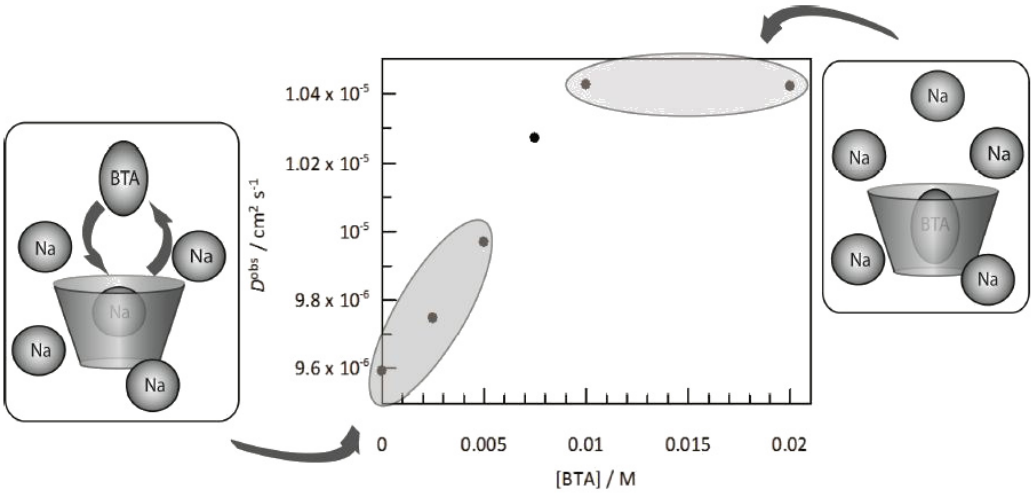

Figure 6. Influence of BTA concentration in the diffusion coefficient of Na^+ for a 10mM sulfonatocalix[4]arene solution in D_2O at 25 °C.

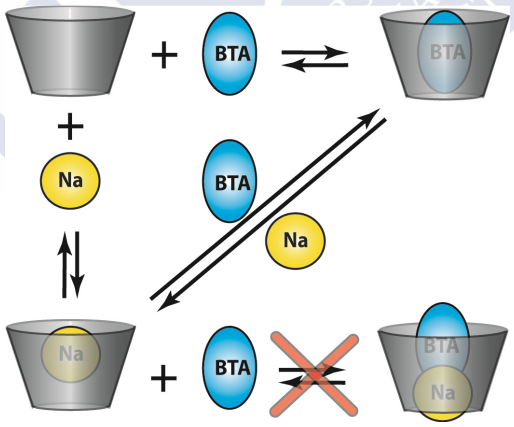

Scheme 1

Opposite experiments, i.e., BTA displacement from the cavity of the calixarene on adding sodium counterions, have been carried out by using the ^1H NMR signals of the trimethylammoniun group and confirm the hypothesis of an ionic exchange complexation (see below).

In an effort to gain further insights into the influence of Na^+ cation in the complexation of BTA by SC4, ^1H NMR and ITC experiments were performed to determine the influence of the cation concentration on the binding constants (Table 1).

In the NMR experiments, different concentrations of NaCl were added to the experiments in which SC4 was successively added to a constant concentration of BTA. We choose keep the BTA concentration constant instead of the SC4 concentration because despite changing the SC4 concentration we change the fraction of Na^+ concentration inside the calixarene, this is the titration method employed by other authors.[19] The K_{obs} values (Table 1, right) have been determined through an iterative method as explained above.

When we compare the K_{obs} obtained by NMR with ITC experiments, we can observe a discrepancy in the higher values of the binding constants obtained at small concentration of added sodium cations (typically binding constants higher than 10^4 M^{-1}). This can be explained with the reliability of the K_{obs} determined by NMR experiments for the concentration of guest chosen, since for 1 mM of BTA the limit for direct NMR titration is about 10^4 M^{-1} and therefore the K_{obs} obtained above this limit can only be estimated. The problem with measuring large K_{obs} (>10^4 M^{-1}) is that there is no curvature in the $\Delta\delta$ versus $[H]_0/[G]_0$ plot at realistic reagent concentrations. The guest is effectively completely complexed by any available host and the graph therefore rises linearly with increasing $[H]_0$ until $\Delta\delta_{max}$ is reached at the 1:1 stoichiometry.[20,21]

A representative titration curve obtained by ITC for the complexation of BTA by SC4 at different NaCl concentration is shown in Figure 7. We noted that at 150mM of added NaCl (ITC experiments) the constant is similar to the literature when comparing the results obtained by other groups through NMR[19] and calorimetric[22] techniques using buffer solutions. We also performed titration in the presence of two different concentrations of phosphate buffer solution at pH 7.2. By changing the buffer concentration from 50 mM to 100 mM, the binding constant for the complex between SC4 and BTA is reduced by half (see Appendix, Table S1 and Figure S2). These values are comparable with the change in the binding constant obtain when the experiments were performed in the presence of different NaCl concentrations.

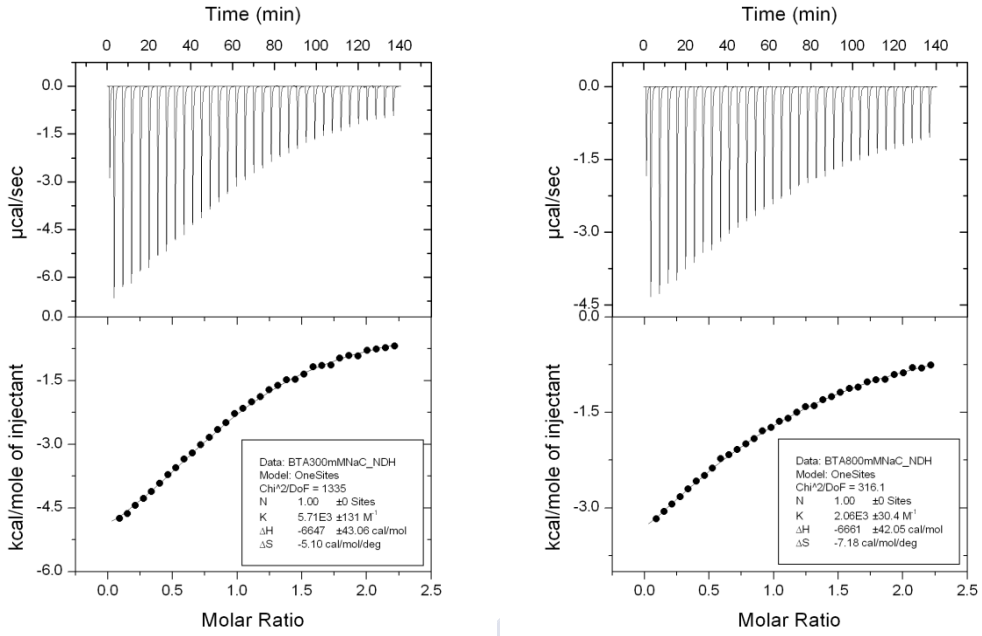

Figure 7. Microcalorimetric titration of BTA with SC4 at 25 °C: raw data for sequential 34 injections (8 μL per injection) of BTA solution (5.2 mM) injecting into SC4 solution (0.5 mM) in the presence of 300 mM of NaCl (left) and 833 mM NaCl (right): apparent reaction heat obtained from the integration of calorimetric traces.

Table 1. Binding constants (K_{obs}) determined by ITC and NMR experiments for 1:1 intermolecular complexation of BTA with SC4 at different added Na^+ concentration.[a]

$[Na^+]_{add}$ (mM)	K_{obs} (M^{-1}) (ITC)	$[Na^+]_{add}$ (mM)	K_{obs} (M^{-1}) (NMR)
---	220000 ± 780	10	185000
10	81700 ± 309	20	95000
20	54600 ± 184	50	45000
40	31000 ± 196	100	24500
80	17100 ± 253	200	11500
150	11000 ± 141	400	5200
300	5711 ± 89	700	2650
833	2060 ± 55	1000	1850
1666	1007 ± 67		

[a] ITC binding constants were obtained in experiments keeping constant the SC4 concentration, 0.5 mM, and varying the BTA concentration. NMR binding constants were obtained in experiments keeping constant the BTA concentration, 1 mM, and varying the SC4 concentration.

In order to analyze the data in Table 1, we propose a complexation model where the Na^+ ions compete with BTA to be complexed by SC4 (Scheme 2).

$$\text{BTA} + \text{SC4} \overset{K_{\text{BTA}}}{\rightleftharpoons} \text{BTA@SC4} \qquad (a)$$

$$\text{Na}^+ + \text{SC4} \overset{K_{\text{Na}}}{\rightleftharpoons} \text{Na@SC4} \qquad (b)$$

$$\text{BTA} + \text{Na@SC4} \overset{K_{\text{E}}}{\rightleftharpoons} \text{BTA@SC4} + \text{Na}^+ \qquad (c)$$

Scheme 2

In this scheme, the exchange constant that measures the affinity of Na@SC4 for BTA, K_E, can be defined as $K_{\text{BTA}}/K_{\text{Na}}$. Moreover, according to the above scheme, the observed binding constant can be defined by equation 6.

$$K_{\text{obs}} = \frac{[BTA@SC4]}{[BTA]([SC4] + [Na@SC4])} \qquad (6)$$

Combining this equation with equations *a* and *b* from Scheme 2, and assuming that the added amount of sodium cation, $[\text{Na}^+]_0$, is much higher than the sodium cations supplied by the SC4, we can deduce the equation that define the dependence of K_{obs} with Na^+ concentration:

$$K_{\text{obs}} = \frac{K_{\text{BTA}}}{(1 + K_{\text{Na}}[\text{Na}^+]_{\text{o}})} \qquad (7)$$

$$\frac{1}{K_{\text{obs}}} = \frac{1}{K_{\text{BTA}}} + \frac{K_{\text{Na}^+}}{K_{\text{BTA}}}[\text{Na}^+]_{\text{o}} \qquad (8)$$

Figure 8 (left) shows the influence of sodium concentration on the observed binding constant, K_{obs}, for BTA by SC4 for experiments carried out by ITC. Figure 8 (right) shows a plot of the inverse of K_{obs} against Na^+ concentration according to equation 8. From the linear fit of the experimental data to eq 8 we get K_{Na} = 138 M^{-1}, which is compatible with the value reported in the previous section (2.1). The value

obtained for K_{BTA} was 3.29×10^5 M^{-1}. The curve-fitting analysis of K_{obs} obtained by NMR experiments at different Na^+ concentration (see Appendix, Figure S4) is comparable with the results obtained by ITC since the association constant obtained for K_{BTA} was 3.28×10^5 M^{-1} and 100 $M^{-1}$for K_{Na} despite the accuracy of the K_{obs} obtained by this technique.

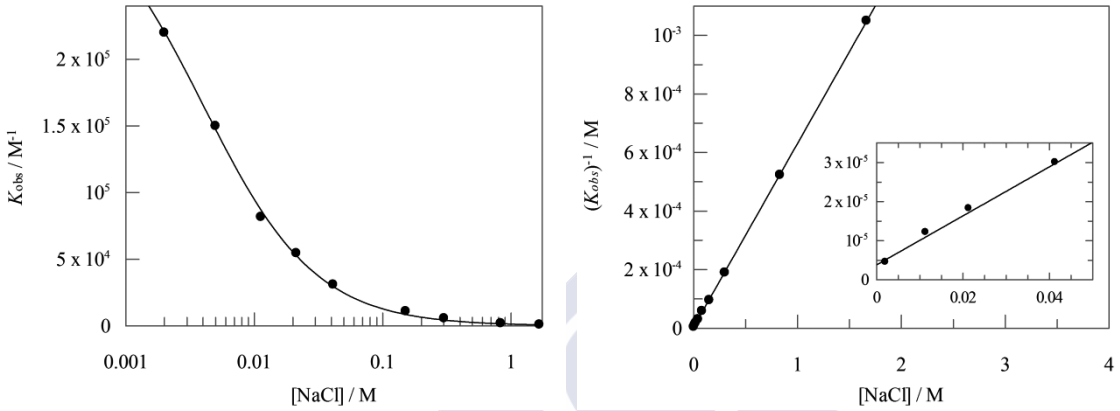

Figure 8. Influence of NaCl concentration in K_{obs} (left) and $1/K_{obs}$ (right) for the complex formation between BTA and SC4. The $K_{obs}$was obtained by microcalorimetric titration and fitted to the "one set of binding sites" model.

In order to test the validity of the ion-exchange model for BTA complexation by SC4, the influence of adding NaCl on the ^{1}H NMR signals of BTA was studied. For this experiment, we add NaCl to a equimolar solution of BTA and SC4 (4 mM) and a downfield shift of the signals is observed. The chemical shift of the trimethylammoniun group increases on increasing the concentration of sodium counterions due to its expulsion to the bulk water (Figure 9).

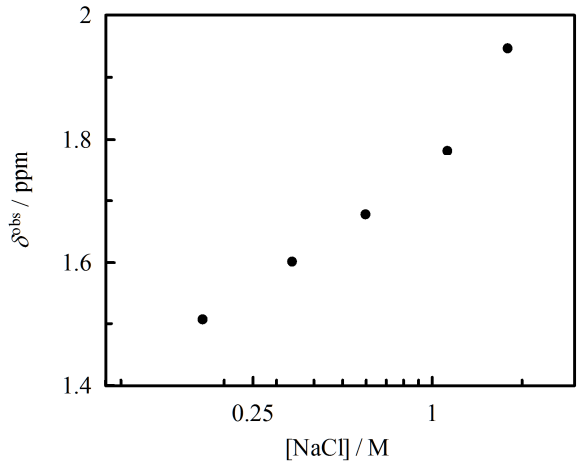

Figure 9. Chemical shift changes for trimethylammonium group signal of BTA(4mM) in the presence of SC4 (4 mM) *vs* NaCl concentration in D_2O at 25 °C. A coaxial tube with DMSO-d_6 was used as external standard.

This behavior is the opposite to that showed in Figure 1 and is consistent with an ionic exchange where sodium complexation by the calixarene compels BTA out of the cavity. Without adding NaCl, the δ value of $N(CH_3)_3$ headgroup of BTA has an appreciably upfield shift after complexation ($|\Delta\delta|$ = 1.73 ppm), but adding NaCl to the equimolar mixture of SC4 and BTA, the δ value of $N(CH_3)_3$ shows a smaller upfield shift ($|\Delta\delta|$ = 1.19 ppm at 1.8M of NaCl added). From a quantitative point of view and by using the BTA and sodium binding constants, $K_{BTA} = 3.28 \times 10^5$ M^{-1} and $K_{Na} = 183$ M^{-1}, and the total concentration of SC4 and BTA (4 mM) we can calculate that the 30% of BTA is displaced from the calixarene in the presence of 1.8M of NaCl. For this displacement, a chemical shift for the trimethylammonium group of BTA close to $\delta^{obs} \approx$ 2 should be expected, as is observed in Figure 9. This indicate that BTA is being expelled from SC4 cavity by exchange with Na^+ cation.

2.2.4. Conclusions

The results show that complexation of organic cations by sulfonatocalixarenes should be considered as an ion-exchange equilibrium with the counterions of SC4. Increasing the calixarene concentration leads to an increment of the counterions present in solution, and consequently, the fraction of cation-free calixarene decreases. As a consequence, the observed binding constant of organic cations by SC4 decreases both on increasing SC4 or added Na^+ concentration. According to these findings, the binding constants of cations to sulfonatocalixarenes obtained by varying the host concentration or in the presence of buffers or other salt sources should be revised. In order to get the true binding constants, experimental results should be extrapolated to zero sulfonatocalixarene concentration.

2.2.5. Appendix

Potentiometric experiments:

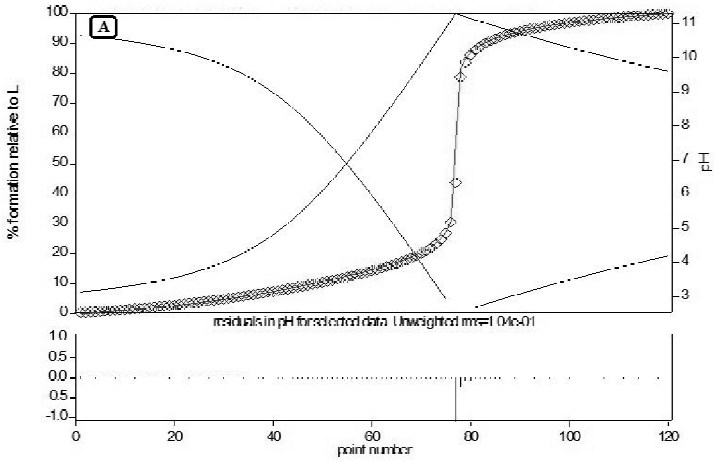

	Value	relative std devn	log beta	standard deviation		
Beta A refined	0.8445E+12	0.0389	11.9266	0.0169	1	1
Beta B refined	0.3353E+16	0.0422	15.5254	0.0183	1	2
Beta C constant	0.1259E-13		-13.9000		0	-1

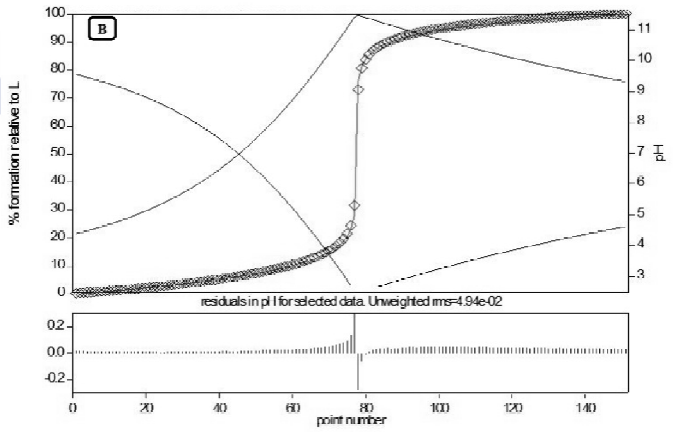

	Value	relative std devn	log beta	standard deviation		
Beta A refined	0.3223E+13	0.0362	12.5082	0.0157	1	1
Beta B refined	0.3643E+16	0.0370	15.5614	0.0161	1	2
Beta C constant	0.1413E-13		-13.8500		0	-1

Figure S1. Potentiometric titration curve obtained for SC4 (A) and SC4 with BTA (B) at 25ºC.

ITC Experiments:

Observed binding constants for the host-guest complexation in phosphate buffer of different concentrations are listed in Table S1.

Table S1. Observed binding constants, K_{obs}, for 1:1 intermolecular complexation of BTA (5 mM) with SC4 (0.5 mM) in presence of buffer of different concentration at 298.15 K.

[Buffer] mM	K_{obs}, M^{-1}
---	220000 ± 780
50	19400 ± 607
100	9860 ± 212

ITC experiments in the presence of phosphate buffer solution:

The phosphate buffer solution of pH 7.2 was prepared by dissolving disodium hydrogen phosphate (Na_2HPO_4–$12H_2O$, 25.79g) and sodium dihydrogen phosphate (NaH_2PO_4–$2H_2O$, 4.37g) in Milli Q water (1000 ml) to make a 0.1 $mol.dm^{-3}$ solution and then diluted to make another solution of 0.05 $mol.dm^{-3}$. The pH values of buffer solutions were verified on a Crison GLP 21 pH-meter calibrated with two standard buffer solutions.

The net reaction heat in each run was analyzed by using "one set of binding sites" model (ORIGIN software, Microcal Inc.) to simultaneously compute the complex stability constant (K), standard molar reaction enthalpy (ΔH°) and standard deviation from the titration curve.

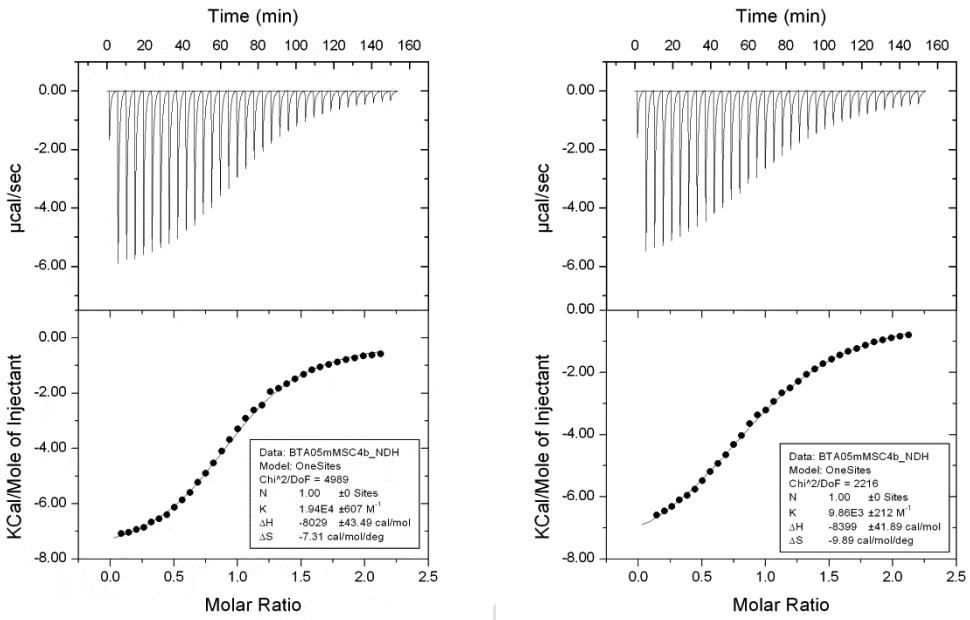

Figure S2. Microcalorimetric titration of BTA with SC4 at 25ºC: raw data for sequential 34 injections (8 μL per injection) of BTA solution (5 mM) injecting into SC4 solution (0.5 mM) in the presence of aqueous phosphate buffer solution (50 mM, left) and (100 mM, right): apparent reaction heat obtained from the integration of calorimetric traces.

NMR experiments:

BTA@SC4 complex. The inclusion of BTA by SC4 has been studied by NMR technique, and a close comparison of $\Delta\delta$ values of BTA protons after complexation with SC4 shows that BTA is encapsulated from either the aromatic moiety or the methyl group without regioselectivity[S1]. As shown in the ^{1}H NMR spectra (Figure S3), our results are compatible with literature, since all BTA protons included into the SC4 cavity experience an upfield shift, as compared with the uncomplexed BTA, due to the ring current effect of SC4[S2]. Depending of the inclusion mode, different types of interactions are involved, as electrostatic and CH-π when the charged group is in the SC4 cavity or mainly π - π and electrostatic when is the aromatic group inserted in the cavity[S2c].

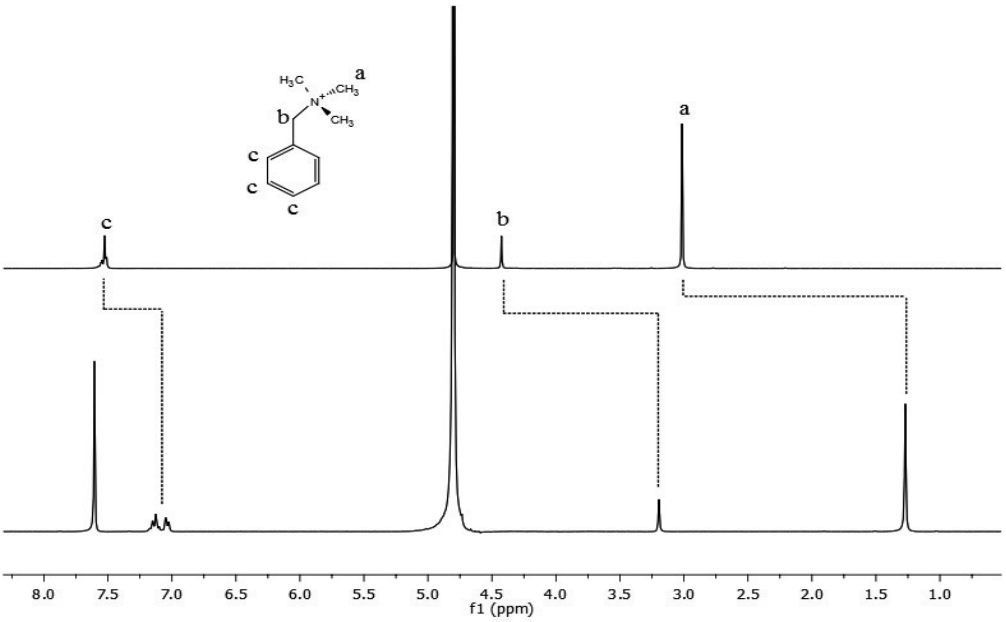

Figure S3. ^{1}H NMR spectra of BTA (2 mM) at 25ºC in D_2O in absence (top) and in presence of 2 mM of SC4 (bottom).

Influence of salt:

As shown in Figure S5, the NaCl concentration has a strong effect in the association constant observed. K_{obs} decrease from 3.25×10^5 M^{-1} to $1.85 \times 1\ 0^3$ M^{-1} in presence of 1M of NaCl.

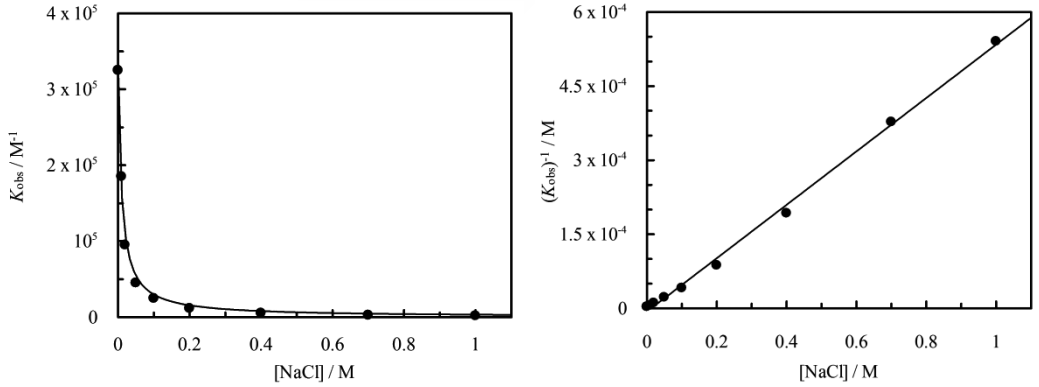

Figure S4. Influence of NaCl concentration in K_{obs} (left) and 1/ K_{obs} (right) for the complex formation between BTA and SC4. All the experiments has been done at 25 °C in D_2O. Solid lines show the best fit to the competitive model.

2.2.6. References

1. Perret, F.; Lazar, A. N.; Coleman, A. W. *Chem. Commun.* **2006**, 2425–2438.
2. Perret, F.; Coleman, A. W. *Chem. Commun.* **2011**, *47*, 7303–7319.
3. Souchon, V.; Leray, I.; Valeur, B. *Chem. Commun.* **2006**, 4224– 4226.
4. Atwood, J. L.; Barbour, L. J.; Hardie, M. J.; Raston, C. L. *Coord. Chem. Rev.* **2001**, *222*, 3–32.
5. Dalgarno, S. J.; Atwood, J. L.; Raston, C. L. *Chem. Commun.* **2006**, 4567–4574.
6. Shinkai, S.; Mori, S.; Koreishi, H.; Tsubaki, T.; Manabe, O. *J. Am. Chem. Soc.* **1986**, *108*, 2409–2416.
7. Bakirci, H.; Koner, A. L.; Dickman, M. H.; Kortz, U.; Nau, W. M. *Angew. Chem. Int. Ed.* **2006**, *45*, 7400–7404.
8. Hennig, A.; Bakirci, H.; Nau, W. M. *Nat. Methods* **2007**, *4*, 629– 632.
9. Douteau-Guével, N.; Perret, F.; Coleman, A.W.; Morel, J.-P.; Morel-Desrosiers, N. *J. Chem. Soc. Perkin Trans. 2* **2002**, 524–532.
10. Arena, G.; Casnati, A.; Contino, A.; Magrì, A.; Sansone, F.; Sciotto, D.; Ungaro, R. *Org. Biomol. Chem.* **2006**, *4*, 243–249.
11. Guo, D.-S.; Wang, K.; Liu, Y. *J. Incl. Phenom. Macrocycl Chem.* **2008**, *62*, 1-21.
12. Morel, J. P.; Morel-Desrosiers, N. *Org. Biomol. Chem.* **2006**, *4*, 462–465.
13. Bonal, C.; Israëli, Y.; Morel, J.-P.; Morel-Desrosiers, N. *J. Chem. Soc. Perkin Trans.* **2001**, *2*, 1075–1078.
14. Gans, P.; Sabatini, A.; Vacca, A. *Talanta* **1996**, *43*, 1739–1753.
15. Suga, K.; Ohzono, T.; Negishi, M.; Deuchi, K.; Morita,Y. *Supramolecular Science* **1998**, *5*, 9-14.

15. Price, W. S. *Concepts Magn. Reson.* **1997**, *9*, 299–336.
16. Antalek, B. *Concepts Magn. Reson.* **2002**, *14*, 225–258.
18. Price, W. S. *Concepts Nucl. Magn. Reson.* **1998**, *10*, 197–237.
19. Arena, G.; Gentile, S.; Gulino, F. G.; Sciotto, D.; Sgarlata, C. *Tetrahedron Lett.* **2004**, *45*, 7091–7094.
20. Fielding, L. *Tetrahedron* **2000**, *56*, 6151-6170.
21. Thordarson, P. *Chem. Soc. Rev.* **2011**, *40*, 1305-1323.
22. Wang, L.; Guo, D.; Chen, Y.; Liu, Y. *Thermochim. Acta* **2006**, *443*, 132–135.

S1. Arena, G.; Gentile, S.; Gulino, F. G.; Sciotto, D.; Sgarlata, C. *Tetrahedron Lett.* **2004**, *45*, 7091–7094.

S2 (a) Shinkai, S.; Araki, K.; Manabe, O. *J. Am. Chem. Soc.* **1988**, *110*, 7214 - 7215. (b) Shinkai, S.; Araki, K.; Matsuda, T.; Nishiyama, N.; Ikeda, H.; Takasu, L.; Iwamoto, M. *J. Am. Chem. Soc.* **1990**, *112*, 9053 – 9058. (c) Franke, J.; Vögtle, F. *Complexation of Organic Molecules in Water Solution*, in Top. Curr. Chem., *Vol. 132* (Eds.: F. Vögtle, E. Weber), Springer, Heidelberg, **1986**, pp. 135–170.

USC
UNIVERSIDADE
DE SANTIAGO
DE COMPOSTELA

2.3. Simultaneous cooperative complexation of a neutral guest and cations by *p*-sulfonatocalix[4]arene

2.3.1. Introduction

Supramolecular interactions are responsible for the three-dimensional structures of enzymes molecules and therefore these type of interactions provide an alternative way to understand the principle of enzyme catalysis and their potential applications.[1] In an effort to reproduce and simulate the cavity functions of enzymes, numerous macrocyclic compounds have been studied.[2–5] This can be related with an important feature of the macrocycles, which is the ability to isolate chemical reactions from the surrounding medium.

Calixarenes are a special class of macrocycles, which due the concave surface and being recognized receptors,[6] can act as a model for natural systems such as the binding sites of enzymes.[7] The ability of this type of macrocycles to accommodate a wide range of guest molecules can be related with the facile modifications at the lower and upper rim, as well as the capability to adopt different conformations.[8] In the last decade, great advances have been made in the field of calixarene-based artificial enzymes. A series of calixarene with different number of catalytic sites and flexibility were synthesized, where the authors concluded that: (i) the calixarene cavity is involved in the catalysis, (ii) the catalytic sites have function cooperativity in the catalysis, (iii) and also the flexibility within the calixarene structure is necessary to achieve the cooperative effects between the catalytic sites.[9,10] Another example was reported with the use of the most common water-soluble calixarene, *p*-sulfonatocalix[4]arene (SC4), where the authors by mixing the macrocycle, a metal ion and a selected guest obtain a structural metalloenzyme model.[11]

In the last years, our laboratory gave special attention to the complexation of different guests by water-soluble calixarenes.[12–14] Moreover, detailed experiments were performed on the influence of cations in the complexation of other guests by *p*-sulfonatocalix[4]arene (SC4).[15,16] The results evidence that to obtain the true binding constant, a competitive binding scheme should be considered. Although the host-guest binary systems with SC4 has been extensively studied,[17,8,18] the formation of ternary complexes with SC4 has been less reported in the literature.[11,19,14]

In this work we report the influence of the presence of an alkali metal and a transition-metal cation on the complexation of a water-soluble calixarene with a selected neutral guest molecule in neutral aqueous solution (Scheme 1).

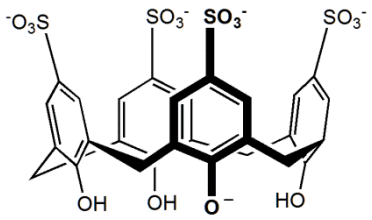

SC4

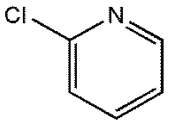

1

Scheme 1. Structure of *p*-sulfonatocalix[4]arene and pyridine guest (**1**).

2.3.2. Experimental Section

Materials: NaCl from Fluka (assay ≥99.5%), $CuCl_2 \cdot 2H_2O$ (assay ≥99%) and 2-Chloropyridine (assay ≥99%) from Sigma-Aldrich were used without further purification. *p*-Sulfonatocalix[4]arene (SC4) was prepared using a procedure described in a previous work.[16] All solutions were prepared with Mili-Q water.

Microcalorimetry: The microcalorimetric titrations were performed on an isothermal titration microcalorimeter (VP-ITC) from Microcal Co. (Northampton, MA) at atmospheric pressure and 25 °C.

NMR Spectroscopy: ^{1}H NMR spectra were recorded in a 300 MHz instrument while 2D NOESY (Nuclear Overhauser Effect Spectroscopy) experiments were obtained in a 500 MHz instrument. DOSY NMR spectra were recorded at 25 °C on a Varian Inova 500 spectrometer.

2.3.3. Results and Discussion

The selection of molecule **1** as a guest to study the influence of different ions in the host-guest complexation between a neutral guest and the calixarene can be relat: (i) with the sufficiently water solubility to obtain direct information on the binding constant by ITC and ^{1}H NMR experiments, (ii) and due the pK_a value (pK_a = 0.72)[22] which is sufficiently low to avoid pK_a displacements upon complexation with SC4 in

neutral aqueous solution.[23] The binding mode and binding constant for the host–guest complexation has already been determined by different techniques at pH = 2 for the 1:1 stoichiometry.[24] However, since the experiments were performed at neutral pH, and knowing the different π-electron density between pH 2.0 and pH 7.0, the binding mode and binding constant were determined again.

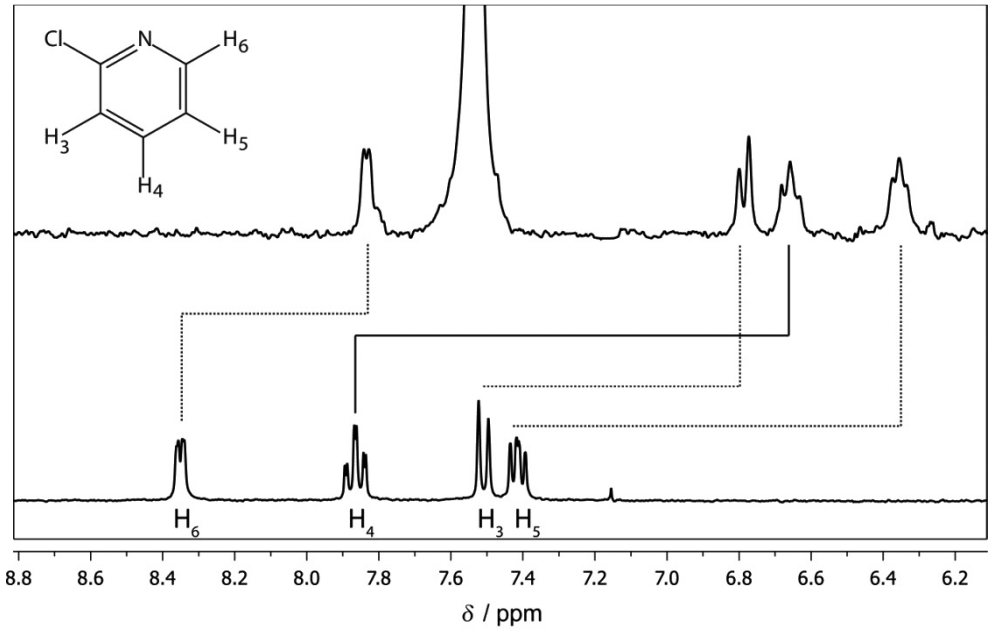

Figure 1. ^{1}H NMR spectra of **1** (1 mM) in D_2O at 25 ºC: (down) in absence of SC4, (upper) in presence of 2.5 mM of SC4.

Figure 1 shows the signals of guest **1** upon interaction with SC4. As can be seen, the signals are observed as a averaged single resonances because of the fast exchange on the NMR timescale between free and complexed guest.[25] The chemical shift to higher field in the order $H_4 > H_5 > H_3 > H_6$ indicates that the guest molecule should be incorporated in the SC4 cavity by the H_4 position, with the N atom located near the sulfonato group of SC4, as also observed at pH 2.0.[24] The observed binding constant (K_{obs}) for the 1:1 complex was determined by ITC experiments, where a value of K_{obs} = 155 ± 2 M^{-1} was obtained at neutral pH (7.0) (Figure 2). As can be seen from Figure 2, the intermolecular interaction between **1** and SC4 is mainly enthalpy driven (ΔH° = –32.3 ± 0.1 kJ mol^{-1}), accompanied with a negative entropy change ($T\Delta S^\circ$ = –19.8 ± 0.2 kJ mol^{-1}), in line with the results for the complex formation at pH = 2.[24] A comparison of the binding constant for the complex formation obtained at different pH, shows that

the value obtained at neutral conditions is about 10-fold lower than in acidic conditions. This difference is related with the stronger binding abilities of SC4 at pH 2.0 than at pH 7.0 and is also in line with the values obtained for others pyridine guests.[26]

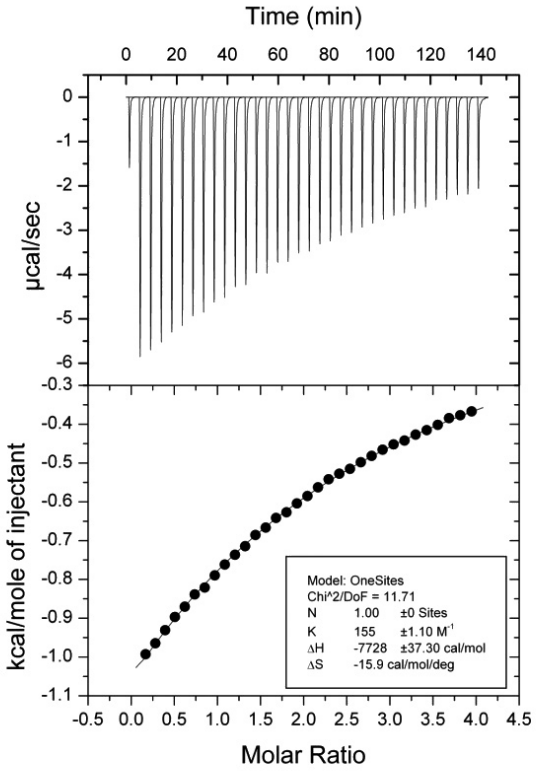

Figure 2. Microcalorimetric titration of **1** with SC4 at 298.15 K: (top) raw data for the sequential 34 injections (8 µL per injection) of **1** solution (20 mM) into SC4 solution (1 mM); (bottom) heat of reaction obtained from the integration of the calorimetric trace after subtracting the dilution heat from the reaction heat and fitted with the "one set of binding sites" model.

2.3.3.1. Influence of sodium ions on the binding constant

We have recently reported the influence of sodium cations, which are always present in aqueous neutral solution as counterion of SC4, in the complexation of a quaternary ammonium ion by the macrocycle (section 2.2).[16] It was conclude that in order to obtain the real binding constant of the guest molecule, a competitive binding model must be employed. However, in this work a neutral guest was selected, and therefore the possible steric constraints between the positive charged ion and the guest molecule were minimized.

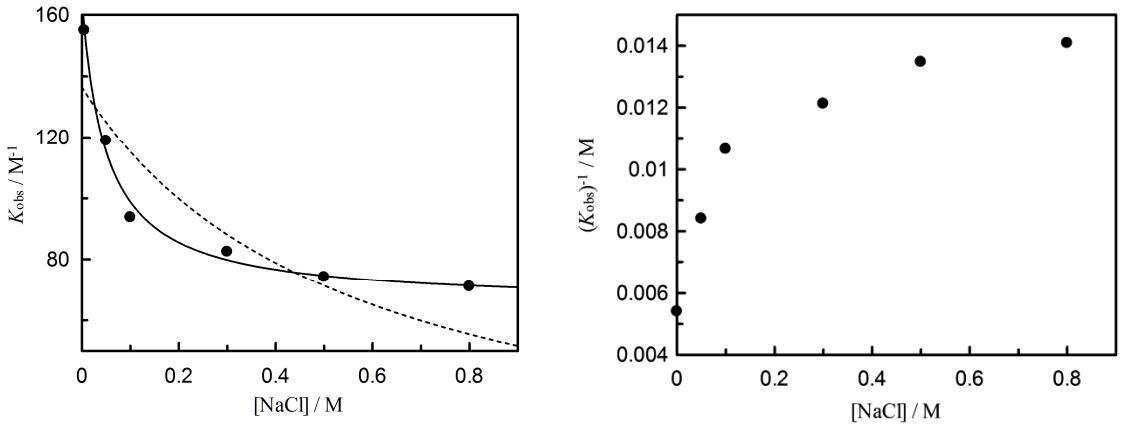

Figure 3. Influence of NaCl concentration in K_{obs} (left) and $1/K_{obs}$ (right) for the complex formation of **1** with SC4. The K_{obs} was obtained by microcalorimetric titrations and fitted with the "one set of binding sites" model. The solid line represents the fit according to eq 2, and the dotted line the fit to a competitive binding model.

Figure 3 shows the influence of sodium cations in the complexation of **1** by SC4 in neutral aqueous solution, carried out by ITC and fitted with the "one set of binding sites" model (Figure S1). As can be seen, the observed binding constant decrease from 155 ± 2 M^{-1} to 71 ± 2 M^{-1} in the presence of 800mM of NaCl, which suggest a competitive binding as shown in the case of the quaternary ammonium ion (section 2.2).[16] However, Figure 3 (right) shows a plot of the inverse of K_{obs} against NaCl concentration, where the absence of a linear dependence evidence that the competitive model is not compatible with the behavior observed. Moreover, in Figure 3 on the left it is also represented the fit to a competitive binding model, where is evidenced that this model cannot explain the trend observed for the binding constant obtained. In this way, a ternary binding model, with the Na^+ ion and **1** inside the cavity of SC4 was proposed. More specifically, the following chemical equilibria were employed to fit the apparent binding constant:

$$\mathbf{1} + \text{SC4} \overset{K_1}{\rightleftharpoons} \mathbf{1}@\text{SC4} \quad \text{(a)}$$

$$\text{Na} + \text{SC4} \overset{K_{\text{Na}}}{\rightleftharpoons} \text{Na}@\text{SC4} \quad \text{(b)}$$

$$\mathbf{1} + \text{Na}@\text{SC4} \overset{K_{\mathbf{T1}\cdot\text{Na}}}{\rightleftharpoons} \mathbf{1}\cdot\text{Na}@\text{SC4} \quad \text{(c)}$$

$$\text{Na} + \mathbf{1}@\text{SC4} \overset{K_{\text{TNa}}}{\rightleftharpoons} \text{Na}\cdot\mathbf{1}@\text{SC4} \quad \text{(d)}$$

Scheme 2

In this scheme, the binding constant that measure the affinity of **1**@SC4 for Na^+ ions, K_{TNa}, can be defined as $K_{\text{TNa}} = K_{\mathbf{T1}\cdot\text{Na}}K_{Na}/K_{\mathbf{1}}$. Moreover, according to the above scheme, the observed binding constant can be defined by eq 1.

$$K_{\text{obs}} = \frac{[\mathbf{1}@SC4] + [\mathbf{1}\cdot Na@SC4]}{([SC4] + [Na@SC4])[\mathbf{1}]} \quad (1)$$

Combining this equation with equilibrium a, b and c from Scheme 2 and assuming that the amount added of sodium cation, $[Na^+]_0$, is much higher than the sodium cations supplied by the SC4, we can deduce the equation that defines the dependence of K_{obs} with Na^+ concentration:

$$K_{\text{obs}} = \frac{K_{\mathbf{1}} + K_{\text{Na}}K_{\mathbf{T1}\cdot\text{Na}}[\text{Na}]_0}{1 + K_{\text{Na}}[\text{Na}]_0} \quad (2)$$

From the non-linear fit of K_{obs} to eq 2, we get K_{Na} = 20 ± 4 M^{-1}, $K_{\mathbf{T1}\cdot\text{Na}}$ = 68 ± 10 M^{-1} for the ternary complex, and $K_{\mathbf{1}}$ = 165 ± 6 M^{-1} for the inclusion of **1** in the SC4 cavity extrapolated in absence of Na^+ counterions.

To obtain further evidences of the formation of a ternary complex, 2D ROESY and ^{23}Na DOSY NMR experiments were performed. 2D ROESY NMR experiments are a common method to study interactions in inclusion complexes,[27–29] since the cross peaks are indicative of the specific proximity between the guest and the host (generally 4 Å or less).[30] Figure 4 shows the region of the 2D ROESY spectrum obtained for **1** with SC4 in the presence of NaCl. The results are consistent with the inclusion of **1** in

the SC4 cavity, due the cross peaks observed between the aromatic protons of SC4 and H_3, H_4, H_5 of **1**. Taking into account the binding constant for the complexation of Na^+ by SC4 (K = 183 M^{-1}, section 2.1) and the total amount of Na^+ added (140 mM), the observation of cross peaks between the guest and the host, indicate a formation of a ternary complex, rather than a competitive binding. Considering a competitive binding in this conditions, the molar fraction of **1**@SC4 is about 2.4% and therefore cannot be responsible for the correlations between the protons of **1** and SC4.

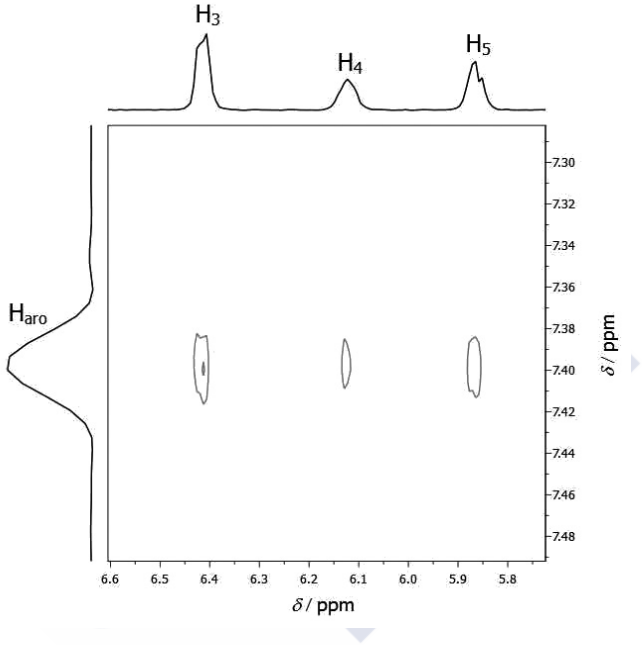

Figure 4. The 2D ROESY NMR spectrum region of **1** (4 mM) with SC4 (8 mM) in the presence of 140 mM of Na^+ in D_2O, with a mixing time of 500 ms at 298.15 K.

The diffusion experiments were performed in a 10 mM solution of SC4, where as demonstrated in a previous work, ca. 8.8 mM exists in the form of Na@SC4 complex. In this way, if only a 1:1 complex between **1** and SC4 is present in solution, the diffusion coefficient of Na^+ should increase to a level close to that observed to free Na^+ when **1** is successively added. Figure 5 shows the observed diffusion coefficient of Na^+ upon the addition of **1** in the solution of SC4Na, and as a comparison, the results obtain for the addition of benzyltrimethylammonium ion (BTA). As can be seen, the observed diffusion coefficient between **1** and BTA is quiet different, in the way that for BTA ions the observed diffusion coefficient of Na^+ almost reach the value of free Na^+ in bulk solution, but on the other hand the same behavior is not observed for the addition of **1**.

The experiments confirm that the complexation of the quaternary ammonium ion by the SC4 is ruled by a competitive binding, while for the neutral pyridine guest, a ternary binding model as proposed in scheme 2 should be employed to fit the data.

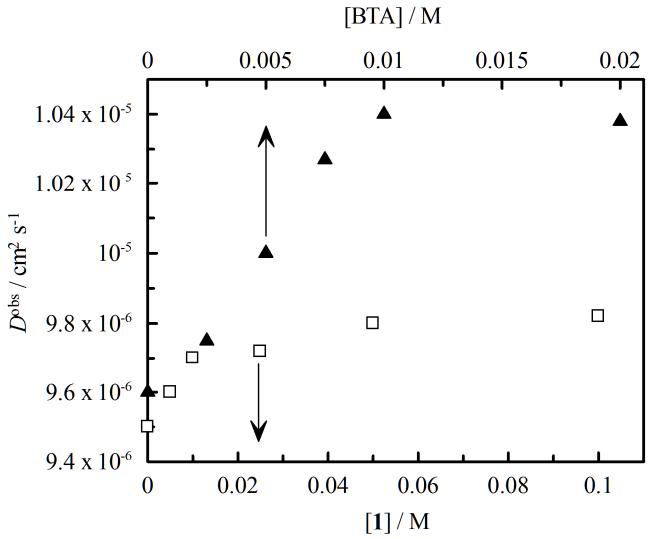

Figure 5. Influence of **1** (□) and benzyltrimethylammonium ion (▲) (data from ref 16) in the self-diffusion coefficient of Na^+ in a solution of SC4Na (10 mM) in D_2O at 25 °C.

2.3.3.2. Influence of copper ions on the binding constant

The addition of transition metal, such as Zn^{2+}, Co^{2+} and Mn^{2+} to the host–guest complexation between SC4 and azo compounds was already been explored by Nau and co-workers.[11,19] Since the formation of an interesting ternary complex with a cooperative binding found in that approach, and after the negative cooperative found with Na^+ cations despite the formation of a ternary complex, it was decided to study the binary system **1**–SC4 in the presence of a divalent transition-metal cation. In this way, the influence of the addition of **1** into SC4 was studied in the presence of Cu^{2+} cations by microcalorimetry.

Figure 6 shows a representative titration curve obtained by ITC for the complexation of **1** by SC4 in the presence of the transition-metal ion. As can be seen, the binding constant increase from 165 ± 6 M^{-1}, extrapolated at zero concentration of salt, to 795 ± 25 M^{-1} when SC4 is fully occupied by Cu^{2+} cations, considering $K_{Cu^{2+}}$ = 5650 ± 290 M^{-1} (section 2.1).

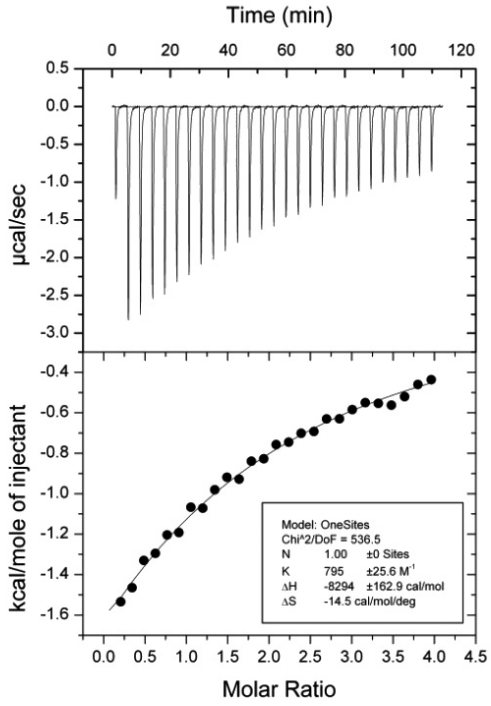

Figure 6. Microcalorimetric titration of **1** with SC4 at 25 °C: (top) raw data for sequential 12 µL injections of **1** (6 mM) into SC4 solution (0.3 mM) in the presence of $CuCl_2$ (5 mM); (bottom) heat of reaction obtained from the integration of the calorimetric trace after subtracting the dilution heat from the reaction heat and fitted with "one set of binding sites" model.

To determine the binding constant for the formation of the ternary complex, the experiments were performed in the presence of different Cu^{2+} concentration in neutral aqueous conditions. Figure 7 shows the dependence of the observed binding constant of **1** with SC4 against the concentration of Cu^{2+}. The results show that increasing the concentration of Cu^{2+} in solution increase the binding affinity of **1** by SC4. To exclude the increase of the binding constant due the **1**·Cu^{2+} complex formation, control experiments were performed. The microcalorimetric titration revealed that the addition of the metal cation to an aqueous solution of **1** did not produced a significant reaction heat (Figure S2), which is in line with the complexation of other transition metal ions by azo compounds.[11] This shows that the formation of the complex between **1** and Cu^{2+} cations has a very low binding constant in solution, and therefore could not be responsible for the increase in the observed binding constant.

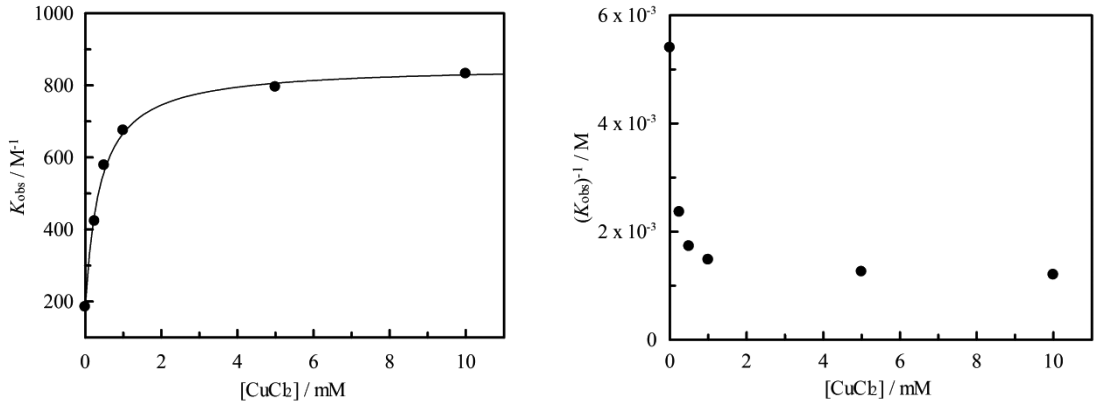

Figure 7. (Left) Dependence of the apparent binding constant of **1** with SC4 on the concentration of $CuCl_2$. The K_{obs} was obtained by microcalorimetric titration and fitted to the "one set of binding sites" model. The line represents the fit according to eq 5. (Right) $1/K_{obs}$ for the complex formation of **1** with SC4.

In order to analyze the data in Figure 7, we propose a complexation model identical to Scheme 2, but adding the complexation of Cu^{2+} (Scheme 3).

$$\mathbf{1} + \text{SC4} \overset{K_1}{\rightleftharpoons} \mathbf{1}@\text{SC4} \quad \text{(e)}$$

$$\text{Na} + \text{SC4} \overset{K_{Na}}{\rightleftharpoons} \text{Na}@\text{SC4} \quad \text{(f)}$$

$$\text{Cu} + \text{SC4} \overset{K_{Cu}}{\rightleftharpoons} \text{Cu}@\text{SC4} \quad \text{(g)}$$

$$\mathbf{1} + \text{Cu}@\text{SC4} \overset{K_{\mathbf{1}\cdot\text{Cu}}}{\rightleftharpoons} \mathbf{1}\cdot\text{Cu}@\text{SC4} \quad \text{(h)}$$

$$\mathbf{1} + \text{Na}@\text{SC4} \overset{K_{\mathbf{1}\cdot\text{Na}}}{\rightleftharpoons} \mathbf{1}\cdot\text{Na}@\text{SC4} \quad \text{(i)}$$

Scheme 3

According to Scheme 3, the observed binding constant can be defined by eq 3:

$$K_{\text{obs}} = \frac{[\mathbf{1}@\text{SC4}] + [\mathbf{1}\cdot\text{Na}@\text{SC4}] + [\mathbf{1}\cdot\text{Cu}@\text{SC4}]}{[\mathbf{1}]([\text{SC4}] + [\text{Na}@\text{SC4}] + [\text{Cu}@\text{SC4}])} \quad (3)$$

Combining equation 3 with the equilibria of Scheme 3, we can deduce the equation that defines the dependence of K_{obs} with Cu^{2+} concentration:

$$K_{obs} = \frac{K_{\mathbf{1}} + K_{Na}K_{\mathbf{T1}\cdot Na}[Na]_0 + K_{Cu}K_{\mathbf{T1}\cdot Cu}[Cu]_0}{1 + K_{Na}[Na]_0 + K_{Cu}[Cu]_0} \quad (4)$$

Assuming a constant amount of sodium supplied by SC4 ($[Na^+]_0 = 1.5mM$)

$$K_{obs} = \frac{a + b\,[Cu]_0}{1 + c\,[Cu]_0} \quad (5)$$

where,

$$a = \frac{K_{\mathbf{1}} + K_{Na}K_{\mathbf{T1}\cdot Na}[Na]_0}{1 + K_{Na}[Na]_0} \quad (6)$$

$$b = \frac{K_{Cu}K_{\mathbf{T1}\cdot Cu}}{1 + K_{Na}[Na]_0} \quad (7)$$

$$c = \frac{K_{Cu}}{1 + K_{Na}[Na]_0} \quad (8)$$

From the non-linear fit of the experimental data to eq 5, we get the binding constant for the formation of the ternary complexes $K_{\mathbf{T1}\cdot Cu} = 855\ M^{-1}$ (Scheme 4).

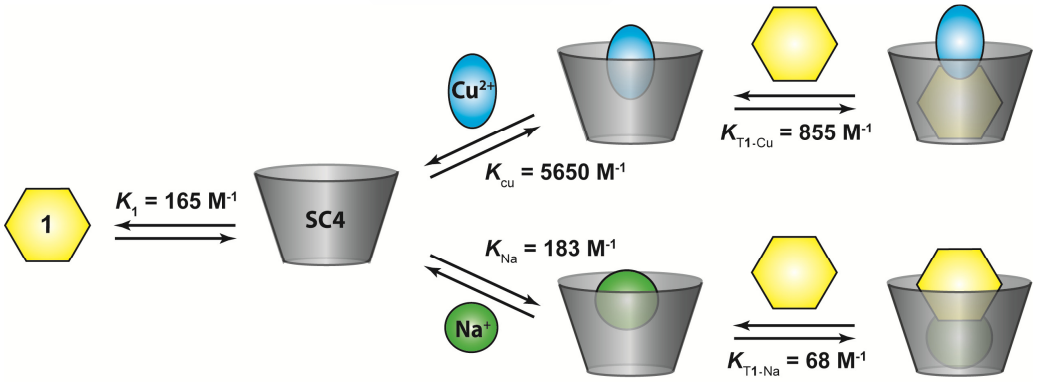

Scheme 4

From Scheme 4 it is also possible to estimate the value for the **1**·Cu^{2+} complex. By the relation $K_{\mathbf{T1}\cdot Cu}/K_{\mathbf{1}}$, a value of 4 M^{-1} was obtained for the complex formation, which is in agreement with the absence of heat of reaction obtained by ITC.

Essentially, the effect of salt (added or as counterion of the macrocycle) on the binding of SC4 with different guests, charged and non-charged, showed that the inorganic cations can influence the formation of complexes in the following two ways: they can compete with the guest molecules for the host cavity;[15,16] or they can form a ternary complex due the additional electrostatic interactions and H-bonding.[11,19] Biologically relevant salts can make significant effects on biomolecules,[31] and consequently, they should always be considered in the host-guest binding. In this work, the results shows that Na^+ and Cu^{2+} influence in a different way on the complexation of **1** by SC4. For Na^+ cations a negative cooperativity is observed for the formation of the ternary complex, **1**·Na@SC4, due the decrease of the binding constant upon addition of Na^+, when compared with the binding constant in absence of salt. The decrease of K_{obs} should be related with the absence of the cation stabilization by the metal-ligand bond, despite the formation of the ternary complex. However, this behavior is in contrast with the expected release of the cation or guest as a result of a competitive binding.[11] On the other hand, the increase in the binding constant for the complex between **1** with Cu^{2+}@SC4 complex, evidences the positive cooperativity of the binding constant by host-assisted metal-ligand bond formation, thus mimicking a metalloenzyme model binding as observed in other ternary systems.[11] In essence, by changing the cation inserted in the calixarene cavity, we are modulating the specificity of the calixarene and therefore simulating the cavity function of enzymes.

2.3.4. Conclusions

In conclusion, we have studied the complexation of a neutral guest by SC4 in the presence of different cations in water at neutral pH. The formation of ternary complexes between the cations and the host-guest molecules have been investigated by ITC and NMR methods. The results show that the presence of the different cation concentration in aqueous solution influence the binding constant for the complex formation between **1** and SC4. In the presence of Na^+ cations the binding constant decrease, although the cation remains in the cavity of SC4 in the presence of the neutral guest, indicating a negative cooperativity, while for the divalent cation Cu^{2+}, a positive cooperativity is evidenced by the increase in the binding constant observed for the **1**@SC4 inclusion complex.

2.3.5. Appendix

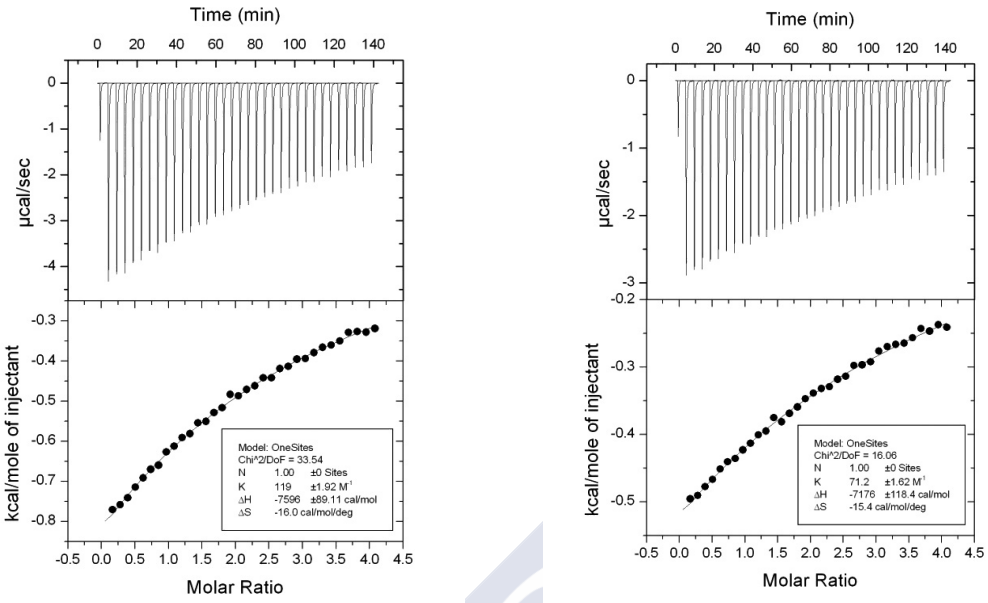

Figure S1. Microcalorimteric titration of **1** with SC4 at 298.15 K: (upper) raw data for the sequential 34 injections (8 µL per injection) of **1** solution (20 mM) injecting into SC4 solution (1 mM) in the presence of 50mM NaCl (left) and 800 mM NaCl (right); (down) heat of reaction obtained from the integration of the calorimetric trace after subtracting the dilution heat from the reaction heat and fitted with "one set of binding sites" model.

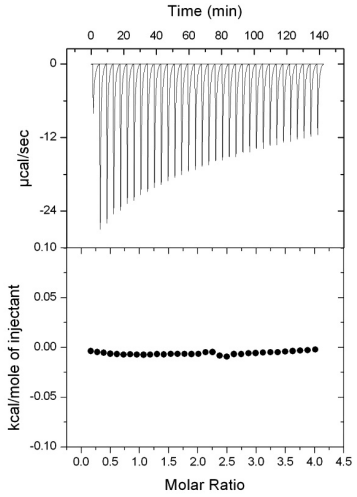

Figure S2. Microcalorimetric titration of **1** with Cu^{2+} at 298.15 K in aqueous solution: (upper) raw data for the sequential 8 µL of Cu^{2+} (200mM) into **1** (10mM); (down) heat of reaction obtained from the integration of the calorimetric trace after subtracting the dilution heat from the reaction heat.

2.3.6. References

1. Z. Dong, Q. Luo, and J. Liu, *Chem. Soc. Rev.*, 2012, **41**, 7890–7908.

2. A. Ikeda and S. Shinkai, *Chem. Rev.*, 1997, **97**, 1713–1734.

3. R. J. Hooley and J. Rebek, *Chem. Biol.*, 2009, **16**, 255–264.

4. T. Brotin and J.-P. Dutasta, *Chem. Rev.*, 2009, **109**, 88–130.

5. C. Klöck, R. N. Dsouza, and W. M. Nau, *Org. Lett.*, 2009, **11**, 2595–2598.

6. Z. Asfari, V. Bohmer, J. Harrowfield, and J. Vicens, *Calixarenes 2001*, Kluwer Academic Publishers, Dordrecht, The Netherlands, 2001.

7. R. Breslow, *Artificial Enzymes*, Wiley-VCH, Weinheim, Germany, 2005.

8. D.-S. Guo, K. Wang, and Y. Liu, *J. Incl. Phenom. Macrocycl. Chem.*, 2008, **62**, 1–21.

9. P. Molenveld, W. M. G. Stikvoort, H. Kooijman, A. L. Spek, J. F. J. Engbersen, and D. N. Reinhoudt, *The Journal of Organic Chemistry*, 1999, **64**, 3896–3906.

10. P. Molenveld, J. F. J. Engbersen, and D. N. Reinhoudt, 1999, 3269–3275.

11. H. Bakirci, A. L. Koner, M. H. Dickman, U. Kortz, and W. M. Nau, *Angew. Chem. Int. Ed.*, 2006, **45**, 7400–7404.

12. N. Basilio and L. García-Río, *Chem. Eur. J.*, 2009, **15**, 9315–9319.

13. V. Francisco, N. Basilio, L. Garcia-Rio, J. R. Leis, E. F. Marques, and C. Vázquez-Vázquez, *Chem. Commun.*, 2010, **46**, 6551–3.

14. N. Basílio, V. Francisco, and L. García-río, *J. Org. Chem*, 2012.

15. N. Basilio, L. García-Río, and M. Martín-Pastor, *J. Phys. Chem. B*, 2010, **114**, 7201–7206.

16. V. Francisco, N. Basilio, and L. García-Río, *J. Phys. Chem. B*, 2012, **116**, 5308–5315.

17. G. V. Oshovsky, D. N. Reinhoudt, and W. Verboom, *Angew. Chem. Int. Ed.*, 2007, **46**, 2366–2393.

18. W. Sliwa and T. Girek, *J. Incl. Phenom. Macrocycl. Chem.*, 2010, **66**, 15–41.

19. R. N. Dsouza and W. M. Nau, *J. Org. Chem.*, 2008, **73**, 5305–5310.

20. W. S. Price, *Concepts Magn. Reson.*, 1997, **9**, 299–336.

21. B. Antalek, *Concepts Magn. Reson.*, 2002, **14**, 225–258.

22. C. B. Brown and D. H. Mcdaniel, *J. Am. Chem. Soc.*, 1955, **77**, 3752–3755.

23. H. Bakirci, A. L. Koner, T. Schwarzlose, and W. M. Nau, *Chem. Eur. J.*, 2006, **12**, 4799–4807.

24. Y. Liu, E.-C. Yang, Y. Chen, D.-S. Guo, and F. Ding, *European Journal of Organic Chemistry*, 2005, **2005**, 4581–4588.

25. G. Arena, S. Gentile, F. G. Gulino, D. Sciotto, and C. Sgarlata, *Tetrahedron Letters*, 2004, **45**, 7091–7094.

26. Y. Liu, Y.-H. Ma, Y. Chen, D.-S. Guo, and Q. Li, *The Journal of organic chemistry*, 2006, **71**, 6468–73.

27. H. Bakirci, A. L. Koner, and W. M. Nau, *J. Org. Chem.*, 2005, **70**, 9960–9966.

28. Y. Liu, D.-S. Guo, H.-Y. Zhang, Y.-H. Ma, and E.-C. Yang, *J. Phys. Chem. B*, 2006, **110**, 3428–3434.

29. Y. Liu, J. Shi, and D.-S. Guo, *J. Org. Chem.*, 2007, **72**, 8227–8234.

30. X. Zhang and W. M. Nau, *Angew. Chem. Int. Ed.*, 2000, **39**, 544–547.

31. M. V Fedorov, J. M. Goodman, and S. Schumm, *Chem. Commun.*, 2009, **7345**, 896–898.

USC
UNIVERSIDADE
DE SANTIAGO
DE COMPOSTELA

Chapter 3

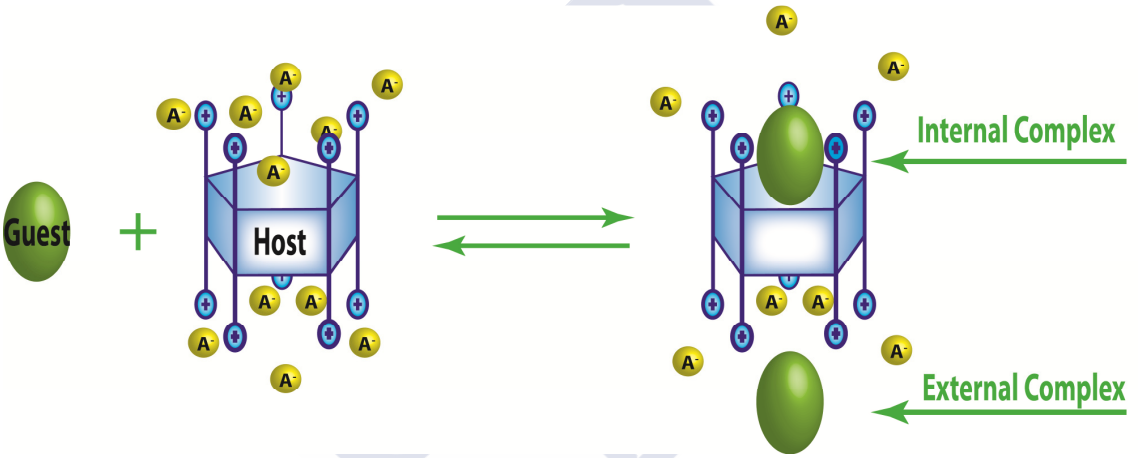

USC
UNIVERSIDADE
DE SANTIAGO
DE COMPOSTELA

3. Internal and external guest binding by pillar[5]arene

3.1. Introduction

The introduction of a new macrocycle host in the host-guest panorama is rare and always interesting. In addition to the well known macrocycles, such as crown ethers, cyclodextrins, calixarenes, cucurbiturils, among others,[1] in 2008 a new macrocycle was synthesized, and was conveniently termed "pillararene".[2] The pillar shape of this new class of macrocycle is made up of disubstituted hydroquinones linked by methylene bridges at *para* positions. Rapidly, new routes were exploited to functionalized these molecules[3–5] in order to complex different guests in organic solvents,[6,7] but particularly in aqueous media,[8–12] where most of the biological process occur. As an example, by introduction carboxylic[8] or ammonium groups[12] at both rims, enables the water solubility of the macrocycles. The introduction of charged groups, in addition to an electron-rich cavity[13] makes them good candidates as host molecules for charged or neutral guests, as demonstrated by the studies of the inclusion of aminoacids,[14] viologen derivatives,[8] aromatic or *n*-alkyl alcohols,[15] among other guests. Therefore, application of pillararenes as chemosensors, drug delivery and supramolecular polymers can be expected.

Between the various analogues of macrocycles, the calixarenes are probably the most similar to pillararenes. Although there exists some structural differences between them, such as the symmetry and flexibility of the cavity,[16,3] one characteristic shared by the two hosts in neutral aqueous solutions, is the presence of counterions. We have recently put a lot of effort to demonstrate the influence of counterions in the complexation of guests, cationic[17] or neutral,[18] by water-soluble calixarenes. This influence concerns with the binding constant for the complex formation, but also in the thermodynamic parameters. In the case of pillararenes, where both rims are substituted, a large amount of counterions are present in aqueous solution and therefore a large effect is expected.

In this work, we report the influence of BF_4^- as a counterion of trimethylammonium substituted pillar[5]arene (**H**) on the complexation of an anionic guest (**G**) (Scheme 1) studied by isothermal titration calorimetry along with ^1H and ^{19}F diffusion ordered spectroscopy NMR experiments.

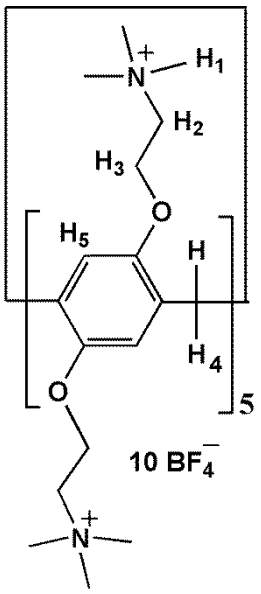

H

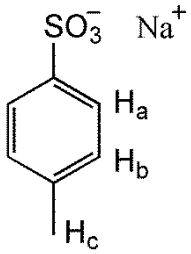

G

Scheme 1

3.2. Experimental Section

Materials: Sodium *p*-toluenesulfonate (95%) (**G**), KBF_4 (≥ 99.99%) were purchased from Sigma-Aldrich and used without further purification. The cationic water-soluble pillar[5]arene (**H**) was synthesized according to the literature (see Appendix, Figure S1-S6).[12] The exchange of the counterion Br^- by BF_4^- was obtained with the following procedure. To a solution of **H** with Br^- counterion (1.17 g, 0.514 mmol) in Milli-Q water, $AgBF_4$ was slowly added in small portions under stirring at room temperature. A thin grayish precipitated was got. The suspension was separated by centrifugation and the supernatant collected was filtered through a 0.45 μm filter. After the solvent was removed, a yellowish solid was obtained (1.15 g, 96 %). **^{1}H NMR** (300 MHz, D_2O, 25 °C): 6.89 (s, 10H); 4.36 (s, 20H); 3.91 (s, 10H); 3.72 (s, 20H); 3.19 (s, 90H). **^{13}C NMR** (75 MHz, D_2O, 25 °C): 149.2 (C, 10C); 129.8 (C, 10C); 115.9 (CH, 10C); 64.8 (CH2, 10C); 62.3 (CH2, 10C); 53.7 (CH3, 30C); 29.3 (CH2, 5C). **ESI-MS:** *m/z* [TMAP510+.9BF4-]+ 2253.2 (calcd: 2253.4); [TMAP510+.8BF4-]2+ 1083.1 (calcd: 1083.3). The **H** was also analyzed by thermal gravimetric analysis (TGA) to assess volatile content.

Microcalorimetry: The microcalorimetric titrations were performed on an isothermal titration microcalorimeter (VP-ITC) from Microcal Co. (Northampton, MA) at atmospheric pressure and 25 °C.

NMR experiments: ^{1}H NMR and ^{1}H and ^{19}F Diffusion-ordered NMR spectroscopy (DOSY) were carried out at 25 ºC on a Varian Inova 500 spectrometer. The ^{1}H DOSY spectra were acquired with stimulated-echo pulse sequence with bipolar gradient pulses (DOSY-Dbppste),[19] while for ^{19}F diffusion NMR a spin-echo pulse sequence with simple gradient was employed (DOSY-Doneshot).[20] The pulsed gradients (G) were incremented from 4.0 to 141.8 cm^{-1} for ^{1}H and 1.85 to 17.7 cm^{-1} for ^{19}F in 20 steps. The duration of the pulse field gradients (δ) applied to encode and decode the diffusion was set to 1.6 ms for ^{1}H and 2 ms for ^{19}F. To obtain reliable results for the diffusion coefficient, the diffusion time (Δ) of the experiment was optimised to 50 ms for ^{1}H and 300 ms for ^{19}F. The reference sample for the ^{1}H diffusion experiments was 99% D2O at 25 °C (D = 1.87 × 10^{-5} cm^{2} s^{-1})[21] and for the ^{19}F diffusion experiments was 0.3 mM NaF solution in 10% D_2O in H_2O at 25 °C (D = 1.37 × 10^{-5} cm^{2} s^{-1}).[22] The raw data were processed by using the MestreC program and fitting with the following equation:

$$\ln I/I_0 = -\gamma^2\delta^2G^2\left(\Delta - \frac{4\delta}{3}\right)D = -bD \qquad (1)$$

where I and I_0 are the echo intensity, in the presence and absence of the gradient pulse, respectively, γ is the gyromagnetic ratio, G is the pulse gradient strength, δ is the length of the pulse gradient, τ is the gradient stabilization delay, Δ is the time interval between the leading edges of the pulse gradient used and D is the diffusion coefficient. For the spin-echo pulse sequence with simple gradient the term $\left(\Delta - \frac{4\delta}{3}\right)$ in eq. 1 was replaced by $\left(\Delta - \frac{\delta}{3}\right)$. The diffusion coefficients were extracted from the slope of the plot of ln I/I$_0$ versus the b value.

3.3. Results and Discussion

The macrocycle **H** is known due to its electron-rich cavity, which allied with the presence of five positive charges in each rim makes this molecule a good receptor for anions. In this way**,** the complexation of **H** with **G** (Scheme 1) was first studied by isothermal titration calorimetry (ITC) to investigate the thermodynamic origin of the inclusion complex. As shown in Figure 1, each titration of **G** into the sample cell with **H** gave an apparent reaction heat caused by the formation of an inclusion complex **G@H**. The titration data could be well fitted by the "one set of binding sites" model to simultaneously obtain the binding constant (K) and the thermodynamic parameters. The results indicate that the complexation is mainly enthalpy-driven (ΔH° = –27.6 ± 0.1 kJ.mol^{-1}), accompanied by favorable entropic changes ($T\Delta S^{\circ}$ = 6.7 ± 0.1 kJ.mol^{-1}). From the experiments performed between guests and other macrocycles, it is well known that noncovalent interactions such as electrostatic, π–π, C–H···π, contribute to the enthalpic changes, while the conformation change and desolvation effect contribute to the entropic changes.[23] Therefore the thermodynamic parameters obtained suggests that π–π, C–H···π between the aromatic ring of **G** and **H,** as well as the interaction of the methyl group of **G** with the electron-rich cavity of **H** should contribute for the favorable enthalpy. Simultaneously, the water molecules around the guest and the host are released to the aqueous bulk phase, and should be the main reason for the entropic gain. The binding constant obtained, $K = (1.06 \pm 0.1) \times 10^6$ M^{-1}, constitutes one of the highest values recorded so far for the complexation of guests by pillar[5]arenes in aqueous solution. However, a simple comparison with anionic calixarenes where identical noncovalent interactions are the basis of the host-guest complex formation,[24,25,17] binding constant values up to 10^6 are expected.

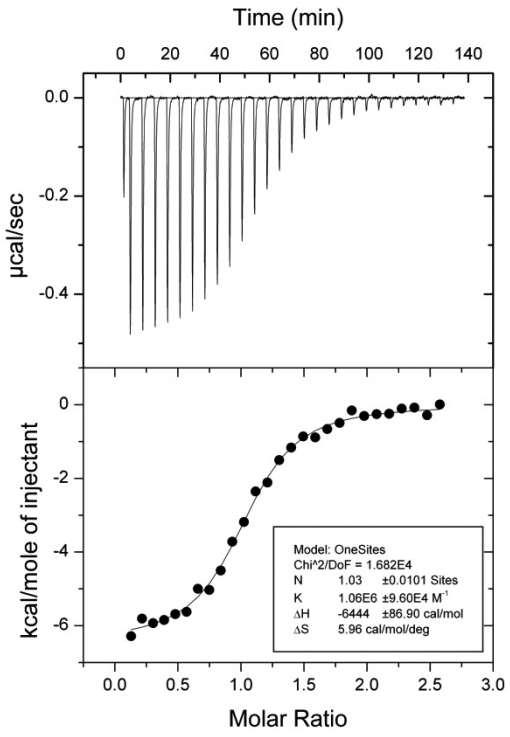

Figure 1. Microcalorimetric titration of **G** with **H** in water at 25 °C: (top) raw data for the sequential 28 injections (10 µL per injection) of **G** solution (0.3 mM) into 0.02 mM of **H**; (bottom) "net" heat effects obtained by subtracting the dilution heat from the reaction heat, which was fitted by computer simulation using "one set of sites" model.

In order to obtain information of the inclusion binding mode between **H** and **G,** ^{1}H and 2D NMR experiments were performed. Figure 2 shows the ^{1}H NMR spectra of **G** in D_2O recorded in absence and presence of 1 equiv. of **H**. As can be seen, the upfield chemical shift displayed by the **G** protons upon complexation with **H** suggest an inclusion complex. The upfield shifts in the order $H_c > H_b > H_a$ indicate that the methyl group of **G** should be more incorporated in the magnetically shielding region of the cavity of **H,** while the sulfonato group should be pointing to trimethylammonium groups of **H**.[24,26] Moreover, the host protons signals (H_5, H_4 and H_2) also experience upfield shifts, with the peak of H_2 further split into two separate peaks. The split observed is possible due the asymmetric structure of **G** and how is inserted in the host cavity, which lead the methylene protons of **H** close to the methyl group and the aromatic ring exhibit different chemical shifts.

On the other hand, the protons H_1 and H_3 of **H** experience deshielding in the presence of **G** molecules, due the downfield shift observed for these proton signals. This

behavior was also observed in the complexation of other guests by **H**.[14,15] A possible origin for the downfield shift could be related with the exchange between the complexed counterion BF_4^- by **G** in the rim of **H**. A more detail analysis of this behavior will be given after the DOSY NMR results have been presented.

The 2D NOESY NMR experiments are shown in Figure 3. As can be seen, all protons of **G** exhibits cross-peaks with $H_{3,4}$ and H_5 of the host, on contrary with H_1, where inexistent or insignificant cross-peaks were observed. This indicate that **G** should be well included into the cavity of **H** and therefore further away from the entrance of the macrocycle. The correlation between H_c and H_5 are stronger than that between H_c and $H_{3,4}$ or H_c and H_2, suggesting that the methyl group of **G** are closer of the aromatic protons of **H** than the trimethylammonium functional group. In this way, the 2D NMR results are in line with the structural assignment based on the complex-induced shifts.

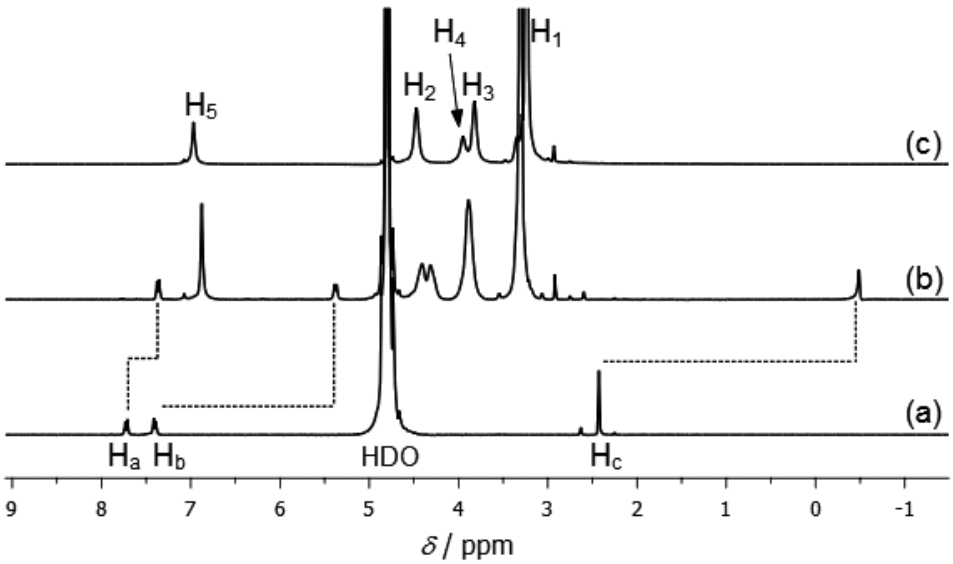

Figure 2. ^{1}H NMR spectra in D2O at 25 °C: (a) 2.0 mM **G**; (b) 2 mM **G** and **H**; 2 mM **H**.

In order to corroborate the binding stoichiometry obtained by ITC, a NMR titration at a constant **G** concentration was performed. As shown in Figure 4, the protons signals of **G** upfield shift more and more upon gradual addition of **H**, and then reach a plateau. By the tangent method, the inflection point appears at the host-guest molar ratio of 1.0, indicating a 1:1 binding stoichiometry, which is in accordance with the ITC experiments.

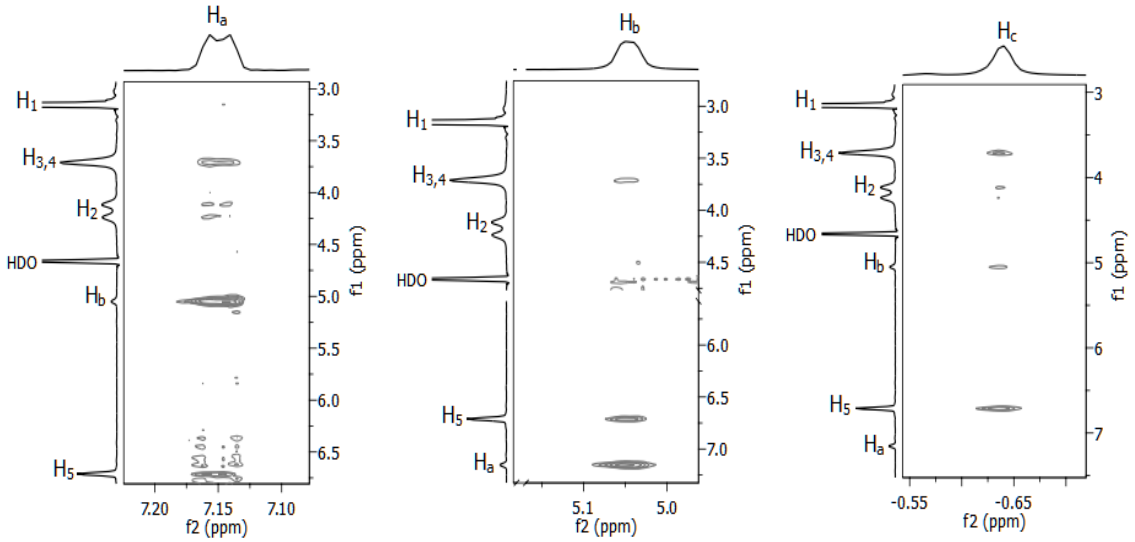

Figure 3. Portion of the 2D NOESY NMR spectrum of **H** (3 mM) with **G** (3 mM) with a mixing time of 500 ms in D_2O at 298.15 K.

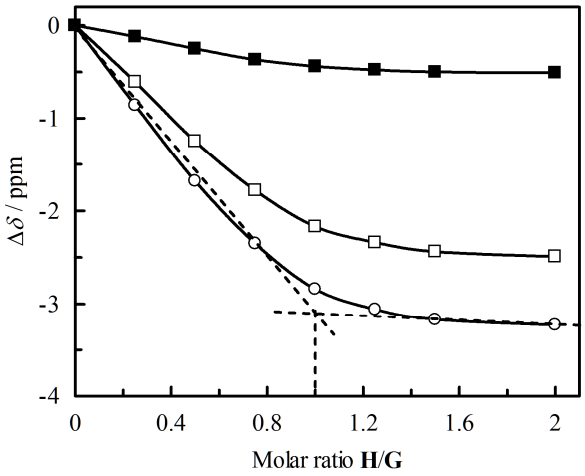

Figure 4. Chemical shifts changes experienced by the **G** protons (2.0 mM) by increasing the amounts of **H** in D_2O at 25 °C: H_a (■); H_b (□) and H_c (○).

3.3.1. Influence of the pillararene concentration

The complexation of cations and anions by macrocycles has been well reported in the literature.[27,28] However, some neglects have been made concerning the counterion of the macrocycles, as in the case of calixarenes.[28,29] In a previous work, we have reported the influence of the counterion in the complexation of a guest by a water-soluble

calixarene.[17] A decrease of almost 10 times in the binding constant for the formation of host-guest complex was observed when the concentration of the calixarene was increased from 0.07 mM to 7 mM. The pillar[5]arene with both rims functionalized and in neutral aqueous solution have ten counterions, BF_4^- in this case, which represent a large amount of counterion in solution. Therefore, it is recommended to study the counterion influence in the binding constant and thermodynamic parameters in the complexation of guests by the pillararene. For this purpose, the binding constant for the complex formation between **G** and **H** was analyzed by microcalorimetric titration at different **H** concentration (Figure S7). Figure 5 shows the dependence of the observed binding constant with increasing the concentration of **H**. As can be seen, K_{obs} decrease from 1.37×10^6 to 3.18×10^4 M^{-1} by increasing the **H** concentration from 0.01 mM to 1 mM. From the decrease in the observed binding constant, more than 40 times, it is intuitive to state that the experiments to determine the binding constants for the host-guest complexation, should be performed with the pillararene concentration constant.

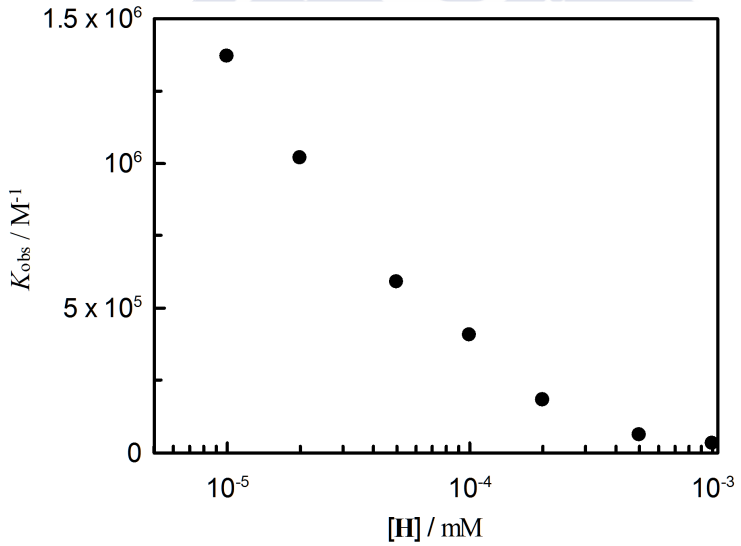

Figure 5. Influence of **H** concentration on K_{obs} for the inclusion complex between **G** and **H** at 25 °C. The K_{obs} values were obtained by microcalorimetric titration and fitted with the "one set of binding sites" model.

^1H and ^{19}F DOSY NMR experiments were also performed to further confirm the complexation of the counterion BF_4^- by **H** (Figure S8). Diffusion NMR experiments are a powerful technique, since it allows the determination of the diffusion of species in solution. Because the diffusion is dependent on the size and shape of the molecules, it is

usually employed for the study of host-guest complexes.[30] Figure 6 shows the D_{obs} obtained for the counterion BF_4^- at different **H** concentration. As can be seen, increasing the concentration of **H**, the diffusion coefficient of the counterion decrease due to formation of the complex between BF_4^- and **H**. For comparison, the diffusion coefficient of pure BF_4^- anion is 1.67×10^{-5} cm^2 s^{-1} (dotted black line), which is independent of KBF_4 salt concentration, and therefore ruled out changes in the solution viscosity in the concentration range studied. In addition, the constant self-diffusion coefficient obtained for **H** in the concentration range studied discard the self-aggregation of the host. Due the fast exchange in the NMR time scale, D_{obs} is given by the weight average of the molecules in the free and complexed states:

$$D_{\text{obs}} = \chi_{\text{bound}} D_{\text{bound}} + (1 - \chi_{\text{bound}}) D_{\text{free}} \quad (2)$$

Since the hydrodynamic radius of **H** is not changed upon guest complexation, and if we consider that the diffusion coefficient for the complexed counterion is the same as that for **H**, we can calculate the fraction of bound BF_4^-, $\chi_{bound}^{BF_4^-}$:

$$\chi_{bound}^{BF_4^-} = \frac{D_{\text{free}}^{BF_4^-} - \left(D_{BF_4^-}^{\mathbf{H}}\right)_{\text{obs}}}{D_{\text{free}}^{BF_4^-} - D_{\text{H}}^{\mathbf{H}}} \quad (3)$$

where $D_{\text{free}}^{BF_4^-}$ is the diffusion coefficient of free BF_4^-, $\left(D_{BF_4^-}^{\mathbf{H}}\right)_{\text{obs}}$ the observed diffusion coefficient at each BF_4^- counterion concentration and $D_{\text{H}}^{\mathbf{H}}$ the diffusion coefficient of **H** (Table 1). The results shows that increasing the concentration of **H**, the fraction of BF_4^- associated with the host also increase, which explain the decrease in the binding constant obtained at higher **H** concentration. Since the host:counterion molar ratio was keep constant in all experiments, 1:10, the calculated values $\chi_{bound}^{BF_4^-}$ indicate that in a 5 mM **H** solution, approximately half of BF_4^- counterions are complexed in the cavity (Figure 6, right).

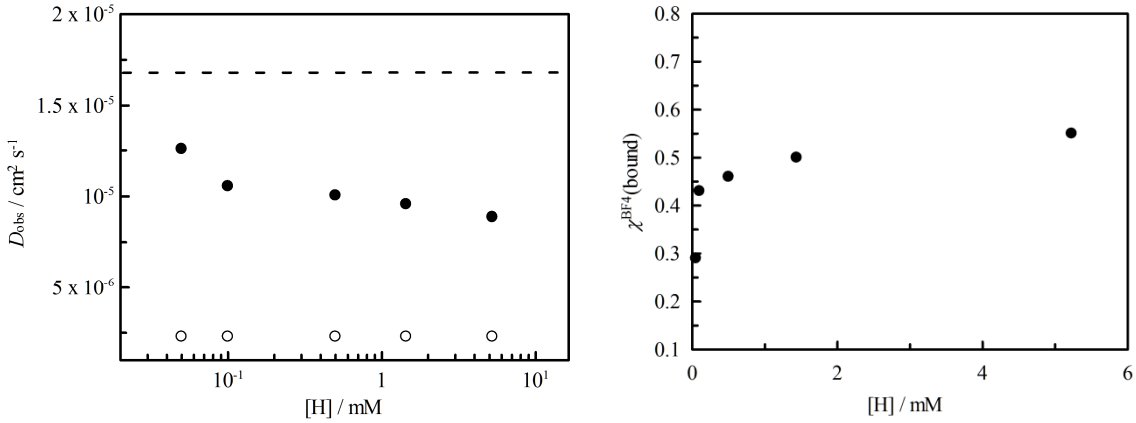

Figure 6. Influence of **H** concentration (○) in the diffusion coefficient of the counterion BF_4^- (●) in D_2O at 25 °C (left). Molar fraction of BF_4^- bound against the concentration of **H** (right).

Table 1. Observed self-diffusion coefficients for BF_4^- counterion ($D^{\mathbf{H}}_{BF_4^-}$) in different **H** sample concentration and the corresponding self-diffusion coefficients for the **H** host ($D^{\mathbf{H}}_{H}$).[a,b]

[**H**] (mM)	$D^{\mathbf{H}}_{BF_4^-}$ (10^{-5} cm^2 s^{-1})	$D^{\mathbf{H}}_{H}$ (10^{-6} cm^2 s^{-1})	$\chi^{BF_4^-}_{bound}$
0.05	1.26	2.28	0.29
0.10	1.05	2.28	0.43
0.50	1.00	2.28	0.46
1.44	0.96	2.28	0.50
5.23	0.89	2.28	0.55

[a] The fraction of complexed BF_4^- ($\chi^{BF_4^-}_{bound}$) was calculated by using eq 3. All measurements were carried out in D2O at 25 °C. To determine the diffusion of **H** ($D^{\mathbf{H}}_{H}$), the trimethylamonium group was followed. [b] 5 % error.

3.3.2. Influence of adding salt

In order to gain further insights into the influence of BF_4^- anions in the complexation of **G** by **H**, and also to corroborate the results obtained at different **H** concentrations (Figure 5), new ITC experiments were performed. In these experiments, the observed binding constant for the **G@H** complex formation was obtained in the presence of different KBF_4 concentrations (Table 2). It should be noted that the total concentration of KBF_4 added to the syringe (with the titrant **G**) takes into account the

BF_4^- as counterion of the **H** host plus the BF_4^- as salt added to the sample cell. As can be seen, and in accordance with the experiments above (Figure 5), the observed binding constant decrease with increasing the concentration of BF_4^- anions in aqueous solution. In the presence of 0.4 mM of anions, a binding constant of 6.37×10^5 M^{-1} was obtained, while in the presence of 12.0 mM the observed binding constant decrease to 2.4×10^4 M^{-1}. From Table 2, it also noteworthy the change in the thermodynamic parameters. An unfavorable difference of about 5 kJ mol^{-1} in the enthalpic gain (ΔH°) was found when the concentration of the anions was increased, while for the entropic term ($T\Delta S^\circ$) a favorable difference of 2.8 kJ mol^{-1} was observed. The difference observed in the enthalpic term could be related with the availability of free **H**, since with the increase of the BF_4^- amount in solution, a higher fraction of host is occupied and therefore less available to form complex with **G**, and/or also due the release of BF_4^- anions upon complexation of **G** by **H**. The more unfavorable entropic change could be attributed with the loss of conformational freedom of the complex in the presence of higher concentration of BF_4^- anions.

In the literature, a wide range of host-guest complexation studies has been performed and are reported in the presence of buffer solution.[31,26] More importantly, full thermodynamics characterization of the inclusion of guest series into macrocycles were based on the thermodynamic parameters obtained in that particular conditions. However, since the experiments were performed in the presence of buffer solution, an amount of salt in being added to the aqueous solution, and therefore will interfere with the complexation of guests by the host. Until now, only ^{1}H NMR experiments were performed to determine the complexation of guests by pillar[5]arenes, in which was maintained constant the concentration of the guest and the concentration of the hostwas changed. Despite the experiments were performed in absence of buffer solution, the complexation of the counterion by the macrocycle has been neglected.[15,14] In this work, we reported for the first time the determination of the complex formation between a guest and a pillararene host by microcalorimetry. Moreover, it is shown the influence of the host counterion in the binding constant and thermodynamic parameters in the complex formation. From the results shown in Table 2, we state that the experiments should be performed in absence of buffer solution and that the thermodynamic parameters are influenced by the counterion of the host. Furthermore, the decrease in the binding constant for the complexation of **G** by **H** suggests that a competitive binding scheme should be employed to determine the true binding constant.

Table 2. Binding constants (K_{obs}) and thermodynamic parameters determined by ITC for the intermolecular complexation of **G** with **H** in the presence of different BF_4^- anion concentration in water at neutral pH and 25 °C.[a]

$[BF_4^-]$/mM	K_{obs} /$(M^{-1})^b$	$\Delta G°$/(kJ $mol^{-1})^c$	$\Delta H°$/(kJ $mol^{-1})^c$	$T\Delta S°$/(kJ $mol^{-1})^c$
0.4	6.37×10^5	-33.1	-26.4	6.7
0.6	4.46×10^5	-32.2	-25.6	6.6
1.0	3.00×10^5	-31.3	-24.9	6.4
1.8	1.89×10^5	-30.1	-24.2	5.9
3.4	1.06×10^5	-28.5	-23.0	5.5
6.0	7.4×10^4	-27.8	-20.2	7.6
12.0	2.4×10^4	-25.4	-21.5	3.9

[a] The binding constants were obtained in experiments keeping constant the **H**. concentrations, 0.02 mM, and titrating with 0.25 mM of **G**. The reaction heat was fitted with the "one set of binding sites" model. [b] 5% error. [c] Error ± 0.1 kJ mol^{-1}.

In order to corroborate that a competitive binding should be employed in the complexation of **G** by **H**, ^1H and ^{19}F DOSY NMR experiments were performed. Figure 7 shows the observed diffusion coefficients (D_{obs}) for different concentrations of **G** in the presence of a constant concentration of **H.** As expected, the diffusion coefficient of BF_4^- increase upon increasing the concentration of **G**. However, a closer examination of D_{obs} values of BF_4^- with increasing the concentration of **G** (Figure 7 and Table S1), show that the diffusion coefficient do not increase to values close to that of free BF_4^- in bulk solution (dotted black line). This indicate that although a fraction of the counterion is being expelled from the **H** cavity, approximately 30% of BF_4^- remains in the cavity. Due the pillar shape of **H** with two rims, the results point toward that while **G** is being complexed in the cavity, there is still enough space to bind the counterion BF_4^-. Therefore, it is formed a ternary complex between the pillararene **H**, the counterion BF_4^- and **G**.

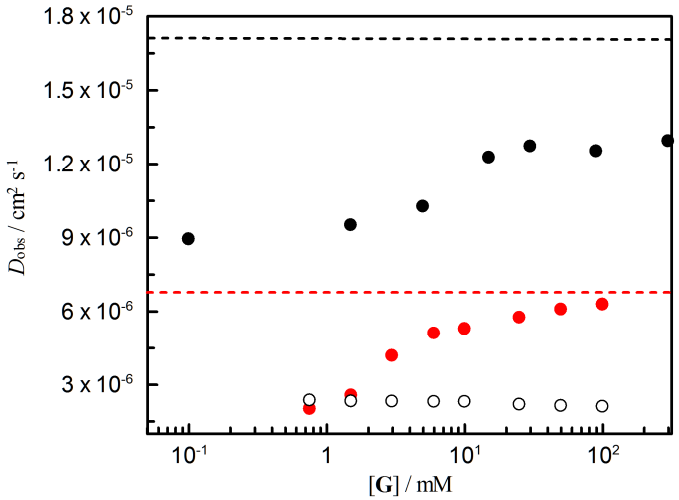

Figure 7. Observed diffusion coefficient (D_{obs}) of 1.5 mM of **H** (○) and the counterion BF_4^- (●) as a function of **G** (●) in D_2O at 25 °C. The dotted black and red line represents the diffusion coefficient of free BF_4^- and free **G** in aqueous solution, respectively.

Regarding with the D_{obs} of **G**, the results show that the diffusion of the guest and the host is equal until molar ratio 1, confirming the inclusion complex, and then increases until the diffusion value of free **G** (dotted red line). However, a qualitative analysis of the diffusion coefficient of **G**, reveals that more than one guest molecule is being complexed by the host (Table S2). Until molar ratio 2, only one molecule form an inclusion complex with **H**, which is in accordance with the previous ITC experiments, but at higher concentration of **G,** the results show that approximately two molecules of **G** are being complexed by the host. Despite no significant reaction heat associated with the intermolecular interaction was detected, as shown in the previous microcalorimetric titration (Figure S7), new ITC experiments were repeated in order to reach higher molar ratio of **G.** In this way, to confirm the formation of a host–guest complex with stoichiometry 1:2, a solution of **H** with **G** in the sample cell (at a molar ratio guest/host of 2), was titrated with **G** (Figure S9). As observed, no heat reaction was detected, which suggests a purely entropy-driven complexation of the second **G** by **H**. Since the complexation of the first guest is associated with a favorable enthalpic gain, the absence of an apparent reaction heat, suggests that the complexation of the second guest molecule should be external. Such as ion-pairing is often thermoneutral,[32] this could be the case of the interaction of the external **G** with the trimethylammonium rim of **H**. Consequently, we propose a ternary model with stoichiometry 1:2:3 (host–guest–counterion) where one **G** molecule is included in the cavity of the host, in

addition to the $BF4^-$ counterions that remain inside of **H**, while the other molecule form an external complex with **H** (Scheme 8). The diffusion coefficient of **H** also corroborate this model, since at higher concentration of **G**, the D_{obs} value of **H** decrease (Table S2). This fact can be related with the higher size and shape of the complex between **H** with the external molecule of **G**, in comparison with the inclusion complex **G@H** at lower concentration of **G**, where the complex assume approximately the same size as **H**.[33,34]

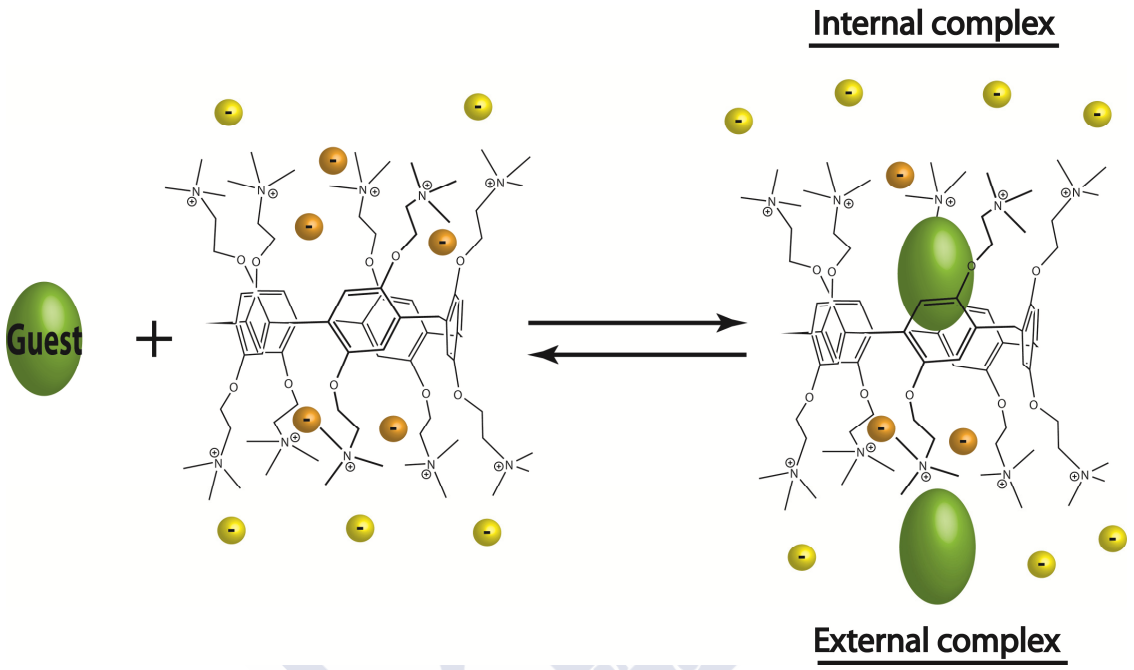

Scheme 8

3.4. Conclusions

In conclusion, we demonstrated the influence of the **H** counterion, BF_4^-, in the complexation of an anionic guest. Increasing the concentration of **H** or the amount of BF_4^- in solution leads to a decrease in the binding constant for the complex formation between **G** and **H**. This is a consequence of the complexation of the counterion BF_4^- by the host. Since BF_4^- is always present in solution as counterion of **H**, the experiments should be performed by keeping the concentration of **H** constant. Otherwise, a competitive binding scheme should be employed to determine the true binding constant. Diffusion experiments show that, despite the inclusion of **G** in the cavity of **H**, a fraction of counterion remain in the cavity of **H**, indicating the formation of a ternary complex. Moreover, at higher concentration of **G**, an external complex is formed with **H** in addition to the internal complex. The arrangement of external complexes between guests and pillararenes might be useful for the formation of supramolecular polymers or other high-order structures.

3.5. Appendix

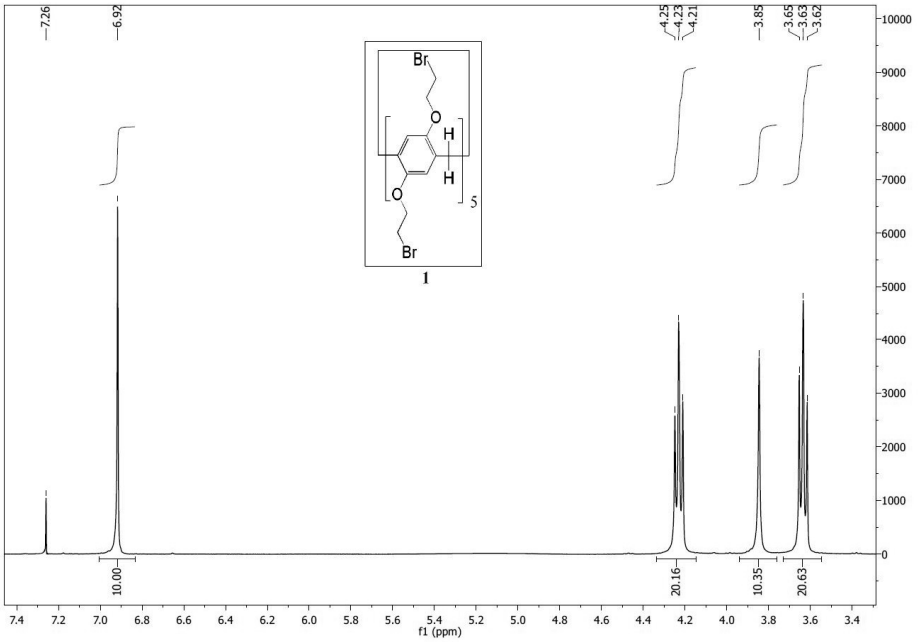

Figure S1. ^{1}H NMR spectrum (500 MHz, $CDCl_3$, 25 °C) of **1**.

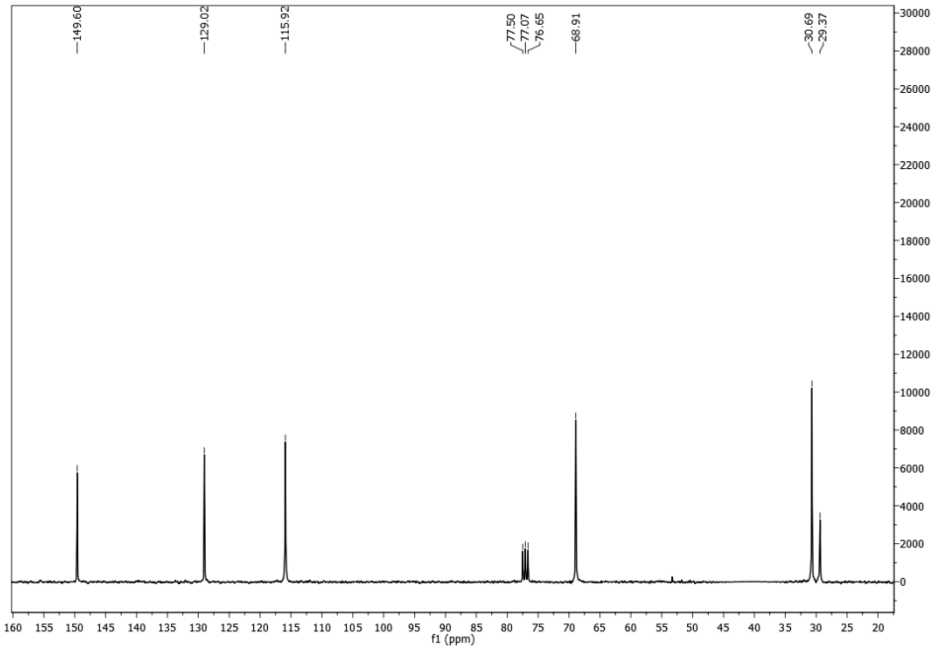

Figure S2. ^{13}C NMR spectrum (75 MHz, $CDCl_3$, 25 °C) of **1**.

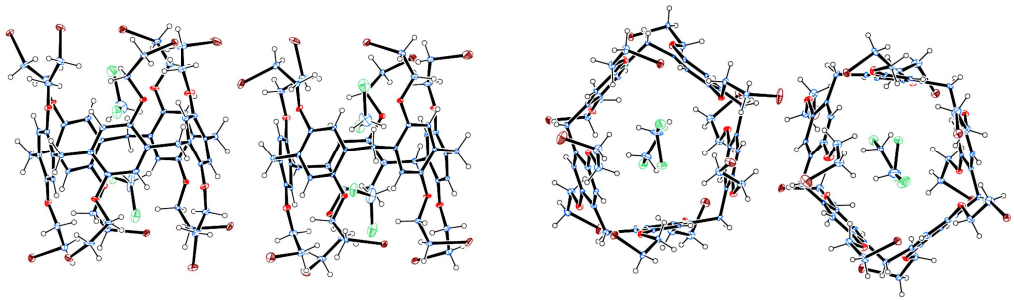

Empirical formula	$C_{55}H_{60}Br_{10}O_{10}$, $2(CH_2Cl_2)$
Formula weight	1849.89
Temperature	100(2) K
Wavelength	0.71073 Å
Crystal system	Monoclinic
Space group	$P2_1$
Unit cell dimensions	a = 13.0967(3) Å α= 90°
	b = 21.4895(5) Å β= 95.3140(10)°
	c = 23.5943(5) Å γ = 90°
Volume	6611.9(3) $Å^3$
Z	4
Density (calculated)	1.858 Mg/m^3
Absorption coefficient	6.275 mm^{-1}
F(000)	3616
Crystal size	0.37 x 0.30 x 0.18 mm^3
Theta range for data collection	0.87 to 26.73°
Index ranges	-16<=h<=16, -27<=k<=24, 0<=l<=29
Reflections collected	108500
Independent reflections	27104 [R(int) = 0.0824]
Completeness to theta = 26.73°	100.0 %
Absorption correction	Semi-empirical from equivalents
Max. and min. transmission	0.2978 and 0.1813
Refinement method	Full-matrix least-squares on F^2
Data / restraints / parameters	27104 / 1813 / 1543
Goodness-of-fit on F^2	1.051
Final R indices [I>2sigma(I)]	R1 = 0.0598, wR2 = 0.1232
R indices (all data)	R1 = 0.0944, wR2 = 0.1359
Absolute structure parameter	0.467(8)
Largest diff. peak and hole	1.802 and -1.243 e.$Å^{-3}$

Figure S3. X-ray crystal structure of **1**.

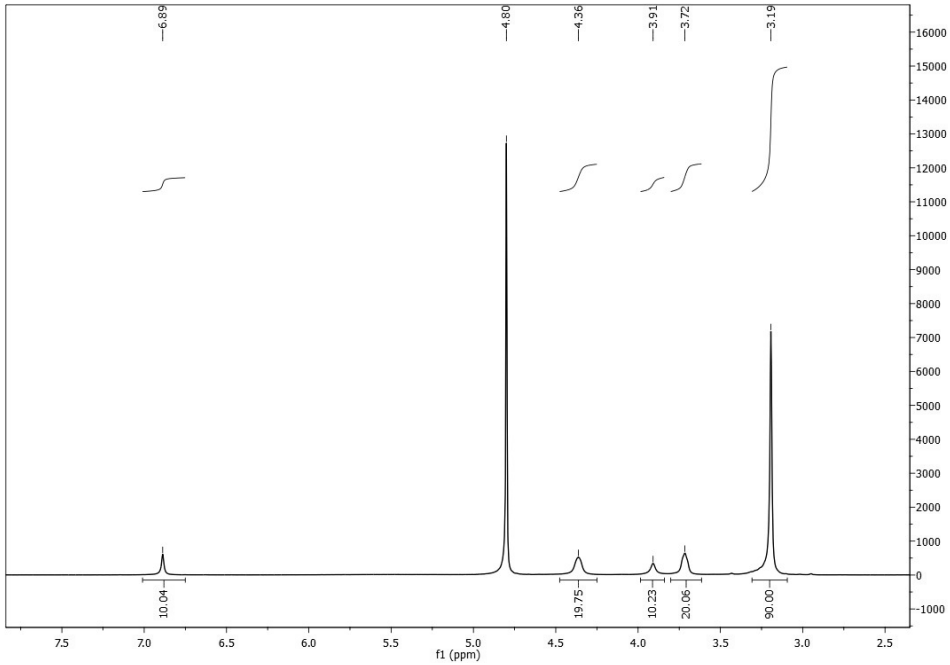

Figure S4. ^{1}H NMR spectrum (500 MHz, D_2O, 25 °C) of **H**.

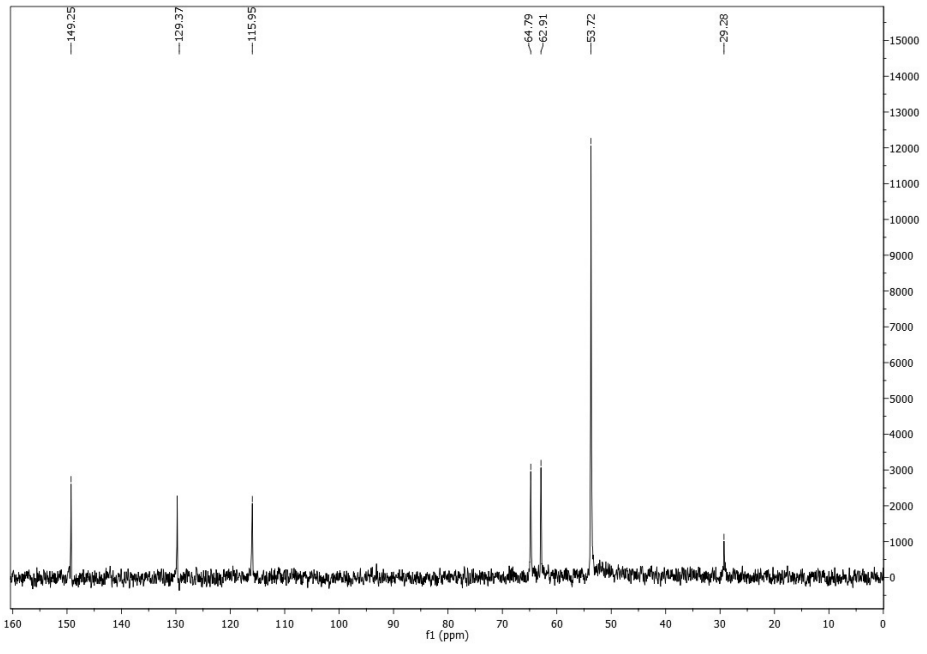

Figure S5. ^{13}C NMR spectrum (75 MHz, D_2O, 25 °C) of **H**.

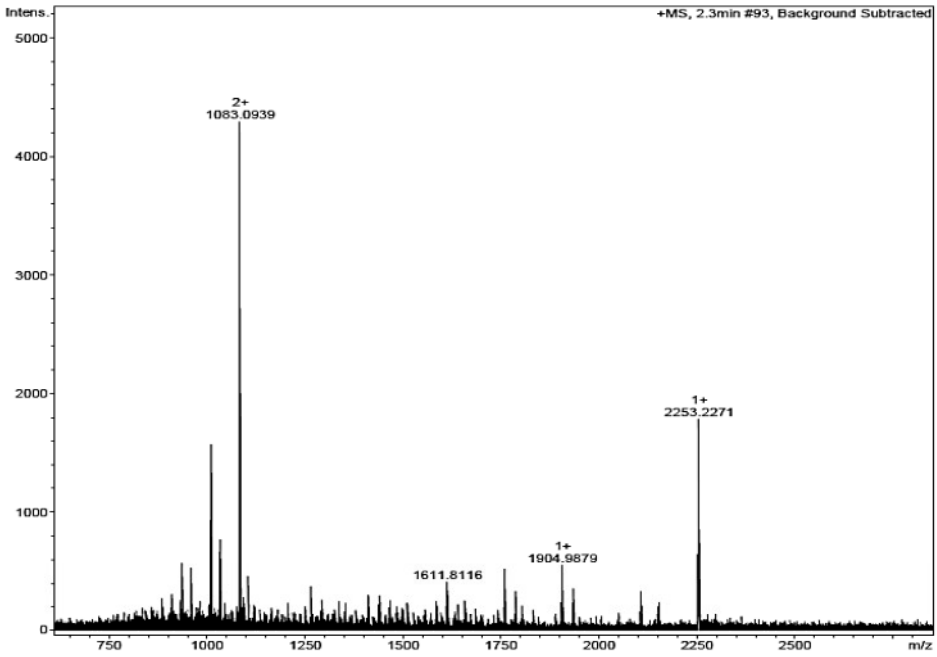

Figure S6. Electrospray ionization mass spectrum of **H**.

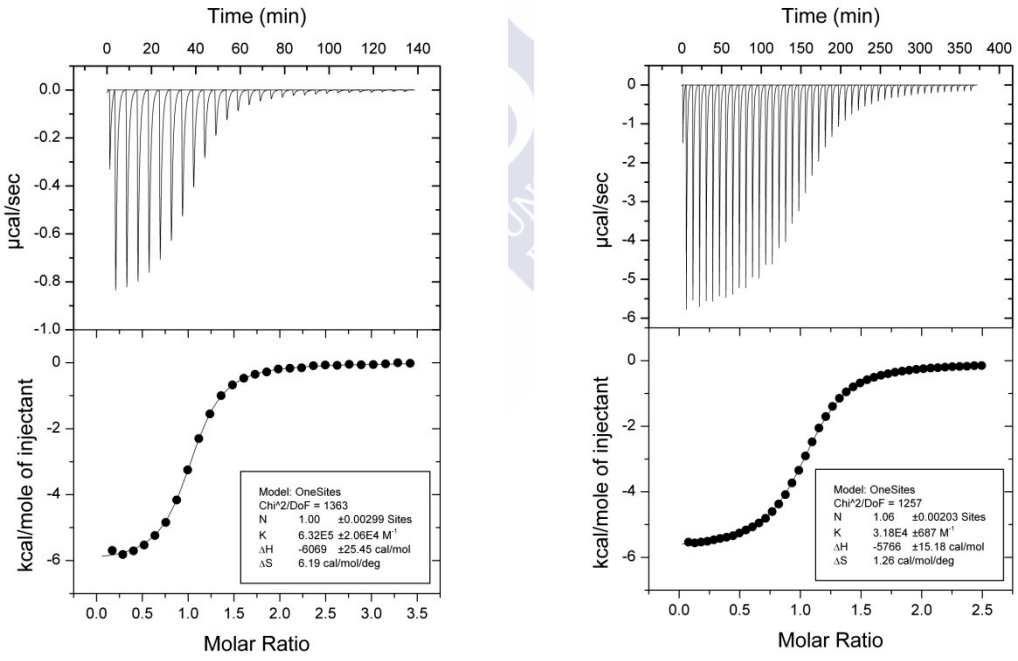

Figure S7. Microcalorimetric titration of **G** with **H** at 25 °C in aqueous solution: (upper) raw data for sequential injections of **G** solution (1 mM or 15 mM) into **H** solution (0.05 mM, left) and (1 mM, right); (down) heat of reaction obtained from the integration of the calorimetric trace after subtracting the dilution heat from the reaction heat and fitted with "one set of binding sites" model.

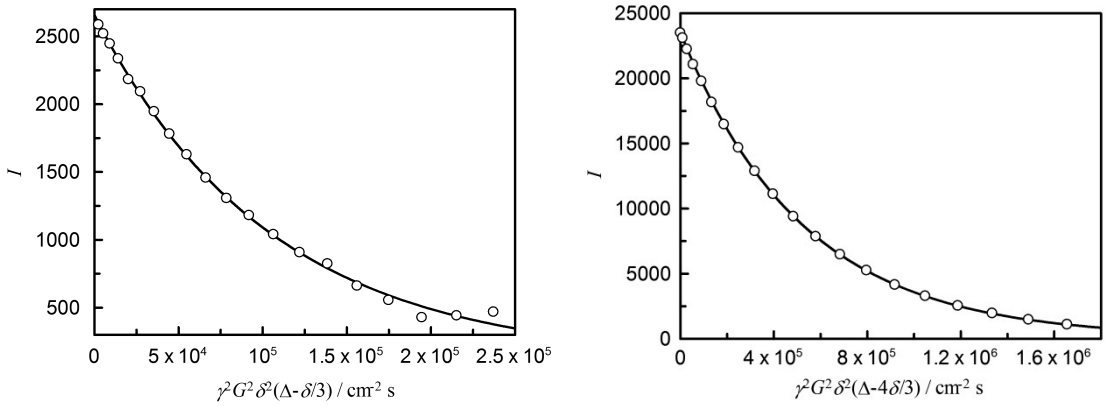

Figure S8. ^{19}F (left) and ^{1}H (right) signal decay for a 1.5mM **H** sample in D_2O at 25 °C. The solid line shows the non linear fit to eq 1.

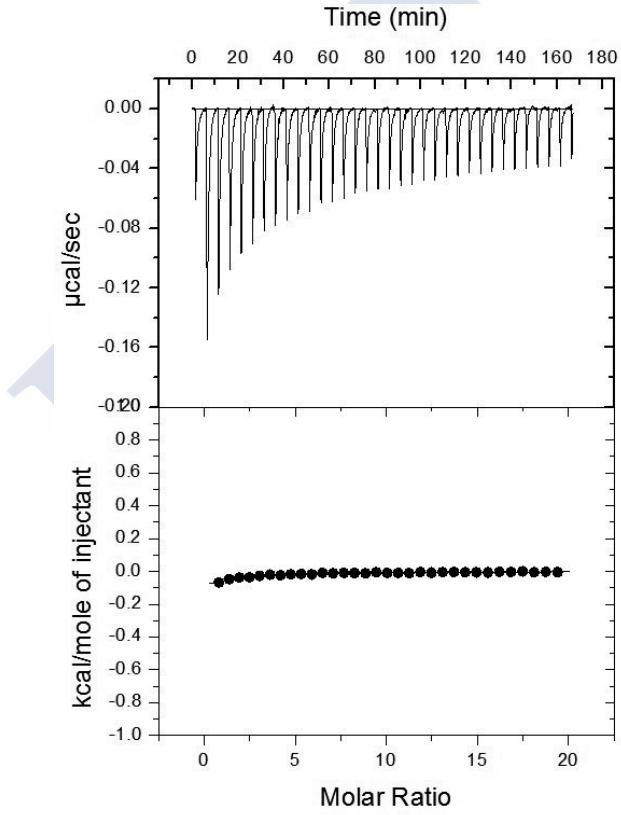

Figure S9. Microcalorimetric titration of **H** with **G** at 298.15 K in aqueous solution: (top) raw data for the sequential 8 µL injections of **G** (10 mM) into **H+G** (0.1 mM + 0.2 mM); (bottom) heat of reaction obtained from the integration of the calorimetric trace after subtracting the dilution heat from the reaction heat.

Table S1. Observed self-diffusion coefficients for BF_4^- ($D^{\mathbf{H}}_{BF_4}$) upon addition different concentrations of **G** to an 1.5 mM solution of **H**.[a,b]

[**G**] (mM)	$D^{\mathbf{H}}_{BF_4}$ (10^{-5} cm^2 s^{-1})	$\chi^{BF_4}_{bound}$
0.1	0.89	0.54
1.5	0.95	0.50
5.0	1.03	0.45
15.0	1.23	0.31
30.0	1.27	0.28
90.0	1.27	0.28
300.0	1.29	0.27

[a] The fraction of complexed BF_4^- ($\chi^{BF_4}_{bound}$) was calculated by using eq 3. $[BF_4^-] = 15.0$ mM. To determine the fraction of BF_4^- was considered a diffusion coefficient of $D^{\mathbf{H}}_{H} = 2.29 \times 10^{-6}$ cm^2 s^{-1}. All measurements were carried out in D_2O at 25 °C. [b] 5 % error.

Table S2. Observed self-diffusion coefficients for **G** ($D^{\mathbf{H}}_{\mathbf{G}}$) and **H** ($D^{\mathbf{H}}_{H}$) upon addition different concentrations of **G** to an 1.5 mM solution of **H**.[a,b]

[**G**] (mM)	$D^{\mathbf{H}}_{\mathbf{G}}$ (10^{-6} cm^2 s^{-1})	$D^{\mathbf{H}}_{H}$ (10^{-6} cm^2 s^{-1})	$\chi^{\mathbf{G}}_{bound}$	[**G**]$_{bound}$ (mM)
0.75	2.20	2.29	1.02	0.51
1.50	2.53	2.27	0.94	0.95
2.00	3.73	2.30	0.71	0.93
3.00	4.25	2.28	0.54	1.08
6.00	4.91	2.26	0.32	1.27
10.00	5.36	2.29	0.27	1.81
25.00	5.68	2.18	0.15	2.58
50.00	6.17	2.11	0.07	2.42
100.00	6.27	2.08	0.03	1.71

[a] The fraction of complexed **G** ($\chi^{\mathbf{G}}_{bound}$) was calculated by using eq 3. All measurements were carried out in D_2O at 25 °C. To determine the diffusion coefficient of **H** ($D^{\mathbf{H}}_{H}$), the trimethylamonium group was followed. [b] 5 % error.

3.6. References

1. (a) C. J. Pedersen, *J. Am. Chem. Soc.*, 1967, **89**, 7017–7036; (b) C. D. Gutsche, in *Calixarenes, An Introduction*, The Royal Society of Chemistry, Cambridge, U.K., 2nd ed., 2008; (c) F. Hapiot, S. Tilloy, and E. Monflier, *Chem. Rev.*, 2006, **106**, 767–781; K. Kim, N. Selvapalam, and D. H. Oh, *J. Incl. Phenom. Macrocycl. Chem.*, 2004, **50**, 31–36.

2. T. Ogoshi, S. Kanai, S. Fujinami, and T. Yamagishi, *J. Am. Chem. Soc.*, 2008, **130**, 5022–5023.

3. M. I. N. Xue, Y. Yang, X. Chi, Z. Zhang, and F. Huang, *Acc. Chem. Res.*, 2012, **45**, 1294–1308.

4. P. J. Cragg and K. Sharma, *Chem. Soc. Rev.*, 2012, **41**, 597–607.

5. T. Ogoshi and T. Yamagishi, *Eur. J. Org. Chem.*, 2013, **2013**, 2961–2975.

6. N. L. Strutt, R. S. Forgan, J. M. Spruell, Y. Y. Botros, and J. F. Stoddart, *J. Am. Chem. Soc.*, 2011, **133**, 5668–5671.

7. C. Han, G. Yu, B. Zheng, and F. Huang, *Org. Lett.*, 2012, **14**, 1712–1715.

8. T. Ogoshi, M. Hashizume, T. Yamagishi, and Y. Nakamoto, *Chem. Commun.*, 2010, **46**, 3708–3710.

9. G. Yu, X. Zhou, Z. Zhang, C. Han, Z. Mao, C. Gao, and F. Huang, *J. Am. Chem. Soc.*, 2012, **134**, 19489–19497.

10. C. Li, X. Shu, J. Li, S. Chen, K. Han, M. Xu, B. Hu, Y. Yu, and X. Jia, *J. Org. Chem.*, 2011, **76**, 8458–65.

11. X.-B. Hu, L. Chen, W. Si, Y. Yu, and J.-L. Hou, *Chem. commun.*, 2011, **47**, 4694–6.

12. Y. Ma, X. Ji, F. Xiang, X. Chi, C. Han, J. He, Z. Abliz, W. Chen, and F. Huang, *Chem. Commun.*, 2011, **47**, 12340–12342.

13. N. L. Strutt, H. Zhang, M. A. Giesener, J. Lei, and J. F. Stoddart, *Chem. Commun.*, 2012, **48**, 1647–1649.

14. C. Li, J. Ma, L. Zhao, Y. Zhang, Y. Yu, X. Shu, J. Li, and X. Jia, *Chem. Commun.*, 2013, **49**, 1924–6.

15. Y. Ma, M. Xue, Z. Zhang, X. Chi, and F. Huang, *Tetrahedron*, 2013, **69**, 4532–4535.

16. Z. Asfari, V. Bohmer, J. Harrowfield, and J. Vicens, *Calixarenes 2001*, Kluwer Academic Publishers, Dordrecht, The Netherlands, 2001.

17. V. Francisco, N. Basilio, and L. García-Río, *J. Phys. Chem. B*, 2012, **116**, 5308–5315.

18. N. Basilio, V. Francisco, and L. García-Rio, *to be submitted*.

19. A. Jerschow and M. Norbert, *J. Magn. Reson.*, 1997, **375**, 372–375.

20. D. Wu, A. Chen, and C. S. Johnson, *J. Magn. Reson. A*, 1995, **115**, 260–264.

21. W. S. Price, *Concepts Magn. Reson.*, 1998, **10**, 197–237.

22. A. C. F. Ribeiro, V. M. M. Lobo, A. J. F. N. Sobral, H. T. F. C. Soares, A. R. J. Leal, and M. A. Esteso, *Acta Chim. Slov.*, 2010, **57**, 410–414.

23. N. Douteau-Guével, A. W. Coleman, J.-P. Morel, and N. Morel-Desrosiers, *J. Chem. Soc., Perkin Trans. 2*, 1999, 629–633.

24. G. Arena, S. Gentile, F. G. Gulino, D. Sciotto, and C. Sgarlata, *Tetrahedron Lett.*, 2004, **45**, 7091–7094.

25. D.-S. Guo, L.-H. Wang, and Y. Liu, *J. Org. Chem.*, 2007, **72**, 7775–8.

26. Y. Liu, D.-S. Guo, H.-Y. Zhang, Y.-H. Ma, and E.-C. Yang, *J. Phys. Chem. B*, 2006, **110**, 3428–3434.

27. P. D. Beer and P. A. Gale, *Angew. Chem. Int. Ed.*, 2001, **40**, 486–516.

28. H. Bakirci, A. L. Koner, and W. M. Nau, *Chem. Commun.*, 2005, 5411–5413.

29. N. Basilio, L. García-Río, and M. Martín-Pastor, *J. Phys. Chem. B*, 2010, **114**, 7201–7206.

30. Y. Cohen, L. Avram, and L. Frish, *Angew. Chem. Int. Ed.*, 2005, **44**, 520–554.

31. G. Arena, A. Casnati, A. Contino, A. Magrì, F. Sansone, D. Sciotto, and R. Ungaro, *Organic & biomolecular chemistry*, 2006, **4**, 243–249.

32. S. L. Tobey and E. V Anslyn, *J. Am. Chem. Soc.*, 2003, **125**, 10963–70.

33. B. Antalek, *Concepts Magn. Reson.*, 2002, **14**, 225–258.

34. G. A. Morris, *Diffusion-Ordered Spectroscopy*, John Wiley & Sons, Ltd, Chichester, UK, 2009.

USC
UNIVERSIDADE
DE SANTIAGO
DE COMPOSTELA

Chapter 4

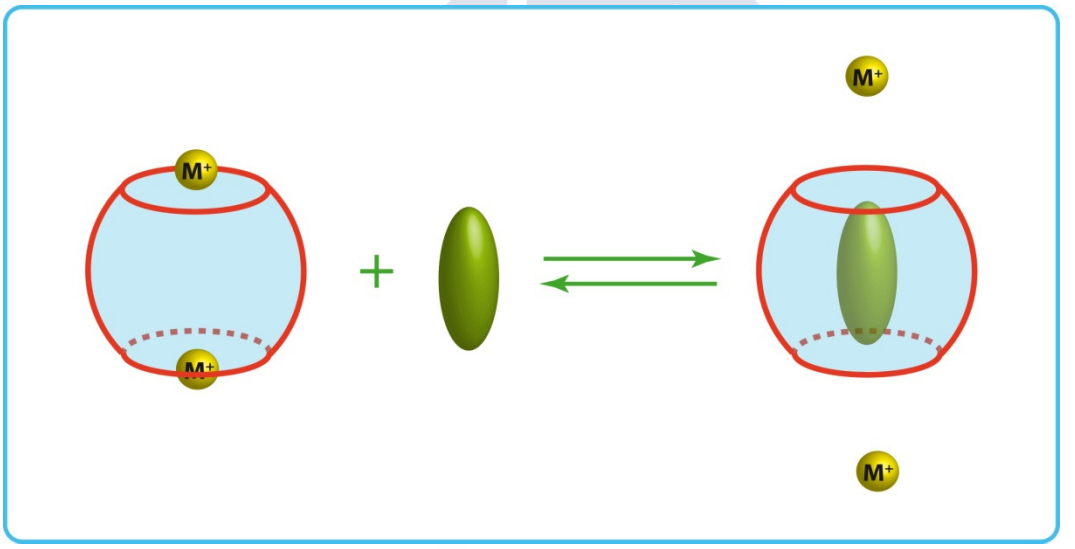

USC
UNIVERSIDADE
DE SANTIAGO
DE COMPOSTELA

4. Kinetic studies of the interaction of a guest with cucurbit[6]uril: influence of cations*

4.1. Introduction

The molecular recognition of cucurbit[*n*]urils has been extensively studied in the last few years, mainly after the synthesis of homologues of the first macrocycle obtained, the cucurbit[6]uril.[1] A wide range of guests can be incorporated in the macrocycle cavity, but since the two density charged portals and a hydrophobic cavity, neutral and positive charged molecules are preferred by these hosts.[2,3] These macrocycles share some characteristics with the analogues cyclodextrins (CD), such as the cavity size and a hydrophobic cavity. On the other hand, regarding with binding affinities, the cucurbiturils show higher binding constants than the analogues.[4,5] Due the recognized host capabilities of the cucurbiturils, these macrocycles have been employed in several applications, such as supramolecular catalysis,[6,7] drug delivery,[8,9] enzyme assays[10] and dye encapsulation.[11] Most of these studies are performed in aqueous solution, despite these macrocycle are not particularly known for their high solubility in water. In this way, the addition of metal cations is often required to enhance the solubility. The increase in water solubility can be related with the complexation of the cations by the two portal of the cucurbiturils, which as reported by Kim and coworkers, function as "lids" to seal the portals and promote binding.[12] Since the portals of the macrocycle provide the accessibility to the hydrophobic cavity, besides the complexation of guests through ion-dipole interactions, the presence of metal cations influence the host-guest chemistry of these hosts. In this way, Nau and coworkers studied the influence of salt addition in the complexation of cyclohexylmethylammonium ions by cucurbit[6]uril (CB6) by NMR experiments.[13] In this chapter it is studied the influence of the temperature and the size of the added salt in the kinetics for the complexation of a fluorescence dye, *trans*-4-[4-(dimethylamino)styryl]-1-methylpyridinium iodide (DSMI) by cucurbit[6]uril (Scheme 1).

---

* This work was performed at the Jacobs University Bremen (Germany), under the supervision of professor Werner M. Nau.

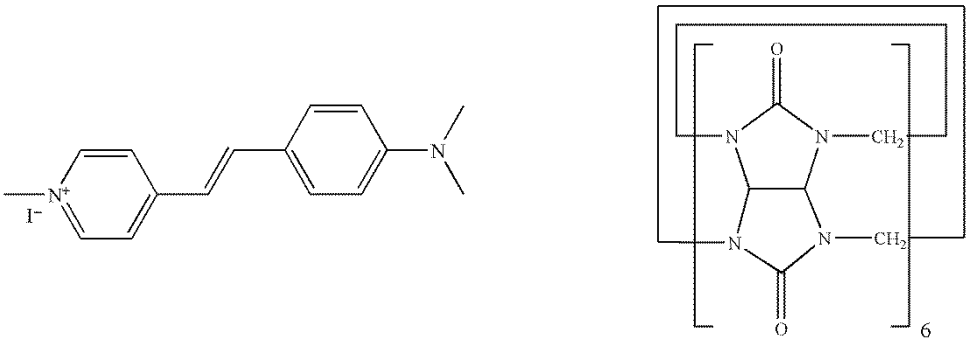

DSMI CB6

Scheme 1. The chemical structure of DSMI and CB6

4.2. Experimental Section

NaCl, CsCl, $BaCl_2$ and tetramethylammonium chloride salts were purchased from Sigma-Aldrich and used as received. CB6 and DSMI were synthesized according to the literature.[1,14] All experiments were performed in Milli-Q water, and the pH values of the solutions were adjusted by addition of HCl or NaOH until pH ≈ 7. pH readings were taken with a WTW 330i pH meter with a combined pH glass electrode (SenTix Mic).

UV–Vis experiment was recorded by using a Varian Cary 4000 spectrophotometer, while the fluorescence experiment was with a Varian Cary Eclipse fluorimeter. A FP-8500 stopped-flow sytem (Jasco) was employed for the kinetic measurements. Excitation and emission bandwidth were fixed at 10 nm and 20 nm, respectively.

4.3. Results and Discussion

The maximum absorption for the guest DSMI in the presence of CB[6] was determined by UV–vis. A peak centered at 450 nm was obtained. In addition, a fluorescence peak at 580 nm was observed from the fluorescence experiments (Figure 1). This behavior is in accordance with the results reported in the literature.[15] As can be seen in Figure 1, the inclusion of the guest in the macrocycle cavity leads to a great enhancement in the fluorescence response of DSMI. The enhancement performance can be related with the restricted rotation of the guest inside the host cavity. Since the narrow cavity of CB6 prohibits the twisted intramolecular charge transfer, which is responsible for the nonradiative decay of the guest, resulting in the significant fluorescence enhancement observed.[15]

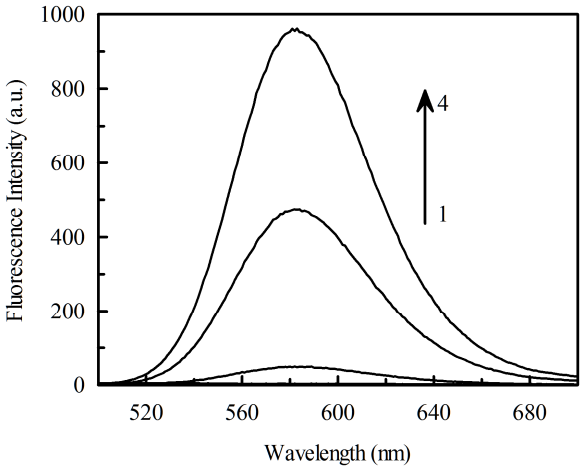

Figure 1. Fluorescence emission spectra for DSMI (2.5 μM) with increasing concentration of CB[6], from 0.0 μM (1) to 3.3 μM (4) at pH ≈ 7.

4.3.1. Kinetics for the formation of the DSMI@CB6 complex

The kinetics for the formation of the complex between DSMI and CB6 were measured by fluorescence stopped-flow experiments. It should be noted that the experiments are performed at pH ≈ 7, where the dimethylamino group of DSMI is unprotonated, since the pKa of DSMI only change from 3.1 to 3.9 upon complexation with CB6.[15] Figure 2 shows the monoexponential growth upon complex formation, indicating that only one relaxation process was observed when the guest and the host were mixed in the sample cell. As can be seen, increasing the concentration of CB6 leads to an increase in the amplitude of the signal and therefore higher k_{obs} values (Figure 3).

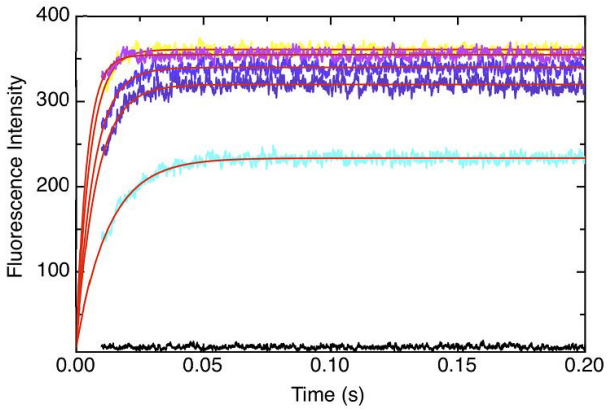

Figure 2. Stopped flow traces fit with a mono-exponential function (red line) for the mixing of DSMI (0.05 μM) with increasing CB[6] concentration (0.0–6 μM), at pH ≈ 7, 25 °C. λ_{ex} = 450 nm, λ_{ex} = 580 nm.

The observed rate constants were obtained by fitting the growth kinetics to eq 1, where I_0 and I_∞ are the intensities at time zero and the total amplitude for the kinetics, respectively.

$$I = I_0 + I_\infty(1 - e^{-k_{obs}t}) \quad (1)$$

The one-step kinetic model that describe the stopped-flow data is the following:

$$G + CB6 \underset{k_{-1}}{\overset{k_1}{\rightleftharpoons}} G@CB6 \quad (2)$$

The differential rate law and the expression of the equilibrium constant for the one-step model are as follows:

$$\frac{d[V]}{dt} = -k_1[G][CB6] + k_{-1}[G@CB6] \quad (3)$$

$$K_1 = \frac{k_1}{k_{-1}} = \frac{[G@CB6]_{Eq}}{[G]_{Eq}[CB6]_{Eq}} \quad (4)$$

The concentration of CB6 is always higher than the DSMI concentration, and consequently the reaction was studied under pseudo-first order conditions. As can be seen, the dependence of k_{obs} with the concentration of CB6 is linear. From the linear fit of the data, it was obtained the association rate constant $k_1 = (3.50 \pm 0.40) \times 10^7$ M^{-1} s^{-1} and for the dissociation $k_{-1} = 50.5 \pm 10.4$ s^{-1}. The kinetically deduced value of the binding constant is $K_1 = k_1/k_{-1} = (6.93 \pm 0.7) \times 10^5$ M^{-1}. The high equilibrium constant obtained for the complex formation is related with the slow dissociation rate constant, ca. 50 s^{-1}. Moreover, the binding constant can also be determined taking in consideration the equilibrium K_1 = [G@CB6]/[CB6][G]. Inserting the mass balance and since the concentration of CB6 is higher than that of the complex, $[CB6_0] \sim [CB6]$, the following equation is used to fit the data:

$$I = \frac{I_0 + I_1K_1[CB6]_0}{1 + K_1[CB6]_0} \quad (5)$$

where I_0 and I_1 denote the fluorescence intensity in pure water and in the complex, respectively, and I is the fluorescence intensity at a given CB6 concentration. The binding constant $K = 1.45 \pm 0.23 \times 10^6$ M^{-1} was obtained. This binding constant show some discrepancy with the value reported in the literature, however this could be due the fact that the authors obtained the binding constant by a linear regression approach (Benesi-Hildebrand plot), instead of a more reliable nonlinear least-square regression analysis.

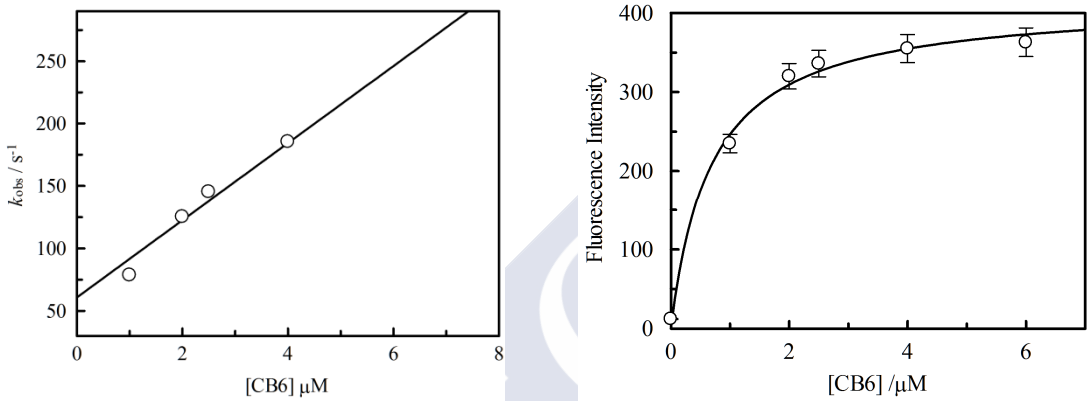

Figure 3. (Left) Dependence of the observed rate constant (k_{obs}) for the formation of the complex between DSMI and CB6, at a constant concentration of DSMI (0.05 μM), pH ≈ 7, 25 °C. The black line represents the linear regression analysis for the data points. (Right) Plot of the fluorescence intensity against the concentration of CB6 for guest DSMI complexed to CB6. The black line is the nonlinear fit to eq 5.

To determine the influence of the temperature in the kinetics for the complexation of DSMI by CB6, experiments at different temperatures were performed (Figure 4). Table 1 shows the results from the linear fitting of the observed rate constant with increasing the concentration of CB6 at each temperature. As can be seen, both association and dissociation rate constant increase with the temperature. On the contrary, the corresponding binding constant for the complex formation decrease with increasing the temperature. Due the small temperature range studied, using the classical method of plotting ln$K$ against 1/T (van't Hoff method) to obtain the thermodynamic parameters, will lead to a relatively large error. However, the trend observed, which was also observed for other guests,[13] suggests that the complexation of DSMI by CB6 is enthalpy-driven. In the temperature range studied, it was also calculated the activation enthalpy, $\Delta H_1^{\ddagger} = 28.0$ kJ mol^{-1}.

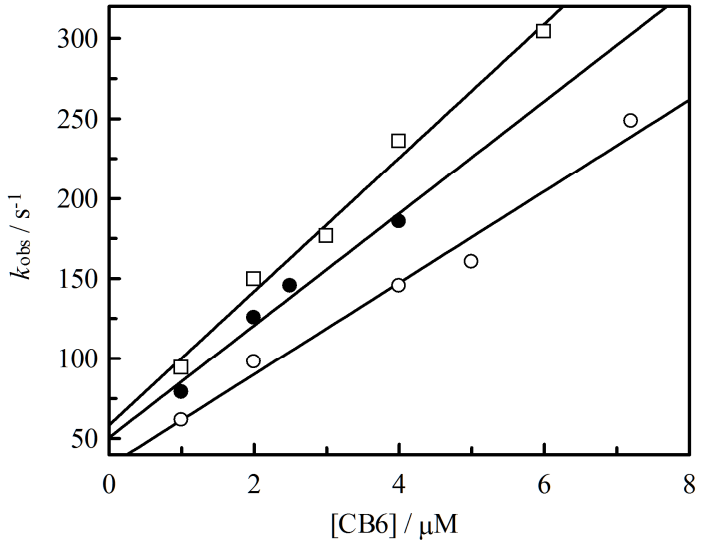

Figure 4. Dependence of the observed rate constant for the formation of the DSMI@CB[6] complex at different temperatures: 20 °C (○), 25 °C (●), 30 °C (□).

Table 1. Rate and binding constants for the complex formation DSMI@CB6, monitored via fluorescence at different temperatures.

T (ºC)	$10^{-6}\ k_1$ /($M^{-1}\ s^{-1}$)	k_{-1} /s^{-1}	K/ M^{-1}
20	28.6 ± 2.3	32.9 ± 10	$8.9 \pm 0.9 \times 10^5$
25	35.0 ± 4.0	50.5 ± 10	$6.9 \pm 0.7 \times 10^5$
30	41.8 ± 2.5	58.3 ± 9.1	$7.2 \pm 0.7 \times 10^5$

4.3.2. Influence of different cations on the kinetics

The kinetics for the complexation of DSMI by CB6 was also studied as a function of the size and cation concentration. The experiments were performed in the presence of different concentration of NaCl and CsCl salts, and also to study the cation size influence, experiments were performed in the presence of $BaCl_2$ and tetramethylammonium chloride (TMACl). As an example, Figure 5 shows the fluorescence stopped-flow experiments by mixing DSMI with CB6 at various CB6 concentrations, in the presence of different concentration of CsCl. As can be seen, all curves follow a monoexponential growth, in comparison with the kinetics in absence of salt, suggesting that binding of the cations to both portals of CB6 is a fast process and can be treated as a pre-equilibrium steps.

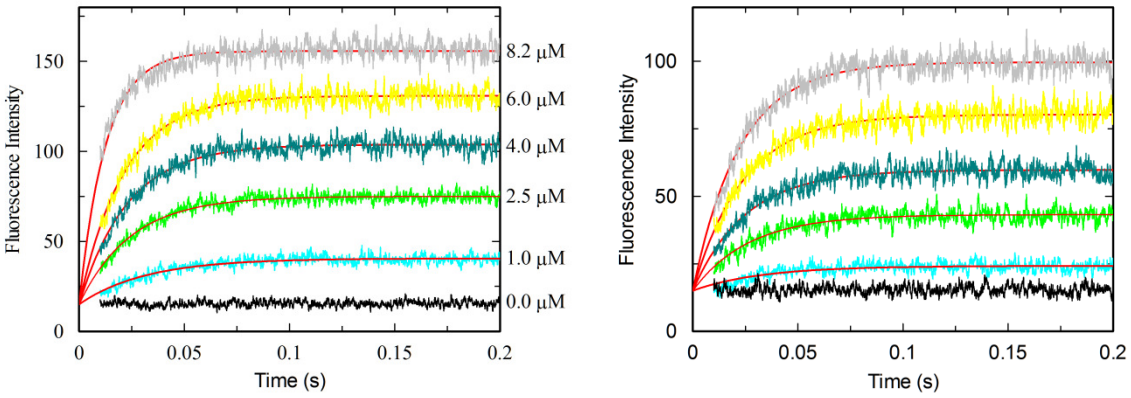

Figure 5. Kinetics for the formation of DSMI@CB6 complex by mixing a DSMI (0.1 μM) solution at various CB6 concentration (0–8.2 μM) in the presence of 0.2 mM (left) and 0.5 mM CsCl (right). The solid red lines represents the fit of the data to eq 1. λ_{ex} = 450 nm, λ_{ex} = 580 nm, pH ≈ 7, 25 °C.

Figure 6 shows the dependence of the observed rate constant for the formation of the DSMI@CB6 complex with the concentration of CB6 in the presence of different concentration of CsCl. The k_{obs} values are recovered by fitting the growth kinetics to eq 1. As can be seen, a linear trend is observed with increasing the concentration of the host. The cucurbiturils are well known for their two portals, which in the presence of protons or metal cations, can accommodate the cations (rather than inclusion in the cavity) to form 1:1 or 1:2 complexes. Consequently, CB6 with one metal cations in one portal or both portals with one metal cation should be considered in the equilibria. The mechanism for the complexation of DSMI by CB6 in the presence of salt is proposed in Scheme 2.

$$\mathrm{CB6} + \mathrm{G} \overset{K_1}{\rightleftharpoons} \mathrm{G@CB6}$$

$$\mathrm{CB6} + \mathrm{M^+} \overset{K_2}{\rightleftharpoons} \mathrm{CB6 \cdot M^+}$$

$$\mathrm{CB6M^+} + \mathrm{M^+} \overset{K_3}{\rightleftharpoons} \mathrm{M^+ \cdot CB6 \cdot M^+}$$

Scheme 2

Assuming that the total concentration of CB6 is much higher than the concentration of DSMI, the following expression can be deduced to fit the dependence of k_{obs} with the concentration of CB6.[16]

$$k_{obs} = m[CB6]_0 + k_{-1} \quad (6)$$

where

$$m = k_1 \frac{1}{1 + K_2[M^{n+}] + K_2K_3[M^{n+}]^2}$$

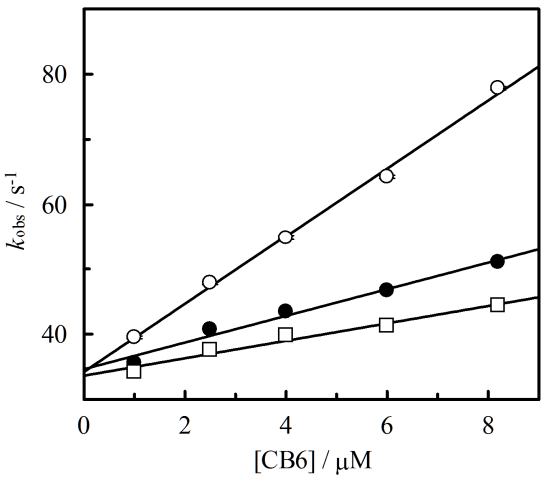

Figure 6. Dependence of the observed rate constant for the complex formation between DSMI (0.1 μM) and CB6 (1–8.3 μM) in the presence of different CsCl concentration: 0.1mM (○), 0.2 mM (●), 0.5mM (□).

The results obtained from the kinetics for the formation of the DSMI@CB6 complex at different salt concentration and salt size, are listed in Table 2. A comparison of the term *m*, where is included the association rate constant, shows that increasing the concentration of M^{n+} leads to a decrease in the association rate constant, as also observed with other guests.[13] This can be explained by the fact that increasing the concentration of salt, it is increasing the concentration of CB6 with the portals occupied by M^{n+}, and therefore less available to form complex with DSMI. On the other hand, changing the concentration of salt in solution did not influence the dissociation rate constant of DSMI from the complex. A constant k_{-1} value suggests that a ternary complex between DSMI, M^{n+} and CB6 is not formed. Regarding with the size of the cations added, the results from Table 2 shows that is necessary to add a large amount of sodium cations to decrease the association rate constant (included in the term *m*) to similar values of the other cations. This probably indicates a cation size selectivity, with the largest TMA^+ cation having a high binding constant than the smallest Na^+.

Table 2. Kinetic rates for the formation of DSMI@CB6 complex monitored via fluorescence with different salts at 25 °C and neutral pH.

Cation	Radius /Å [a]	$[M^{n+}]$ / mM	10^{-6} *m* /(M^{-1} s^{-1}) [b]	k_{-1} /s^{-1} [b]
Na^+	1.02	5.0	2.82	53.45
		10.0	2.31	60.05
Cs^+	1.67	0.10	5.21	34.21
		0.20	2.04	34.62
		0.50	1.33	33.63
Ba^{2+}	1.35	0.10	2.11	37.95
		0.25	0.52	45.76
TMA^+	3.22	0.10	3.37	43.03

[a] From reference 17. [b] 10% error.

4.4. Conclusions

In this chapter, it was studied the effect of the temperature as well as the dependence of the salt concentration and size of the cations on the kinetics for the formation of the complex between a fluorescent dye and a cucurbituril. A qualitative analysis of the temperature dependence for the complex formation, indicate that the complexation is enthalpy-driven. The kinetics obtained at different salt concentration shows a low influence in the dissociation rate constant, and therefore indicate that a ternary complex between DSMI–CB6–M^{n+} is not formed. On the other hand, it was observed a decrease of the association rate constant with the salt concentration, which suggest a sizable binding of the cations to the portals of CB6. Despite the low number of experiments performed, the results also indicate a size selectivity trend for the cations studied. Due the poor solubility of cucurbiturils in water, and after the approach of add salt to improve the solubility of these macrocycles in water, study the guest binding dynamics in the presence of cations are essential.

4.5. References

1. J. Kim, I. Jung, S. Kim, E. Lee, J. Kang, S. Sakamoto, K. Yamaguchi, and K. Kim, *J. Am. Chem. Soc.*, 2000, **122**, 540–541.

2. J. W. Lee, S. Samal, N. Selvapalam, H.-J. Kim, and K. Kim, *Acc. Chem. Res.*, 2003, **36**, 621–30.

3. K. Kim, N. Selvapalam, and D. H. Oh, *J. Incl. Phenom. Macrocycl. Chem.*, 2004, **50**, 31–36.

4. S. Liu, C. Ruspic, P. Mukhopadhyay, S. Chakrabarti, P. Y. Zavalij, and L. Isaacs, *J. Am. Chem. Soc.*, 2005, **127**, 15959–15967.

5. K. a. Connors, *Chem. Rev.rev.*, 1997, **97**, 1325–1358.

6. C. Klöck, R. N. Dsouza, and W. M. Nau, *Org. Lett.*, 2009, **11**, 2595–2598.

7. N. Basilio, L. García-Río, J. a Moreira, and M. Pessêgo, *J. Org. Chem.*, 2010, **75**, 848–55.

8. M. Salehi, S. J. Johnson, and J.-T. Liang, *Langmuir*, 2008, **24**, 14099–14107.

9. N. Saleh, A. L. Koner, and W. M. Nau, *Angew. Chem. Int. Ed.*, 2008, **47**, 5398–5401.

10. A. Hennig and W. M. Nau, *Nature Methods*, 2007, **4**, 629–632.

11. J. Mohanty and W. M. Nau, *Angew. Chem. Int. Ed.*, 2005, **44**, 3750–3754.

12. Y.-M. Jeon, J. Kim, D. Whang, and K. Kim, *J. Am. Chem. Soc.*, 1996, **118**, 9790–9791.

13. C. Márquez, R. R. Hudgins, and W. M. Nau, *J. Am. Chem. Soc.*, 2004, **126**, 5806–5816.

14. Y. Huang, T. Cheng, F. Li, C.-H. Huang, T. Hou, A. Yu, X. Zhao, and X. Xu, *J. Phys. Chem. B*, 2002, **106**, 10020–10030.

15. Z. Li, S. Sun, F. Liu, Y. Pang, J. Fan, F. Song, and X. Peng, *Dyes and Pigments*, 2012, **93**, 1401–1407.

16. H. Tang, D. Fuentealba, Y. H. Ko, N. Selvapalam, K. Kim, and C. Bohne, *J. Am. Chem. Soc.*, 2011, **133**, 20623–20633.

17. R. D. Shannon, *Acta Cryst. A*, 1976, **32**, 751–767.

Chapter 5

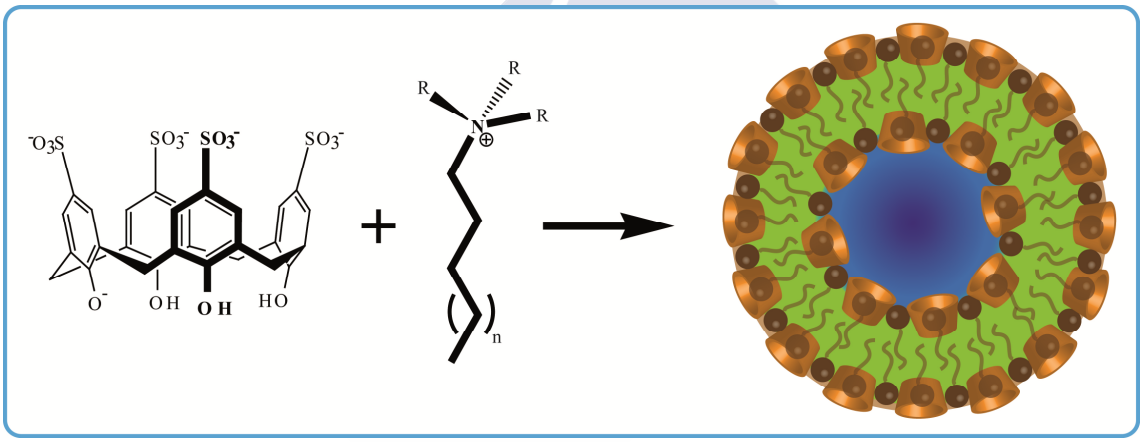

USC
UNIVERSIDADE
DE SANTIAGO
DE COMPOSTELA

5. Complexation of *p*-sulfonatocalix[4]arene with surfactants

5.1. Interaction of bolaforms with *p*-sulfonatocalix[4]arene*

5.1.1. Introduction

Bolaamphiphiles, also known as bolaforms, are usually described as molecules with a hydrophobic skeleton and hydrophilic head group on both ends.[1] The difference in the structure when compared with conventional surfactant enable this type of molecules to have other properties and useful applications. They are capable of self-organizing themselves to form colloidal aggregates such as spheres, cylinders, vesicles, *etc*.[2–4] Due to the double polar head groups, one of the potential applications is for example, the binding of one head group to a solid surface while the other head group is free and can be used to fixate colloids, transition-metal ions or electrophilic organic molecules.[1]

Despite the interest in these molecules in the past three decades, only recently has some attention been given to the interactions of bolaforms with macrocyles. The interest in studying bolaamphiphiles as guest molecules is mainly due the hydrophobic effect which tends to protect the alkyl chain from the aqueous environment, the requirement of dehydration of the head groups during complexation, as well as effects due steric hindrances.[5] The complexation behavior and stoichiometry of some bolaforms with cyclodextrins, cucurbiturils and calixarenes were studied by means of different techniques such as ^{1}H NMR, diffusion experiments and calorimetry.[5–11] Although the simple or higher order complexation find in some binary systems, the host-guest recognition between these two type of molecules enable them for building supramolecular structures.[12–14] Therefore, it is of great interest to study and understand the binding behavior between these molecules to improve and increase the applications of the formed structures. In a previous paper, we have reported the complexation of a conventional alkyltrimethylammonium bromide surfactant by a calixarene, which in some molar ratios and after sonication, occurs the formation of unilamellar vesicles.[15]

* The synthesis and characterization of the bolaform surfactant were performed at the Universidade do Algarve (Portugal), under the supervision of professor José Moreira.

In this work, the complexation of bolaforms with different spacer length between the head groups and with different head groups volume by a water-soluble calixarene were studied in neutral aqueous solution. *p*-sulfonatocalix[4]arene (SC4) which is a recognized macrocyle for the complexation of several guest, like inorganic cations,[16] organic ammonium cations,[17] neutral molecules,[18] *etc*, was employed as a host for the complexation of the selected amphiphiles. Several NMR methods were performed, which allied with the thermodynamic parameters obtained by ITC gives a complete binding behavior for the complexation of bolaform surfactant by SC4.

5.1.2. Experimental Section

Material: Hexane-1,6-bis(trimethylammonium bromide), hexyltrimethylammonium bromide (assay ≥98.0%), tetramethylammonium bromide (assay ≥98.0%), tetraethylammonium bromide (assay ≥98.0%) supplied by Sigma-Aldrich and NaCl from Fluka (assay ≥99.5%) were used as received. The bisquaternary ammonium salt were synthesized using the following procedure: 1,12-dibromododecane (Aldrich, 98%) was dissolved in ethanol and an excess of trimethylamine (Aldrich, 31-35% in ethanol) or triethylamine (Sigma-Aldrich, ≥99%) was added and kept under stirring at 80 ºC for 3 days to obtain G2 and G3, respectively. G4 was prepared according to the method of Ng *et at*.[19] *p*-Sulfonatocalix[4]arene (SC4) was prepared using a procedure described in a previous work.[20]

NMR experiments: ^{1}H NMR spectra were recorded in a 300 MHz instrument while 1D and 2D NOESY (Nuclear Overhauser Effect Spectroscopy) were obtained in a 500 MHz instrument. 1D and 2D NOESY experiments were carried out by applying the pulse sequence defined in the literature.[21] Different spin-lock mixing times (ranging between 200 and 800 ms) were used to ensure the validity of the linear approximation for the NOE cross-peaks and to obtain the best signal-to-noise ratio, which was achieved at 600 ms. Thirty two scans were collected in each spectrum. Before the subsequent Fourier transformation and 2D phase tuning, zero-filling in F1 and cosine square apodization in both dimensions were applied to the FIDs.

For assignment purposes of G4, the two dimensional HSQC, HMBC and TOCSY were performed at 750 MHz using standard Varian software. Saturation transfer difference NMR (STD-NMR) were also performed on a Varian Inova 750MHz spectrometer. All solutions used in the NMR experiments were prepared in D_2O

(Aldrich, 99.9 %). Diffusion-ordered NMR spectroscopy (DOSY) were carried out at 25 ºC on a Varian Inova 400 spectrometer. The DOSY-Dbppste spectra were acquired with stimulated-echo pulse sequence with bipolar gradient pulses.[22] The pulsed gradients (*G*) were incremented from 2.0 to 64.4 cm^{-1} in 20 steps. To obtain reliable results for the diffusion coefficient, the diffusion time (Δ) of the experiment was optimised for each sample to a value between 60 and 70 ms. The raw data were processed by using the MestreC program.

Microcalorimetry: The microcalorimetric titrations were performed in aqueous neutral solution on an isothermal titration microcalorimeter (VP-ITC) from Microcal Co. (Northampton, MA) at atmospheric pressure and 298.15 K. All solution were prepared with Milli-Q water. In each run, a solution of guest (or guest and inhibitor) in a 0.270 mL syringe was sequentially injected with stirring at 459 rpm into a solution of host (or host with a inhibitor) in the sample cell (1.459 mL volume). Each solution was degassed and thermostatted using a ThermoVac accessory before titration. In each titration the reference cell was filled with the same sample that in sample cell. The heat of dilution was measured by injecting the guest solution into a blank solution or in a solution containing only the inhibitor. The ORIGIN software (Microcal Inc.), which was used to compute the binding constant and molar reaction enthalpy from a single titration curve, gave a standard deviation based on the scatter of the data points in the titration curve. The net reaction heat in each run was calculated by the "one set of sites" model, the "competitive binding" model in cases of extremely large binding constants and the "sequential binding" model with two sites. Additionally, the first point was removed from the titration curve before doing the curve-fit, because of the probable leakage resulting from having the syringe stirring all the time in the sample cell a long time before the first injection, giving a smaller heat effect than it should have.

5.1.3. Results and Discussion

5.1.3.1. Binding mode of bolaform G1

The binding modes for the interaction between SC4 and the bolaform guests shown in Scheme 1 has been establish using several techniques such as microcalorimetry (ITC), ^1H chemical shifts, diffusion ordered spectroscopy (DOSY), 1D and 2D Nuclear Overhauser effect spectroscopy (NOESY) and saturation transfer difference NMR spectroscopy (STD-NMR). The guests analyzed were selected in order

to study the influence of the spacer between the positive charges as well as the terminal volume in the formation of different types of complexes with SC4.

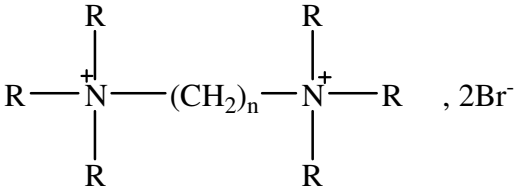

Guest	R	*n*
G1	CH_3	6
G2	CH_3	12
G3	C_2H_5	12
G4	C_3H_7	12

Scheme 1. Structures of bisquaternary ammonium salts

In order to obtain the thermodynamics parameters associated with the complexation of G1 by SC4, ITC experiments were performed. As can be seen in Figure 1, each titration of G1 into the sample cell with SC4 gave an apparent reaction heat caused by the formation of an inclusion complex SC4:G1. Due to the high binding affinity obtained for the complexation of the guests by SC4 (see Figure S1), the experiments were performed in the presence of an inhibitor. Since the host SC4 in neutral aqueous solution is in the pentaanion form with Na^+ as a counterion, and knowing that SC4 can complex its own counterions, the inhibitor selected was the NaCl salt.[20] Although exist the possibility of Na^+ cations decrease the charge repulsion between the sulfonato groups of the calixarene and therefore the formation of other stoichiometry occur, such as expected in 2:1 complexes, the ITC experiments performed in the presence and absence of salt confirm that there is no change in the stoichiometry of the complex. Also as a control experiment, the terminal head group of G1, tetramethylammonium cation (TMA^+) and its equivalent conventional surfactant, hexyltrimethylammonium surfactant (C_6TA^+), were examined.

The net reaction heat obtained for the complexation of TMA^+ or C_6TA^+ by SC4 was analyzed by using the "one set of binding sites" model as expected for a 1:1 stoichiometry. Unexpectedly, since the two positive charges of the bolaform, fitting the net reaction heat obtained for G1 with the "one set of binding sites" model, also reproduces the data as shown in Figure 1, and therefore indicating the same 1:1 stoichiometry as observed with TMA^+ and C_6TA^+. The thermodynamic parameters

obtained, complex binding constant (K), standard molar reaction enthalpy (ΔH°), and the calculated standard free energy (ΔG°) and entropy changes ($T\Delta S^{\circ}$) are listed in Table 1.

The binding constant obtain for TMA^+ and for the surfactant C_6TA^+ are in the same range, however the binding constant for the association of G1 with SC4 is about 10-fold higher. A close examination on the thermodynamic parameters between the three guests shows that the enthalpy is almost the same, but the entropy for the complexation of G1 is higher than C_6TA^+ or TMA^+. This means that the higher binding constant for SC4:G1 complex is not attributed to the enthalpy gain, but to more favorable entropy changes. The enthalpy gain can be attributed to C–H$\cdots\pi$ interaction between the methyl group of the guests and the aromatic nuclei of the SC4,[23] as observed for other ammonium organic cations, whereas the entropy gain can be attributed to release of the ordered water molecules from the bolaform as well as the sulfonato groups of the calixarene. The positive entropy term show that the desolvation effect is more important rather than the loss of the conformational freedom. The higher binding constant and entropy gain (higher desolvation effect) for the complexation of G1 indicates the possibility that the complexation not only occur with one polar head group, but probably both heads groups of bolaform are inserted in the cavity of the calixarene. Otherwise, the binding constant should be in the same range of the other two guests. This complex stoichiometry is in contrast with the 2:1 complexation found in other dicationic guests with a water-soluble calixarene,[24,25] but it is in accordance with a work reported recently.[11]

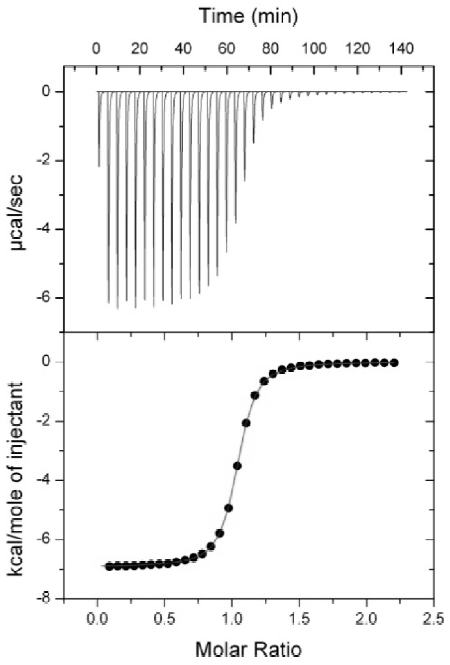

Figure 1. Microcalorimetric titration of G1 with SC4 in the presence of 50 mM of NaCl in water at 25 °C: (top) raw data for the sequential 34 injections (8 µL per injection) of G1 solution (3 mM) into 0.3 mM of SC4. (bottom) Net heat effects obtained by subtracting the dilution heat from the reaction heat, fitted by computer simulation using the "competitive binding" model.

Table 1. Complex binding constant (*K*) and thermodynamic parameters for the 1:1 intermolecular complexation of guests by SC4 in aqueous neutral solution at 25 °C. The titration data were fitted with the "competitive binding" model.

Guest	K /(M^{-1})	ΔG° /(kJ mol^{-1})	ΔH° /(kJ mol^{-1})	$T\Delta S^\circ$ /(kJ mol^{-1})
C_6TA^+	$(2.4 \pm 0.1) \times 10^5$	–30.7 ± 0.1	–22.3 ± 0.1	8.4 ± 0.2
TMA^+	$(6.1 \pm 0.1) \times 10^5$	–33.0 ± 0.1	–25.2 ± 0.1	7.8 ± 0.2
G1	$(5.8 \pm 0.1) \times 10^6$	–38.6 ± 0.1	–22.4 ± 0.1	16.2 ± 0.2

NMR spectroscopy experiments were performed to better understand the binding mode of complexation of G1 by SC4. In addition to providing information about the stoichiometry of the host-guest complex, ^{1}H NMR spectra also provide the manner of how the guest can be inserted in the host cavity, through the direction of the complexation-induced chemical shift change ($\Delta\delta = \delta_{complex} - \delta_{free}$) of the guest nuclei. The different upfield chemical shifts of the guest indicate if the nuclei are more or less

incorporated inside the SC4 cavity and also which region of the guest is being complexed.

Figure 2 shows the chemical shifts for the titration of G1 with SC4. In all cases the signals of the guest protons are observed as an averaged single resonances because of the fast exchange on the NMR timescale between the free and the complexed guest.[26] As can be seen, all the protons of the alkyl chain as well as the protons of the head group experience a considerable upfield shift upon addition of SC4. The head group protons exhibit large upfield shifts in comparison with the protons of the alkyl chain in the order $H_\alpha > H_1 > H_2 > H_3$. However, after the addition of 1 equiv of SC4 the chemical shifts of the G1 protons reached a plateau, indicating a 1:1 binding stoichiometry in accordance with the ITC experiments.

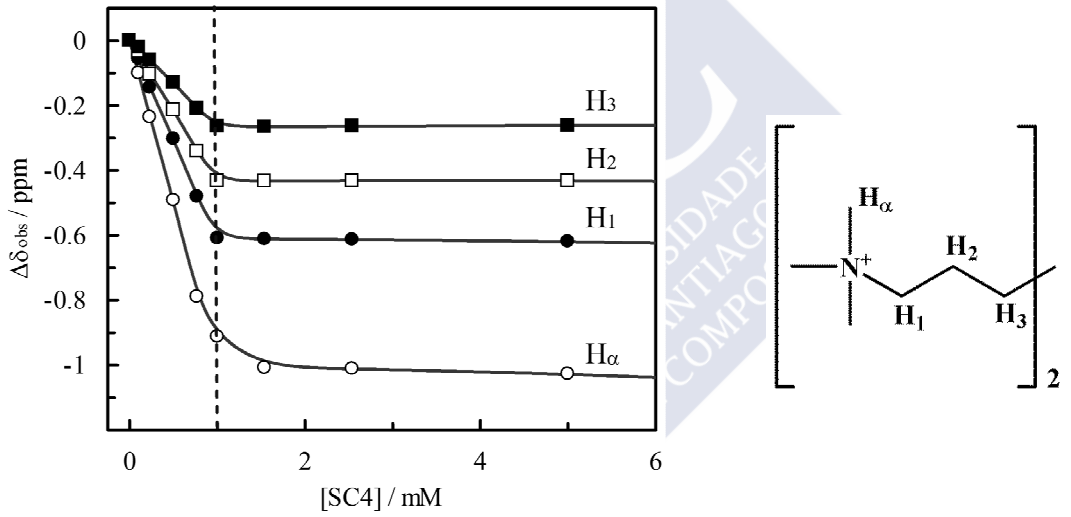

Figure 2. Chemical shifts changes experienced by the G1 protons with increasing the concentration of SC4 in D_2O at 25 °C, [G1] = 1 mM.

The inclusion of organic ammonium guests is usually associated with large chemical shifts upon complexation with SC4. However, the inclusion of both positive groups of G1 in the small cavity of SC4 should displace the chemical shifts of the bolaform protons to a lesser extent due a more external complex. Therefore, experiments with the homologous conventional surfactant of the bolaform were performed. The results of the chemical shifts of C_6TA^+ and G1 protons upon complexation with SC4 are listed in Table 2.

Table 2. The chemical shift changes $\Delta\delta_{obs}$ values (ppm) of C_6TA^+ (1 mM) and G1 (1 mM) in the presence of SC4 (5 mM).[a]

Guest	H_α	H_1	H_2
C_6TA^+	-2.02	-1.23	-0.69
G1	-1.04	-0.63	-0.44

[a] Negative values indicate upfield shift.

As can be seen, the δ_{obs} values of the C_6TA^+ protons shift to higher field after complexation with SC4, especially the head group, indicating that the surfactant is encapsulated into the calixarene cavity by the polar head group. However, a comparison between the conventional surfactant and the bolaform G1 confirms that the polar head groups are less incorporated in the SC4 cavity. Since the chemical shifts for the G1 protons are approximately half of the C_6TA^+ protons upon complexation, this could indicate a more external complex.

Unlike ^{1}H NMR shifts, 2D NOESY cross-peaks are indicative of specific proximity relationships between host and guest protons (generally 4Å or less).[27] This technique is a powerful qualitative method that has previously been used to monitor weak through-space proton coupling interactions in calixarene inclusion complexes.[28,29] Therefore, 2D NOESY NMR experiments were carried out to obtain complementary information in the inclusion geometry between G1 and SC4. In 2D NOESY, the small molecules usually give rise to positive cross peaks while the diagonal signals are phased negative. While NOE give rise to positive cross peaks, chemical exchange provides negative cross peaks.[30] From ^{1}H NMR experiments it can be seen that the calixarene is in cone conformation upon complexation with G1, since the methylene protons of the bridge change from a single peak to two doublets peaks, H_{endo} (4.4 ppm) and H_{exo} (3.4 ppm).[31] Consequently, the distances of the aromatic SC4 protons (H_{aro}) to G1 are substantially shorter than those of the methylene protons. This is the reason why the NOESY cross-peaks only were observed between H_{aro} of SC4 and the protons of G1.

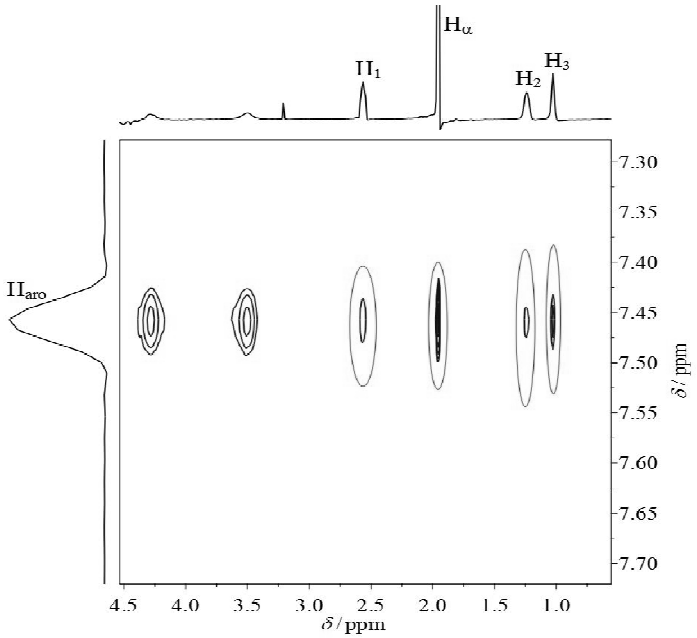

Figure 3. 2D NOESY NMR spectrum of SC4:G1 at equimolar solution (4 mM) with mixing time of 600 ms, in D_2O at 25 °C.

From Figure 3, it can be seen the NOE enhancements specially strong for the cross peaks between the H_{aro} from SC4 with the terminal polar groups H_α, but also with the protons of the alkyl chain, where the cross peak with H_3 is stronger than H_1 and H_2. Therefore, the results obtained from the NOESY experiments are in accordance with the data obtained from ITC and ^1H NMR, indicating that both polar heads of G1 are incorporated in the cavity of SC4. A possible inclusion mode of G1 in SC4 is represented in Figure 4. The accommodation of two polar group in the same macrocycle cavity is related not only with the particular shape of the guest but with the special flexibility of SC4.

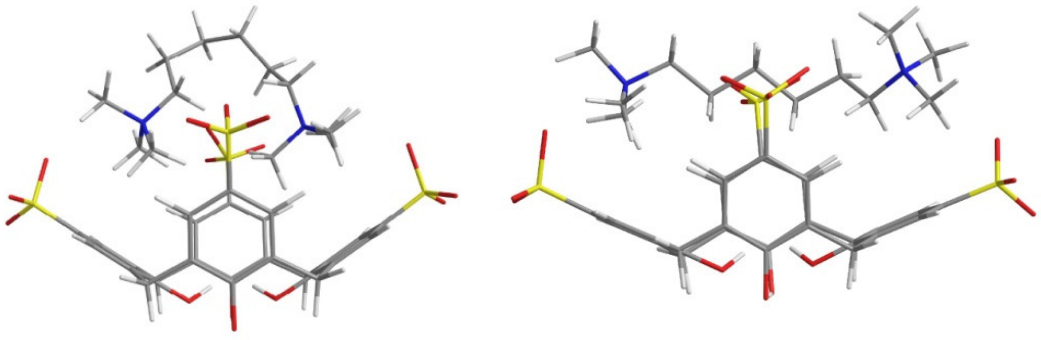

Figure 4. Schematic representation of possible complex binding mode between SC4 and G1**.**

5.1.3.2. Influence of the spacer

The complexation of the bolaform with shorter spacer by SC4 shows that the host can complex both polar head groups of the guest, however increasing the spacer length, different stoichiometry and complexation behavior are expected. Therefore, several experiments were performed to study the complexation of G2 by SC4. To obtain the thermodynamic data for the complex formation, ITC experiments were performed in neutral aqueous solution by injecting G2 in SC4 at the sample cell and in the presence of 50 mM of NaCl. As can be seen in Figure 5, although the microcalorimetric titration shows a trend of a simple 1:1 complexation, fitting the net reaction heat obtained from the integration of the calorimetric traces with "one set of binding sites" model fails to reproduce the experimental data (Figure S2). Instead, fitting the nonsymmetrical sigmoidal curve with the "sequential binding" model reproduces very well the data and the results are listed in Table 3.

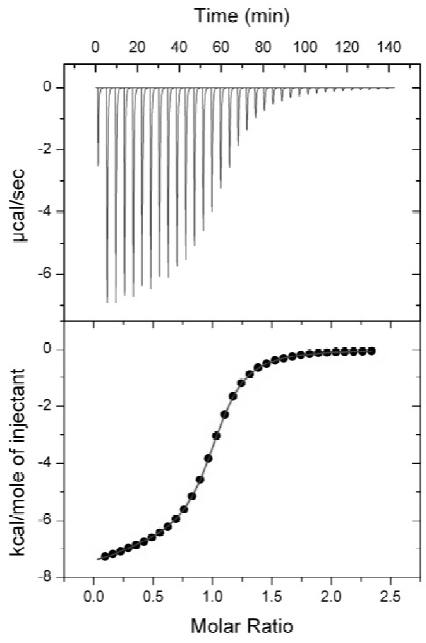

Figure 5. Microcalorimetric titration of G2 with SC4 in the presence of 50 mM of NaCl in water at 25 °C: raw data for the sequential 34 injections (8 µL per injection) of G2 solution (3 mM) into 0.3 mM of SC4.

Table 3. Complex binding constant (K) and thermodynamic parameters for the 1:1 and 2:1 intermolecular complexation of SC4 with G2 in the presence of 50 mM NaCl in aqueous neutral solution at 25 °C. The titration data were fitted with the "sequential binding" with two sites model.

Guest	K /(M^{-1})	ΔG° /(kJ mol^{-1})	ΔH° /(kJ mol^{-1})	$T\Delta S^{\circ}$ /(kJ mol^{-1})
G2	$(2.4 \pm 0.1) \times 10^{5}$[a]	–30.7 ± 0.1	–28.6 ± 0.1	2.1 ± 0.2
	$(1.2 \pm 0.1) \times 10^{3}$[b]	–17.7 ± 0.1	–8.4 ± 0.1	9.4 ± 0.2

[a] $K_{1:1}$ and [b] $K_{2:1}$

The thermodynamic parameters show that the complexation is enthalpy-driven accompanied with a small positive entropy change for the 1:1 complex, whereas in the complexation of the second calixarene it is observed a decrease in the enthalpy gain and increase in the entropic term. Increasing the alkyl chain length of the spacer from 6 to 12, allows the complexation of two SC4 by G2, with the binding constant for the second complexation being about 100-fold lower than the formation of 1:1 complexes. However, as observed for G1, the binding association of the first SC4 with G2 is higher than the complexation of TMA^+ or C_6TA^+ (Table 1), indicating that although the increase of the spacer length, the binding mode for the 1:1 complex could be similar in both cases. Although the binding constant obtained for G2 and TMA^+ or C_6TA^+ are in the same magnitude, it should be noted that $K_{1:1}$ for the complex SC4:G2 is obtained in the presence of 50 mM of NaCl, while for TMA^+@SC4 and C_6TA^+@SC4 were performed in absence of added salt (only in the presence of Na^+ as counterion of SC4).

To answer the unlikely complexation in the 1:1 stoichiometry for the mixture SC4:G2, 2D NOESY NMR experiments were performed to better understand the binding mode. The experiments were performed in 1:1 molar ratio solutions, which from the binding constant obtained from ITC, indicates that the mixture is mainly in 1:1 complexes. As can be seen from Figure 6, and in comparison with the NOE performed for SC4:G1, the aromatic protons of SC4 has cross peaks with all the protons of G2.

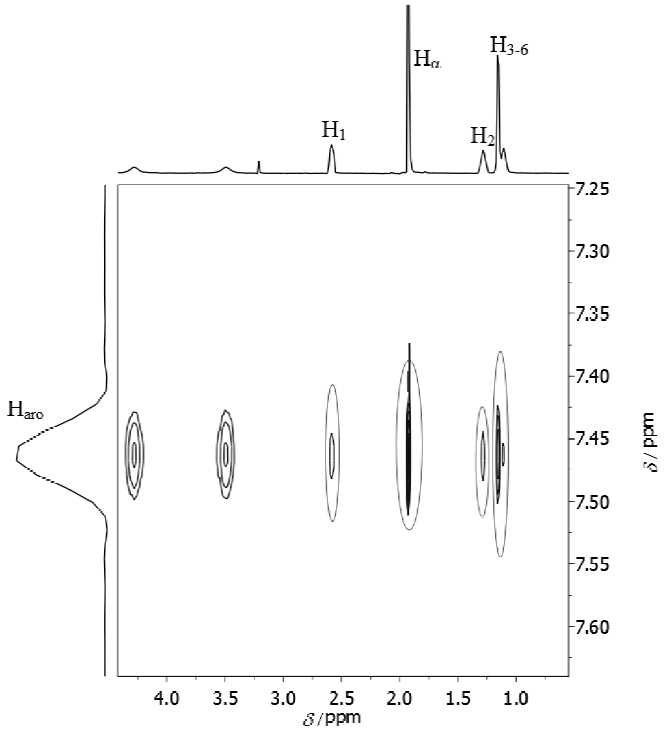

Figure 6. 2D NOESY NMR spectrum of an equimolar mixture of SC4 and G2 (4 mM) with mixing time of 600 ms, in D_2O at 25 °C.

Although the results from ITC and NOESY seems indicate a similar binding behavior between G1 and G2 by SC4 for 1:1 complexes, we cannot discard an inclusion complex as shown in Figure 7, and also pointed out in a recent work.[11] However, a qualitative analysis of the distance between the H_{aro} protons of SC4 in C_{4v} cone conformation and the $H_{3–6}$ protons of G1, shows a higher distance than 5 Å and therefore is incompatible with the cross-peak observed in the NOESY experiments.

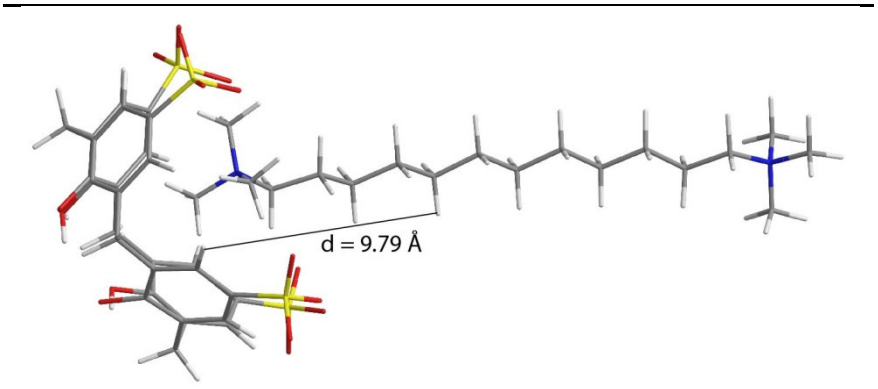

Figure 7. Possible inclusion mode for the complexation of SC4 and G2 in the 1:1 complex using MM2 force field energy minimization.

A possible inclusion mode to explain all the cross peaks observed for the inclusion of G2 by SC4 is represented in Figure 10a, with the calixarene in a flattened cone conformation (C_{2v}) and G1 with a slight curvature conformation.

To confirm the 2:1 stoichiometry between SC4 and G2 indicated in the ITC experiments, we also performed ^{1}H NMR and diffusion experiments. As can be seen in Figure 8, all protons of G2 underwent to upfield shifts upon complexation with SC4 and where the $\Delta\delta_{obs}$ are in the order $H_\alpha > H_1 > H_2 > H_{3\text{-}4} > H_{5\text{-}6}$. On contrary to the experiments with G1, the protons of G2 still decrease after the molar ratio 1 (dotted line) and almost reach the chemical shift for C_6TA^+ (*ca.* $\Delta\delta$= –2.0 ppm). From the chemical shifts it can be concluded that each calixarene is inserted at the polar head group of G2 as shown in Figure 10b.

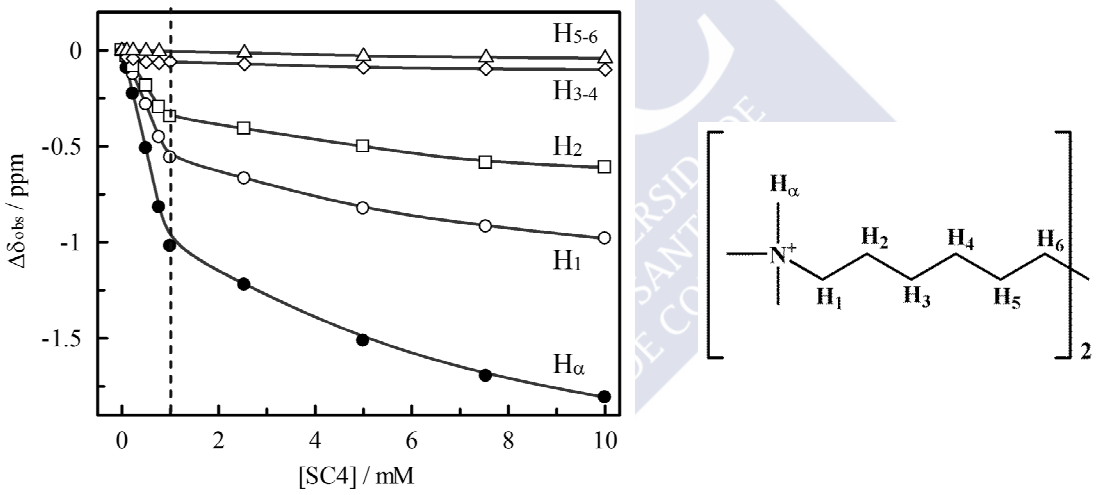

Figure 8. Chemical shifts changes experienced by the G2 protons with increasing the concentration of SC4 in D_2O at 25 °C, [G2] = 1 mM.

The 2:1 complex was also confirmed by diffusion experiments (DOSY), in which the guest G2 was kept constant and the SC4 concentration was varied. As can be seen in Figure 9, the diffusion of G2 decrease rapidly until molar ratio 1 (dash blue line), due the high binding constant for K_1, and then a moderately decrease with increase concentration of SC4. Since G2 in SC4:G2 complexes is in a fast exchange of free and bound state on the NMR time scale, the diffusion coefficient is a time-weighted average of the diffusion coefficients in each state. The experimental data were fitted to an 1:1 stoichiometry model, but as can be seen the model fails to reproduce the data. Only with

a model that take in consideration the formation of 1:1 and 2:1 complexes can reproduce the experimental data (eq S2-S11). A diffusion of D_{SC4-G2} = 3.4 × 10^{-6} cm^2 s^{-1} and D_{SC4_2-G2} = 2.6 × 10^{-6} cm^2 s^{-1} were obtained from the fitting. All experiments performed to identify the binding mode between SC4 and G2 are in accordance and it can be assumed that G2 is complexed with both polar head group incorporated in the calixarene cavity in the 1:1 complex, while the 2:1 stoichiometry is formed by the complexation of one SC4 at each end of G2 (Figure 10b).

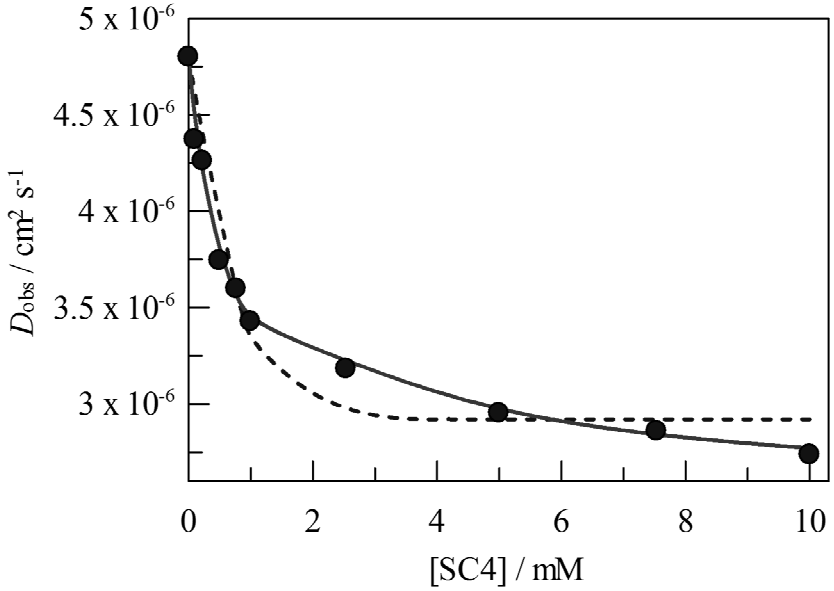

Figure 9. Dependence of the self-diffusion coefficients for the H_α protons of G2 (1 mM) with increasing concentration of SC4. The dotted line shows the fit to the model with only 1:1 complex, and the solid line to the model including 1:1 and 2:1 complexes.

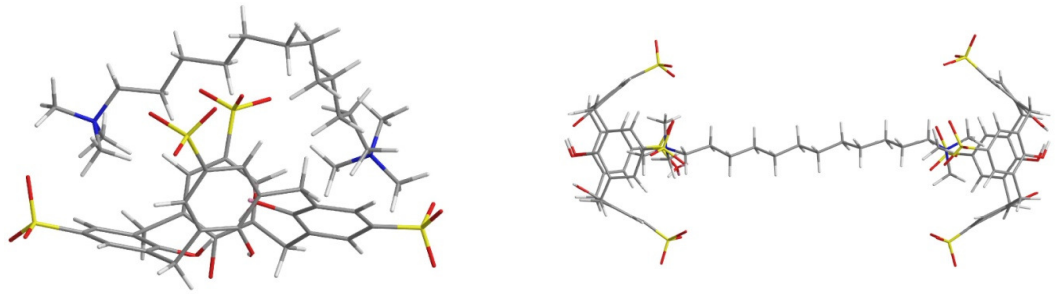

(a) (b)

Figure 10. Possible inclusion modes for the complexation of SC4 and G2 in 1:1 (a) and 2:1 complexes (b).

5.1.3.3. Influence of the polar head volume

To study the influence of the bolaform terminal group, G3 which has the same spacer length as G2 but with a higher head group volume was selected. ITC experiments were performed to determine the binding constant for the complex formation between G3 and SC4 (Figure S3). In Table 4 are shown the results by fitting the microcalorimetric titration data with the "sequential binding" model with two sites. The binding constant obtained for the complexation of G3 by SC4 shows that $K_{2:1}$ is, as observed for the complexation of G2, up to 3 orders of magnitude lower than the binding constant for the 1:1 complex formation. As a control experiment, the binding constant and thermodynamic parameters for the complexation of the terminal group of the bolaform, tetraethylammonium cation (TEA^+), were determined. In comparison with G2, the binding constant obtained for the complexation of the respective terminal group of bolaform are lower than the formation of the complex between the bolaform and SC4. This behavior suggests a similar mode inclusion of G2 and G3 by SC4 in 1:1 complexes.

Table 4. Complex binding constant (K) and thermodynamic parameters for the 1:1 and 2:1 intermolecular complexation of SC4 with G3 and the parameters for complex SC4:TEA^+ in aqueous neutral solution at 25 °C. The titration data were fitted with the "sequential binding" model with two sites for G3 and "competitive binding" model for TEA^+.

Guest	K /(M^{-1})	ΔG° /(kJ mol^{-1})	ΔH° /(kJ mol^{-1})	$T\Delta S^\circ$ /(kJ mol^{-1})
G3	$(8.2 \pm 0.3) \times 10^{6[a]}$	-39.5 ± 0.1	-38.9 ± 0.1	0.6 ± 0.2
	$(5.9 \pm 0.3) \times 10^{3[b]}$	-21.5 ± 0.1	-1.7 ± 0.1	19.8 ± 0.2
TEA^+	$(1.8 \pm 0.1) \times 10^6$	-35.7 ± 0.1	-34.5 ± 0.1	1.2 ± 0.2

[a] $K_{1:1}$ and [b] $K_{2:1}$

However, to obtain detail information of the complexation mode, ^1H NMR experiments were performed. In Figure 11 it can be seen the chemical shifts of the protons of G3 upon complexation with SC4. All the protons shifts to upfield, especially the protons of the polar head groups, resembling the case of G2. The chemical shifts also show that the binding stoichiometry of the mixture is higher than 1:1, since all protons shifts to higher magnetic field when the concentration of SC4 is increased above the molar ratio 1 (dotted line).

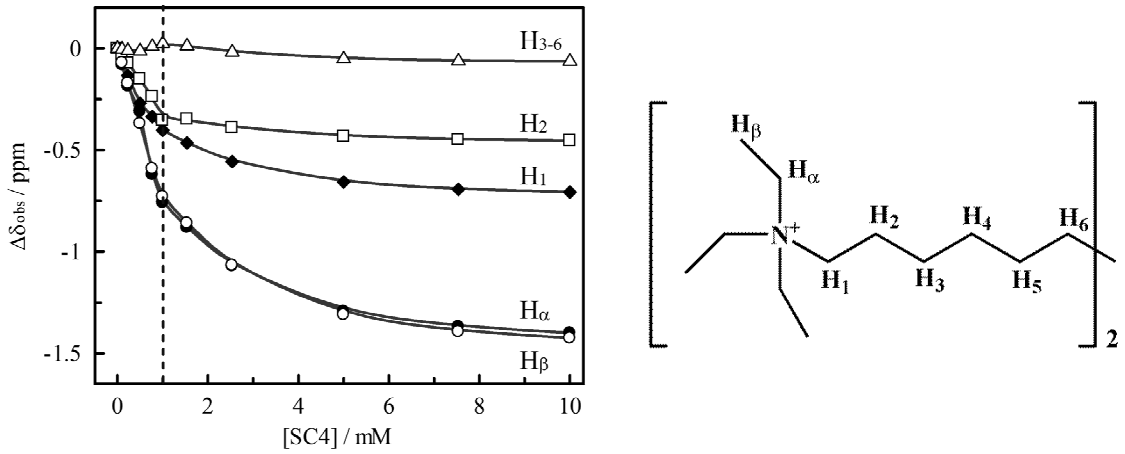

Figure 11. Chemical shifts changes experienced by the G3 protons with increasing the concentration of SC4 in D_2O at 25 °C, [G3] = 1 mM.

In order to confirm that the binding mode for the complexation of G3 by SC4 in the 1:1 complex is similar to the previous bolaforms, 1D NOESY experiments were performed (Figure S4). The results show interactions between the aromatic protons of SC4 with the protons of the bolaform heads, H_α and H_β, but also with the protons of the alkyl spacer, confirming the similar binding mode between G3 and SC4 with the complexation of G2 (Figure 10a).

Driven by these observations, a bolaform with tripropyl terminal groups was synthesized (G4), to proceed with the study of the influence of the head group volume in 1:1 complexes. The complexation of G4 by SC4 was studied by ^{1}H NMR. The ^{1}H NMR titration show that for higher molar ratio of SC4 in the mixture, and in line with G2 and G3, the results are consistent with the formation of 1:1 and 2:1 complexes, as demonstrated by the upfield shifts of the bolaform protons, especially H_γ, after the molar ratio 1 (spectra f, Figure 12). In Figure 12, it can also be seen that after complexation of G4 with SC4, the signals of the protons, H_α, H_β and H_γ of the propyl chain of G4 terminal head, splits into different peaks. A comparison in the head volume of G3 and G4 show that the triethyl terminal of G3 could be better accommodated in the SC4 cavity, while in the case of G4 possibly only one propyl chain of the terminal can be inserted in the cavity of SC4, as proposed by Morel-Desrosiers and coworkers .[32]

Therefore, to prove this hypothesis and to assign the proton and carbon resonances of G4 upon complexation with SC4, 2D NMR analysis (HSQC, HMBC and TOCSY) at equimolar ratio were performed (Figure 13) (Figures S5-S6).

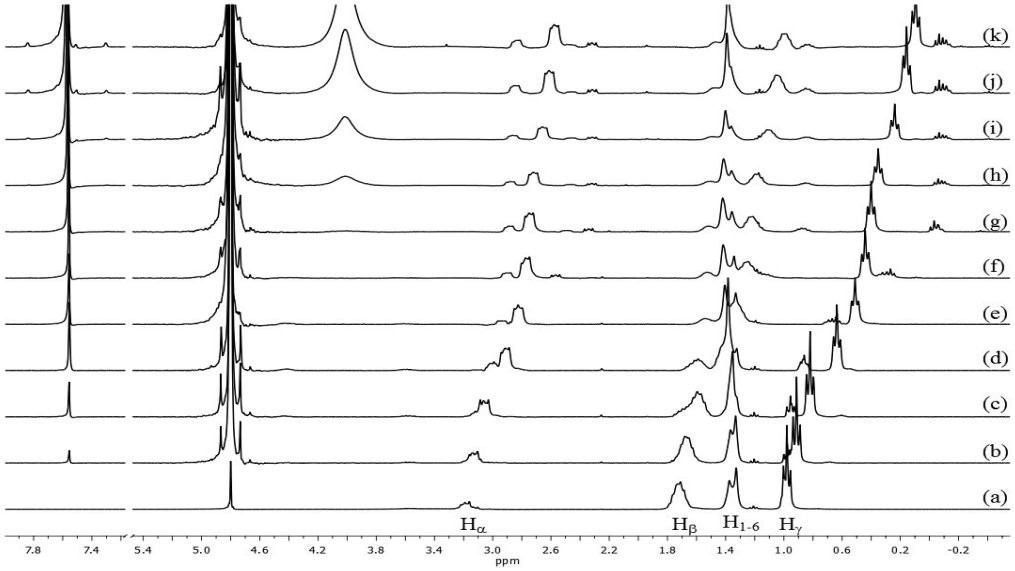

Figure 12. ^{1}H NMR spectra (D_2O, 25 °C) of G4 (1 mM) with different concentrations of SC4: (a) 0.0, (b) 0.1, (c) 0.25, (d) 0.5, (e) 0.75, (f) 1.0, (g)1.5, (h) 2.5 (i) 5.0, (j) 7.5, (k) 10 mM.

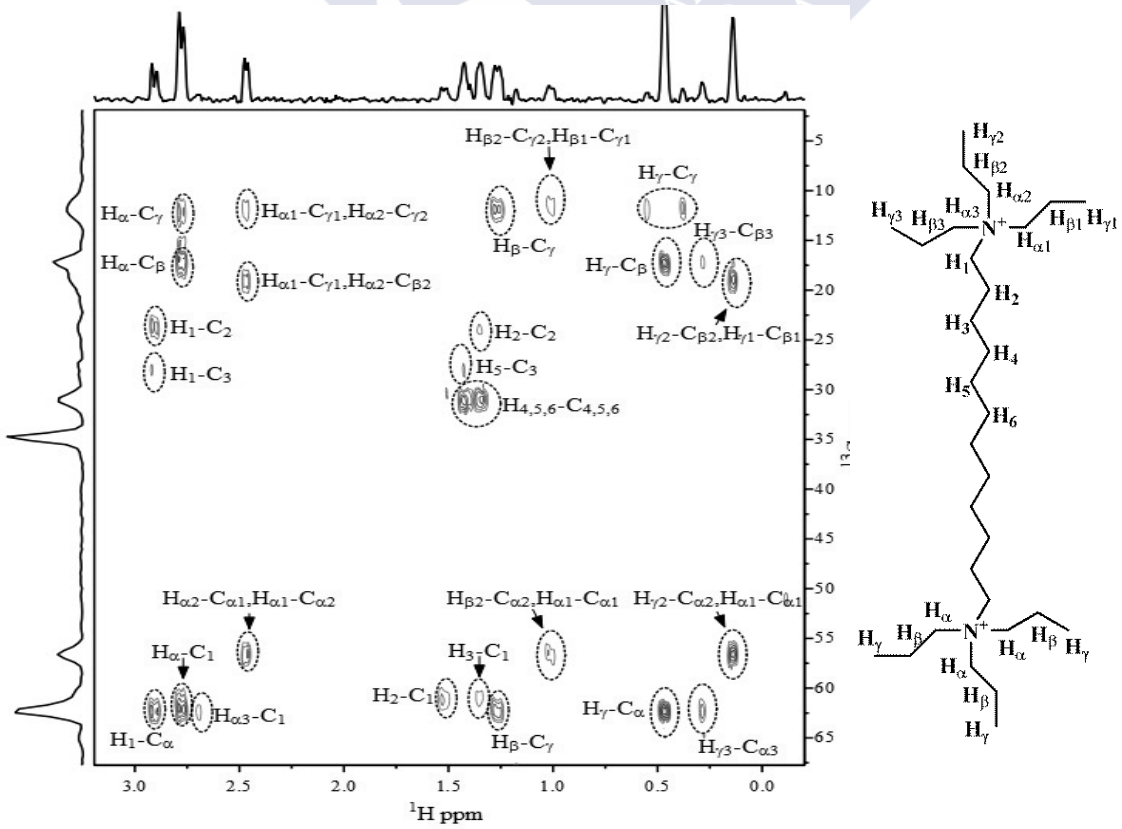

Figure 13. ^{1}H–^{13}C HMBC spectra region of G4 (10 mM) in the presence of SC4 (10 mM) at 750MHz, in D_20 at 25 °C.

Figure 13 shows the $^{1}H–^{13}C$ HMBC region of G4 upon complexation with SC4 at equimolar ratio. Combining all the experiments obtained for the complex SC4:G4 (^{1}H, HMBC, HSQC and TOCSY), it is possible to assign the protons of G4 and identify the number of alkyl chain of the G4 terminal which are inserted in the SC4 cavity. After assignment of the protons in G4 and integration of the proton peaks, it indicates that opposed to expected, two propyl chain of the G4 terminal group should be inserted in the SC4 cavity, due the observed higher upfield shift of $H_{\alpha1,\alpha2}$, $H_{\beta1,\beta2}$ and $H_{\gamma1,\gamma2}$ in comparison with the other propyl terminal chain ($H_{\alpha3}$, $H_{\beta3}$ and $H_{\gamma3}$). However, unlike the results obtained with the other bolaforms in 1:1 complexes, from the ^{1}H and HSQC-HMBC NMR spectra analysis, it is possible to differentiate the two terminal group of G4. From a quantitative point of view, the integration of G4 proton peaks is compatible with a model where the molar fraction χ_{bound} = 0.35 but with only one terminal group complexed with SC4 and a molar fraction of free species of about 0.65. The absence of correlation between the proton $H_{\alpha3}$ with the carbons separated with two or three bonds $C_{\alpha1}$,$C_{\alpha2}$, H_{α} with $C_{\alpha1}$,$C_{\alpha2}$ and H_1 with $C_{\alpha1}$,$C_{\alpha2}$, as well the observed peaks $H_1–C_{\alpha}$, $H_{\alpha2}–C_{\alpha1}$ and $H_{\alpha3}–C_1$ corroborate that in the molar fraction of bounded species, only one terminal group is being complexed by the calixarene cavity. The analysis of the NMR spectra also provide useful information to assign and differentiate the protons of the alkyl spacer ($H_{1\text{-}6}$) from the H_{β} of the terminal groups that appears between δ=1.0–1.5 ppm. The different environment experienced by the two terminals in the molar ratio 1 could indicate a binding mode as shown in Figure 7, where one terminal is being complexed by the SC4 cavity while the other is uncomplexed.

However, to define as clearly as possible the binding mode of complexation of G4 by SC4 at equimolar ratio, we performed 1D saturation transfer difference NMR (1D STD-NMR) and 1D NOESY experiments. STD-NMR, together with transfer NOE, is one of the most popular NMR techniques for the study of the interactions between small guests and macrocyles receptors.[33] Essentially, an STD experiment involves subtracting a spectrum in which the macrocycle was selectively saturated, from one without macrocycle saturation. In the difference spectrum only the signals of the guest that receive saturation from the macrocycle will remain. The size of the STD signal is not only dependent on the distance between the guest and the macrocycle, but the saturation of a signal in the bound state is counteracted by their longitudinal relaxation times in the free state.[33,34] To prevent possible misinterpretations due to T1 effects, the

construction of STD build-up curves was proposed,[35] and the slope of the STD build-up curves at 0 saturation time can be used to eliminate T1 bias at long saturation times (Figure S7). Since the cavity of SC4 is in cone conformation upon complexation with G4, it was selected to saturate the aromatic protons of SC4.

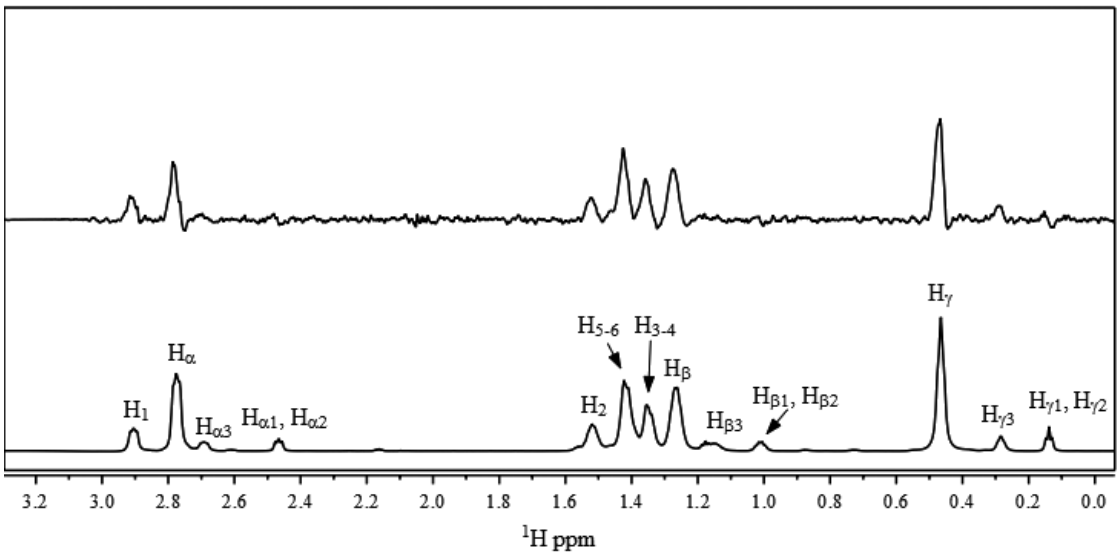

Figure 14. 1D STD spectrum (STDon - STDoff) of G4 (10 mM) in the presence of SC4 (10 mM) at 25 °C: ^{1}H NMR reference spectrum (bottom); 1D STD with saturation of aromatic protons of SC4 (7.44 ppm) with saturation time of 600 ms (top).

As can be seen in Figure 14, the results show intermolecular interaction between the protons of the terminal group of G4 (H_α, H_β, H_γ) but also and more importantly, intermolecular interaction of the aromatic protons of SC4 with the protons that correspond with the alkyl spacer of G4 (H_{1-6}). Therefore, these results are fairly compatible with a complex structure as shown in Figure 7, since the spacer is more than 4Å of distance to the aromatic protons of SC4. The experiment of 1D NOESY is as well in line with the STD experiments, due the observed intermolecular interactions between the aromatic protons of SC4 and the protons of the alkyl chain of the spacer (H_{3-6}) in addition to the terminal group (Figure S8). In this way, a possible inclusion mode between G4 and SC4 is shown in Figure 15 for 1:1 complexes, where one terminal head is inserted in SC4 cavity while the rest of the bolaform surrounds the macrocycle. Since all the experiments were performed in water at neutral pH, one of the lower-rim phenolic groups of SC4 is deprotonated and could be responsible for the binding mode between G4 and SC4. Despite do not exist many studies reporting the complexation of

guests at the lower rim,[36–38] it is known that the lower rim affect the complex formation and binding mode of host-guest complexes.[39] Therefore it is plausible that the lower rim of the calixarene may play a crucial rule in the complexation of G4 in 1:1 complexes.

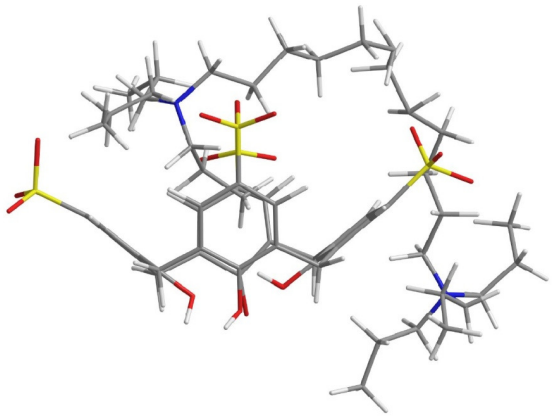

Figure 15. Schematic representation of one possible binding mode between SC4 and G4 at 1:1 molar ratio.

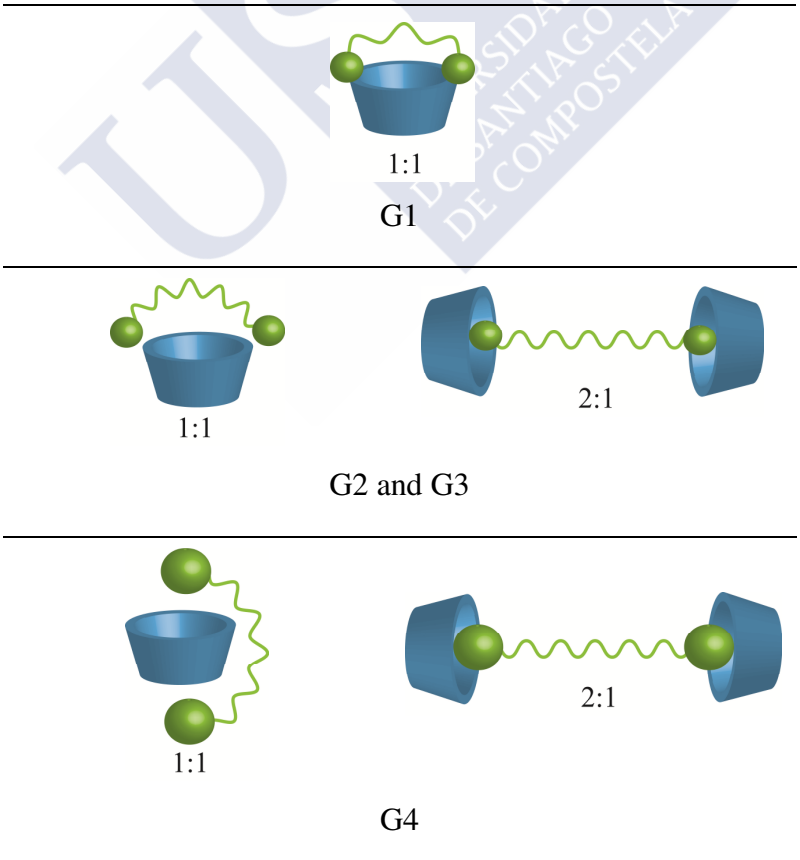

Scheme 2

5.1.4. Conclusions

In conclusion, we have shown that the inclusion of different bisquaternary ammonium guests by SC4 can adopt various binding modes as demonstrated by the several techniques employed (Scheme 2). The thermodynamics parameters obtained by ITC experiments shows that the complexation of the bolaform studied are enthalpy driven due C–H···π interaction and entropy favorable mainly due to the release of water molecules from the bolaform guests. The bolaform with the smaller spacer and polar head group can only form 1:1 complexes with the host, however with the particularity that the calixarene allows the complexation of both polar terminal groups of the bolaform. Increasing the spacer of the guest from n = 6 to n = 12 still allows the complexation of both polar head of bolaform in 1:1 complexation, however increasing the molar ratio of host in solution, 2:1 complexes are also formed for G2, G3 and G4. The binding mode of the bolaform with the higher polar head volume, G4, is different from the other three bolaforms in 1:1 complex, since only one terminal group of bolaform is complexed by the cavity of SC4, indicating that the complexation depends on the size of the bolaform head volume. Although one terminal group is being complexed by the SC4 cavity, the lower rim of the calixarene have some influence in the other terminal that remained uncomplexed and therefore influence the binding mode.

5.1.5. Appendix

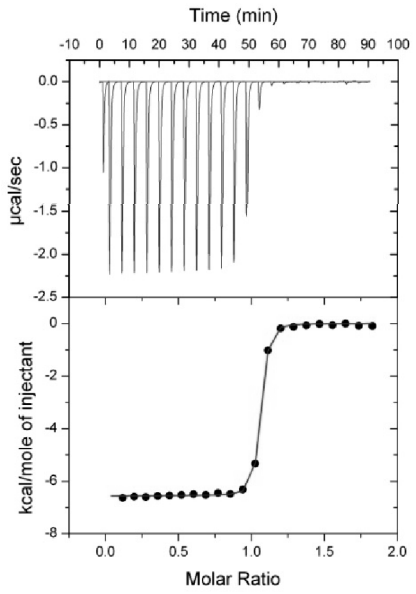

Figure S1. Microcalorimetric titration of G1 with SC4 in water at 25ºC: (top) raw data for sequential 23 injections (12 µL per injection) of G1 solution (1 mM) into SC4 solution (0.1 mM). (bottom) "net" heat effects obtained by subtracting the dilution heat from the reaction heat, which was fitted by computer simulation using "one set of binding sites" model.

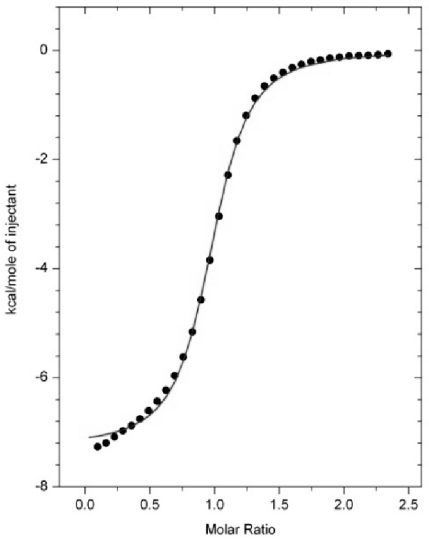

Figure S2. Microcalorimetric titration of G1 with SC4 in the presence of 50 mM of NaCl in water at 25 °C. Data for the sequential 34 injections (8 µL per injection) of G2 solution (3.5 mM) into 0.3 mM of SC4, fitted with the "one set of binding sites" model.

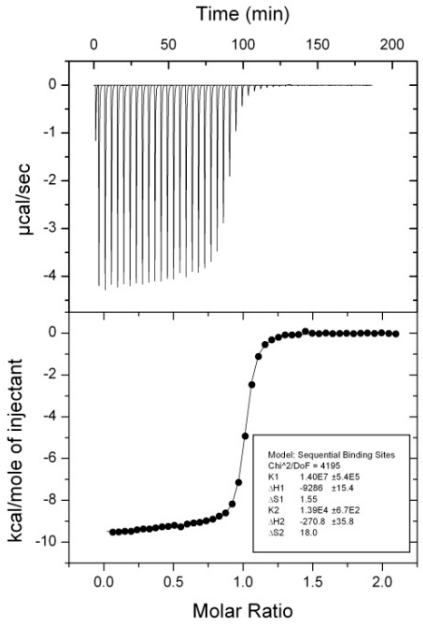

Figure S3. Microcalorimetric titration of G3 with SC4 in water at 25 °C: (top) raw data for sequential 45 injections (6 µL per injection) of G3 solution (2.1 mM) into 0.2 mM of SC4, (bottom) "net" heat effects obtained by subtracting the dilution heat from the reaction heat, which was fitted by computer simulation using "sequential binding" with two sites model.

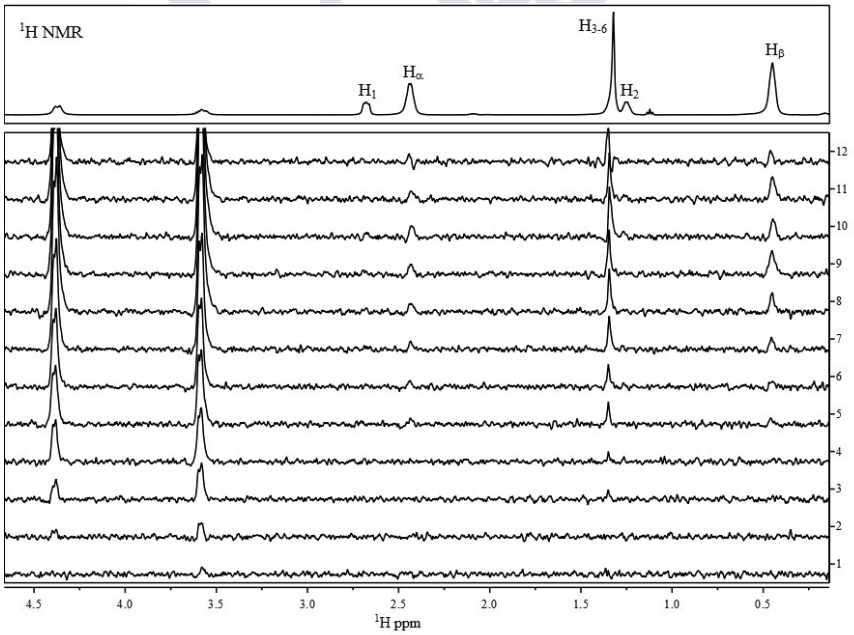

Figure S4. (top) ^{1}H NMR spectra of G3 (7 mM) in the presence of SC4 (7 mM) in D_20 at 25ºC. (bottom) 1D NOESY spectra of the mixture at different mixing time (from 0 s to 3 s at spectra 12) irradiating the aromatic proton of SC4 (7.44 ppm).

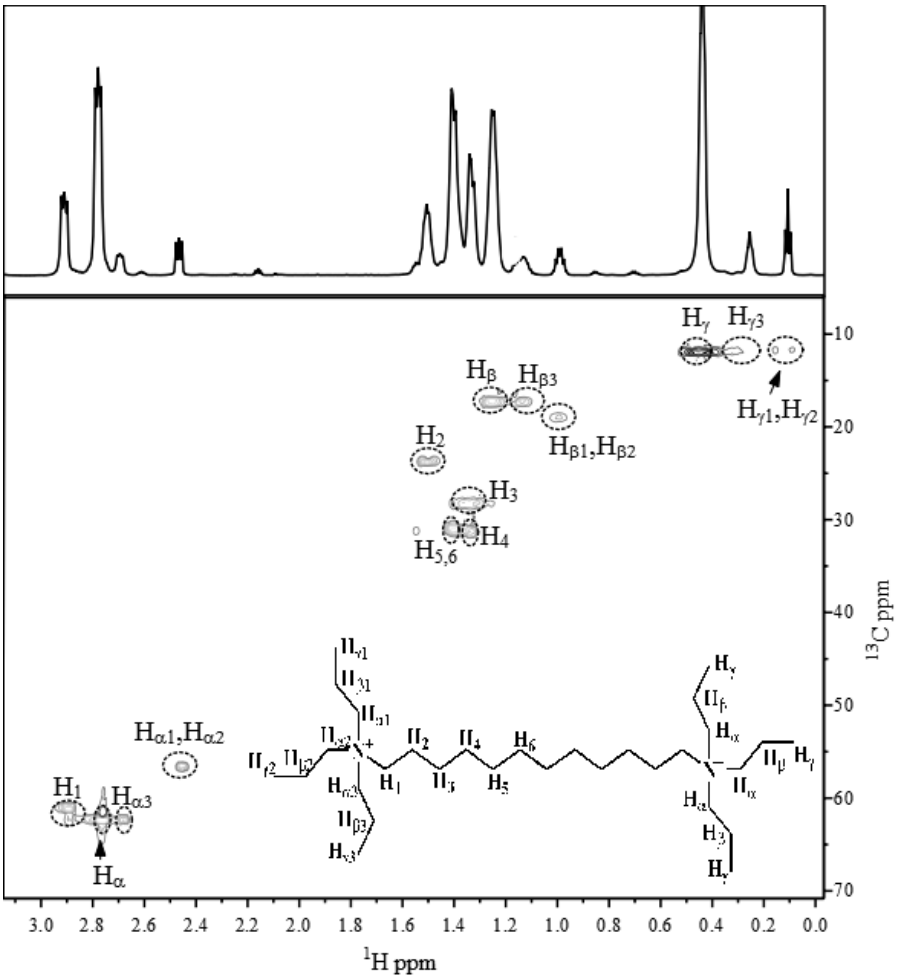

Figure S5. ^{1}H-^{13}C HSQC spectra region of G4 (10 mM) in the presence of SC4 (10 mM) in D_20 at 25 °C.

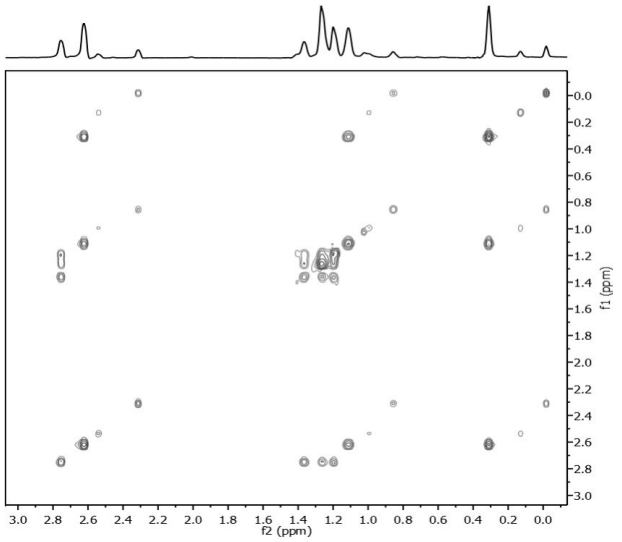

Figure S6. G4 region of an TOCSY spectrum of equimolar mixture of SC4 and G4 (10 mM) in D_2O, 25 °C.

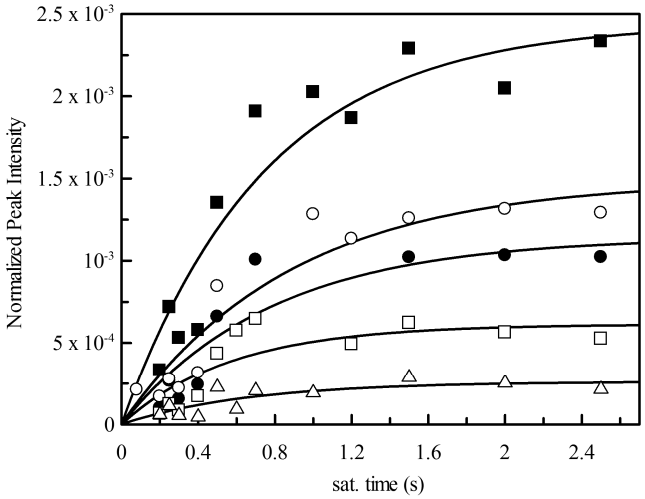

Figure S7. Normalized STD build-up curves of G4 (10 mM) in the presence of SC4 (10 mM) with saturation of the aromatic protons of SC4. (■) $H_{\gamma 1}$, (○) H_{5-6}, (●) $H_{\beta 1}$, (□) H_1 and (Δ) $H_{\gamma 3}$.

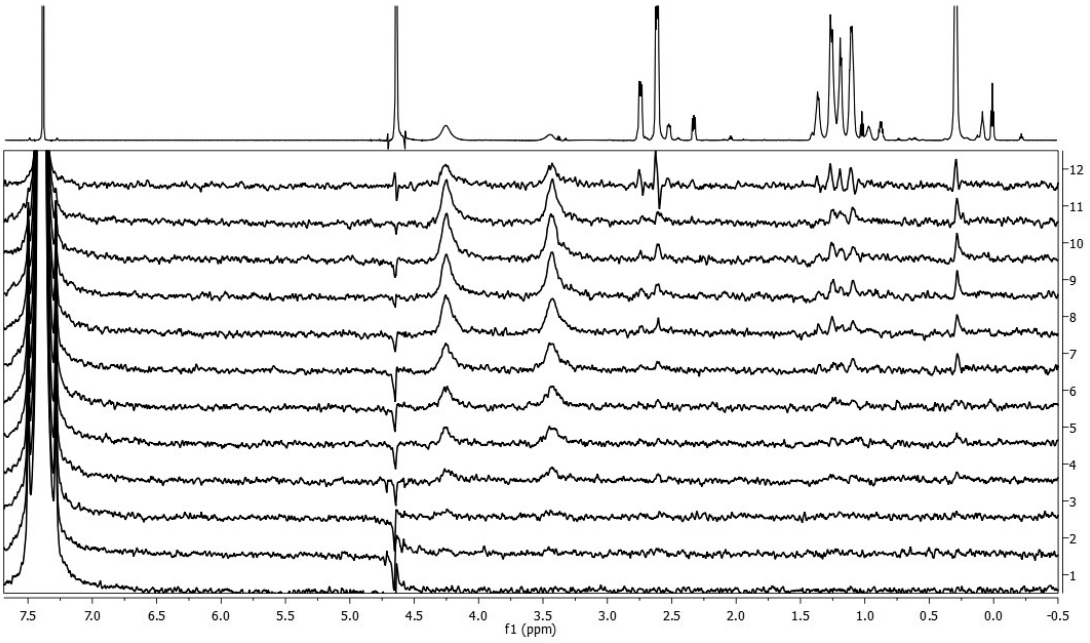

Figure S8. (top) ^{1}H NMR spectra of G4 (10 mM) in the presence of SC4 (10 mM) in D_20 at 25 °C. (bottom) 1D NOESY spectra of the mixture at different mixing time (from 0 s to 3 s at spectra 12) irradiating the aromatic proton of SC4 (7.44 ppm).

Diffusion experiments:

The diffusion coefficients were obtained using the pulse sequence, DOSY bipolar pulse pair stimulated echo (Dbppste), according to which the ratio of the signal intensity is given by equation S1:

$$\ln I/I_0 = -\gamma^2\delta^2G^2\left(\Delta - \frac{4\delta}{3}\right)D = -bD \quad \text{(S1)}$$

where I and I_0 are the echo intensity, in the presence and absence of the gradient pulse, respectively, γ is the gyromagnetic ratio, G is the pulse gradient strength, δ is the length of the pulse gradient, τ is the gradient stabilization delay, Δ is the time interval between the leading edges of the pulse gradient used and D is the diffusion coefficient. The diffusion coefficients were extracted from the slope of the plot of ln I/I_0 versus the b value.

Modeling the self-diffusion for the 1:1 Complex.

The model was taking into account the equilibrium between SC4 and the bolaform

$$SC4 + G \underset{}{\overset{K_{1:1}}{\rightleftharpoons}} SC4{:}G \quad \text{(S2)}$$

The binding constant for the 1:1 inclusion complex is given by:

$$K_{1:1} = [SC4{:}G]/([SC4][G]) \quad \text{(S3)}$$

The experimental bolaform self-diffusion coefficient $D_{\mathrm{G,obs}}$, can be described according to equation (4),

$$D_{\mathrm{G,obs}} = f_{\mathrm{G,f}}D_{\mathrm{G,f}} + \left(1 - f_{G,\mathrm{f}}\right)D_{\mathrm{SC4:G}} \quad \text{(S4)}$$

where $D_{\mathrm{SC4:G}}$ is the self-diffusion coefficient of the complex and $D_{\mathrm{G,f}}$ is the surfactant self-diffusion coefficient; $f_{\mathrm{G,f}}$ is the fraction of the free bolaform, which is given by

$$f_{\mathrm{G,f}} = \left(C_{\mathrm{G,t}} - C_{\mathrm{SC4:G}}\right)/C_{\mathrm{G,t}} \quad \text{(S5)}$$

where $C_{G,t}$ and $C_{SC4:G}$ represents the concentration of the complex and the total concentration of the surfactant, respectively. The concentrations of all the components in solution are connected by the corresponding mass action law, and the overall binding constant; K and $D_{SC4:G}$ have been estimated by using a non linear fitting of equation S6. The observed self-diffusion for the surfactant (eq S4) previously defined can be expressed in terms of binding constant and the total concentrations of SC4 and bolaform.

$$D_{G,obs} = \frac{D_{G,f} + K_{1:1} D_{SC4:G}[SC4]}{1 + K_{1:1}[SC4]} \quad \text{(S6)}$$

Modeling the self-diffusion for the 1:1 and 2:1 complexes

Assuming that higher order complexes than the 1:1 complex are formed and exist simultaneously, a second equilibrium is established.

$$\begin{aligned} SC4 + G &\overset{K_{1:1}}{\rightleftharpoons} SC4{:}G \\ SC4{:}G + SC4 &\overset{K_{2:1}}{\rightleftharpoons} SC4_2{:}G \end{aligned} \quad \text{(S7)}$$

Binding constants are defined as

$$K_{1:1} = [SC4{:}G]/[SC4][G] \quad \text{(S8)}$$

$$K_{2:1} = [SC4_2{:}G]/[SC4][SC4{:}G] \quad \text{(S9)}$$

Following the same procedure as before, observed self-diffusion values can be obtained for the bolaform and SC4

$$D_{G,obs} = f_{G,f} D_{G,f} + f^{G}_{SC4:G} D_{SC4:G} + f^{G}_{SC4_2:G} D_{SC4_2:G} \quad \text{(S10)}$$

where $D_{G,f}$, $D_{SC4:G}$ and $D_{SC4_2:G}$ are the diffusion coefficients for bolaform in 1:1 complex and 2:1 complex, respectively.

Assuming the molar fractions for the different species, the observed self-diffusion for the bolaform can be expressed in terms of binding constants and total concentrations of SC4 and bolaform.

$$D_{\mathrm{G,obs}} = \frac{D_{\mathrm{G,f}} + K_{1:1}D_{\mathrm{SC4:G}}[\mathrm{SC4}] + K_{1:1}K_{2:1}D_{\mathrm{SC4_2:G}}[\mathrm{SC4}]^2}{1 + K_{1:1}[SC4] + K_{1:1}K_{2:1}[SC4]^2} \quad \text{(S11)}$$

5.1.6. References

1. J.-H. Fuhrhop and T. Wang, *Chem. Rev.*, 2004, **104**, 2901–2937.
2. X. Cheng, F. Liu, X. Zeng, G. Ungar, J. Kain, S. Diele, M. Prehm, and C. Tschierske, *J. Am. Chem. Soc.*, 2011, **133**, 7872–7881.
3. Z.-X. Chen, X.-X. Su, and S.-P. Deng, *J. Phys. Chem. B*, 2011, **115**, 1798–1806.
4. Y. Kaufman, S. Grinberg, C. Linder, E. Heldman, J. Gilron, and V. Freger, *Langmuir*, 2013, **29**, 115211–61.
5. G. González-Gaitano, a. Guerrero-Martínez, F. Ortega, and G. Tardajos, *Langmuir*, 2001, **17**, 1392–1398.
6. C. Cabaleiro-Lago, M. Nilsson, A. J. M. Valente, M. Bonini, and O. Söderman, *J. Colloid Interface Sci.*, 2006, **300**, 782–787.
7. A. Müller and G. Wenz, *Chem. Eur. J.*, 2007, **13**, 2218–2223.
8. M. Nilsson, A. J. M. Valente, G. Olofsson, O. Söderman, and M. Bonini, *The journal of physical chemistry. B*, 2008, **112**, 11310–6.
9. I. W. Wyman and D. H. Macartney, *J. Org. Chem*, 2009, **74**, 8031–8038.
10. K. Baek, Y. Kim, H. Kim, M. Yoon, I. Hwang, Y. H. Ko, and K. Kim, *Chem. Commun.*, 2010, **46**, 4091–4093.
11. H.-X. Zhao, D.-S. Guo, and Y. Liu, *J. Phys. Chem. B*, 2013, **117**, 1978–1987.
12. M. Dreja, I. T. Kim, Y. Yin, and Y. Xia, *J. Mater. Chem.*, 2000, **10**, 603–605.
13. I. A. Banerjee, L. Yu, and H. Matsui, *J. Am. Chem. Soc.*, 2003, **125**, 9542–9543.

14. H. Zhang, J. Shen, Z. Liu, A. Hao, and Y. Bai, *Supramol. Chem.*, 2010, **22**, 297–310.

15. V. Francisco, N. Basilio, L. Garcia-Rio, J. R. Leis, E. F. Marques, and C. Vázquez-Vázquez, *Chem. Commun.*, 2010, **46**, 6551–6553.

16. H. Bakirci, A. L. Koner, and W. M. Nau, *Chem. Commun.*, 2005, 5411–5413.

17. L. Wang, D. Guo, Y. Chen, and Y. Liu, *Thermochimica Acta*, 2006, **443**, 132–135.

18. M. Rehm, M. Frank, and J. Schatz, *Tetrahedron Lett.*, 2009, **50**, 93–96.

19. C. K. L. Ng, D. Obando, F. Widmer, L. C. Wright, T. C. Sorrell, and K. a Jolliffe, *J. Med. Chem.*, 2006, **49**, 811–816.

20. V. Francisco, N. Basilio, and L. García-Río, *J. Phys. Chem. B*, 2012, **116**, 5308–5315.

21. S. Berger and S. Braun, *200 and More Basic NMR Experiments, A Practical Course*, Wiley-VCH, Weinheim, Germany, 2004.

22. A. Jerschow and M. Norbert, *J. Magn. Reson.*, 1997, **375**, 372–375.

23. M. Nishio, H. Hirota, and Y. Umezawa, *The CH-pi Interactions: Evidence, Nature and Consequences*, Wiley-VCH, New York, 1998.

24. D.-S. Guo, X. Su, and Y. Liu, *Cryst. Growth Des.*, 2008, **8**, 3514–3517.

25. C. Bonaccorso, A. Ciadamidaro, C. Sgarlata, D. Sciotto, and G. Arena, *Chem. Commun.*, 2010, **46**, 7139–7141.

26. G. Arena, S. Gentile, F. G. Gulino, D. Sciotto, and C. Sgarlata, *Tetrahedron Lett.*, 2004, **45**, 7091–7094.

27. X. Zhang and W. M. Nau, *Angew. Chem. Int. Ed.*, 2000, **39**, 544–547.

28. Y. Liu, D.-S. Guo, H.-Y. Zhang, Y.-H. Ma, and E.-C. Yang, *J. Phys. Chem. B*, 2006, **110**, 3428–3434.

29. R. N. Dsouza and W. M. Nau, *J. Org. Chem.*, 2008, **73**, 5305–5310.

30. D. Neuhaus and M. P. Williamson, *The Nuclear Over-hauser Effect in Structural and Conformational Analysis*, Wiley-VCH, New York, 2nd ed., 2000.

31. Z. Asfari, V. Bohmer, J. Harrowfield, and J. Vicens, *Calixarenes 2001*, Kluwer Academic Publishers, Dordrecht, The Netherlands, 2001.

32. C. Bonal, Y. Israëli, J.-P. Morel, and N. Morel-Desrosiers, *J. Chem. Soc., Perkin Trans. 2*, 2001, 1075–1078.

33. M. Mayer and B. Meyer, *Angewandte Chemie International Edition*, 1999, **38**, 1784–1788.

34. B. Meyer and T. Peters, *Angew. Chem. Int. Ed.*, 2003, **42**, 864–890.

35. M. Mayer and T. L. James, *J. Am. Chem. Soc.*, 2004, **126**, 4453–4460.

36. I. Yoshida, N. Yamamoto, F. Sagara, K. Ueno, D. Ishii, and S. Shinkai, *Chem. Lett.*, 1991, **20**, 2105–2108.

37. N. Iki, T. Horiuchi, H. Oka, K. Koyama, N. Morohashi, C. Kabuto, and S. Miyano, *J. Chem. Soc., Perkin Trans. 2*, 2001, 2219–2225.

38. J. L. Atwood, L. J. Barbour, M. J. Hardie, and C. L. Raston, *Coord. Chem. Rev.*, 2001, **222**, 3–32.

39. J. Cui, V. D. Uzunova, D.-S. Guo, K. Wang, W. M. Nau, and Y. Liu, *Eur. J. Org. Chem.*, 2010, **2010**, 1704–1710.

5.2. Novel Catanionic Vesicles from Calixarene and Single-Chain Surfactant

5.2.1. Introduction

The construction of well-defined structures in the nanometer or micrometer length scale based on molecular self-assembly is one of the most important challenges facing modern chemistry. For instance, noncovalent interactions have been used to obtain a wide-range of structured aggregates such as tubules, fibers, micelles, vesicles, and disks through molecular self-assembly of small organic compounds.[1–6]

Mixtures of anionic and cationic surfactants (catanionic mixtures) offer an attractive approach for the construction of complex self-assembled nanostructures. The formation of spontaneous vesicles in mixtures of oppositely charged surfactants was first demonstrated by Kaler[7] and since then, intense research has been devoted to the study of self-assembled structures formed in catanionic surfactant systems.[8–14] Globular micelles, cylindrical micelles, long threadlike micelle, discs, and large lamellar sheets have also been observed in some of the aqueous cationic-anionic systems. The molecular assemblies formed in these systems are mainly attributed to a strong electrostatic association modulated by chain packing interactions, which generally result in a reduced head-group area promoting a dense packing of surfactant molecules in the aggregate.

We have recently demonstrated that when the anionic surfactant is replaced with a non-aggregating and surface inactive hexamethylated *p*-sulfonatocalix[6]arene (SC6HM) the micellization of single chain trimethylammonium amphiphiles is promoted at concentrations below the critical micelle concentration (cmc) of neat surfactant.[15] It was suggested that the complexation of the cationic surfactant with SC6HM yields an aggregate with surface active properties that aggregates at lower concentrations than that of neat surfactant. Motivated by this observation, we decided to study the mixed system formed by the most common *p*-sulfonatocalix[4]arene (SC4) with a single chain surfactant, tetradecyltrimethylammonium bromide (TTABr), as well as a serine-based surfactant (16Ser) (Scheme 1).

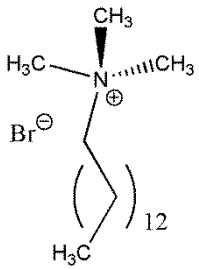

TTABr

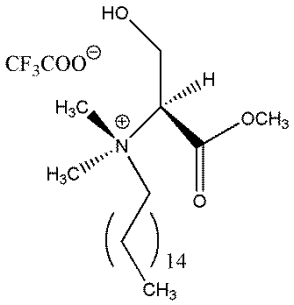

16Ser

Scheme 1

5.2.2. Experimental Section

Materials: *p*-sulfonatocalix[4]arene was obtained from sulfonation of (*p*-tert-Butyl)calixarene in concentrated sulfuric acid (98%). The cationic serine-based surfactant N-hexadecyl-N-(2-hydroxy-1-methyloxycarbonyl)ethyl-N-N-dimethylammonium trifluoroacetate was synthesized according to previously described method.[16] Tetradecyltrimethylammonium bromide (assay ≥99%) from Sigma-Aldrich was used without further purification. All solutions were prepared with Milli-Q water.

Sonication procedure. The vesicles were prepared as follows: a certain amount of p-SC4 and TTABr was dispersed in 40 mL of water at 60 °C. Then the solution was sonicated using a Branson Sonifier 450 with a probe containing a 13 mm flat tip. The tip was submerged approximately two-thirds of the sample height and the power monitor indicated 20%. After every 5 min of sonication, the sample was left at rest during 2 min. The sonication time was always 30 min in total. Samples were then equilibrated to room temperature and filtered through a 0.45 μm pore size filter in order to eliminate possible titanium particles.

NMR. The ^{1}H NMR spectra in D_2O solution were measured with a Varian Mercury 300 MHz NMR spectrometer. Diffusion NMR experiments were recorded at 35 °C on a Varian Inova 500 spectrometer.

Zeta-potential measurement. Vesicle electrophoretic mobilities were measured using a Malvern Zetasizer 2000. The ζ-potentials were calculated using the Smoluchowski equation. All samples were filtered prior to the measurement that was performed at 25 °C.

TEM. Vesicles were imaged with a PHILIPS CM-12 transmission electron microscope at 100kV using the negative staining method. A drop of vesicle solution was spread on a 200-mesh copper grid coated with a Formvar film, and the extra droplet was instantly wiped off by filter paper. After being naturally desiccated, a drop of 2% phosphotungstic acid solution was dropped on the copper grid for about 60 s and the extra droplet was also removed. Then the grid was dried naturally for about 3 h before TEM observation.

Lyophilization. The sample is cooled with liquid nitrogen, causing ice crystals to nucleate and grow. The sublimation of the ice with a TELSTAR lyophilizator yielded a freeze-dried powder.

Light scattering. Light scattering was performed using an ALV SP-86 goniometer, ALV 5000 Multi-tau correlator and a Coherent Sapphire optically pumped semiconductor laser operating at a wavelength of 488 nm and a power of 200 mW. The correlation functions were accumulated for 100 s and analysed using the ALV Correlator Software (ALV-5000/E version 3.0) based on the CONTIN algorithm adapted to the specific correlator noise. Temperature was fixed to 25 ºC. The logarithmically sampled relaxation time spectra (amplitude vs. log(τ)) were obtained from the CONTIN inversion of the normalised correlation functions. Assuming homodyne light beating, the distribution of diffusivities were obtained applying the relation $D = 1 / (q^2\tau)$, and transformed using the Stokes-Einstein relation, the electrolyte solvent viscosity η_0 and refractive index n at the actual temperature T in order to yield the hydrodynamic radius $R_H = kTq^2\tau / 6\pi\eta_0$ where k is the Boltzmann constant, $q = (4\pi n/\lambda)\cdot sin(\theta/2)$ is the scattering vector as a function of wavelength in vacuum, λ, and scattering angle θ. Measurements were performed at angles between 30 and 150º with increments of 15º.

Light Microscopy. An Axioplan Universal light microscope from Carl Zeiss, equipped with differential interference contrast (DIC) lenses and a video-camera system, was used.

***Cryo*-SEM.** SEM/EDS experiments were performed using a High resolution Scanning Electron Microscope with X-Ray Microanalysis and CryoSEM experimental facilities: JEOL JSM 6301F/ Oxford INCA Energy 350/ Gatan Alto 2500. The specimen was rapidly cooled (plunging it into sub-cooled nitrogen – slush nitrogen) and transferred under vacuum to the cold stage of the preparation chamber. The specimen

was fractured, sublimated ('etched') for 120sec. at -90°C, and coated with Au/Pd by sputtering for 35 sec. The sample was then transferred into the SEM chamber and studied at a temperature of -150°C. The conditions in which images and spectrum were obtained are described in the respective labels.

5.2.3. Results and Discussion

SC4 is a well known receptor for organic ammonium cations in water and displays specially strong binding abilities for these guests due to their π-rich cavities and to five negative charges at pH 7. Though ammonium cations are typical guests for SC4 host, reported studies on the complexation of alkylammonium cations are scarce.[17,18] In this section are shown the results obtained for the mixed system between SC4 and TTABr and as well as for the system SC4–16Ser.

5.2.3.1. Binary mixture SC4–TTABr

When 2 mM of SC4 is mixed with TTABr, it is observed the formation of a white dispersion at TTABr concentrations between 0.1 mM and 50 mM, and a precipitate zone near the charge neutrality. Below and above this gap a clear solution is observed. Since this last behavior is common in some catanionic systems, experiments were carried out to identify the aggregates formed in that region. In the literature, it is know that the mixture between the above calixarene and some biorelevant molecules, such as aliphatic amines, polyamines and amino acid isomers, is organized in bilayer-type structures in the solid state.[19] In this work it was study the host-guest system in liquid state and the use of conventional amphiphilic surfactants, which increase the number of molecules that can form bilayer structures with the calixarene.

When a milky dispersion of 50 mM SC4/TTABr with molar ratio 1:2.5 was examined under Nomarski light microscopy between glass and cover slide, a high concentration of giant vesicles (0.5–5 μm) was visible (Figure 1), with the smaller ones in fast Brownian motion. The presence of these very large vesicles is the reason for the white opaque appearance of the dispersion and was detected throughout the 0.1–50 mM range.

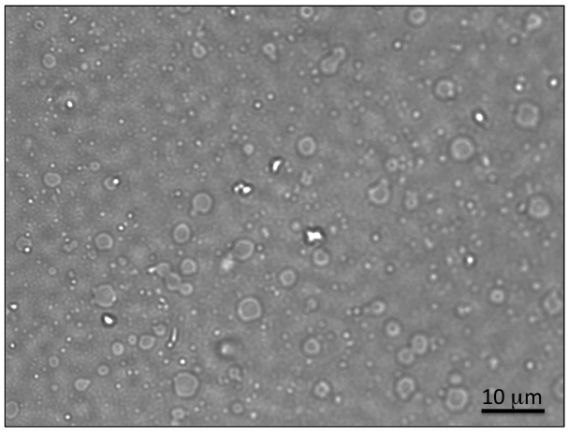

Figure 1. A light micrograph of a 50 mM white dispersion of SC4/TTABr with a molar ratio 1:2.5, showing the presence of polydisperse and very large vesicles. The smallest vesicle visible appears in Brownian motion.

In the diluted region, after sonication of a dispersion containing 2 mM of SC4 and 5 mM of TTABr, the sample was studied by dynamic light scattering (DLS) and transmission electron microscopy (TEM). As shown below our results are compatible with the presence of unilamellar vesicles in the solution. When the aqueous mixture of components in the sample is examined by DLS two relaxation modes are observed: a fast mode at short relaxation times, related to the diffusion of large aggregates, and (within the low experimental precision because of bad statistics for such slow fluctuations in a limited sampling time) a slow mode at long relaxation times which is independent of the scattering vector q, indicating that it is a "viscoelastic" mode (Figure 2a). The average diffusion coefficient of the vesicles is obtained by fitting the angular dependence relaxation times of the fast mode, $D = (4.29 \pm 0.05)\ \mu m^2\ s^{-1}$, which corresponds to an average hydrodynamic radius of *ca.* 57.2 ± 0.7 nm (Figure 2b).

The size distribution was also investigated by TEM, and the experimental results are in agreement with the average size obtained by DLS, showing that the vesicles are generally smooth and spherical (Figure 4). It was also measured the charge of these vesicles in a Z-Sizer equipment and a ζ-potential about -23 ± 5mV was obtained at 25 $^{\circ}$C. This value met our expectations since we worked with an excess of negative charge due to the calixarene. The diameter obtained by the Z-Sizer is 135 nm and it is in accordance with TEM and DLS data.

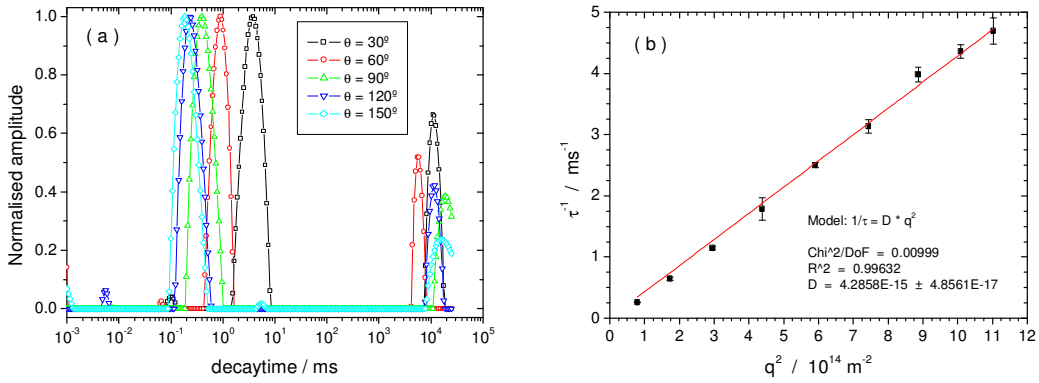

Figure 2. DLS data of negatively charged catanionic vesicles a few hours after preparation: (a) angular dependence; (b) determination of the diffusion coefficient of the vesicles.

To obtain more information on the structure of the aggregates NMR spectra of neat SC4, neat TTABr and mixed vesicles were performed. The assigned chemical shifts are listed in Table 1. The terminal protons of the surfactant alkyl chain are unaffected in the complex. However, in contrast, the $N(CH_3)_3$ and the protons bonded to the alpha Carbon (C_α) show large changes in chemical shifts, compatible with an inclusion complex where the surfactant polar head is located in the aromatic cavity of the calixarene (Scheme 2). In Scheme 2 the calixarene is represented in the simplified shape, "cone" conformation, but the ^1H NMR spectrum indicates that the calixarene is exchanging rapidly in the NMR time-scale between several possible conformations, since the $ArCH_2Ar$ methylene protons give one singlet.

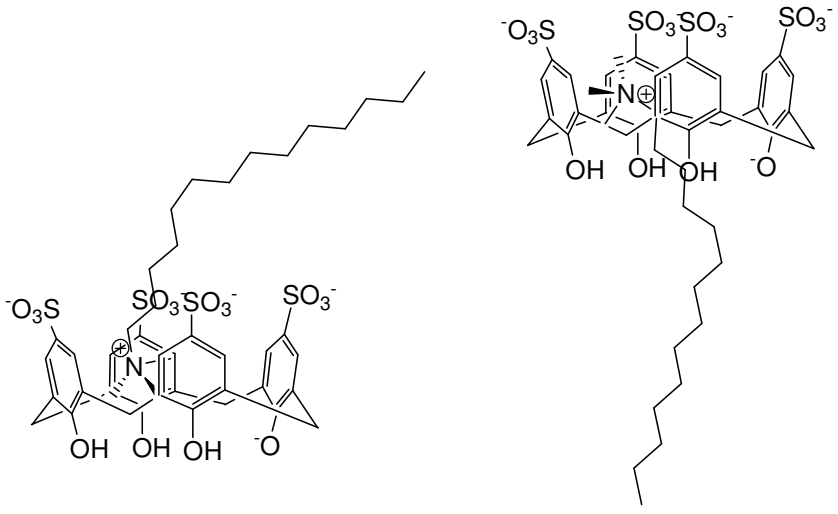

Scheme 2. Two possible inclusion modes of TTABr in SC4.

Table 1. Chemical shift changes ($\Delta\delta$, ppm) for the inclusion complex formed between the surfactant TTABr and the *p*-sulfonatocalix[4]arene. Negative values indicate up-field shift.

	ArH aromatic	$ArCH_2Ar$	RCH_3	$RCHC_{2\alpha}$	$N^+(CH_3)_3$
p-SC4	7.58	4.01	——	——	——
TTABr	——	——	0.87	3.41	3.17
Complex	7.61	4.04	0.85	2.15	1.31
$\Delta\delta$	0.03	0.03	–0.02	–1.26	–1.86

In order to study the stability of the vesicles, the evolution of the relaxation time spectra was studied by DLS (Figure 3). No change was observed within 4–5 days from preparation; however, after 7 days, a new relaxation mode is observed at longer times than the fast diffusive mode. The relative amplitude of the new mode increases, while the corresponding to the fast mode decreases; this feature is an indication that the vesicles are either coalescing and growing in size or flocculating.

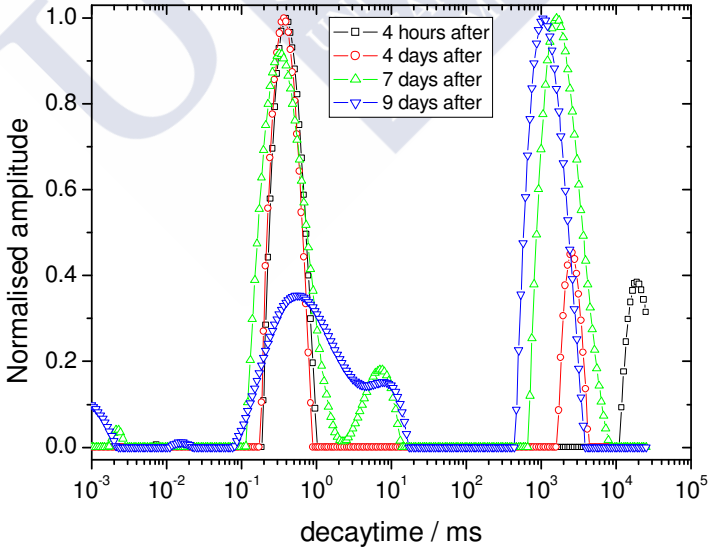

Figure 3. Time evolution of the DLS for negatively charged vesicles.

This behavior is quite usual since often the high curvature vesicles are metastable aggregates and consequently, the size distribution evolves with time to larger structures (e.g. lamellar sheets). The initial aqueous dispersions may even show phase separation.

In addition, chemical or biological degradation may also develop. Due to this issue, dispersions that contain vesicles must be freshly prepared just prior to use. Since this process is often poorly defined and difficult to control,[20] this procedure presents some disadvantages (i.e., when preparing liposome/DNA complexes).

To circumvent colloidal instability and/or avoid degradation and to allow for long-term storage of vesicles, water may be removed through the most common and frequent method to dehydrate, that is the freeze-drying technique.[21,22] The complete process to stabilize and store our vesicles can be summarized in the following four points: (A) SC4 and TTABr are dissolved in water yielding a whitish dispersion. (B) The aqueous cloudy dispersion is sonicated for approximately 30 min, and a homogenous clear solution is obtained. (C) The solution is then frozen with liquid nitrogen, causing ice crystals to nucleate and grow. Sublimation of ice yields the freeze-dried powder. (D) The dried power is rehydrated again with water (Figure 4).

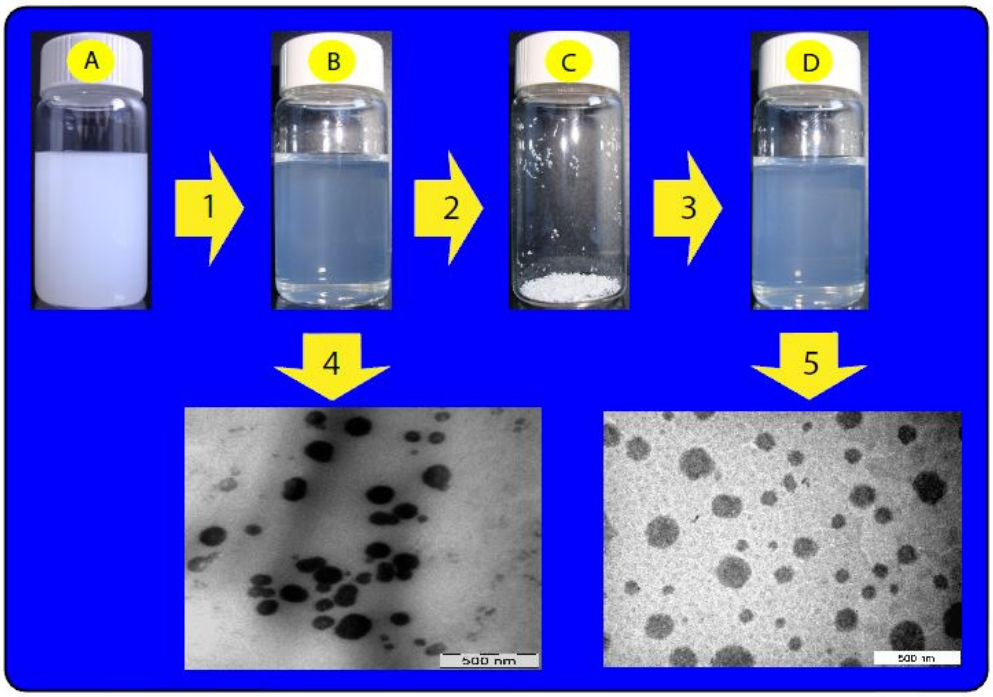

Figure 4. Schematic representation for vesicle storage method and rehydration. Step 1,2 and 3 corresponds to sonication, lyophilization and rehydration, respectively. The TEM images (negatively stained 2% phosphotungstic acid, pH=7) are before (step 4) and after the lyophilization (step 5).

After sample lyophilization (step C), a white powder is obtained that completely redisperses in water forming again the vesicles, without any need of sonication. Usually

simple hydration of the dried vesicles powder does not completely redisperse them in water, but produces a mixture of suspended vesicles and larger aggregates and therefore requires the sample to be sonicated again.[23]

Consequently we can deduced that the structure of vesicles formed when the solution is sonicated for the first time maintains their organization when water escapes and later enters the structure again. Also we can conclude that this process does not significantly change the size of the vesicles as one might expect. Usually the conventional vesicle structure is lost during the freeze-drying process, and as a result the use of carbohydrates was introduced.[24,25] The sugar coating on the surface of the vesicles results in a low molecular mobility, which minimizes damage caused by the fusion process or crystal formation after drying.[23] To confirm that these vesicles do not need any cryoprotectant it was performed a new set of DLS measurements after rehydration. Figure 5 shows the results for the sample measured after 3 days of the redispersion. From the linear fit, the average diffusion coefficient obtained is D = (3.44 ± 0.06) μm^2 s^{-1}, which corresponds to an average hydrodynamic radius of 71 ± 1 nm.

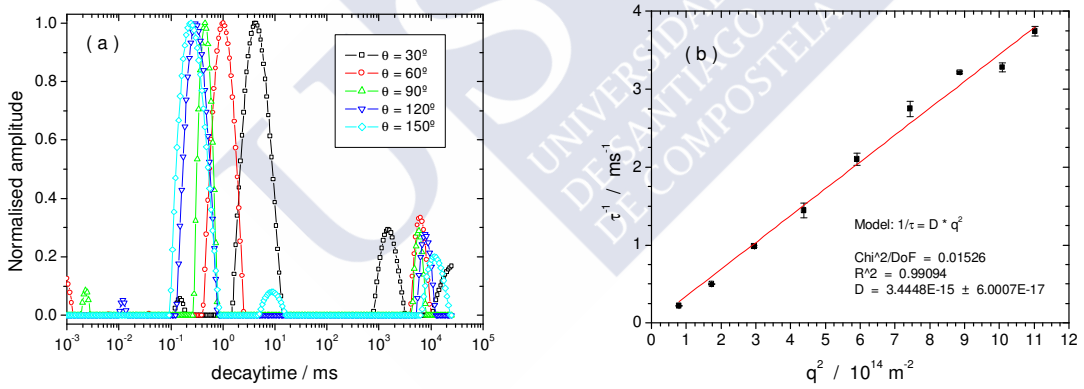

Figure 5. DLS for negative vesicles after lyophilization, measured 3 days after redispersion: (a) angular dependence; (b) determination of the diffusion coefficient of the vesicles.

This value confirms that when these vesicles are lyophilized and hydrated again they do not yield the thermodynamically preferred lamellar phase domains. With respect to the process of water leaving and entering the mixed amphiphilic film, the effect cannot be considered very remarkable since the water permeability of usual lipids is very high, for instance, almost 10 orders of magnitude larger than that of sodium

ion.[26,27] We can derive from this fact that the inclusion complex between *p*-SC4 and TTABr does not significantly change the transport of water across the vesicle bilayer.

5.2.3.2. Binary mixture SC4–16Ser

The interest to study amino acid-based surfactants can be related with their lower toxicity and facile biodegradation when compared with other conventional surfactants.[16] Sulfonatocalixarenes are also known to be friendly to organisms,[28] in addition to the recognized ability to build supramolecular aggregates.[29–31] Therefore, a mixed system could be a smart strategy to design supramolecular architectures with the necessary biocompatibility for applications in the fields of biotechnology.

In this sense, the mixture between the water-soluble calixarene and the serine-based surfactant was studied at different molar ratio. At lower molar ratio of SC4, a clear solution is observed, but when the concentration of SC4 is increased, a gap with a bluish appearance solution is formed. At higher molar ratio of SC4 it is observed the formation of solid particles and the solution becomes colorless. In Figure 6 is shown the macroscopic phase behavior in the binary mixture of SC4–16Ser at different molar fraction of SC4, $\chi_{SC4} = nSC4/(nSC4 + n16Ser)$. The total concentration of the mixed system was kept constant near 5mM, since at higher concentrations occur the formation of solid particles/precipitate. It should be noted that all experiments were performed at temperatures above the Krafft temperature of the serine-based surfactant (T_{Kr} = 31.2 °C).[16]

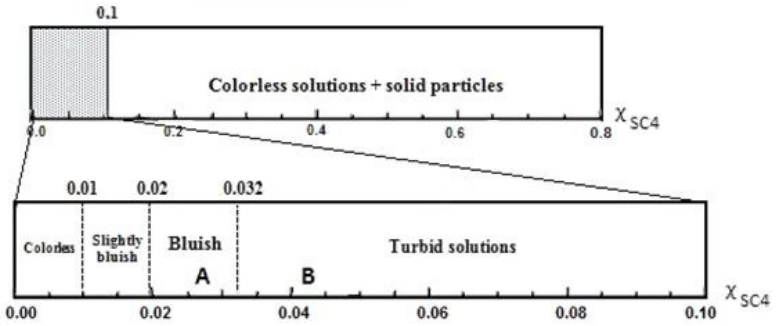

Figure 6. Schematic representation of the macroscopic phase behavior observed for the binary mixture of SC4–16Ser at a total concentration of ca. 5 mM and at 40 °C. χ_{SC4} is the molar fraction of SC4 in the mixture.

In order to identify which type of aggregates are formed in the bluish and turbid region, light microscopy and *cryo*-SEM experiments were performed. Observations of

freshly prepared aqueous mixture solutions by light microscopy do not show the formation of any aggregates (visible in the microscope, size ≥ 100 nm). However, from the continuously inspection during the following days after samples preparation, approximately 15 days, it was possible to identify the formation of large aggregates. From the light microscopy observations in the bluish region, $\chi_{SC4} = 0.01 - 0.032$, it can be observed the formation of spherical particles, possibly multilamellar vesicles, and tubules. The spherical particles show a diameter up to 1 μm and the tubules with approximately the same diameter have length up to 50 μm, with both aggregates in fast and slow Brownian motion (Figure 7). When compared against the turbid region, $\chi_{SC4} = 0.032 - 0.063$, a large number of tubular and spherical aggregates were also observed. However, while in bluish solutions the number of tubules are higher when compared with the number of spherical particles, in turbid solutions the opposite is observed. The different number of spherical aggregates and tubules with increasing the amount of SC4 in the mixture was also confirmed by *cryo*-SEM experiments (Figure 7).

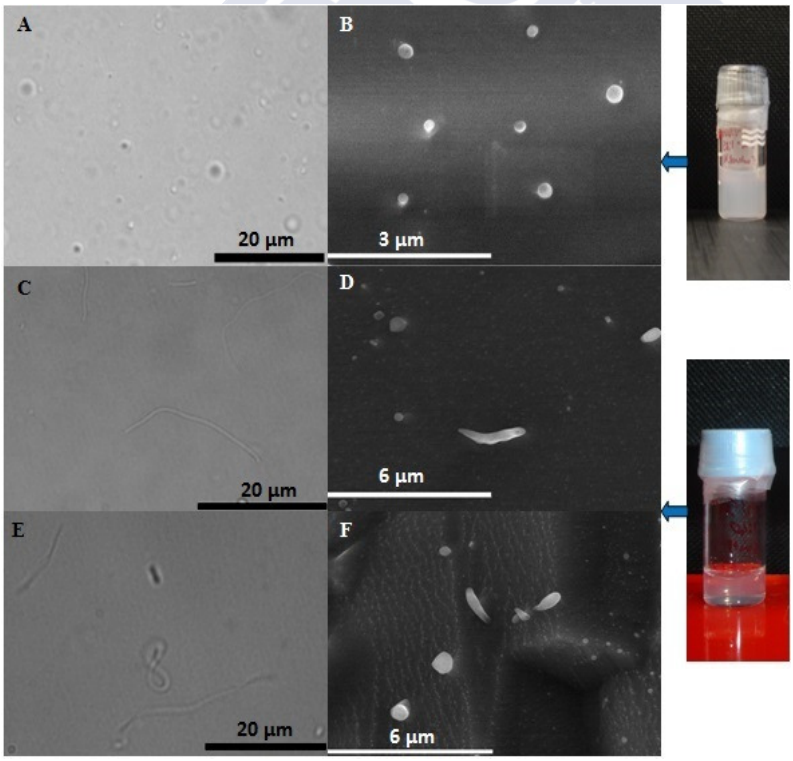

Figure 7. Light microscopy (A, C and E) and Cryo-SEM (B, D and F) micrographs of SC4–16Ser mixtures with different composition, showing the presence of spherical particles and flexible supramolecular tubules. The letters A and B represent the sample turbid with χ_{SC4} = 0.042 and the letters C to F represent the sample bluish with χ_{SC4} = 0.024.

From the light microscopy and *cryo*-SEM experiments, it was also possible to observe that the tubules break and gives rise to the formation of the spherical aggregates (Figure 8).

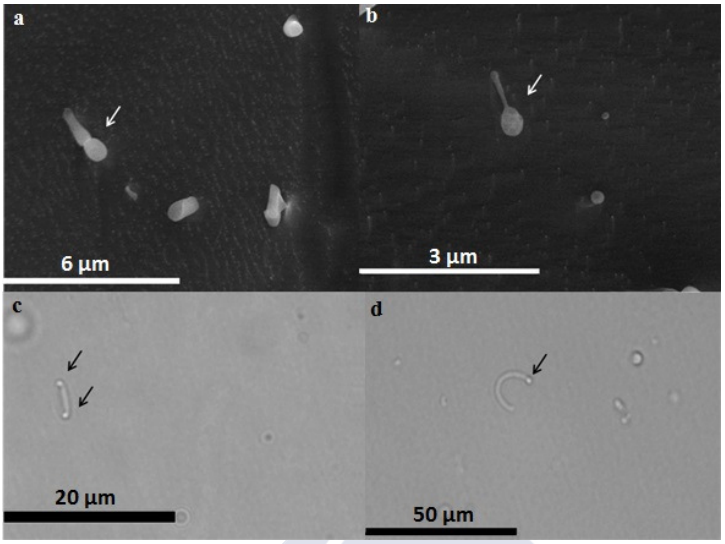

Figure 8. Cryo-SEM (a, b) and light microscopy (c, d) micrographs of 16Ser/SC4 mixtures, showing the morphology of tubules.

To obtain further information about the mixed system, diffusion measurements were performed. Firstly, knowing the critical micelle concentration (cmc) of the "pure" surfactant (cmc = 0.33 mmol kg^{-1}),[16] the diffusion coefficients were determined for the monomer and the micellar structure. The surfactant self-diffusion was monitored from the alkyl chain peak. A diffusion coefficient of $(3.67 \pm 0.17) \times 10^{-6}$ cm^2s^{-1} was obtained for the monomer. Above the cmc, where the monomers and micelles exist in a dynamic equilibrium, the self-diffusion coefficient decrease to $(1.47 \pm 0.11) \times 10^{-6}$ cm^2s^{-1}. The value obtained for the diffusion of micelles of 16Ser is in good agreement with the value reported in the literature.[16] The same experiments were then carried out for the binary mixture, where the molar ratio of SC4 was gradually increased. Since these experiments were performed above the cmc of 16Ser, and in the presence of SC4, the observed diffusion coefficient should be the mole fraction weighted average of the diffusion of four species: "pure" surfactant as monomer and as micelle, host–guest complex and as supramolecular aggregates. The aggregates include the large spherical particles, the tubules as well as the micelles formed by the surfactant and SC4 (see below). As can be seen in Table 2, the diffusion coefficients obtained at different molar fractions of SC4 are lower than the diffusion of the micelles formed only by 16Ser, as

expected for the formation of large aggregates, but more importantly is the trend observed with increasing the amount of SC4 in the binary system. Increasing the molar ratio of SC4 leads to an increase of the surfactant self-diffusion coefficient, from 1.0×10^{-7} cm^2 s^{-1} at $\chi_{SC4} = 0.004$ to 5.2×10^{-7} cm^2 s^{-1} when the $\chi_{SC4} = 0.063$. From the Stokes–Einstein equation it is possible to calculate the size of the aggregates, although only as a qualitative indication once the equation assumes a spherical shape for the aggregates. At molar ratio $r = 0.4\%$, an average diameter of ca. 60 nm was obtained for the aggregates, but the size decreases to ca. 10 nm when the molar ratio of SC4 is increased to 6.3%. Since the diameter of pure surfactant micelles is in the range of 4–5 nm, the formation of aggregates with diameter of ca. 10 nm could be due to the formation of supramolecular micelles, such as the mixed system SC6HM–DTAB.[15] A comparison of the particles sizes obtained by light microscopy or *cryo*-SEM (ca. 300–500 nm for the spherical particles and up to 20 μm for tubules) and the sizes obtained by self-diffusion reveal some discrepancy. However, in every molar ratio studied, the peaks of the surfactant monitored only shows single-exponential echo decays. This behavior indicates that despite the size polydispersity of the aggregates in the different region studied, the observed echo decay corresponds only to the smaller aggregates, and therefore excludes the large tubules and the spherical aggregates observed by light microscopy.

Table 2. Observed self-diffusion coefficients for the surfactant 16Ser in the presence of different molar fraction of SC4 for a constant $C_t \approx 5$mM at 35 °C.

r_{SC4} (%)	D_{obs} (10^{-7} cm^2 s^{-1})
0.4	1.044 ± 0.066
1.4	1.101 ± 0.140
4.2	2.707 ± 0.113
6.3	5.277 ± 0.086

As mentioned above, the addition of SC4 to a solution of 16Ser could also lead to the formation of a catanionic micelle. Recently, it was reported that the complexation of calixarene derivatives with single chain surfactant gives rise to the formation of a supraamphiphile that promotes micelle formation, with diameter size near 10 nm.[15,32] Moreover, it was observed that the mixed macrocyclic-surfactant system is associated

with a large decrease of the surfactant cmc value. Therefore, in order to corroborate the formation of supramolecular micelles, surface tension experiments were performed. The variation of the surface tension with the "pure" surfactant concentration (ln *c*) as well as in the presence of different amount of SC4 is plotted in Figure 9. The cmc value is determined from the inflection point in the curve. The results show that the addition of a small amount of SC4, induces a decrease in the cmc value of the surfactant. Therefore, corroborating the results obtained from the self-diffusion experiments, the addition of SC4 to a solution of 16Ser leads to the formation of a supra-amphiphile and its aggregation as a catanionic micelle.

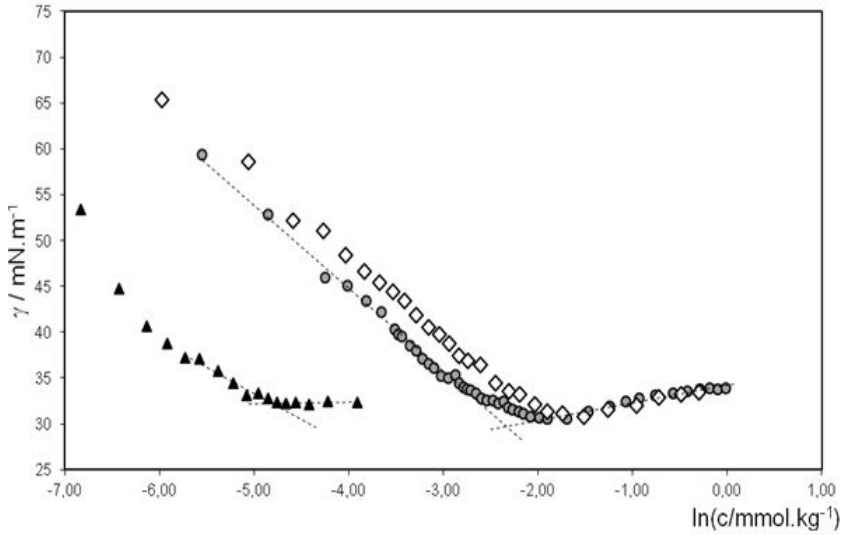

Figure 9. Surface tension vs ln concentration (*c*) curves for the "pure" surfactant 16Ser (◊) and in the presence of different molar fraction of SC4 at 35 °C. (●) χ_{SC4} = 0.004 and (▲) χ_{SC4} = 0.024.

To obtain more insights into the structure of the aggregates, ^{1}H NMR spectra were obtained. Based on the ability of SC4 to complex a wide range of organic ammonium cations, the complexation of the serine-based surfactant should not be an exception. Unfortunately, at lower χ_{SC4} the fraction of complex is too small to observe changes in the proton signals and at higher molar fraction of SC4 occurs the formation of solid particles/precipitate. Moreover, as observed in other systems,[40] signal broadening owing the formation of aggregates was also observed in D_2O. In this way, the experiments were performed with the homologue surfactant 12Ser, with 12 carbon atoms at the aliphatic tail. The observed changes in the proton signals of the surfactant 12Ser upon

complexation with SC4 are shown in Figure 10. The mixture resulted in averaged signals for the free and complexed components. This indicates that the assembly formation is fast on the NMR time scale. As can be seen, the terminal protons of the surfactant alkyl chain are unaffected, in contrast with the upfield shifts experienced by the head group of the surfactant. Although the peaks for methyl protons (H_3 and H_4) of 12Ser displays the higher upfield shifts compared to the free guest, the protons H_1 and H_2 also reveal substantial upfield shifts. The chemical shifts observed for the head group region are the result of the shielding provided by the calixarene cavity upon interaction with the surfactant.[41,42]

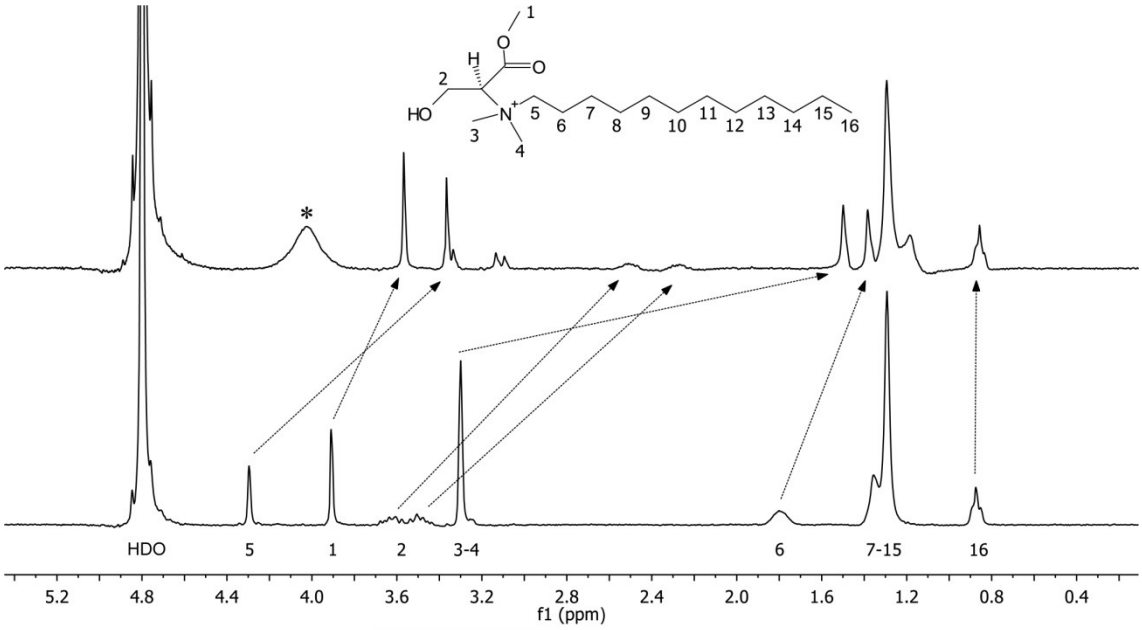

Figure 10. ^{1}H NMR spectra of: (bottom) 12Ser (1 mM), (top) 12Ser (1 mM) in the presence of SC4 (1 mM), in D_2O at 25 °C. The (∗) correspond to the methylene protons of SC4.

Assuming a similar binding mode between 12Ser and 16Ser when complexed with SC4, we propose a model of forming supramolecular aggregates based on host–guest complexation as that illustrated in Scheme 3. In all cases, the aggregates should have a positive surface charge, since the amount of SC4 added (despite the five negative charges in neutral conditions)[36] is always in deficit in relation to the amount of 16Ser. For the mixed micelles, the complexation of 16Ser by SC4 acts as a new amphiphile that promotes the formation of micelles, while for the construction of giant vesicles and

tubules, the hydrophobic alkyl chain of 16Ser should be packed together in the middle of the layer, and the calixarene attached by host-guest interactions in the inner and outer-layer surface.

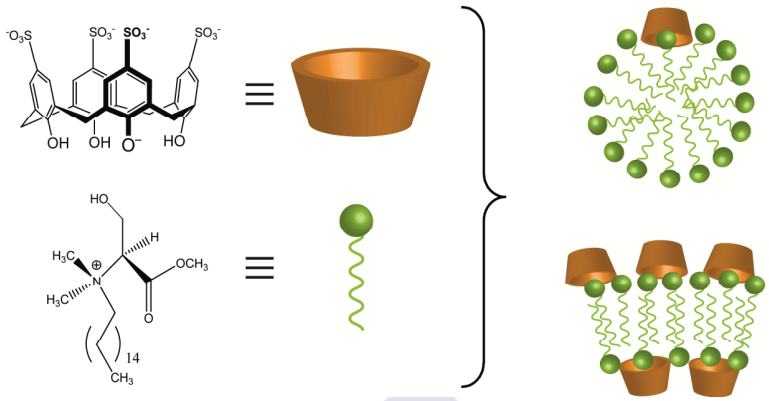

Scheme 3. Schematic representation of the construction of supramolecular aggregates formed by the complexation of 16Ser by SC4.

The formation of the different aggregates can be explained in terms of molecular packing parameter (*P*), which is based on geometrical considerations and therefore depends on the molecular structure.[37] Here, since the aggregates are formed through a binary mixture, the individual components have to be considered. In the solid state, it is know that the *p*-sulfonatocalix[4]arene sodium salt shows a bilayer-type arrangement, with the counterions intercalated between the layers.[38] However, in aqueous solution there is no evidence for the formation of a well organized struture.[39] Regarding with the other component, 16Ser, the results reported only show the formation of micelles.[40,16] Therefore, none of the individual components show trend to form large aggregates in aqueous solution. On the other hand, when combined with other molecule, the calixarene[41] as well as the serine-based surfactant[40] can successfully lead to the formation of well-organized structures, such as vesicles.

Based on the ability of SC4 to complex the serine-based surfactant by the head group region, a new amphiphilic host-guest complex is formed.[15] The molecular packing parameter is defined as $P = v_o/al_o$, where v_o and l_o are the volume and length of the surfactant hydrophobic tail and a_o is the area of the surfactant head group. When 16Ser is complexed by SC4, it can be intuitively estimated an increase in the a_o parameter which in turn favor the formation of micelles. Based on this assumption, this is probably the reason why when the amount of SC4 was increase in the binary mixture,

the diffusion experiments show a decrease in the aggregates size, corresponding to the formation of supramolecular micelles. To expect the formation of tubules or spherical vesicles the packing parameter should be in the range from 0.5 to 1. In order to explain the formation of the tubules and the spherical aggregates observed, probably more than one surfactant molecule should be complexed by the calixarene, in order to increase the v_o parameter and therefore $P \geq 0.5$.

5.2.4. Conclusions

In this work, it was shown that for the mixed system SC4–TTABr, a new type of catanionic vesicles are formed, in which the principal feature is the possibility of being stored and rehydrated on demand without any significant change in size. Further investigations have to be done related to other water-soluble calixarene and surfactants, as well as in the combined properties of calixarenes as macrocyclic hosts and self-organizing systems able to form vesicles. In the mixed system SC4–16Ser, further investigations have to be performed to better characterize the aggregates and the transition between the various morphological structures, as well as stimuli-responsive properties. However, the preliminary results show that the complexation of the serine-based surfactant by the water soluble calixarene give rise to the formation of a very rich region of aggregates. The lack of toxicity and immune response of calixarene derivates as well as the serine-based surfactant, enable new applications of the supramolecular aggregates in biomedical and pharmaceutical sciences.[43]

5.2.5. References

1. J. Bae, J.-H. Choi, Y.-S. Yoo, N.-K. Oh, B.-S. Kim, and M. Lee, *J. Am. Chem. Soc.*, 2005, **127**, 9668–9669.

2. Y. Chen, B. Zhu, F. Zhang, Y. Han, and Z. Bo, *Angew. Chem. Int. Ed.*, 2008, **47**, 6015–6018.

3. T. Kunitake and Y. Okahata, *J. Am. Chem. Soc.*, 1977, **99**, 3860–3861.

4. S. I. Stupp, *Science*, 1997, **276**, 384–389.

5. T. Shimizu, M. Masuda, and H. Minamikawa, *Chem. Rev.*, 2005, **105**, 1401–1443.

6. T. Zemb, *Science*, 1999, **283**, 816–819.

7. E. W. Kaler, A. K. Murthy, B. E. Rodriguez, and J. a. Zasadzinski, *Science*, 1989, **245**, 1371–1374.

8. E. W. Kaler, K. L. Herrington, A. K. Murthy, and J. a. Zasadzinski, *J. Phys. Chem.*, 1992, **96**, 6698–6707.

9. P. K. Yuet and D. Blankschtein, *Langmuir*, 1996, **12**, 3802–3818.

10. H. T. Jung, B. Coldren, J. a Zasadzinski, D. J. Iampietro, and E. W. Kaler, *Proc. Natl. Acad. Sci. U. S. A.*, 2001, **98**, 1353–1357.

11. E. . Marques, O. Regev, A. Khan, and B. Lindman, *Adv. Colloid Interface Sci.*, 2003, **100-102**, 83–104.

12. M. Bergmeier, M. Gradzielski, H. Hoffmann, and K. Mortensen, *J. Phys. Chem. B*, 1999, **103**, 1605–1617.

13. J. Hao and H. Hoffmann, *Curr. Opin. Colloid Interface Sci.*, 2004, **9**, 279–293.

14. M. Bergstro, J. S. Pedersen, and P. Schurtenberger, *J. Phys. Chem. B*, 1999, **103**, 9888–9897.

15. N. Basilio and L. García-Río, *Chem. Eur. J.*, 2009, **15**, 9315–9319.

16. S. G. Silva, J. E. Rodríguez-Borges, E. F. Marques, and M. L. C. do Vale, *Tetrahedron*, 2009, **65**, 4156–4164.

17. Y. Zhou, C. Liu, H. Xu, H. Yu, Q. Lu, and L. Wang, *Spectrochim. Acta Part A*, 2007, **66**, 919–923.

18. M. Stödeman and N. Dhar, *J. Chem. Soc., Faraday Trans.*, 1998, **94**, 899–903.

19. O. Danylyuk and K. Suwinska, *Chem. Commun.*, 2009, 5799–5813.

20. Y. Maitani, Y. Aso, A. Yamada, and S. Yoshioka, *Int. J. Pharm.*, 2008, **356**, 69–75.

21. J. H. Crowe and L. M. Crowe, *Biochim. Biophys. Acta, Biomembr.*, 1988, **939**, 327–334.

22. L. M. Crowe and J. H. Crowe, *Liposome Technology*, CRC Press, Boca Raton, 1993.

23. S. Liu and D. F. O'Brien, *J. Am. Chem. Soc.*, 2002, **124**, 6037–6042.

24. L. M. Crowe, J. H. Crowe, J. F. Carpenter, A. S. Rudolph, C. A. Wistrom, B. J. Spargo, and T. J. Anchordoguy, *Biochim. Biophys. Acta*, 1988, **947**, 367–384.

25. E. C. van Winden and D. J. Crommelin, *J. Controlled Release*, 1999, **58**, 69–86.

26. R. Fettiplace, *Biochim. Biophys. Acta, Biomembr.*, 1978, **513**, 1–10.

27. W. D. Stein, *Transport and Diffusion across Cell Membranes*, Academic Press, San Diego, 1986.

28. A. W. Coleman, S. Jebors, S. Cecillon, P. Perret, D. Garin, D. Marti-Battle, and M. Moulin, *New J. Chem.*, 2008, **32**, 780–782.

29. K. Wang, D.-S. Guo, and Y. Liu, *Chem. Eur. J.*, 2010, **16**, 8006–8011.

30. Z. Li, C. Hu, Y. Cheng, H. Xu, X. Cao, X. Song, H. Zhang, and Y. Liu, *Sci. China Chem.*, 2012, **55**, 2063–2068.

31. K. Wang, D.-S. Guo, X. Wang, and Y. Liu, *ACS nano*, 2011, **5**, 2880–2894.

32. G. Gattuso, A. Notti, A. Pappalardo, S. Pappalardo, M. F. Parisi, and F. Puntoriero, *Tetrahedron Lett.*, 2012, **54**, 188–191.

33. F. Sansone, L. Baldini, A. Casnati, and R. Ungaro, *New J. Chem.*, 2010, **34**, 2715–2728.

34. G. Arena, S. Gentile, F. G. Gulino, D. Sciotto, and C. Sgarlata, *Tetrahedron Lett.*, 2004, **45**, 7091–7094.

35. Y. Liu, D.-S. Guo, H.-Y. Zhang, Y.-H. Ma, and E.-C. Yang, *J. Phys. Chem. B*, 2006, **110**, 3428–3434.

36. K. Suga, T. Ohzono, M. Negishi, and K. Deuchi, *Supramol. Sci.*, 1998, **5**, 9–14.

37. S. Segota and D. Tezak, *Adv. Colloid Interface Sci.*, 2006, **121**, 51–75.

38. A. W. Coleman, S. G. Bott, S. D. Morley, C. M. Means, K. D. Robinson, H. Zhang, and J. L. Atwood, *Angew. Chem. Int. Ed.*, 1988, **1**, 1361–1362.

39. N. Basilio, L. García-Río, and M. Martín-Pastor, *J. Phys. Chem. B*, 2010, **114**, 7201–7206.

40. E. F. Marques, R. O. Brito, S. G. Silva, J. E. Rodríguez-Borges, M. L. do Vale, P. Gomes, M. J. Araújo, and O. Söderman, *Langmuir*, 2008, **24**, 11009–11017.

41. N. Basilio, V. Francisco, and L. Garcia-Rio, *Int. J. Mol. Sci.*, 2013, **14**, 3140–3157.

42. F. Perret, A. N. Lazar, and A. W. Coleman, *Chem. Commun.*, 2006, 2425–2438.

6. Resumen

La química supramolecular es una de las áreas de la química experimental que ha mostrado mayor crecimiento en los últimos años. Esto se debe esencialmente a la contribución de científicos no solo de química, sino también de otras áreas como la física, biología, bioquímica, matemática, etc. La química supramolecular estudia el reconocimiento molecular y la formación de agregados supramoleculares como resultado de fuerzas intermoleculares. El reconocimiento molecular se basa en la interacción, frecuentemente inclusión, de una pequeña molécula (huésped, *guest*) en la cavidad de un macrociclo (anfitrión, *host*), mientras que la formación de agregados supramoleculares consiste en la organización de un gran número de moléculas originando estructuras tipo micelas o vesículas. De este modo se puede considerar que el reconocimiento molecular es la base de la química supramolecular (que incluso ha aparecido antes del término química supramolecular), ya que la construcción de cualquier sistema supramolecular implica una combinación molecular selectiva. Las designadas "supermoleculas", que resultan de la interacción de dos o más especies moleculares, suelen tener propiedades diferentes que la suma de los propiedades de cada componente. Las fuerzas frecuentemente involucradas en la formación de las supermoleculas incluyen interacciones de tipo hidrofóbico, tipo π–π, van der Waals, electrostáticas, enlace de hidrógeno, y otras, que no sólo se suman unas a las otras sino que también son cooperativas. La gran ventaja de esto tipo de interacciones, en comparación con las del tipo covalente, se debe a la reversibilidad de las interacciones intermoleculares. Considerando que la mayor parte de los procesos biológicos ocurren en medio acuoso y se basan en interacciones no-covalentes entre las especies moleculares, es de gran importancia el estudio de las interacciones intermoleculares para que se pueda crear nuevos sistemas supramoleculares.

En este sentido, una parte del trabajo de esta Tesis Doctoral pretende estudiar el reconocimiento molecular mediante la formación de complejos de inclusión entre distintas moléculas anfitrión, con pequeñas moléculas e iones (huésped). En una segunda parte, se ha estudiado la formación de agregados supramoleculares, por la interacción de macrociclos con surfactantes. En el primer capítulo se hace una breve introducción a las distintas fuerzas intermoleculares responsables por las interacciones entre los anfitriones y las moléculas huésped, así como a los principales métodos experimentales empleados en el desarrollo de este trabajo. En este capítulo también se

hace un pequeño resumen del reconocimiento de moléculas huésped por los macrociclos empleados en la Tesis, que están descritos en la literatura. Al final de este capítulo también se resumen los trabajos descritos en la literatura en el empleo de macrociclos para la formación de agregados supramoleculares.

En el capítulo 2, se ha estudiado la influencia de los contraiones del macrociclo en la complejación de moléculas huésped. Dado que los contraiones, frecuentemente iones inorgánicos, siempre están presentes en disolución y normalmente no se tienen en cuenta, se estudiado su influencia sobre la constante de estabilidad, así como su influencia en los parámetros termodinámicos de los procesos de complejación. En este sentido, el capitulo 2 se divide en tres secciones mediante el tipo de huésped: iones, pequeñas moléculas cargadas positivamente y pequeñas moléculas sin carga. En la sección 2.1 se ha estudiado la complejación de cationes metálicos monovalentes y divalentes, por un macrociclo soluble en agua, *p*-sulfonatocalix[4]arene (SC4). La técnica elegida para estudiar este tipo de complejación ha sido la calorimetría isoterma de titulación (ITC), ya que con un solo experimento se pueden obtener la constante de estabilidad y los parámetros termodinámicos. Además esta técnica es bastante útil en la determinación de complejos de inclusión donde la constante de estabilidad es baja ($K \leq 20$ M^{-1}). Con los experimentos de microcalorimetría fue posible determinar por primera vez los parámetros termodinámicos para la complejación de metales alcalinos (Li^+, Na^+, K^+, Rb^+, Cs^+) y de la plata (Ag^+) con el SC4 a pH neutro. Teniendo en cuenta que el cation Na^+ está rutinariamente presente como contraión del macrociclo en disoluciones acuosas neutras (se consideran 5 cationes Na^+ por cada molécula de SC4), consecuentemente se tiene que tener en cuenta cuando se determinan las constantes de estabilidad y los parámetros termodinámicos para la complejación de cationes. Para la determinación de la constante de estabilidad y los restantes parámetros de complejación del cation Na^+ se ha considerado un modelo secuencial, mientras que para los restantes cationes metálicos se empleó un modelo competitivo. Se debe destacar también que ya que el catión Na^+ está presente como contraión y puede ser complejado en la cavidad del SC4, los experimentos de ITC tienen que ser ejecutados dentro de un determinado rango de concentraciones. Para concentración altas de SC4 en la celda de la muestra del ITC, la cavidad del calixareno estará ocupada con el contraión, y puede que no se vea calor de reacción al ser complejado con los cationes metálicos, mientras que a concentraciones bajas, el flujo de calor puede ser suficientemente bajo para que no sea detectable. Este ha sido precisamente el problema encontrado por otro grupo de

investigación, en cuyo caso la ausencia de flujo de calor era interpretado como debida a la falta de interacción entre cationes metálicos y a que tenían constantes de interacción muy pequeñas ($K_{M^+} \leq 15\ M^{-1}$). Los valores determinados para las constantes de estabilidad, que van desde $K_{Li^+} = 139\ M^{-1}$ hasta $K_{Cs^+} = 760\ M^{-1}$ están claramente en desacuerdo con los valores de la literatura determinados por ITC, ya que los trabajos publicados no tienen en cuenta da complejación del contraión con el macrociclo. Sin embargo las constantes de estabilidad están de acuerdo con los valores publicados por el grupo de Werner M. Nau, en que las constantes fueran determinadas por un método competitivo de desplazamiento de una molécula fluorescente.

Los parámetros termodinámicos obtenidos para la complejación de los cationes por el SC4 (ΔH° and ΔS°) indican que el proceso de inclusión está dominado por el término entrópico, aunque una influencia de la temperatura en los experimentos ha revelado que el término entálpico también contribuye en la complejación. Los resultados también muestran que una compensación entalpía-entropía equilibra la ganancia de una contribución con la correspondiente pérdida en la otra.

La determinación de los parámetros termodinámicos y la constante de estabilidad para la complejación del contraión Na^+ permiten avaluar la complejación de otras moléculas con el SC4. Este es el trabajo que se presenta en la sección 2.2, donde la constante de estabilidad entre el SC4 y un ion amonio cuartanario ha sido determinada por experimentos de RMN y calorimétricos. Los resultados demuestran que la constante de estabilidad depende tanto de la concentración de calixareno en disolución como de la adición de sales. A concentraciones bajas de SC4 (0.075mM), $K_{obs} = 3.05 \times 10^5\ M^{-1}$ fue determinado para la complejación del benziltrimetilamomio (BTA) con el SC4, mientras que este valor ha disminuido hasta $3.40 \times 10^4\ M^{-1}$ cuando la concentración de SC4 ha sido incrementada hasta 7 mM.

Sin embargo, ya que el counterion en mayor o menor fracción estará en la cavidad del SC4, se han realizado experimentos de difusión (^{23}Na) para verificar si el contraión sale de la cavidad y es reemplazado por el BTA, o si se forma un complejo ternario. Los resultados demuestran que la titulación de una disolución de 10 mM de SC4 con BTA, en lo cual 90 % del SC4 estará ocupado con el contraión Na^+, la difusión del Na^+ se incrementa hasta valores proximos a la difusión del Na^+ libre en disolución, al incrementar la concentración de BTA en disolución. Del experimento de difusión se ha

concluido que para analizar los datos de ITC y RMN a distintas concentraciones de SC4 se tiene que considerar un modelo competitivo.

En la literatura, la mayoría de los experimentos que se realizan para la determinación de las constantes de estabilidad de complejación de huéspedes con el SC4 son hechos en presencia de tampones. Frecuentemente se usan tampones de fosfatos para controlar al pH con concentraciones próximas a 100 mM, los cuales tienen en su composición iones Na^+ y, por tanto, se está incrementado la concentración de sal en disolución. Así, la constante de estabilidad que se determina para la formación del complejo no es el valor real, sino una constante aparente. Para determinar la verdadera constante, se tiene que extrapolar la constante de estabilidad a concentración cero de SC4 y a concentración cero de sales añadidas.

Después de estudiar la influencia de los iones Na^+ en la complejación del BTA, una molécula cargada positivamente, se ha decidido estudiar la complejación de una molécula neutra. En la sección 2.3 se describe el estudio de complejación de la 2-cloropiridina (**1**) con el SC4 en presencia de un ion metálico alcalino, Na^+, y un alcalinotérreo, Cu^{2+}. Las constantes de estabilidad fueran determinadas por ITC a pH neutro. Los resultados obtenidos para la influencia de los cationes Na^+ muestran que la constante de estabilidad disminuye al incrementar la concentración de sal en la disolución. Sin embargo, al intentar ajustar los datos a un modelo competitivo, lo esperable para un comportamiento en que la constante de estabilidad disminuye, el ajuste al modelo no consigue reproducir la tendencia de la constante de estabilidad observadas. Se han realizado experimentos de difusión (DOSY) mostrando que el cation Na^+ permanece dentro de la cavidad del SC4 cuando el macrociclo forma complejo con la molécula neutra. La formación de un complejo triple también fue confirmado por experimentos de 2D NOESY. A una disolución de SC4 (8 mM) con molécula neutra (4 mM) en presencia de 140 mM de Na^+, es posible observar señales NOE entre los protones de la molécula neutra con los protones del SC4, indicando la inclusión de la molécula neutra en la cavidad del SC4, incluso en la presencia de una gran cuantidad de sal.

En relación al cation metálico Cu^{2+}, se ha observado un comportamiento distinto al detectado con Na^+, ya que la constante de estabilidad para la complejación de la molécula neutra con el SC4 se ha incrementado en presencia de distintas concentraciones del cation Cu^{2+}. Los resultados indican que en presencia de Na^+ y Cu^{2+} se observa la formación de complejos triples, pero en presencia del catión metálico

alcalino la cooperatividad es negativa, mientras que para el catión alcalinotérreo la cooperatividad es positiva.

Para comprobar que la complejación del contraión por el macrociclo no se puede restringir a los calixarenos o únicamente al SC4 , se ha estudiado este comportamiento con una otra clase de macrociclo. En el capítulo 3, se describe el estudio de la complejación de un huésped cargado negativamente, toluenosulfonato de sodio (TSNa), con un pilarareno, en disolución acuosa a pH neutro. Esta nueva clase de macrociclo, que ha sido recientemente sintetizado por Tomoki Ogoshi (2008), está caracterizada por tener una forma de cilindro, en que la parte de superior y la inferior pueden ser funcionalizada con distintos grupos. En este caso fue estudiado el tetrafluoborato de bis[(trimetilamonio)etoxi]pilar[5]areno (en que 5 representa el número de unidades repetidas). Cada grupo trimetilamonio tiene su respectivo contraión, BF_4^-, de tal modo que en cada macrociclo existen 10 contraiones. Para estudiar la complejación del TSNa con el macrociclo, fueran realizados experimentos de ITC y también de difusión de protón (^1H) y flúor (^{19}F). Los resultados obtenidos por ITC indican que al variar la concentración de pilarareno de 0.01 mM a 1mM, la constante de estabilidad para la inclusión del TSNa cambia de 1.37×10^6 a 3.18×10^4 M^{-1}, lo que supone una cambio de más de 40 veces. Este cambio en la constante de estabilidad se puede atribuir debido a la complejación del contraión con el macrociclo, ya que los experimentos de difusiometría de RMN con el pilarareno puro en medio acuoso, permitirán concluir que para una disolución de 5 mM, sensiblemente la mitad del contraión de pilarareno está complejado en la cavidad del macrociclo.

La confirmación de que el contraión es complejado por el macrociclo induce a investigar que ocurre al BF_4^- cuando se compleja el TSNa con el pilarareno. En este caso es posible verificar que aunque hay una fracción de contraión BF_4^- que es expulsado de la cavidad del macrociclo, una parte permanece complejado en el interior del mismo. Los experimento de difusiometría también permiten verificar que además de la complejación de una molécula de TSNa en el interior del pilarareno, existe también la formación de un complejo externo. En conclusión, los experimentos evidencian que cuando se mezcla TSNa con pilarareno, se induce la formación de un complejo ternario, en que una molécula de TSNa y el contraión BF_4^- están dentro de la cavidad, y a mayores el pilarareno aun puede formar un complejo externo con otra molecula de TSNa.

En el capítulo 4 se ha estudiado la complejación de un colorante fluorescente, hemicianina, con un cucurbiturilo. Los cucurbiturilos son macrociclos que han sido bastante estudiados en los últimos anos por el reconocimiento de pequeñas moléculas, cargadas positivamente o neutras. El macrociclo debe sus propiedades de reconocimiento molecular a su cavidad hidrofóbica y sus dos portales con densidad de carga negativa. Los cucurbiturilos comparten algunas características con sus análogos ciclodextrinas, como las dimensiones y la cavidad hidrofóbica, sin embargo los cucurbiturilos presentan constantes de estabilidad con órdenes de magnitud superiores a las ciclodextrinas.

Unas de las grandes limitaciones de los cucurbiturilos es su solubilidad en medio acuoso, ya que es demasiada baja. Una manera de incrementar la solubilidad de estos macrociclos, es la adición de sales a una disolución de cucurbiturilo. Sin embargo, la adición de sal afecta a la accesibilidad de las moléculas a la cavidad de los cucurbiturilos, ya que los cationes funcionan como tapa que sellan los portales. El trabajo de este capítulo consiste en estudiar la influencia de la temperatura y de la presencia de distintos sales, sobre la cinética de complejación del yoduro de *trans*-4-[4-(dimetilamino)stiril]-1-metilpiridinio (DSMI) con el cucurbit[6]uril (CB6). Los experimentos fueran realizados en un *stopped-flow* para monitorizar reacciones rápidas. En relación a los experimentos realizados a distintas temperaturas, se puede concluir que la complejación del DSMI con el CB6 es entalpicamente favorable.

La influencia de la concentración de sales en disolución, muestra que la constante de velocidad de disociación permanece constante, mientras que la constante de velocidad de asociación disminuye al incrementar la concentración de sal. Se ha propuesto un modelo competitivo para la complejación del DSMI con el CB6 en presencia de sales. Cuando los experimentos fueran realizados en presencia de distintos tipos de sales, se puede concluir que existe una afinidad por tamaño de la sal por los portales del cucurbiturilo.

En el último capítulo de esta tesis se ha estudiado la complejación de distintos tipo de surfactantes con un calixareno. En la sección 5.1 se ha estudiado la interacción de surfactantes tipo bolaform con estructura $C_nR_6^{2+}$ $2Br^-$ con distintos espaciadores (n = 6 y 12) y los grupos terminales con distintos volúmenes (R = metil, etil, propil) con el macrociclo SC4. Los surfactantes bolaform difieren de los surfactantes convencionales por tener dos grupo polares en vez de uno. La interacción de los distintos bolaform ha sido estudiado por distintas técnicas de RMN (^{1}H, NOESY, DOSY, KMBC, HSQC,

TOCSY) y también por ITC. Los modos de complejación de los bolaform con el SC4 han sido estudiados en primero lugar teniendo en cuenta el espaciador entre los grupos polares del bolaform (*n* = 6 o 12, R = metil). Los datos indican que el bolaform con el espaciador más pequeño sólo forma un complejo con estequiometria 1:1, mientras que el bolaform con *n* =12 puede formar complejos 1:1 pero también con estequiometria 2:1, en que cada grupo polar del bolaform compleja su respectivo SC4. Sin embargo, la comparación de las constantes de estabilidad de los dos bolaform con la constante de estabilidad para la complejación del surfactante convencional con sólo un grupo polar (bromuro de hexiltrimetilamonio) con el SC4, muestra que los bolaform tienen una afinidad más grande con el macrociclo. Esto se debe al hecho de que en la estequiometria 1:1 de ambos bolaform, los dos grupos polares están incluidos en la cavidad del SC4.

Al incrementar el volumen del grupo polar del bolaforme (*n* = 12, R= etil), se ha verificado la existencia de dos modos de inclusión, con estequiometria 1:1 y también con la 2:1 (SC4−bolaform−SC4), de un modo similar a lo observado para el bolaform con *n* = 12, R= metil. Cuando se ha estudiado la interacción del bolaform con los grupos polares más voluminosos (*n* = 12, R= propil), se ha verificado se sigue formando complejos con estequiometria 1:1 y 2:1, sin embargo en el caso del complejo 1:1 no se verifica que los dos grupos polares del bolaforme están dentro de la cavidad del SC4. En este caso, solamente un grupo polar esta dentro de la cavidad mientras que la cadena alquílica esta plegada por fuera a los anillos aromáticos del SC4 e el otro grupo polar en contacto con la parte inferior del SC4.

En la sección 5.2 se ha estudiado la complejación de dos surfactantes de cadena simples, uno con grupo polar trimetilamonio (TTABr) y el otro con un grupo serina (16Ser), con el SC4 en medio acuoso. Al estudiar el sistema mixto SC4−TTABr para distintas relaciones molares se ha verificado una región en que se forma una dispersión blanca. Al analizar una muestra de esa región en un microscopio de luz, se ha verificado la existencia de vesículas gigantes con tamaños entre 0.5 y 5 μm, y en que las pequeñas presentaban un movimiento browniano. Con el objetivo de obtener vesículas de tamaños inferiores y para disminuir la polidispersidad de las vesículas, se ha sometido una muestra compuesta por 2 mM de SC4 con 5 mM de TTABr a sonicación. Al analizar las muestras después de sonicadas por las técnicas de difusión dinámica de luz (DLS) y microscopia electrónica de transmisión (TEM), se ha verificado por ambas técnicas la formación de vesículas con diámetros medios de 120 nm.

La estabilidad de las vesículas también fue estudiada, pudiendo destacar el hecho de que presentan una gran estabilidad durante un periodo de 4-5 días. A tiempos mayores se observa su evolución a estructuras de mayor tamaño. Debido a este problema, se ha retirado el agua del sistema mixto mediante la técnica de liofilización, para que así se puedan almacenar las vesículas. Al redisolver el polvo conteniendo las vesículas, se ha verificado por DLS que estas mantienen el tamaño sin que se tenga que adicionar crioprotectores antes de liofilizar. En conclusión se ha construido una vesícula que puede ser almacenada y luego se redispersa en agua sin que se altere el tamaño de las mismas y sin tener que adicionar ningún tipo de protección.

En relación al sistema SC4-16Ser también se ha verificado por microscopia de luz y experimentos de difusión (DOSY) la formación de agregados supramoleculares, como túbulos y vesículas. La gran ventaja de este sistema mixto en relación al SC4−TTABr tiene que ver con la biocompatibilidad de los componentes. Del macrociclo, los experimentos iniciales han demostrado buena compatibilidad *in vivo*, mientras que comparando los dos surfactantes, el derivado de serina tendrá mejor biocompatibilidad que el TTABr. De esta forma se espera poder usar este tipo de agregados en aplicaciones biomédicas y farmacéuticas.